Investigating the Molecular Mechanisms of Vomocytosis

By

Andrew Stephen Gilbert

A thesis submitted to the University of Birmingham for the degree of DOCTOR OF PHILOSPHY

School of Biosciences
Institute of Microbiology and Infection (IMI)
University of Birmingham
Birmingham, UK

September 2016

Abstract

The opportunistic fungal pathogen *Cryptococcus neoformans* is the major etiological agent of the life threatening disease cryptococcosis, which is responsible for over half a million human deaths per annum (**Park *et al.,* 2009**). Professional phagocytes, such as alveolar macrophages, phagocytose inhaled spores and attempt to destroy the pathogen. However, this process is inefficient in immunocompromised hosts, such as those suffering from HIV/AIDS. In such hosts the macrophage is thought to behave like a "Trojan Horse", acting as both a cryptococcal dissemination vector and as a protective niche against antifungal agents/cells present in the circulation (**Casadevall *et al.,* 2010**).

Vomocytosis, first discovered in *C. neoformans* (**Ma *et al.,* 2006**) (**Alvarez and Casadevall 2006**), is a non-lytic expulsive mechanism whereby *C. neoformans* or *C. gattii* exit the macrophage leaving both pathogen and the host macrophage with a morphologically normal phenotype. The clinical implications of vomocytosis are poorly understood however; data from this research suggests that the induction of a pro-inflammatory response increases vomocytosis rates, suggestive of a pathogen escape mechanism from a harsh antimicrobial environment i.e. the pro-inflammatory primed macrophage. Regulating the rates of vomocytosis *in vivo* may have dramatic consequences on pathogen dissemination and also patient prognosis. For instance, enhancing the rate of vomocytosis within circulation could allow other antifungal cells and compounds access to destroy the freshly released cryptococci, hence reducing pathogen burden and improving patient prognosis.

Using a combination of pharmacological inhibitors and genetic approaches, I now demonstrate a key role for the atypical MAP-kinase ERK5 in regulating cryptococcal vomocytosis. By inhibiting ERK5 activity pharmacologically, we have been able to increase the rate of vomocytosis in both murine cell lines and primary human phagocytes without modifying cryptococcal extracellular growth. Addition of two ERK5 inhibitors, XMD17-109 and AX15836, reduces intracellular proliferation and the viable colony forming units. Furthermore, XMD17-109 modifies the levels of IFNγ secreted from infected macrophages. My data suggests that ERK5 inhibition may result in the induction of a pro-inflammatory response, analysed through cytokine profiling, enhancing pathogen killing and vomocytosis. I hypothesise an antimicrobial M1 macrophage phenotype is generated and either the pathogen escapes from the cell via vomocytosis or the cryptococci are destroyed intracellularly. Mass spectrometry experiments have revealed a functional group of murine peptides involved in cytoskeletal regulation to be involved in vomocytosis, correlating with the previous evidence of actin cage formation and the restriction of vomocytosis (**Johnston and May 2010**).

These pharmacological approaches thus offer a potentially powerful route to subtly modify this host-pathogen interaction during systemic cryptococcal infection. *In vivo* models are now being used to investigate the effects of pathogen dissemination, severity and clearance from both a zebrafish and a murine host.

To Grandad and Nana,

"I wish you were here" – Pink Floyd, 1975.

Love

Andrew

Acknowledgements

Four years ago I made a difficult decision to move away from my family, friends and football team to pursue a PhD at the University of Birmingham. This was not an easy choice, as Gemma and I regard family as the single most important thing in life, but it was a necessary choice in an increasingly competitive world. The University and particularly the IMI are fantastic and I couldn't have chosen a better place to begin my scientific career. A PhD is not an easy qualification to achieve and as many before me would agree it has been a rollercoaster – one of which I would not want to ride again in a hurry! Along the way I have met some fantastic people - too many to thank them all individually but there are some key people I must thank and this is where you will find them.

The first is to my supervisor, Robin – a great microbiologist and friend. Your support and advice, not just academically, has been outstanding making my PhD enjoyable, challenging and rewarding. The attitude and care you show to your team is unbelievable. I would also like to thank all past and present HAPI lab members many of you are great friends who are very dear to me and I promise to keep in touch. The lab is a special place where great people do great research, and I feel very privileged to have been a part of it.

I must also thank the BBSRC for funding my research and keeping the rain off my feet. I am grateful for the trust and support the MIBTP directors placed in me four years ago and hope that trust has been rewarded. I must also thank the Microbiology Society, the Federation of European Microbiological Societies (FEMS) and the British Society for

Medical Mycology (BSMM) for providing travel grants to attend various conferences and allowing me to present some of this work to the world's best mycologists and microbiologists.

I would also like to thank our many collaborators who through their own kindness and curiosity have helped make this project so engaging. These include: Dario Alessi, Nathanael Gray, Kathy Tournier, Greetje Van der Velde, Anne Puel and Apoorva Bhatt. I would also like to thank my internal assessor, Dave Grainger and external assessor, Darius Armstrong James for agreeing to read the entirety of my thesis.

I would like to thank my family and friends at home in Lincolnshire for always been at the other end of the phone when I have needed them – a few cases stick out rather vividly. I have missed you all terribly and look forward to seeing more of you. I would also like to thank Lincoln City Football Club – who have tried their best to give me something to cheer about when experiments weren't going to plan!

Most importantly of all I would like to thank my wife, Gemma, for being the one constant in my life, except possibly the cat, Jim. I will forever be grateful for your love, support, patience and kindness over the last four years. It has been difficult but it has made who we are today and I wouldn't change that. I love you xxx.

Anyway, thanks for reading this but I'm off home now, UTI.

Thesis Table of Contents:

List of Figures:

List of Tables:

List of Abbreviations

ACN - Acetonitrile

AGS - Alpha (1,3) glucan synthase

AIDS – Acquired Immune Deficiency Syndrome

AM – Alveolar Macrophages

APP1 – anti-phagocytic protein 1

ATCC – American Tissue Culture Collection

ATP – Adenosine tri-phosphate

AMP – Adenosine mono-phosphate

BBB – Blood Brain Barrier

BMDM – Bone Marrow Derived Macrophages

BMM – Bone Marrow Media

BRD4 – Bromodomain containing protein 4

BSA – Bovine Serum Albumin

CFU – Colony Forming Unit

CK1 – Casein Kinase 1

CNS – Central Nervous System

CSF – Cerebrospinal Fluid

DHM - dihydroxynapthalene

DMEM – Dulbecco's Modified Eagle's Media

cDMEM – complete Dulbecco's Modified Eagle's Media

sfDMEM – serum free Dulbecco's Modified Eagle's Media

DMSO – dimethyl sulphoxide

DNA – Deoxyribonucleic Acid

DTT - Dithiothreitol

DYRK – Dual specificity tyrosine-phosphorylation-regulated kinase

ECL – Enhanced chemiluminescemce

EDTA – ethylenediaminetetraacetic acid

EGF - Extracellular Growth Factor

ELISA – Enzyme Linked Immunosorbant assay

ERK 5 – Extracellular – signal – regulated Kinase 5

FBS – foetal bovine serum

FHB1 – flavoheamoglobin 1

GFP – Green Fluorescent Protein

GM-CSF – granulocyte macrophage-colony stimulating factor

GSK3 – Glycogen synthase kinase 3

GXM – glucuronoxylomannan

GXMGal - glucuronoxylomannogalactan

HIV – Human Immunodeficiency Virus

HPLC – High Pressure Liquid Chromatography

IFN – Interferon

IKK - IκB Kinase

IL – Interleukin

IPR – Intracellular Proliferation Rate

IQGAP – Ras GTPase activating-like protein IQGAP1

IRAK-4 - Interleukin1 Receptor Associated Kinase 4

L-DOPA – 3, 4-dihydroxyphenylalanine

JAK/STAT – Janus Kinase/ Signal Transducer and Activator of Transcription

JNK – c-Jun N-terminal Kinase

LPS – Lipo-polysaccharide

LRRK2 – Leucine Rich Repeat Kinase 2

LRRK2 IN1 – Leucine Rich Repeat Kinase 2 Inhibitor 1

MAPK (KK) – Mitogen Activated Protein Kinase (Kinase Kinase)

M-CSF – Macrophage-colony stimulating factor

MEK5 – Dual specificity mitogen-activated protein kinase kinase 5

MEKK2/3 – Mitogen activated protein kinase kinase kinase 2/3

MEP1 - metalloproteinase

MLST – Multi Locus Sequence Typing

MOI – Multiplicity of Infection

MyD88 – Myeloid Differentiation primary response 88

NEMO - Nuclear Factor – κB (NF – κB) Modulator

NFAT - Nuclear Factor of Activated T-Cells

NF – κB - Nuclear Factor – κB

NGF – Nerve Growth Factor

NRON – ncRNA repressor of the nuclear factor of activated T-cells

PAGE – Polyacrylamide gel electrophoresis

PAMPs – Pathogen Associated Molecular Patterns

PBMC – peripheral blood mononuclear cell

PBS – phosphate buffered saline

PCR – Polymerase Chain Reaction

PDGF - Platelet Derived Growth Factor

PFA - Paraformaldehyde

PFP – Pore Forming Protein

pH – potential Hydrogen

PKC – Protein Kinase C

PLB – Phospholipase B

PMA – Phorbol myristate acetate

PNW – Pacific North West

PRR – Pathogen Recognition Receptor

PVDF – Polyvinylidene fluoride

OD – Optical Density

RBC – Red Blood Cell

RHAMM – Hyaluronan-mediated motility receptor

RIP1 - Receptor Interacting Protein 1

RNA – Ribonucleic Acid

rRNA – ribosome ribonucleic acid

RNS – Reactive Nitrogen Species

ROS – Reactive Oxygen Species

RPM – revolutions per minute

RPMI – Roswell Park Memorial Institute medium

cRPMI – complete Roswell Park Memorial Institute medium

sfRPMI – serum free Roswell Park Memorial Institute medium

RT – Room Temperature

SDS – sodium dodecyl sulphate

SILAC – Stable Isotope Labelling of Amino Acids in Cell Culture

SIT – Siderophore Iron Transporter

SOD – Super Oxide Dismutases

SOWgp – Spherule Outer Wall glycoprotein

TAK1 - TGFβ Activated Kinase 1

TANK - TRAF Family Member Associated NF – κB Activator Binding Kinase

TEMED – tetramethylethylenediamine

TFA – Trifluoroacetic acid

TGF – Tumour Growth Factor

Th – T-helper

TIRAP - Toll Interleukin 1 Receptor Adaptor Protein

TLR – Toll Like Receptor

TNF – Tumour Necrosis Factor

TRAF-6 - TNF Receptor Associated Factor 6

TRAM - TRIF Related Adaptor Molecule

TSA1 – thiol-specific antioxidant 1

TRIF - TIR-domain-containing adaptor – inducing interferonβ

TX-100 – Triton X -100

UPEC – Urinary Pathogenic *E.coli*

URE – Urease

USA – United States of America

UV - Ultraviolet

VIO – Vancouver Island Outbreak

XMD17-109 – ERK5 Inhibitor

YPD – Yeast peptone dextrose

CHAPTER 1: INTRODUCTION

Much of this introduction has been previously published as a book chapter article:

Gilbert, A.S., Wheeler, R.T. and May, R.C. (2014) Fungal Pathogen: Survival and Replication within Macrophages. *Cold Spring Harb Perspect Med.* **10; 5(7):** 179 – 191.

Fungal Pathogens: Survival and Replication within Macrophages

The innate immune system is an important line of defence against pathogenic fungi of which, macrophages are a key element, cells involved in the detection and phagocytosis of infectious propagules. An immunocompromised human body is considered as an adaptable niche environment for a range of pathogenic fungi as macrophage antimicrobial activity and performance is inhibited. Many fungal pathogens are detected by and engulfed by the macrophages of an immunocompromised host but are not readily destroyed. This chapter will discuss five of the most important human fungal pathogens (*C. albicans, A. fumigatus, C. neoformans, C. imitas and H. capsulatum*) and consider the strategies and virulence factors adopted by each to survive and even replicate within macrophages.

Macrophages

Macrophages are phagocytic immune cells, forming part of the host's innate immune system, derived from monocyte differentiation, and are involved in the first line of defence during microbial invasion. They recognise, engulf and destroy foreign bodies such as pathogenic organisms before then presenting antigen to co-ordinate subsequent adaptive immunological responses (Figure 1). Macrophages are found in almost all tissues with various iterations depending upon tissue specificity i.e. Kupffer cells – macrophages of the liver or osteoclasts – macrophages in the bones. Macrophages are particularly abundant at mucosal surfaces, where pathogen exposure is naturally higher, such as the alveoli – alveolar macrophages. The physical size of alveolar macrophages (AM) varies from species to species, ranging between 12- 22 microns in diameter (**Krombach *et al.,* 1997**). They are capable of engulfing particles ranging from 500nm (such as bacteria) to greater than 5μm (such as yeast cells), however an upper diameter size limit does exist (**Chen *et al.,* 1997**). After phagocytosis, the pathogen is trapped in a maturing phagosome, which it must resist or escape from in order to survive (**Kinchen and Ravichandran 2008**).

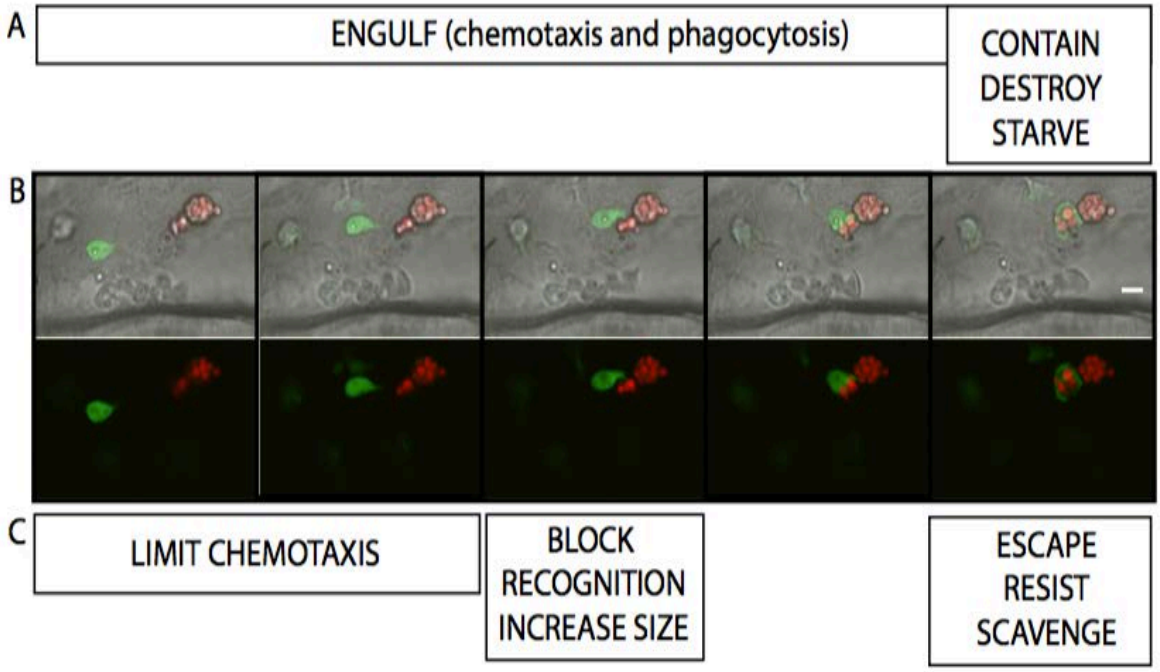

Figure 1: Fungal defences against phagocytic attack. *Figure created by Rob Wheeler.* **A**) For phagocytes to destroy fungal pathogens, they must first arrive at the site of infection and move into contact with fungi by long-range and short-range chemotaxis. Once a macrophage contacts a fungal cell via opsonic and/or non-opsonic receptors, it can initiate phagocytosis. Engulfed fungal cells are then trafficked to the phagolysosome where they are subjected to hydrolases, noxious reactive oxygen species (ROS) and nitrogen species (RNS), and starvation from easily metabolised carbon, nitrogen and trace nutrients. **B**) Schematic of phagocytosis time-lapse taken by intravital imaging in the zebrafish. Macrophages express green fluorescent protein and *C. albicans* yeast express mCherry fluorescent protein. Frames are from 1, 3, 4, 5, 6-minute time-points during this interaction. Scale bar = 10μm. **C**) Pathogenic Fungi have evolved mechanisms to limit chemotaxis, block recognition, inhibit phagocytosis, escape phagolysosomes, resist microbicidal attack and scavenge nutrients within the macrophage.

Macrophages express a wide range of different receptors able to detect foreign particles. These receptors can be split into two groups; opsonic and non-opsonic. Opsonic receptors, such as the Fc receptor or the complement receptor families (**Flannagan *et al.,* 2012**), are able to recognise particles coated (opsonised) in antibody (IgG, IgM, IgE etc.) or complement proteins (C5a) (**Flannagan *et al.,* 2012**). In contrast, non-opsonic receptors are pathogen recognition receptors (PRR), such as the toll-like receptors (TLR) or Dectin 1, which directly detect pathogen associated molecular patterns (PAMPs), such as LPS, flagellin or β-glucans, on the surface of bacteria and fungi respectively. Macrophages are heterogeneous in the receptors they express, and can alter this receptor repertoire when differentiating into different sub-types. Macrophage heterogeneity is controlled significantly via the presence of cytokines (IFNγ, IL-4, IL-10, Il-12, etc.), chemokines (CXCL12) and other small signalling molecules within the local microenvironment where they are differentiating. Differentially differentiated macrophages express different receptors and secrete different cytokines depending upon their microenvironment, including: CD86, IL-12p40 and TNFα for the antimicrobial, aggressive M1 macrophages and CD206, CD301 and Ym1 (murine only) secretion for M2 macrophages, involved in tissue repair and down regulation of the pro-inflammatory immune response. The non-opsonic Dectin-1 receptor, responsible for detecting β-glucans of the fungal cell wall, serves as a marker of M2-type macrophages (**Biswas and Mantovani 2010**; **Gordon and Martinez 2010**). The heterogeneity of receptors provides multiple paths for engulfment and different responses depending on macrophage subtype and activation state, enabling a multitude of foreign particles to be detected at any given time.

Once engulfment has been achieved the macrophage must then digest the pathogen, now segregated into a phagosome (digesting vesicle). To complete the digestion, the phagosome must mature via the fusion of early and late stage endosomes and ultimately fuse with the lysosome, generating a phagolysosome (**Kinchen and Ravichandran 2008; Smith *et al.,* 2015**). The phagolysosome utilises vacuolar ATPases to pump H+ ions into the phagolysosome, reducing the pH. As the pH is reduced, acid dependant proteases such as cathepsin D become more active and begin to degrade the pathogen (Figure 1) (**Kinchen and Ravichandran 2008**).

Many human fungal pathogens have developed strategies to resist phagocytic attack, thus facilitating pathogenicity. The field of fungal research has exploded over the last three decades due to the increase in fungal related illnesses that appears to correlate with the AIDS pandemic and more effective immunosuppressive medicines (**Brown *et al.,* 2012**). Macrophages have been shown to play a role in innate resistance to disseminated candidiasis, cryptococcosis and aspergillosis. However, pathogen resistance is not achieved in isolation by the macrophage. During *Candida* interactions, macrophages are believed to play a supporting role relative to the neutrophil. (**Calderone and Sturtevant 1994; Vazquez-Torres and Balish 1997; Lionakis *et al.,* 2014; Swamydas *et al.,* 2016**). Rigorous testing of the role of macrophages in fungal disease in the human and mouse has lagged behind examination of the neutrophil's role in immunity, as specific ablation of neutrophils is possible experimentally and seen clinically in several patient populations. Here we discuss how many clinically important fungal pathogens resist macrophage attack. Many resistance mechanisms, adopted by human fungal pathogens, discussed in this chapter, are highlighted in Figure 2.

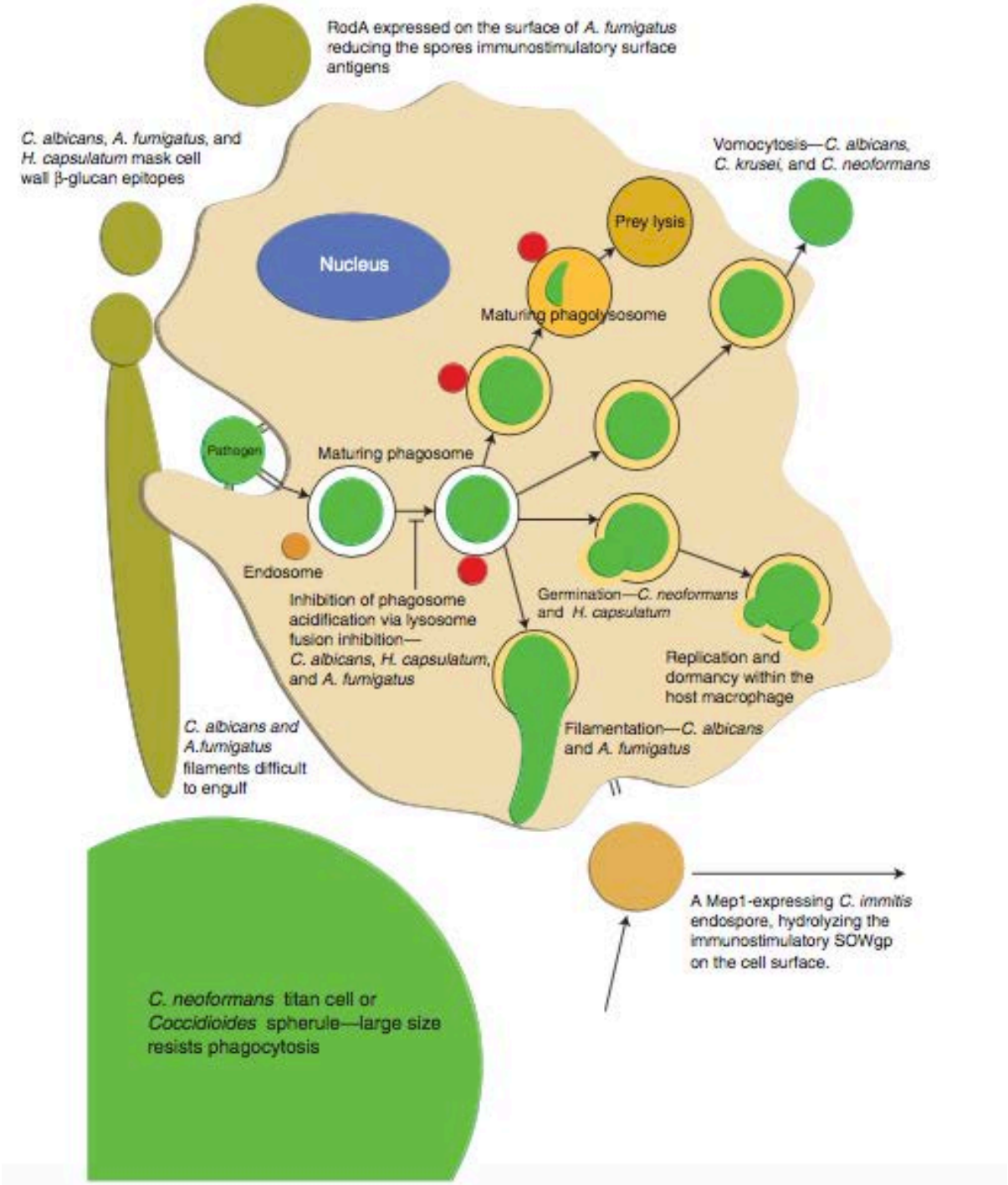

Figure 2: A diagrammatic representation of the strategies used by different fungal pathogens to avoid phagocytosis and destruction by macrophages.

Candida species

Candida albicans, C. glabrata, C. tropicalis and *C. parapsilosis* are well adapted, commensal ascomycetes considered part of the natural human microflora and are commonly associated with warm mucosal regions, such as the gut, mouth and vagina (**Miramon *et al.,* 2013**). It has been estimated that 75% of the population harbours a population of *Candida* species within their oral mucosa, however not all will succumb to symptomatic infection (**Scully *et al.,* 1994; Mayer *et al.,* 2013**). *Candida albicans*, *C. glabrata, C. parapsilosis, C. krusei* and *C. tropicalis* all have the genetic machinery to cause both superficial mucosal infections, commonly known as thrush, and life threatening systemic candidiasis. Typical to many fungal infections, predisposition to initiate invasive infection is predominantly some form of immunosuppression either through disease, such as HIV/AIDS or diabetes, or being placed on immunosuppressive therapies, for example; after organ transplant surgery (**Miramon *et al.,* 2013**). *Candida* infections often arise in patients fitted with a catheter – where the mucosal surface has been breached. Other factors facilitating the initiation of mucosal infections are long-term antibiotic use (which reduces bacterial competition on the mucosal surfaces), extreme age and use of prosthetics such as dentures (**Miramon *et al.,* 2013**).

In immunocompromised hosts or those on anti-bacterial treatments, *Candida* can proliferate. High proliferation results in biofilm formation giving rise to the superficial mucosal form of the disease. The biofilm produced can genetically and biochemically direct a more co-ordinated damaging effect upon the host, which in some instances is able to rupture mucosal barriers (**Ramage *et al.,* 2009; Nailis *et al.,* 2010a**). The biofilms provide protection from antifungal cells and treatments, such as fluconazole

and amphotericin B, with biofilms showing an altered transcription profile compared to planktonic cultures when treated with antifungal agents (**Nailis *et al.,* 2011b**). Yeast cells associated with the biofilm can then systemically invade the host's bloodstream resulting in systemic pathogen spread (**Uppuluri *et al.,* 2010**). The yeast cells interact with the mucosal and systemic macrophages and neutrophils and therefore require a variety of virulence factors involved with macrophage survival and nutrient acquisition to remain viable (**Marcil *et al.,* 2002; Miramon et al. 2013; Kitahara *et al,* 2015**). Three key survival mechanisms will be discussed: phagocyte evasion and escape, acidic/oxidative/hydrolytic survival and nutrient acquisition.

Evasion of macrophage engulfment is a strategy that many fungal and bacterial pathogens adopt, reducing the chance of phagocytic destruction and proinflammatory cytokine production. Some pathogens limit phagocyte chemotaxis cues to prevent internalization, and recent work suggests that changes in *C. albicans* during the yeast-to-hyphal transition can limit phagocyte recruitment (**Brothers *et al.,* 2013**). As with many fungal pathogens, *C. albicans* has been shown to mask the immunostimulatory β glucan constituent of the cell wall, via manno-proteins, thus reducing fungal recognition, via Dectin-1, whilst promoting and maintaining the more tolerable anti-inflammatory response (Figure 2) (**Wheeler *et al.,* 2008**). Ultimately, however, many yeast cells will still be engulfed by macrophages; hence, survival and replication or subsequent escape, remain important features of pathogen survival. *C. albicans* and *C. glabrata* actively limit phagosome maturation in macrophages, preventing acidification, limiting hydrolytic and enzymatic attack (Figure 2) (**Fernandez-Arenas *et al.,* 2009; Seider *et al.,* 2011**). Neither the mechanisms for maturation arrest nor its relative

contribution to fungal survival are known, although blocking phagosome-lysosome maturation plays an important role for many intracellular pathogens (Figure 2).

C. albicans yeast cells sense environmental changes between the external and internal macrophage environment, and use this information to turn on an escape program that includes hyphal germination and induction of pyroptosis. Elevated CO_2 levels, reduced oxygen levels, the presence of reactive oxygen species (ROS) and a neutral pH are known cues of filamentation for yeast cells *in vitro* (**Klengel *et al.,* 2005**; **Vylkova *et al.,* 2011**). *In vitro* experiments suggest that *C. albicans* can germinate within macrophages to cause physical macrophage membrane rupture and eventual lysis (Figure 2), allowing *C. albicans* escape. Intriguingly, this macrophage lysis may be a result of pyroptosis instead of physical membrane rupture (**Wellington *et al.,* 2012**). Although yeast-to-hyphal germination of *C. albicans* inside macrophages at high yeast-to-macrophage ratios *in vitro* is dramatic, at lower ratios the activation of macrophages can restrict proliferation and morphogenesis of engulfed *C. albicans* (**Calderone and Sturtevant 1994**; **Vazquez-Torres and Balish 1997**). Recent work *in vivo* in the zebrafish infection model indicates that macrophages are more active in restricting hyphal growth when in their natural context rather than *in vitro* (**Brothers *et al.,* 2011; Brothers *et al.,* 2013**). Filamentation mutants and *Candida* species that do not filament, such as *C. glabrata*, are not always avirulent, indicating that other mechanisms exist to allow survival, replication and escape from within macrophages see - **Lo *et al.,* 1997 Lorenz *et al.,* 2004**. Indeed, recently *C. albicans* and *C. krusei* yeast cells have also been shown to escape via a non-lytic process first identified in *Cryptococcus neoformans*, in which both the fungus and the macrophage are left intact post expulsion (Figure 2) (**Garcia-Rodas *et al.,* 2011**; **Bain *et al.,* 2012**).

The *C. albicans* genome is rich in genes that, when transcribed, enable macrophage survival. Hog1p is a protein kinase and transcription factor, activated by a diverse range of stressors, such as acidity, heavy metals and differing osmolarity and is known to regulate genes in response to phagosomal conditions (**Smith *et al.,* 2004**). Cap1p, the *C. albicans* homologue of *S. cerevisiae YAP1* (**Enjalbert *et al.,* 2003**), is a transcription factor that induces genes involved in carbohydrate metabolism, drug resistance, anti-oxidant production and energy production (**Wang *et al.,* 2006**). The loss of Hog1p renders *C. albicans* very sensitive to phagocyte killing (**Miramon *et al.,* 2012)**, whilst a six-fold early activation of *CAP1* has been demonstrated *in vitro* in *C. albicans* when exposed to oxidative stress, generated via heat and osmotic shocks, enabling the *C. albicans* to cope with the stressors (**Enjalbert *et al.,* 2003**). *CAP1* is required for full virulence in the moth larva virulence model and for macrophage survival *in vitro*, but unexpectedly is not required for virulence in the intravenous mouse candidiasis model (**Jain *et al.,* 2013; Patterson *et al.,* 2013**).

Sod1 and Sod4, are intracellular and extracellular superoxide dismutases, respectively (**Hwang *et al.,* 2002**). Both Sod1 and Sod4 provide *C. albicans* yeast cells with protection from ROS by converting these species into hydrogen peroxide (H_2O_2). Hydrogen peroxide is highly antimicrobial and thus Cta1p, a catalase enzyme secreted by *C. albicans*, converts H_2O_2 into water and oxygen, further reducing antimicrobial effects (**Hwang *et al.,* 2002; Mayer *et al.,* 2013**). H_2O_2 can also be dealt with by the glutathione peroxidases (Gpxs) that detoxify H_2O_2 by oxidizing the thiol groups of two glutathione molecules (**Miramon *et al.* 2013**). Superoxide dismutases, catalases and glutathione peroxidases thus appear to work synergistically to reduce oxidative stress (ROS) common in a mature phagosome.

Reactive Nitrogen Species, RNS, are secreted into the phagosome by macrophages and are thought to create a fungistatic effect against *Candida* species, maintaining the phagocytosed fungi in a state of limbo, whilst more destructive antimicrobials are secreted leading to pathogen clearance. The *C. albicans* genome contains few genes able to neutralise the effects of RNS. Of the three genomic flavohaemoglobins, enzymes secreted to convert NO to nitrate, one *(YHB1)* is upregulated upon exposure to macrophages and appears to play a critical role in *C. albicans* defence against RNS (**Ullmann *et al.,* 2004**).

Once defensive strategies are in place nutrient acquisition becomes the top priority, enabling growth and replication within macrophages. Macrophage phagosomes pose a nutritional challenge where alternative sources of carbon, nitrogen and trace elements must be utilised to promote growth (**Lorenz *et al.,* 2004**). Needless to say, the genomes of *C. albicans* and *C. glabrata* are rife with genes for such an eventuality. *C. albicans* upregulates genes involved in the glyoxylate cycle and gluconeogenesis (**Lorenz *et al.,* 2004**), allowing the 2-carbon utilisation from alternative sources, whilst down regulating genes involved in glycolysis and protein synthesis to limit processes that demand high energy and consume considerable levels of carbon and nitrogen (**Fradin *et al.,* 2005**). *C. albicans* also increases secreted levels of the enzymes involved in beta-oxidation, presumably to take advantage of the relatively high abundance of fatty acids within the phagosomal environment (**Lorenz *et al.,* 2004; Ramirez and Lorenz 2009**). Similarly, *C. glabrata* upregulates methylcitrate cycle genes in response to macrophages. This pathway enables the degradation of fatty acid chains, allowing lipids to be used as an alternative carbon source (**Kaur *et al.,* 2007**). Increased production of hexose transporter proteins and a maltose transporter proteins post macrophage

exposure further emphasizes the widespread genetic and metabolic shift required to maintain a steady carbon influx to the pathogen (**Lorenz *et al.,* 2004**).

The upregulation of amino acid biosynthetic pathways, in response to macrophage stressors such as ROS, is common practice adopted by *Candida* species in response to nitrogen deprivation. Both *C. glabrata* and *C. albicans* upregulate the arginine biosynthetic pathway, whilst *C. glabrata* also upregulates lysine biosynthesis (**Kaur *et al.,* 2007; Jimenez-Lopez *et al.,* 2013**). The increase in arginine biosynthesis creates CO_2 and urea as waste products; increasing pH and potentially inducing filamentation in *C. albicans*, hence promoting lytic escape via macrophage membrane rupture (**Vylkova *et al.,* 2011**). General amino acid permease genes are more highly transcribed in the phagosome environment in both *C. albicans* and *C. glabrata* (**Lorenz *et al.,* 2004**), further highlighting the importance of nitrogen acquisition in the parasitic intracellular lifecycle.

Aspergillus fumigatus

The ascomycete *Aspergillus fumigatus* is a common worldwide saprotroph, found abundantly in compost heaps, playing a vital role in nutrient recycling and organic decomposition. It is also, however, the cause of the life-threatening aspergillosis in immunocompromised individuals. *Aspergillus fumigatus* exposure is unavoidable with asexual conidia ubiquitous in the air and commonly inhaled; approximately 200 - 300 conidia are inhaled per person per day (**Latge 1999; Morton *et al.,* 2012**). In immunocompromised hosts, such as those with neutropenia or on medication to inhibit the activity of their immune system, *A. fumigatus* has the ability to cause invasive aspergillosis, the most severe and life threatening form of the disease (**Mansour *et al.,* 2012**). According to **Pappas *et al.,* 2010**, 10% of all bone marrow transplant patients develop invasive aspergillosis.

The molecular and genetic evolution of the pathogenicity of *A. fumigatus* suggests that adaptations concerned with "compost heap" survival are transferable to vertebrate macrophage survival. Two good examples of this are: **a**) the evolution of thermostable ribosomes and heat shock proteins enabling appropriate protein translation at elevated temperatures, even up to 55 - 70^{0}C in self-heating compost heaps (**Nierman *et al.,* 2005**) and **b**) the evolution of elastases and other proteases, capable of hydrolysing protein components of the compost heap for amino acid assimilation and hydrolysing elastin proteins in the host's lung tissue, increasing pathogenicity (**Blanco *et al.,* 2002**).

Upon entry into the lung, *Aspergillus* conidia are inefficiently detected and phagocytosed by host leukocytes. Upon engulfment, however, a poorly understood mechanism inhibits acidification/maturation of the phagosome, thus maintaining a

neutral pH and promoting pathogen survival (**Thywissen *et al.,* 2011**). The dihydroxynapthalene, DHM, melanin coat on the conidial surface, which provides the green-greyish colour, is required for restricting acidification of the phagolysosome but curiously does not prevent endosome and lysosome fusion; the underlying mechanism remains uncharacterised (**Thywissen *et al.,* 2011**). Subsequent hyphal growth then physically lyses the macrophage (**Morton *et al.,* 2012**). This finding extends the known functions of melanin, which is more commonly used to provide DNA protection from ultraviolet radiation and hence, DNA pyrimidine dimer formation in mammals (**Meredith and Reisz 2004**) and protection against reactive radicals in fungi, including *A. fumigatus* (**Heinekamp *et al.,* 2013**).

A. fumigatus conidia synthesise a RodA hydrophobin (a hydrophobic protein) that is expressed on the surface of the cells. This hydrophobin conceals the immunostimulatory cell surface proteins and carbohydrates such as the β-glucans and chitin, resulting in poor fungal recognition by the cells of the innate immune system (Figure 2) (**Aimanianda *et al.,* 2009**). Interestingly, evidence suggests that surface RodA has no role in the suppression of macrophage phagosome maturation (**Thywissen *et al.,* 2011**).

A. fumigatus relies on the secretion of secondary metabolites, part of a multiplex of adaptations that allow it to occupy the specialised niche of the phagosome. A distinct set of these secondary metabolites includes a plethora of toxins that often have immunosuppressive characteristics, therefore inhibiting macrophage function (**Latge 1999**). The most well known secreted toxic compound produced by *Aspergillus* is gliotoxin, which inhibits phagocytosis and induces macrophage apoptosis (**Eichner *et***

***al.,* 1986; Latge 1999**). Gliotoxin is capable of inhibiting the functionality of the 20S macrophage proteasome (**Eichner *et al.,* 1986**). *Aspergillus* also encodes a major allergen known as ribotoxin, a toxin able to cleave a single phosphodiester bond of the 28S rRNA of eukaryote ribosomes, hence contributing towards virulence by reducing host protein translation (**Nierman *et al.,* 2005; He *et al.,* 2012**).

Once survival mechanisms are implemented within the macrophage, *A. fumigatus* needs to extract organic materials that can be catabolised into usable organic biological compounds, hence promoting growth and replication. *Aspergillus* has a wide range of transporter proteins for this process. For instance, iron-chelating siderophores are secreted into the surrounding environment whilst iron-consuming process are inhibited (**Schrettl and Haas 2011**). Siderophores have an extremely high affinity for iron and are able to bind to iron freely available within the environment but also remove it from other iron binding compounds such as haemoglobin and transferrin. The iron bound siderophores are then reabsorbed into the fungi via the SIT (Siderophore Iron Transporter) complex to be re-distributed around the fungi for further metabolism, aiding pathogen survival (**Schrettl and Haas 2011**).

Cryptococcus neoformans/gattii

The encapsulated yeast basidiomycete, *Cryptococcus neoformans*, is an opportunistic and lethal fungal pathogen able to cause cryptococcosis in immunocompromised/immunosuppressed individuals, such as those suffering from HIV/AIDS or those administered immunosuppressive therapies respectively (**Johnston and May 2013**). The HIV epidemic has resulted in an explosion of cryptococcosis cases, as well as other fungal infections, in recent years, highlighting the need for new antifungal approaches. The *Cryptococcus* genus has a second pathogenic species, *Cryptococcus gattii* that alarmingly has been associated with infections in immunocompetent hosts (Pacific Northwest Outbreak); however, cases of *C. gattii* infections are rare (**Hoang *et al.,* 2004; Chaturvedi and Chaturvedi 2011**). Contrary to the common infection trends described above *C. neoformans* has been reported to infect the apparently immunocompetant (**Chen *et al.,* 2008**) and *C. gattii* has been reported to infect the immunocompromised (**Byrnes *et al.,* 2011**), suggestive of a genetic predisposition resulting in a susceptibility to infection.

One million patients are diagnosed with cryptococcosis per annum of which approximately 650,000 cases are lethal; furthermore 80% of these cases are in sub-Saharan Africa with poor education and health service infrastructures (**Park *et al.,* 2009**). Treatment is complicated as symptoms are often observed late after disease onset or after re-initiation from dormancy – often treatment begins at the onset of cryptococcal meningoencephalitis (**Perfect *et al.,* 2010; Johnston and May 2013**). Common symptoms include: fever, dry cough and a headache or the more severe symptoms such as blurred vision and haemoptysis. Treatment of cryptococcosis is

further complicated by disease progression and patient status i.e. whether the patient is HIV+/-, pregnant or whether the patient is an organ transplant recipient (**Perfect *et al.,* 2010**). Curiously, more cases of cryptococcosis are reported in men then women with the molecular cause of this remaining unclear (**McClelland *et al.,* 2013**). Common antifungals used clinically include Amphotericin B, Flucytosine and fluconazole, depending upon disease progression and drug availability (**Perfect *et al.,* 2010**). At the late stage of infection, lack of treatment commonly results in death (**Perfect *et al.,* 2010**).

The desiccated yeast cells or basidiospores of *Cryptococcus* are thought to be the infectious agents of cryptococcosis (**Velagapudi et al., 2009**). *C. neoformans* basidiospores are ubiquitous in the air and most of the world's population have been exposed to spores from a young age, hence an antibody response to the spores commonly exists (**Goldman *et al.,* 2001**). The inhaled small spores (2 – 5μm) travel through the lungs, ultimately entering the alveoli. The spores then interact with the alveolar macrophages; cells responsible for protecting the host from potential inhaled pathogens by phagocytosing and destroying foreign bodies (**Velagapudi *et al.,* 2009**). This initial vital interaction between cryptococcal basidiospores and the innate immune defence of the alveolar macrophages determines how the disease will progress (**Voelz *et al.,* 2009**). Ideally these spores are phagocytosed by the macrophages and the spores destroyed by the antimicrobial environment created. Unfortunately *C. neoformans* and *C. gattii* have evolved mechanisms that resist destruction by macrophages, resulting in either escape or dormancy within the macrophage (**Johnston and May 2013**).

The natural environment for *Cryptococcus neoformans* is the soil and bird faeces (**Emmons 1955**), whilst *C. gattii* has been isolated from eucalyptus trees, *E. camaldulensis* (**Ellis and Pfeiffer 1990**). These environments are often rich in predatory amoebae that utilise phagocytosis to engulf cryptococcal spores as a food source. Thus a compelling hypothesis is that cryptococci have evolved mechanisms to avoid amoebal predation and that these survival attributes are therefore transferable when spores find their way into a vertebrate host, such a s a human (**Steenbergen *et al.,* 2001; Derengowski *et al.,* 2012**). The bacterial organism that causes legionnaires disease, *Legionella pneumophilia*, is thought to have evolved in a similar way (**Albert-Weissenberger *et al.,* 2007**).

Cryptococci have several features that, together, facilitate avoidance, survival or replication within phagocytes. Firstly and most importantly, a polysaccharide coat surrounds the basidiospores of *C. neoformans* acting as both a chemical and physical barrier to fungal recognition by the macrophage and ultimately pathogen destruction (**Bose *et al.,* 2003; Doering *et al.,* 2009**). The capsule is ~ 5μm thick and is composed primarily of: glucuronoxylomannan (GXM) 90-95% but also contains a small percentage (5 – 10%) of glucuronoxylomannogalactan (GXMGal) and a small number of immunostimulatory manno-proteins (**Doering 2009**). The capsule can also be "shed" to avoid macrophage attachment and phagocytosis, to disrupt macrophage function and to disrupt T-cell function (**Monari et al., 2006; Pericolini *et al.,* 2006; Doering 2009**). Another unique and unusual technique adopted by *C. neoformans* is the ability for ~20% of the population to become "Titan Cells" upon exposure to the murine pulmonary environment (Figure 2). The size of the whole cell varies from 50 - 100μm

in diameter, each with varying degrees of capsule thickness. These titan cells are too large to be phagocytosed, have increased cross linking within their capsule conferring resistance to phagocytosis and most curiously provide phagocytosis resistance to adjacent normal sized yeast cells via an unknown mechanism (**Okagaki *et al.,* 2010; Okagaki *et al.,* 2012; Zaragoza and Nielsen 2013**). Recently, mutations in *PLB1*, a gene that encodes cryptococcal phospholipase B, were shown to be involved in controlling titan cell morphology *in vitro* in response to macrophage infection and critically in the murine lung environment (**Evans *et al.,* 2015**). App1 (Anti-phagocytic protein 1) is a secreted protein that inhibits complement-mediated phagocytosis (**Stano *et al.,* 2009**), whilst transcriptional regulators such as Gat201 and Gat204, are all involved in the phagocytosis resistance of cryptococci (**Liu *et al.,* 2008**).

The stringent avoidance strategies described above cannot prevent phagocytosis indefinitely; and a substantial proportion of inhaled cryptococci are ultimately phagocytosed, especially in the presence of opsonin, such as antibody or complement proteins (**Johnston and May 2013**). It is well known that cryptococci can persist within a host long after the lifespan of macrophages and these persistence strategies are the subject of much research, including the investigation of granuloma like structures, similar to those found in Tuberculosis infections (**Ma *et al.,* 2007; Ma 2009**). Upon internalisation, however, *C. neoformans* utilises a wide variety of defence strategies to enable growth and replication within the macrophage, an interaction first witnessed in 1973 by **Diamond and Bennett**. As with all parasitic fungal (and bacterial) pathogens, *C .neoformans* must resist antimicrobial attack and directly extract nutrients from the surrounding environment.

Phagosome maturation is an important step required to create the antimicrobial environment, involving the fusion of multiple vesicles (early and late endosomes) and the fusion of the lysosome to produce a fully mature phagolysosome (**Fairn and Grinstein 2012; Smith *et al.,* 2015**). A respiratory surge is the first stage of macrophage maturation followed by the acidification of the phagosome and secretion of acid dependant proteases and hydrolases (**Fairn and Grinstein 2012**). Initially, some aspects of phagosomal maturation appear to proceed normally upon internalisation of cryptococci, with the phagosome pH reported to drop to at least pH 5 (**Levitz *et al.,* 1999**). Recently, **Smith *et al.,* 2015**, reported that live but not dead cryptococci, are able to alter phagosome maturation by inducing the premature removal of the early endosome markers Rab5 and Rab11 (**Smith *et al.,* 2015**). This effect could not be replicated with zymosan particles or latex beads (**Smith *et al.,* 2015**). It was also found that acidification and protease activity of these modified phagosomes was hindered resulting in a less hostile environment for the cryptococci then was originally reported, conflicting with the data produced by **Levitz *et al.,* 1999.** (**Levitz *et al.,* 1999; Smith *et al.,* 2015**).

The thick polysaccharide capsule and melanin coat absorb reactive oxygen/nitrogen species (ROS/RNS), (**Zhu *et al.,* 2001; Zaragoza *et al.,* 2008**) whilst several other genes are also involved in defence against ROS. For instance, *SOD1* encodes a secreted superoxide dismutase enzyme, which converts ROS into hydrogen peroxide and water (see *H. capsulatum* and *C. albicans* for more detail). *URE1* encodes a urease enzyme, involved in the hydrolysis of host and pathogen-produced urea into ammonia and carbamate, resulting in the pH neutralisation of the immature phagosome (see *Coccidioides*) (**Cox *et al.,* 2000**). Two other genes associated with RNS and ROS

resistance are *FHB1* (flavoheamoglobin 1) and *TSA1* (thiol-specific antioxidant 1) respectively – see *Candida* and *Aspergillus* (**Brown *et al.,* 2007; Johnston and May 2013; Smith and May 2013**). Many of these lysophagosome resistance genes are found in a wide variety of fungal pathogens and are almost characteristic to a fungal pathogen.

Both species of *Cryptococcus* have the ability to escape the macrophage by inducing macrophage lysis but also have the ability to escape via a non-lytic process known as vomocytosis (Figure 2) (**Alvarez and Casadevall 2006; Ma *et al.,* 2006**). Vomocytosis is the main area of focus for this thesis, however the mechanism behind lytic escape remains poorly understood, since *Cryptococcus* has no known Pore Forming Proteins (PFP), used by some other pathogens to punch holes into the host's plasma membrane therefore alternative methods of lytic escape must exist (**Johnston and May 2013**). One possibility is that the virulence factor phospholipase B is important for lytic escape, although, the degradation of both phagosomal and cellular plasma membranes via phospholipase B activity is unlikely to perforate the cellular membrane of the macrophage sufficiently to result in lysis. It is also feasible that lysis results from excessive fungal proliferation, depleting nutrients for the host macrophage and causing physical stress inducing the eventual rupture of the cellular membrane. Figure 3 shows three human macrophages infected with multiple cryptococci. The macrophage at the bottom of the image is distorted to the point of loss of focus due to the high number of cryptococci within the macrophage.

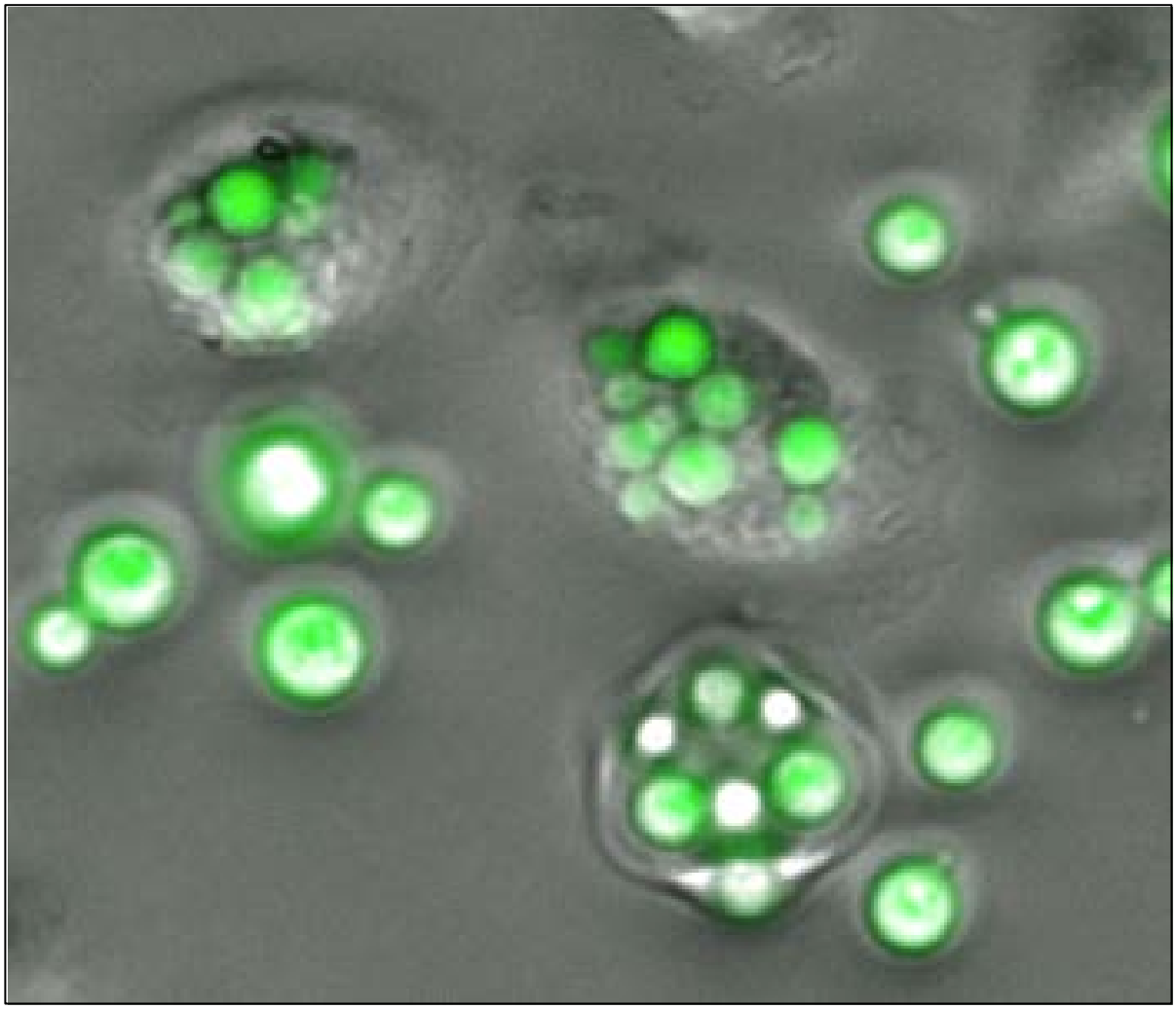

Figure 3: Three human macrophages infected with multiple H99GFP cryptococci.

Vomocytosis is the process of fungal expulsion from the macrophage without causing lysis of the host cell (**Alvarez and Casadevall 2006; Ma *et al.,* 2006**). Recently, similar processes have been noted in *C. albicans* (**Bain *et al.,* 2012**) and *C. krusei* (**Garcia-Rodas *et al.,* 2011)**. It is likely that non-lytic escape offers a distinct advantage by minimising pro-inflammatory signalling and thus ensuring that immune activity is kept to a minimal level. It is also possible that vomocytosis is a result of macrophage exocytosis, that has been hijacked by the cryptococci.

Vomocytosis is hypothesised to be a regulated process similar to cellular exocytosis. Vomocytosis is thought to require cellular signalling and microtubule activity, although the molecular process is still poorly understood. To date, the only pathogen factor known to contribute to vomocytosis is CnPlb1, since loss of this enzyme reduces, but does not entirely block, escape (**Chayakulkeeree *et al.,* 2011**). Interestingly, phagocytic cells have an actin-dependent mechanism to block vomocytosis of cryptococci (**Johnston and May 2010**), although whether this process blocks the escape of other pathogens remains unknown.

Coccidioides posadasii/immitis

Coccidioides posadasii and *C. immitis* are dimorphic fungal pathogens responsible for coccidioidomycosis, a systemic infection commonly known as "Valley Fever" (**Borchers and Gershwin 2010**; **Welsh et al., 2012**). Endemic regions include the semiarid Southern USA (Nevada, Utah and Arizona) and regions of South America (Northern Mexico) (**Welsh *et al.,* 2012**). In immunocompetent patients, coccidioidomycosis primarily manifests as an asymptomatic infection but can develop into a dry cough. As with many other fungal pathogens, immunocompromised patients and pregnant women are at greater risk of being dangerously infected from a disseminated form (meningitis) of the disease (**Borchers and Gershwin 2010; Welsh *et al.,* 2012**).

The natural environment of *Coccidioides* is in semiarid alkaline sandy clay soils (**Welsh *et al.,* 2012**). The mycelia grow saprophytically in the soil producing the infectious arthroconidia that are considered to be small enough to be aerosolised and inhaled by the host during dust storms common to the region (**Welsh *et al.,* 2012**). Upon entry into the host, gene expression within the arthroconidia rapidly alters to transform it into a large (60-100μm) endosporulating spherule (Figure 2) that cannot be phagocytosed due to its size (**Frey and Drutz 1986**). The spherule contains up to 300 small infectious endospores that are released, leading to dissemination throughout the host. Alveolar macrophages (AM) and neutrophils are able to phagocytose both arthroconidia and endospores, but phagocytosed particles are difficult to destroy even for immunocompetent patients, partially because lysosome fusion is inhibited, hence rendering the macrophage incapable of destroying the pathogen (**Beaman and Holmberg 1980; Frey and Drutz 1986**).

The Spherule Outer Wall glycoprotein (SOWgp) is an important, immunostimulatory glycoprotein expressed on the surface of the *Coccidioides* spherules and endospores (**Hung *et al.,* 2000**). **Hung *et al.,* 2000**, found that the SOWgp on the surface of spherules causes the activation of the Th_2 directed immune response and Th_2 type cytokine (IL-6 and IL-10) secretion, providing a significant advantage to the pathogen (**Hung *et al.,* 2007**). Similarly, *Cryptococcus neoformans* drives the immune system towards the Th2 response, by alternative methods (**Shen and Liyun 2015**) – this will be discussed later in this chapter. The *Coccidioides* spherule's method of immunomodulation means that once the endospores are released the immune system is poorly equipped to attack them, resulting in an increased likelihood of pathogen survival and dissemination. However, SOWgp is immunostimulatory on the smaller endospores, potentially resulting in more efficient phagocytosis. To avoid this, endospores secrete a metalloproteinase, Mep1, which hydrolyses surface bound SOWgp, reducing phagocytosis (Figure 2) (**Hung *et al.,* 2005; Hung *et al.,* 2007**). The molecular mechanisms of the variable immunological responses induced by SOWgp are unknown.

Even following phagocytosis, *Coccidioides* is able to resist killing by several mechanisms. **Gonzalez *et al.,* 2011**, demonstrated the presence of a soluble factor produced by *Coccidioides*, which blocks the action of host phagocyte nitric oxide (NO) (**Gonzalez *et al.,* 2011**). In addition, the pathogen secretes urease, which hydrolyses both pathogen and host derived urea into ammonia and carbamate, increasing the phagosomal pH, generating a pH neutral environment (**Mirbod-Donovan *et al.,* 2006**). The secretion of urease is another common virulence factor many human fungal pathogens utilise including: *C. neoformans* and *H. capsulatum*. Up regulation of urease

synthesis genes have been noted in the parasitic spherule phase of both *C. posadasii* and *C. immitis* (**Whiston *et al.,* 2012**).

Whiston *et al.,* 2012, performed transcriptomic analysis comparing gene transcription of both *C. immitis* and *C. posadasii* whilst in the saprobic mycelial natural growth phase and the pathogenic parasitic spherule phase. Phase specific up regulation of genes was identified, highlighting genetic transcripts that were up regulated in the pathogenic phase including *AGS1* (Alpha (1,3) glucan synthase). Alpha glucans act to mask the immunostimulatory beta glucans found on the fungal cell wall, reducing fungal recognition and interaction by the innate immune system (**Whiston *et al.,* 2012**), as is the case for *H. capsulatum* (**Rappleye and Goldman 2007**).

Histoplasma capsulatum

Histoplasma capsulatum is a thermally stable dimorphic fungus and the causative agent of the life threatening disease, histoplasmosis. Histoplasmosis is primarily a respiratory disease able to infect both immunocompetent and immunocompromised hosts and is predominantly found in the USA. In endemic regions, exposure is thought to be as high as 80%, with significant morbidity in 50,000 immunocompetent hosts per annum (**Edwards *et al.,* 1969**; **Chu *et al.,* 2006**). As with many fungal diseases, cases of histoplasmosis are on the rise (**McNeil *et al.,* 2001**).

A *Histoplasma capsulatum* infection initiates when the mycelial-produced microconidia (2 - 6μm diameter) are inhaled into the lungs of the mammalian host (**Helmbright and Larsh 1952**). Upon entry into the host the increase in temperature up to 37^0C triggers a dimorphic switch into the yeast form (**Inglis *et al.,* 2013**). Although yeast cells are rapidly engulfed by neutrophils and alveolar macrophages of the host's innate immune system, fungal defence mechanisms allow the organism to survive and replicate within the macrophage environment (**Inglis *et al.,* 2013**) and successful clearance of the infection requires the adaptive immune response to enhance the antifungal activity of the infected macrophages (**Kroetz and Deepe 2012**).

A major factor enabling *H. capsulatum* survival is its ability to manipulate the phagosome to maintain an internal pH of 6.5, reducing the activity of acid dependant hydrolytic proteases, such as cathepsin D, and generating a more neutral and growth promoting environment (**Strasser *et al.,* 1999**). At the same time, the pathogen up-regulates a siderophore biosynthetic cluster consisting of the genes *ABC1, SID1, SID3, SID4* and *OXR1* (**Inglis *et al.,* 2013**) which aid in iron scavenging in an analogous way

to that which occurs in *Aspergillus species* (**Schrettl and Haas 2011**). *Histoplasma* also secretes two catalases, CatB and CatP. These convert antimicrobial hydrogen peroxide (H_2O_2) to water and oxygen (**Holbrook *et al.,* 2013**). CatP acts intracellularly whilst CatB is secreted and has an association with the cell wall, where it acts downstream of the secreted superoxide dismutase Sod3 (**Youseff *et al.,* 2012**; **Holbrook *et al.,* 2013**).

The transcriptomic study by **Inglis *et al.,* 2013** has also highlighted other genes whose products may play a role in macrophage survival and replication. The *LDF1* gene encodes a protein required to lyse macrophages, although the underlying molecular mechanism is poorly understood, whilst the *LYP1* gene encodes a predicted membrane transporter protein that may potentially facilitate amino acid transport such as lysine or cysteine – enabling the utilisation of alternative nitrogen sources.

Summary

All the fungal pathogens described above have the genetic and metabolic machinery to survive and replicate within human macrophages, thus enhancing their pathogenicity and virulence. Many of these pathogens share common features associated with macrophage survival and replication such as cell surface modification strategies (SOWgp, α glucan, Rod A, polysaccharide capsule), to avoid pathogen recognition and ultimately phagocytosis, ROS resistance (superoxide dismutases and catalases, polysaccharide coat), reducing the antimicrobial activity of the macrophage and the utilisation of alternative nutrient acquisition pathways to enable survival within the nutrient sparse macrophage environment. Inhibiting the defensive strategies described above may enable the macrophage to overwhelm the pathogen, hence removing the threat of systemic infection. Current research in this field is targeted to the common and unique defensive strategies of the individual pathogens.

A Deeper Exploration of Cryptococcosis:

Cryptococcus neoformans and Cryptococcus gattii

The two important human fungal pathogens, *Cryptococcus neoformans* and *Cryptococcus gattii* are capable of causing the life threatening disease, cryptococcosis (**Kwon-Chung *et al.,* 2014)**. Many pathogenic fungal species belong to the phylum Ascomycota, including: *Candida albicans, Candida glabrata, Aspergillus fumigatus, Histoplasma capsulatum* and *Coccidioides immitis* – previously discussed. However, the cryptococcal species are basidiomycetes, distinguishable by their characteristic, thick, polysaccharide rich, extracellular capsule, the ability to produce eumelanin (**Staib 1962; Williamson *et al.,* 1998**) and the enzymatic activity of pathogen derived urease and phospholipase B (**Cox *et al.,* 2000; Chayakulkeeree *et al.,* 2011; Kwon-Chung *et al.,* 2014**).

Serological evidence suggests that cryptococcal infection is common and almost unavoidable in the human population. Many people are exposed to *Cryptococcus* spores during early childhood, as spores are ubiquitous in the air (**Goldman *et al.,* 2001**). Due to the worldwide distribution of *C. neoformans,* antibodies are likely to originate from an early, initial alveolar macrophage interaction with *C. neoformans* spores and the antigen presentation of *C. neoformans* PAMPs via dendritic or macrophage cells (**Goldman et al., 2001**). Disease symptoms, caused by *C. neoformans*, primarily manifest in the immunocompromised such as those undergoing immunomodulatory therapy or those suffering from HIV/AIDS. *C. neoformans* cases are rife in sub-Saharan Africa, predominantly in HIV+ individuals common to the area (**Park *et al.,* 2009**). A

common complication with a *C. neoformans* infection results in the successful cryptococcal traversal of the patients Blood Brain Barrier (BBB) inducing meningoencephalitis, which is fatal without medical intervention (**Chang *et al.,* 2004; Sabiiti and May 2012**). BBB traversal is an interesting but poorly understood area of cryptococcal pathology. Conversely, *C. gattii,* predominantly affects the immunocompetent and is infamous for the Vancouver Island and Pacific North West (PNW) outbreak in 1999 (**Hoang *et al.,* 2004; Chaturvedi and Chaturvedi 2011**). A *C. gattii* infection is commonly associated with lung infections (inducing lung lesions) with the generation of lymph like nodes or granuloma a common phenomena (**Dewar and Kelly 2008**). These granuloma are similar to those caused by *M. tuberculosis* infections and these will be discussed later in the chapter. *C. gattii* has typically been associated in subtropical regions of the world, whilst *C. neoformans* has a global distribution (**Kwon-Chung *et al.,* 1984a; Kwon-Chung *et al.,* 1984b; Kwon-Chung *et al.,* 2014**). The differential immunological responses observed between cryptococcal-infected human populations are a hot topic of research, with evidence suggesting that even men and women react differently to cryptococci (**McClelland *et al.,* 2013**). A study of Chinese cryptococcal patients highlights cases where *C. neoformans* has infected apparently immunocompetent individuals (**Chen *et al.,* 2008**), whilst *C. gattii* has been reported to occasionally affect the immunocompromised (HIV/AIDS population in California, USA), indicative of a genetic predisposition to infection (**Byrnes *et al.,* 2011**).

C. neoformans was first isolated in 1894 by Sanfelice from peaches and peach juice (**Sanfelice 1894**) but the environmental source remained elusive until the 1950's when strains were identified in association with avian faeces (pigeon, parrots and

canaries) (**Emmons 1955**). In 2016, **Johnston *et al.,*** discovered that *C. neoformans* is capable of surviving extracellularly at the elevated avian body temperature (~42^{0}C), but is incapable of surviving and replicating intracellularly in avian macrophages (**Johnston *et al.,* 2016**). This suggests that avian species are carriers of *C. neoformans* but are insufficient hosts. *C. gattii* has never been isolated from avian faeces. The environmental source of *C. gattii* was not discovered until 1990 when it was isolated from eucalyptus trees in Australia (**Ellis and Pfeiffer 1990**). Some mycologists argue that the increasing import of eucalyptus trees, from Australia, and global climate change may have been factors attributed to the outbreak of cryptococcosis in the PNW in 1999 (**Pfeiffer and Ellis 1991;Chakrabarti *et al.,* 1997 Kidd *et al.,* 2007**).

Serotyping in the 1950s defined four serotypes: A, B, C and D (**Evans 1950; Wilson *et al.,* 1968**). The serotypes were distinguished by polyclonal rabbit antibody binding to the glucuronoxylomannan (GXM) of the polysaccharide capsule for the different species (**Wilson *et al.,* 1968**). Before next generation DNA sequencing technologies were readily available, *Cryptococcus* species were separated into two distinct groups: *C. neoformans var. neoformans* – serotypes A, D and AD and *C. neoformans var. gattii* – serotypes B and C (**Kwon-Chung *et al.,* 1982**). During the last two decades the distinguishing features of these groups has expanded due to new modern molecular biology approaches, such as Multi-locus Sequence Typing (MLST) and PCR – restriction fragment length polymorphism analysis (PCR-RFLP). In 1999, Franzot and colleagues used sequencing to identify two separate subgroups within the *C. neoformans var. neoformans* group, *C. neoformans var. grubii* (serotype A) and *C. neoformans var. neoformans* (serotype D) (**Franzot *et al.,* 1999**). *C. neoformans var. gattii* was defined as a separate species in 2002 based on biochemical and molecular characteristics

(**Kwon-Chung *et al.,* 2002**). Both individual *Cryptococcus* species are further divided into at least four subgroups. PCR-RFLP provides repeatable and reliable grouping based on genetic variation of the cryptococcal *URA5* gene: *C. neoformans var. neoformans* – molecular subgroups VNI – VNIV, *C. neoformans var. grubii* – VNI, VNII and VNB and *C. neoformans var. gattii* – VGI and VGII (serotype B) and VGIII and VGIV (serotype C) (**Meyer *et al.,* 2003**). Majority of global cases of cryptococcosis are caused by *C. neoformans var. grubii* VNI, 63 - 95%, with only 3% - 9% of all other cases caused by all the other species subgroups, confirmed using molecular typing of clinical isolates (**Day *et al.,* 2011; Kaocharoen *et al.,* 2013; Kangogo *et al.,* 2015; Gonzalez *et al.,* 2016**).

As with many fungal species *Cryptococcus* has two mating types with the vast majority of global clinical cryptococcosis cases caused by the MATα mating type (**Kwon-Chung and Bennett 1978**). This is unsurprising as these are the most common in nature (40:1 - MATα and MATa). Reasons for the dramatic over abundance of the MATα mating types are unclear, however, McClelland and colleagues postulate that the genetic cost of asexual reproduction for the MATα mating type are less then the MATa mating type (**McClelland *et al.,* 2004**). Both mating types commonly reproduce asexually however, upon spores encountering opposite mating types on an appropriate nutrient source, sexual reproduction can commence (**McClelland *et al.,* 2004**; **Gyawali and Lin, 2011; Kwon-Chung *et al.,* 2014**). MATa and MATα spores secrete the MFa and MFα pheromone respectively upon detection of the opposite mating type (**Moore *et al.,* 1993**). Detection of opposite pheromones induces isotropic growth in MATa spores and the formation of conjugative tubes in the MATα spores. These conjugative tubes fuse with the MATa spores, inducing fused clamp connections, where the haploid

spores become a diploid karyogamy via meiosis (**Kwon-Chung *et al.,* 2014**). As with human reproduction only mitochondria from one parent (maternal) are passed to the offspring. For cryptococcal sexual reproduction the MATα mitochondria are biologically removed, leaving MATa mitochondria to be supplied to the offspring (**Yan *et al.,* 2004; Yan *et al.,* 2007**). The karyogamy produces an equal ratio of haploid basidiospores and disperses them into the environment (**Gyawali and Lin, 2011; Kwon-Chung *et al.,* 2014**).

Cryptococcosis: Treatments and Antifungal Resistance

Treatment of cryptococcosis is complicated, varying from patient to patient. Factors that can affect the treatment options include: pregnancy, species of cryptococci involved, HIV/AIDS+ patients, patients from resource limited regions and whether a patient is currently taking immunomodulatory medication (**Perfect *et al.,* 2010**). Furthermore, cryptococcal capsule is a significant physical barrier protecting cryptococci, whilst immuno-compromised macrophages can also act to inadvertently protect the cryptococci from antifungals in circulation.

Amphotericin B, a secondary metabolite polyene produced by *Streptomyces nodosus,* was discovered in 1953 to have antifungal activity to *Coccidioides* and *Histoplasma capsulatum* (**Dutcher 1968**). Since the 1960's, Amphotericin B, has been used to treat deep seated cryptococcal infections in patients symptomatic for cryptococcal meningoencephalitis, however intravenous treatment is required rendering this antifungal less attractive to developing countries (**Dutcher 1968; Perfect *et al.,* 2010**).

Flucytosine, a fluorinated pyrimidine, was identified to have antifungal activity against *C. albicans* infections in 1963 (**Grunberg *et al.,* 1963**) and anticryptococcal activity in 1968 (**Tassel and Madoff 1968**). Flucytosine is actively imported into the fungal cells where it is metabolised into 5-flurouracil (5-FU) that is antifungal to susceptible cells (**Polak *et al.,* 1975**). Cells lacking the enzymes capable of converting flucytosine to 5-fluorouracil are unaffected by the treatment (**Polak 1977**).

A combination therapy of flucytosine and amphotericin B has been developed (**Perfect *et al.,* 2010**). The combination therapy is able to inhibit both extracellular and intracellular cryptococcal growth and reduce cryptococcal growth in the CNS, hence reducing meningitis; however, treatment is expensive, requires intravenous injection and can induce significant toxicity within the patient, becoming difficult to use effectively in isolated areas where the disease is prevalent (**Perfect *et al.,* 2010**).

Fluconazole (2-(2,4-difluorophenyl)-1,3-bis (1H-1, 2,4-triazol-1-yl)-2-propanol) was developed in 1990 and is capable of eliciting antifungal activity, particularly in the CNS (**Richardson *et al.,* 1990; Perfect *et al.,* 2010**). Fluconazole is an ergosterol synthesis inhibitor that blocks the activity of the Lanosterol 14-alpha-demethylase, responsible for converting Lanosterol to ergesterol. Ergesterol is a key component of the fungal cell membrane similar to cholesterol in humans, providing membrane rigidity. Fluconazole can be taken as an oral tablet, improving its distribution and effectiveness in less developed regions, however its antifungal capabilities are less effective against intracellular cryptococci when compared to amphotericin B (**Perfect *et al.,* 2010**). Cases of fungal resistance to fluconazole have also been reported in AIDS patients (**Sionov *et al.,* 2009; Sionov *et al.,* 2010**). A clinical isolate strain, resistant to

fluconazole, has been sequenced and a missense mutation in the *ERG11* gene, encoding the Lanosterol 14-alpha-demethylase enzyme, has been identified (**Sionov *et al.,* 2012**). Innately fluconazole resistant subpopulations of both *C. neoformans* and *C. gattii* have also been identified (**Sionov *et al.,* 2009**), whereby multiple copies of drug efflux pump genes, such as the Afr1 efflux pumps, are generated. An example of how this has been achieved is through the multiple duplication of chromosome 4 in fluconazole resistant strains (**Sionov *et al.,* 2009**).

Cryptococcal Pathogenicity Factors

Although *C. neoformans* and *C. gattii* have differences both phenotypically and genotypically, including: serotype, biochemical characteristics, differing yeast cell morphology and nitrogen and carbon source utilisation, the two species share common pathogenicity/virulence factors. Virulence factors to be discussed include: polysaccharide capsule, eumelanin, urease and the phospholipase B enzymes.

Polysaccharide Capsule

The polysaccharide capsule is considered by many in the field as the major virulence factor of the *Cryptococcus* genus, as many pathogenic isolates synthesise and secrete a capsule upon pulmonary exposure. Isolates with little are no capsule are commonly avirulent (**Chang and Kwon-Chung 1994; Bose *et al.,* 2003**). The capsule is the most well studied virulence factor and therefore will be considered first.

The capsule synthesis enzymes are expressed in order to make the required polysaccharides, these are synthesised and anchored to the surface of the cryptococcal cell wall, acting as both a physical and chemical barrier to the phagocyte (**O'Meara and Alspaugh 2012**). Capsule is involved in resisting macrophage phagocytosis by masking common fungal antigens, such as the β-glucans – detected by macrophage Dectin-1, hence preventing pathogen recognition from the immune system (**Doering *et al.,* 2009**). The capsule can be "shed", prior to phagocytosis, to prevent successful phagocytosis (**Bose *et al.,* 2003**). Similarly, post phagocytosis, capsule can be deposited into the lysophagosome, dramatically altering macrophage function and commonly resulting in macrophage lysis (**Bose *et al.,* 2003**).

Capsule provides resistance to leukocytes including: macrophages, neutrophils and dendritic cells. Antigens, predominantly mannan proteins, of the capsule have been identified in the blood and cerebrospinal fluid (CSF) particularly among HIV/AIDS patients (**Powderly *et al.,* 1994**). The capsule's fundamental role is to resist phagocytosis by masking immunostimulatory mannans and glucans (**Bolanos *et al.,* 1989**) but is also capable of neutralising the antimicrobial effects of ROS and RNS (**Zaragoza *et al.,* 2008**). Furthermore, capsule has been shown to interfere with cytokine secretion and the class (Th_1, Th_2 and Th_{17}) of cytokines secreted, inducing a predominantly Th2 immune response (IL-4), beneficial to the pathogen (**Ellerbroek *et al.,* 2004b**), whilst inhibiting the Th_1 immune response (TNFα). Capsule has also been shown to inhibit neutrophil recruitment towards the infection site (**Ellerbroek et al., 2004a**). The capsule on the surface of environmental isolates is rarely heavily expressed, however, upon inhalation into the lungs or phagocytosis by macrophages or amoebae, the capsule thickness can increase dramatically (**Feldmesser *et al.,* 2001;**

Steenbergen *et al.,* 2001). Capsule thickness can vary depending upon the organ of infection with the brain, CNS and lung potent inducers of capsule, organs commonly severely affected by cryptococcosis (**Feldmesser *et al.,* 2001**). Inducers of capsule formation include iron depleted, CO_2 rich conditions common within the host.

The capsule is a complicated mix of polysaccharides, glycoproteins and proteins. 95% of the polysaccharide capsule consists of glucuronoxylomannan (GXM), a large polysaccharide with a α-1,3-mannose backbone with β-D-xylopyranosyl side chains (**Doering *et al.,* 2009**). 5% of the capsule consists of glucuronoxylomannogalactan (GXMGal), a polysaccharide with a smaller mass then GXM (**Doering *et al.,* 2009**) composing of α-1,6 galactan backbone with side chains of β-1,3-galactose-α-1,4-mannose-α-1,3-mannose (**Doering *et al.,* 2009**). The capsule also contains over 50 predicted different mannoproteins, sialic acid and importantly hyaluronic acid. Hyaluronic acid is a ligand for CD44 and RHAMM, receptors found on the surface of brain endothelial cells. Hyaluronic acid binds to CD44 and/or RHAMM and initiates transcytosis of the cryptococci into the endothelial cell, thought to be involved in the transcytosis method of BBB traversal (**Jong *et al.,* 2008; Jong *et al.,* 2012**).

The synthesis of the capsule is a highly regulated process, including extensive polysaccharide modification, hypothesised to occur in the Golgi, where polysaccharide donors including; UDP-xylose, GDP-mannose, and UDP-galactopyranose, are polymerised and transported to the cell surface for assembly (**Kwon-Chung *et al.,* 2014**). In the 1990's, four essential genes were discovered to play a role in the capsule synthesis in *C. neoformans var. neoformans* (serotype D): *CAP10, CAP59, CAP60* and *CAP64* (**Ma et al., 2009**), all of which were required for successful murine infection,

however, capsule synthesis and construction are still poorly understood. Other genes involved in capsule synthesis have been identified through genome analysis including: *CAS1p* and *CAS3p* –involved in the acetylation of GXM (**Janbon *et al.,* 2001**; **Moyrand *et al.,* 2004**) and *CAS31-34* (**Moyrand *et al.,* 2004**). These genes are not essential to capsule formation but play a role in GXM modification (acetylation etc.).

Eumelanin

Melanisation is a common process adopted by many species across all domains of life including: humans, insects (*D. melanogaster*) and plants – often associated with the browning of fruits and sun tanning. Many fungal species, including plant pathogenic species such as the black aspergilli, *Aspergillus niger*, synthesise melanin, producing the characteristic black mould – associated with food spoilage. Human fungal pathogens, such as *A. fumigatus*, also synthesise melanin and in the 1960's Staib *et al.,* discovered *C. neoformans* produces a melanin. As with other species, melanin is synthesised by *C. neoformans* to resist environmental (desiccation, temperature fluctuations etc.) and UV stress, however the mode of action is unclear (**Rosas and Casadevall 1997**). Melanins are known to absorb and scatter high energy UV radiation preventing the formation of pyrimidine dimers within the organisms DNA. Melanin is a virulence factor as it has been shown to protect the cryptococci from macrophage derived stressors, such as ROS and peptidases and antifungal compounds, such as amphotericin B (**Casadevall *et al.,* 2000**).

Unlike *Aspergillus fumigatus,* that makes a dihydroxynapthalene-based melanin (DHM), *C. neoformans* synthesises eumelanin via phenolic compound oxidation. The phenolic compound used is 3,4-dihydroxyphenylalanine or L-DOPA, a precursor to a group of natural hormones known at catecholamines, which contain epinephrine and noradrenaline (**Williamson 1998**). Eumelanin is a negatively charged, hydrophobic brown/black pigment with a high molecular weight (**Casadevall *et al.,* 2000**). Interestingly, eumelanin synthesis is induced in the host CNS and brain (**Nosanchuk *et al.,* 2000**) and melanisation was thought to correlate to cryptococcal virulence in humans. In 2014, **Sabiiti *et al.*** cultured cryptococci in the dark, in specific media containing vitamin C and L-DOPA, inducing the melanisation of 5 high and 5 low virulence clinical cryptococcal isolates. The melanin was extracted and weighed for each isolate and the melanin content compared to strain virulence. The most melanised were not necessarily the most virulent, leading to the authors to conclude that laccase activity (melanin synthesis and iron oxidase activity) was critical to virulence (**Liu *et al.,* 1999a; Sabiiti *et al.,* 2014**).

The *LAC1 (*formerly *CnLAC1)* and the *LAC2 (*formerly *CnLAC2)* genes encode the laccase enzymes of *C. neoformans* and are responsible for synthesising eumelanin, commonly in response to environmental and/or host macrophage stressors (**Williamson 1998**). Laccases also have iron oxidase activity (**Liu *et al.,* 1999a**). Mutants and genetic knockouts of the *LAC1* gene result in a reduction of melanised cryptococci, which elicits a reduced virulence in mice (**Liu *et al.,* 1999b; Missall *et al.,* 2005**), whereas the effects of *LAC2* knockdown are negligible. The laccase enzyme localises to the cell wall, where *SEC6* transports the eumelanin across the cell wall through vesicles (**Panepinto *et al.,* 2009**).

Urease and Phospholipase B Activity

C. neoformans utilises a wide range of proteases during host infection of both human and murine macrophages. Two major degradative enzymes are urease and phospholipase B. However, unlike capsule, mutations or knockouts of protease genes result in a reduction of virulence but not complete virulence ablation. The combined efforts of urease and phospholipase B, disrupts the lysophagosomal pH and potentially permeabilise the host lysophagosomal membrane. This reduces the potency of the antimicrobial environment generated in the lysophagosome, protecting the pathogen from the host and providing nutrients to the pathogen (**Kwon-Chung *et al.,* 2014**).

Urea has antimicrobial properties and is produced by a host during both fungal and bacterial infections. As previously mentioned urease is a common virulence factor in pathogenic fungi, such as *H. capsulatum* and *A. fumigatus*, and also in bacteria, capable of hydrolysing host-produced urea to ammonia and carbamate (**Cox *et al.,* 2000; Whiston *et al.,* 2012**). The *URE1* gene encodes urease, which, is secreted by *C. neoformans* via the *SEC6* protein, similar to melanin export, to, the surface of the yeast cell (**Cox *et al.,* 2000; Panepinto *et al.,* 2009**). At the cell surface, urease hydrolyses urea, protecting the pathogen from the antimicrobial agent and simultaneously neutralising phagosomal pH. Genetic knockout of cryptococcal *URE1* reduces pathogen virulence in mice (**Cox *et al.,* 2000**) and furthermore, similar to capsule, *URE1* activity has been shown to induce a Th_2 immune response *in vivo*, which is beneficial to the pathogen (**Osterholzer *et al.,* 2009**).

Phospholipase B (PLB) is a cryptococcal virulence factor transported to the cell surface, through vesicles, before being secreted via the *SEC14* secretory protein (**Chayakulkeeree *et al.,* 2011**). PLB has multiple lipid modifying enzymatic activities to aid pathogen survival including; phospholipase, lysophospholipase hydrolase and lysophospholipase transacylase. PLB activity and virulence in mice was first demonstrated in 1997 (**Chen *et al.,* 1997**) and it has since been shown to be an important factor in human macrophage infection (**Chayakulkeeree *et al.,* 2011; Evans *et al.,* 2015**). Critically for this thesis, PLB activity has been shown to have an effect on the rates of cryptococcal vomocytosis (**Chayakulkeeree *et al.,* 2011**). *C. neoformans* mutants in *PLB1* are less virulent in mice whilst those overexpressing the gene are more virulent (**Chen *et al.,* 1997**). *PLB1* mutants have been shown to replicate more slowly in macrophages then wild type counterparts and both murine and human macrophages are more effective at killing *PLB1* mutants (**Evans *et al.,* 2015**). Interestingly, *PLB1* mutants generate a significant increase in the population of titan cells produced during *in vitro* and *in vivo* murine infection (**Evans *et al.,* 2015**). Cryptococcal titan cells are too large to be phagocytosed and confer phagocytosis resistance to neighbouring regular sized cryptococci and this process appears to be under the control of PLB activity (**Okagaki *et al.,* 2010; Okagaki *et al.,* 2012; Zaragoza and Nielsen 2013; Evans *et al.,* 2015).** PLB is hypothesised to permeabilises the lysophagosomal membrane, subtly modifying the correct maturation of cryptococcal containing phagosomes (**Johnston and May 2013**). The lipid modifying activities of PLB are also thought to have an effect on plasma membrane function, potentially inducing lysis of macrophages in combination with intense cryptococcal intracellular growth.

The Host Response and Vomocytosis

The cryptococcal responses to the macrophage, among other pathogenic fungi, have been explored. The response of the macrophage towards cryptococci will now be considered with particular focus on the process and potential consequences of vomocytosis. As previously stated alveolar macrophages (AM) phagocytose *C. neoformans* yeast cells, however the immunocompromised macrophage host is incapable of destroying the fungi. Three possible outcomes can result from this host pathogen interaction: **a**). The alveolar macrophages successfully phagocytose and digest the engulfed cryptococci. Alveolar macrophages often require T-cells of the adaptive immune system and/or pro-inflammatory cytokines, such as IFNγ, to enhance their antifungal activities in order to achieve this pathogen destruction (**Beaman 1987**). **b**). The cryptococci enter a dormant state within the macrophage whereby the replication of cryptococci is inhibited but the phagocyte is incapable of destroying the pathogen (**Dromer *et al.,* 2011**). Dormant cryptococci can be re-activated when the host becomes immunocompromised at a later date i.e. the host acquires a HIV infection (**Garcia-Hermoso *et al.,* 1999**). Cryptococci can remain dormant within a host for many years, far beyond the life of an individual macrophage and must therefore use a multitude of mechanisms to persist within the host. Dormancy of a cryptococcal infection can occur extracellularly within the lung of the host via the formation of a granuloma similar to a *Mycobacterium tuberculosis* infection (**Cambier *et al.,* 2014**). **c**). Particularly in the immunocompromised, the cryptococci avoid destruction by the host; proliferate within the macrophage phagosome, induce macrophage lysis and release infectious progeny systemically (**Velagapudi *et al.,* 2009**). Upon release, the

cryptococci can be re-phagocytosed by another phagocyte or disseminate throughout the host, often accumulating within the CNS and brain resulting in meningoencephalitis and ultimately death of the patient (**Johnston and May 2013**). The cryptococci may also use vomocytosis to escape the macrophage, hypothesised to allow the cryptococci to travel under the radar of the host immune system by not inducing an aggressive immune response via macrophage lysis.

Characteristic of a *C. neoformans* infection are its immunomodulatory properties. The cryptococcal polysaccharide capsule is capable of reducing the pro-inflammatory response to cryptococcal infection, highlighting the importance of immune evasion. Furthermore cryptococci have been shown to induce an anti-inflammatory response to actively promote the induction of a more tolerable environment within the host (**Monari *et al.,* 2006; Wiesner *et al.,* 2016**).

A Th1 dominant immune response (increased secretion of TNFα and IFNγ) elicited by the host, results in classically activated M1 macrophages, more efficient at eliminating *C. neoformans* spores intracellularly (**Alspaugh and Granger 1991; Hardison *et al.,* 2010; Osterholzer *et al.,* 2011**). Alternative activation of macrophages via the Th2 immune response, associated with IL-4 secretion, results in the generation of M2 polarised macrophages (**Anthony *et al.,* 2006**). M2 macrophages are involved in tissue repair and the down-regulation of the pro-inflammatory response, have a poor fungicidal activity and allow the survival of intracellular cryptococci (**Voelz *et al.,* 2009**). Furthermore, cryptococci secrete prostaglandins to polarise macrophages towards the alternatively activated M2 macrophage phenotype, resulting in a reduced

intracellular cryptococcal killing and increased pathogen survival (**Monari *et al.,* 2006; Shen and Liyun 2015**).

Circulating apoptotic lymphocytes and neutrophils are recognised by macrophages and phagocytosed (efferocytosis), reducing cytokine, protease and toxic metabolite release systemically. This results in the control of inflammation and tissue recovery post infection/trauma (**Haslett *et al.,* 1994**). Phagocytosis of apoptotic cells inhibits a pro-inflammatory response from the live macrophages and this process is regulated through the activation of the MAP Kinase, ERK5 (**Meagher *et al.,* 1992; Fadok *et al.,* 1998; Heo *et al.,* 2014**). Infected macrophage lysis, results in the systemic release of infectious propagules, hypothesised to result in a pro-inflammatory cytokine (TNFα and IFNγ) and chemokine (CXCL12) burst, alerting the immune system that the host is under pathogenic attack. An alternative and more subtle method of phagosome escape is the enigmatic process of vomocytosis, also known as "non-lytic exocytosis". Vomocytosis is a non-lytic form of exocytosis whereby the *C. neoformans* escapes the macrophage leaving both host and pathogen with a morphologically normal phenotype (**Alvarez and Casadevall 2006; Ma *et al.,* 2006**) (Figure 4). Cryptococcal vomocytosis events have been observed in murine, avian and human macrophages and *in vivo* in zebrafish (**Ma *et al.,* 2006; Johnston *et al.,* 2016; Johnston Unpublished**). Vomocytosis has been observed for different fungal species including: *Candida albicans* (**Bain *et al.,* 2012**), *C. gattii* (**Ma *et al.,* 2009**), *Candida krusei* (**Garcia-Rodas et *al.,* 2011**) and in mucorales species (**Unpublished Voelz observation**) suggesting that vomocytosis is important in the infection process of several important human fungal pathogens. Phagosome and leukocyte escape have also been observed in bacterial species, such as *M. tuberculosis*, in which the bacterium can escape the phagosome but remain within the cytoplasm of the

host and urinary pathogenic *E.coli* (UPEC), which have recently been shown to neutralise the phagolysosome pH of bladder epithelial cells, resulting in expulsion of bacteria via exocytosis (**Harriff *et al.,* 2012; Miao *et al.,* 2015**).

Free-living single celled amoebae are capable of feeding on a wide range of microorganisms, many of which are human pathogens, including bacteria (*Legionella, Salmonella, Shigella* and *Burkholderia*) and fungi (*C. neoformans and Histoplasma capsulatum)* (**Price and Vance, 2014**). The cellular biology of macrophage and amoebal phagocytosis and phagosome maturation are similar indicating that many pathogens may have evolved resistance mechanisms towards amoebal predators, which are transferable when macrophages are encountered (**Price and Vance, 2014**). Evidence of this evolution has arisen from a study of *Legionella pneumophila*. The natural host of *L. pneumophila* are freshwater amoebae (**Fields, 1996**) however, alveolar macrophages are commonly encountered when *L. pneumophila,* suspended in water vapour, are inhaled (**Price and Vance, 2014**). The *L. pneumophila* are capable of survival within the alveolar macrophage by delivering over 300 effector proteins into the cytosol of its host (**Hubber and Roy, 2010**). The survival strategies employed in both amoebae and macrophages are the same indicating that *L. pneumophila* may be an accidental human pathogen. Evidence suggests that *C. neoformans* may have experienced similar evolutionary pressures and shares many pathogenic properties with *L. pneumophila*. *C. neoformans* is capable of surviving and replicating in phagocytic amoebae (**Steenbergen *et al.,* 2001**) common to its natural environment and within human alveolar macrophages. Interestingly, acapsular *C. neoformans* mutants are susceptible to destruction in amoebae similarly observed in mammalian cells, suggesting that the capsule acts as a common defence strategy in both systems (**Steenbergen *et al.,* 2001**).

Cryptococcal vomocytosis has been shown to occur from the amoebae *Acanthamoeba castellanii* and *Dictyostelium discoideum*, suggesting that *C. neoformans* may have evolved vomocytosis to avoid natural predators, which drives co-incidental dissemination within a human host (**Steenbergen *et al.,* 2001; Chrisman *et al.,* 2010**).

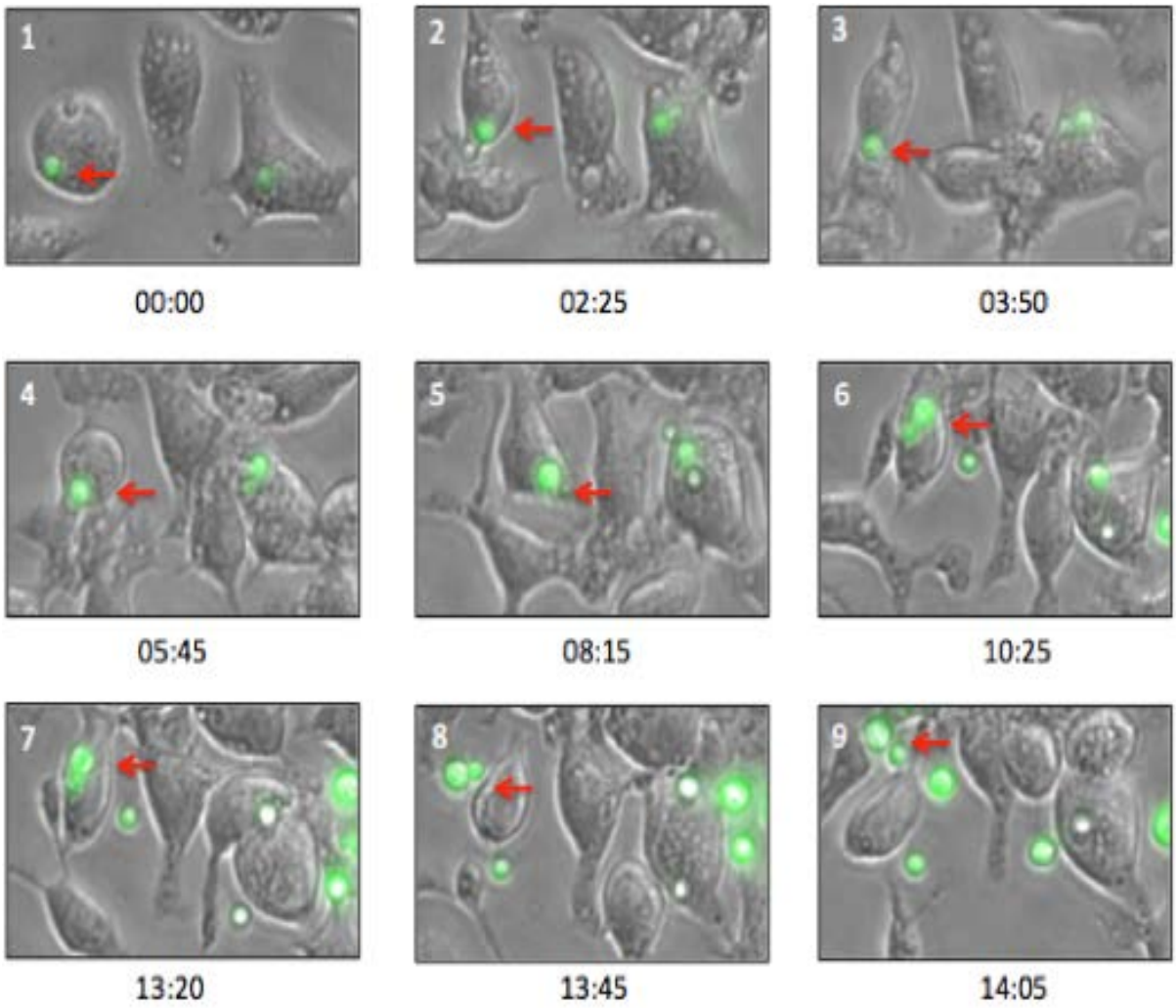

Figure 4. A Time-lapse series of images showing a cryptococcal (H99 GFP) vomocytosis event from a murine macrophage cell line (J774A.1). The time post infection is shown below each panel – Time given in hours and minutes post infection. The red arrow indicates the vomocytosing cryptococci. The vomocytosis event occurs between panels 7 and 8. See Appendix – Movie 1.

Three alternative forms of vomocytosis have been published to date: **I**). Partial emptying of the phagosome – a single or multiple cryptococci from one phagosome are vomocytosed. **II**). Complete emptying of the phagosome – often as a single rapid event involving multiple cryptococci (1 - 10+). **III**). Lateral Transfer – the transfer of cryptococci from one macrophage to the other (**Alvarez and Casadevall 2006; Ma *et al.,* 2006; Ma *et al.,* 2007; Stukes *et al.,* 2014**). Lateral transfer events have also been observed for *Aspergillus fumigatus*, driven by the action of calcineurin, indicating its importance in fungal pathology (**Shah *et al.,* 2016**). Here we report a fourth form of vomocytosis dubbed "tethered vomocytosis" – whereby a single member of a budding pair is inside the macrophage whilst the other member is outside. Throughout the course of time-lapse movies these tethered Cryptococci either become fully phagocytosed, including the second *Cryptococcus*, remain tethered or vomocytose (Figure 5). We have observed single members of an extracellular budding pair of cryptococci become phagocytosed, predominantly but not exclusively the bud. These phagocytosed pairs have been observed to undergo either complete phagocytosis, vomocytosis or remained tethered to the macrophage. This tethering effect has also been observed in zebrafish embryos (**Johnston Unpublished**)

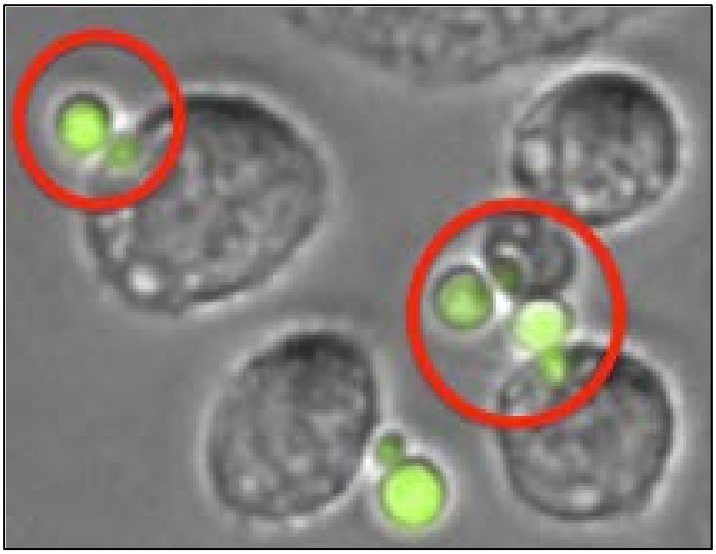

Figure 5: Tethered *Cryptococcus* (H99 GFP) pairs. One member of the pair has been phagocytosed whilst the second is outside of the macrophage (J774A.1) and tethered to its partner. Three cases are circled in red above.

The biological mechanics of a vomocytosis event are poorly understood, however many hypothesise it to require intense cellular signalling (kinase signalling?) and microtubule activity (**Alvarez and Casadevall 2006; Ma *et al.,* 2006; Johnston and May, 2010**). Vomocytosis has never been reported to occur with serum or antibody opsonised latex beads or heat killed cryptococci suggesting that viable pathogens are essential (**Alvarez and Casadevall, 2006**). Similarly vomocytosis has never been reported to occur from neutrophils, possibly due to the aggressive attack unleashed by neutrophils on phagocytosed cryptococci, hence yeast cells are killed before they can vomocytose. However, evidence in the lab suggests that vomocytosis may occur from dendritic cells but these observations remain unpublished. The lysophagosomal membrane fusion to the macrophage cellular membrane is essential to initiate a vomocytosis event (**Johnston and May, 2010**). The mechanism of cryptococcal lysophagosomal transport to the cellular membrane is not clear but *C. neoformans* may "hijack" and manipulate the

lysosome cellular exocytosis machinery to drive this process. **Johnston and May, 2010**, hypothesised that cryptococcal vomocytosis events are naturally inhibited through the formation of macrophage derived actin cages, formed around the phagolysosome. Using confocal imaging, "flashes" of polymerised macrophage derived actin were observed forming around the phagolysosome, creating cage like structures (**Johnston and May, 2010**). These actin cages were hypothesised to inhibit vomocytosis events and were generated through the activity of the WASP/WASH and ARP2/3 protein complexes (**Johnston and May, 2010**). Activation of macrophage actin polymerisation using jaspokinolide, an actin polymerisation-promoting compound, enhances the rate of actin cage formation whilst reducing the rate of cryptococcal vomocytosis, indicating that the hypothesis may be true. Additionally, treatment of infected macrophages with an actin depolymerising drug such as cytocholasin D reduces actin cage formation and enhances the rate of vomocytosis (**Johnston and May, 2010**).

Exocytosis – A Potential Cellular Mechanism of Vomocytosis

Exocytosis and endocytosis are fundamental biological processes governing the vesicular import and export of proteins and large polar molecules, including signalling molecules, hormones and toxins, in and out of a cell. Endocytosis is the biological process of cellular import whilst exocytosis involves cellular export (**Wu *et al.,* 2014**). Exocytosis involves the packaging of proteins into lipid bound vesicles, within the Golgi apparatus, transport of the vesicles through the cytosol, fusion of vesicle with the plasma membrane and release of the contents extracellularly. Exocytosis can also be used to incorporate new ion channels into the cellular membrane. Exocytosis is an

energy consuming and highly regulated process (**Stockli *et al.,* 2011; Wu *et al.,* 2014**). A multitude of cells utilise endo/exocytosis including: neurons – neurotransmitter secretion, α and β Langerhans cells of the pancreas – glucagon and insulin secretors and critically for this research, macrophages – secretion of indigestible material. As previously mentioned the cellular machinery involved in vomocytosis is little understood however, the similarities between vomocytosis and natural exocytosis are striking. Indigestible material within a macrophage are commonly secreted via the process of exocytosis, however, rarely the material is stored within the cell as a residual body known as a lipofuscin granule (**Wu *et al.,* 2014**). Particularly, antimicrobial resistant cryptococci could be treated in much the same way by the macrophage.

Exocytosis begins with the packaging of cellular proteins in the endoplasmic reticulum and Golgi apparatus, whereupon biochemical modification can occur. These vesicular membranes include the proteins: GLUT4, VAMP2 and Rab 10, 11 and 14 enabling the trafficking, docking and plasma membrane fusion of the vesicle (**Stockli *et al.,* 2011**). The vesicle uses the microtubule and actin filament network to travel from the Golgi apparatus to the plasma membrane. The myosin proteins enable vesicle travelling down the microtubules (**Stockli *et al.,* 2011**). After arrival at the plasma membrane, the vesicle is tethered through a combination of the actin filaments and a dimer of the protein TBC1D4 (**Stockli *et al.,* 2011**). The role of actin filaments and microtubule activity are clearly highlighted in the process of vesicle transport. Combined with the data produced by **Johnston and May 2010**, cytoskeletal activity could be a fundamental biological activity during a vomocytosis event.

Upon binding to the cellular membrane the vesicle can begin the docking procedure. The docking process begins when a protein complex forms between the plasma membrane and the vesicle (**Stockli *et al.,* 2011**). The vSNARE, VAMP2 protein, found in the vesicle membrane interacts with a complex of SNAP23, Mun18c, Syntaxin-4 and DOC2B on the plasma membrane. Multiple complexes form which then orchestrate the fusion of the two membranes and hence release of the vesicle contents extracellularly (**Stockli *et al.,* 2011**). As demonstrated this process is complicated and tightly regulated. Protein translation of individual proteins involved in these pathways is a critical upstream process ensuring that vesicle trafficking and exocytosis work as they should.

Phagosome Manipulation, Cytokine Secretion and Vomocytosis

Phagosome maturation and cytokine secretion are hypothesised to play critical roles on the rates of vomocytosis. Fully mature phagosomes, of macrophages classically activated by CD4+ T-cells of the adaptive immune system, fully operational within an immuno-competent host, are capable of eliciting an aggressive anti-fungal response towards *C. neoformans* (**Wager *et al.,* 2014**). The macrophage mounts a significant oxidative burst and increases the synthesis and secretion of pro-inflammatory cytokines (TNFα and IFNγ). This results in pathogen clearance from the macrophage and further classical activation of neighbouring phagocytes improving pathogen elimination from the site of infection. Upon complete pathogen clearance, classical activation signals are reduced and the Th_2 alternative activation become paramount, a response that drives tissue repair and induces fungistasis (**Wager *et al.,* 2014**). The role of the phagosome

and particularly its response to extracellular signals plays a critical role in cryptococcal pathogenesis. Critically, permeabilisation of the lysophagosome membrane allows the cryptococcal-containing vesicle to fuse with the plasma membrane, inducing vomocytosis events (**Johnston and May 2010**).

In 1999, Levitz and colleagues reported that *C. neoformans* does not inhibit the fusion of the lysosome to the developing phagosome, resulting in a fully mature phagolysosome in which the *C. neoformans* can survive (**Levitz *et al.,* 1999**). The phagosomal marker used to show this complete maturation was LAMP1 and ratiometric imaging was used to determine that the phagolysosome was pH5 (**Levitz *et al.,* 1999**); although three years later this was revised to pH4.3 (**Chen *et al.,* 2002**). Cryptococcal containing phagosomes have since been further researched with results indicating that maturation of the phagosome is incomplete (**Smith *et al.,* 2015**). The cryptococci have been implicated in subtly modifying the phagosome maturation process to produce a less hostile environment for the pathogen. The cryptococci modify the recruitment of Rab GTPases, markers of phagosome maturity, to the phagolysosome (**Smith *et al.,* 2015**). Previously, the rates of vomocytosis were measured in context of phagosome maturation (**Ma *et al.,* 2006**). Treatment of the infected macrophages with 10μM Chloroquine, an anti-malarial basic compound, which accumulates within the phagosome, increases phagosome pH and doubles the rate of vomocytosis (**Ma *et al.,* 2006**). The increase in pH mimics an immature phagosome suggesting that regardless of phagosome maturation status, vomocytosis can still be achieved (**Ma *et al.,* 2006**). Interestingly, treatment of infected macrophages with 100nM concanamycin A, a V-ATPase inhibitor, that inhibits acidification of the phagosome, results in a reduction but not an abolishment of vomocytosis (**Ma *et al.,* 2006**). These data indicate that

vomocytosis is not dependant upon phagosome maturation but can be regulated using phagosome modifying drugs. The cryptococci must sense the external environment and respond; a response to increasing acidity may be to escape via vomocytosis.

Addition of endogenous IFNγ has been shown to enhance the rate of vomocytosis in primary human macrophages (**Voelz *et al.,* 2009**). We hypothesise that this effect may be observed as the macrophages are activated and differentiate into classically activated M1 macrophages, better equipped at eliminating the pathogen within the host macrophage. The cryptococci may sense that they are in a more hostile environment and vomocytose to escape destruction. Alternatively the macrophage may sense that it is incapable of destroying the cryptococci and therefore exocytose the indigestible matter. Interestingly, IFNγ and antifungal co-treatment clinically has been shown to improve the prognosis of many, but not all patients (**Joly *et al.,* 1994; Lutz *et al.,* 2000**). We hypothesise that the addition of IFNγ results in an increase in the rate of vomocytosis *in vivo*, exposing the cryptococci to the antifungal compounds present within the patient. This in turn enhances pathogen clearance from the host, reducing fungal burden and improving patient prognosis. Furthermore the addition of TNFα induces an increase in the rates of vomocytosis in human macrophages similar to IFNγ adding further evidence to the hypothesis (**Voelz *et al.,* 2009**). Interestingly, addition of the Th_2 cytokine IL-4 induces a reduced rate of vomocytosis when compared to untreated human primary macrophages (**Voelz *et al.,* 2009**). The effects on cytokine signalling, phagosome maturation and cryptococcal biological activity requires further research, however this is an exciting challenge for this host pathogen interaction.

The macrophages of an immunocompromised host acts as an excellent niche environment for the cryptococci, allowing fungal proliferation whilst offering protection from antifungal compounds (Amphotericin B, Fluconazole and Flucytosine) and other innate immune cells, such as neutrophils much better adapted at killing *Cryptococcus* yeast cells (**Mambula *et al.,* 2000**). Regulating the rate of vomocytosis could be used to expose macrophage-protected cryptococci to more efficient antifungal agents or cells, hence improving patient prognosis.

Cryptococcal Persistence and Dissemination

Key to a cryptococcal infection is the inherent ability of cryptococci to persist within a host for many years (**Garcia-Hermonso *et al.,* 1999**). *C. neoformans* yeast cells have a particular affinity for the CNS and brain, whilst *C. gattii* are associated with lung infections and granuloma formation. A fascinating study in 1999 by **Garcia-Hermonso *et al.*** identified a group of African migrants in France with genetically similar *C. neoformans* infections. The cryptococcal strains identified were endemic in Africa but rare in France. Furthermore the African migrants were known to have developed immuno-compromisation many years after settling in France. The authors therefore hypothesised that the cryptococcal infection was obtained during the patient's life in Africa and the disease only became symptomatic years later in France upon acquiring immuno-compromisation (**Garcia-Hermonso *et al.,* 1999**). The persistence of cryptococci within the human host is a major problem faced by those trying to monitor the epidemiology of the cryptococcal population.

How the persistence of the cryptococci is achieved is a major topic of research. Not only are cryptococci phagocytosed by macrophages capable of entering a dormant state – an effect commonly observed in the lab and extensively reported in the literature (**Spitzer *et al.,* 1993; Kobayashi *et al.,* 2004; Ma *et al.,* 2006**), but are capable of residing within lung granuloma (**Watabe *et al.,* 1984; Fairhurst and Pegues 2002**). The granulomas commonly show up in X-Rays of patients and have been mis-interpreted as TB granulomas by medical professionals, resulting in patients being prescribed medication inadequate for fungal infection, commonly resulting in fatal consequences (**Jarvis *et al.,* 2010**). Awareness of *C. neoformans* has increased in recent decades so mis-diagnoses are becoming rare. Similar to TB granulomas, cryptococcal granulomas are associated with multinuclear cells and large macrophage morphologies, creating an immuno-protective niche whereby the cryptococci can survive (**Fairhurst and Pegues 2002; Dewar and Kelly 2008**). Upon the detection of immuno-suppression the cryptococci can re-activate and trigger symptomatic infection. Curiously, *C. gattii* infections present an increase in the granuloma formation as opposed to *C. neoformans* – why this is the case is little known but fascinating. The methods adopted by the cryptococci within the granuloma to escape are little known but vomocytosis, lateral transfer or cellular transition (transcytosis) across the macrophages composing of the granuloma are all viable explanations.

Cryptococcal meningoencephalitis is the most common cause of fatality in patients with cryptococcosis (**Johnston and May, 2013**). Inflammation of the CNS and brain results from dissemination of the cryptococci around the host; starting with exit from the lungs, travel within blood circulation and deposition to internal organs. A curious aspect of cryptococcal pathogenesis is the ability to cross the blood brain barrier (BBB). The

blood brain barrier is designed to prevent the cerebrospinal fluid and blood combining and most importantly prevent pathogen invasion and neurotoxins entering the CNS. This prevents damage to the brain, which is critical as its regeneration capabilities are poor. The barrier consists of brain endothelial cells connected with tight junctions and allows passive diffusion of small molecules and water whilst utilising active protein transport mechanisms to move essential molecules, such as glucose, into the CNS (**Ballabh *et al.,* 2004; Sabiiti and May 2012**).

The cryptococci within the lungs are required to cross the lung endothelia and epithelia, within the alveoli and enter the blood. This process is not fully understood, however cryptococcal capsule components (glucuronoxylomannan -GXM) have been shown to bind to these layers and induce layer traversal (**Ganendren et al., 2006**). Interestingly the enzyme phospholipase B has been shown to play an important role in lung epithelia invasion (**Santangelo *et al.,* 1999**). Lung surfactant contains a significant concentration of dipalmitoyl phosphatidylcholine (DPPC) and other membrane lipids. Phospholipase B, secreted by extracellular cryptococci, is able to metabolise DPPC, resulting in lung surfactant changes, inducing lung damage and successful traversal across the lung epithelia (**Santangelo *et al.,* 1999**). Upon entry into blood circulation the full arsenal of the immune system meets the cryptococci: including neutrophils, macrophages and dendritic cells etc. These other leukocyte cells will destroy many cryptococci. Neutrophils are particularly efficient at destroying cryptococci however, as previously mentioned ineffectively primed macrophages, such as those in an immuno-compromised patient are inefficient at this process. The cryptococcal yeast cells are able to travel within the blood either within a macrophage ("Trojan Horse") (**Casadevall 2010**) or freely within circulation.

The cryptococcal containing macrophages and the free cryptococci within the bloodstream will find their way to the blood capillaries surrounding the BBB and are capable of crossing this barrier. The traversal of these barrier layers is hypothesised to use three alternative approaches.

a). Transcytosis – the cryptococci freely available within the blood are thought to bind the brain endothelial cells and modulate the host actin cytoskeleton to induce uptake and hence traversal across the BBB. Urease, phospholipases and the incorporation of hyaluronic acid into the cryptococcal capsule have been shown to contribute to this stage of pathogenicity (**Jong *et al.,* 2008**). Hyaluronic acid is the ligand to CD44 and RHAMM (hyaluronan-mediated motility receptor) highly expressed in brain endothelial cells and therefore improves cryptococcal binding to the host cells and potentially increases transcytosis (**Jong *et al.,* 2008; Jong *et al.,* 2012**). Simvastatin can be used to block CD44 and RHAMM *in vivo*, reducing the presence of *C. neoformans* in the murine CNS, suggesting that these two receptors are important for BBB traversal (**Jong *et al.,* 2012**). Transcytosis may also be achieved by cryptococci resident within macrophages. The natural process of lateral transfer between macrophages and the brain endothelial cells has been shown to occur and this process may drive invasion of the BBB (**Ma et al., 2007; Sabiiti and May 2012**).

b). "Trojan Horse" – The cryptococcal containing macrophages, present in the blood capillaries surrounding the BBB, traverse the BBB, hence introducing the cryptococci to the CNS (**Casadevall 2010**). Vomocytosis may then play a critical role in the deposition of the cryptococci within the CNS, driving encephalitis.

c). Paracellular traversal – requires physical damage to the cellular tight junctions in order to be achieved (**Chang *et al.,* 2004**). Damage to the tight junction would allow the passive movement of the cryptococci from circulation to the cerebrospinal fluid between endothelial cells. How this damage might be achieved is little known, however host inflammation may enhance the damaging process.

The cryptococci are then capable of growing within the cerebrospinal fluid inducing the life threatening encephalitis.

THESIS OUTLINE

C. neoformans and *C. gattii* are critically important human fungal pathogens known to interact with macrophages, dendritic cells and neutrophils of the innate immune system. The interaction with macrophages is an important aspect of cryptococcal pathology as macrophages are thought to be able to act as a dissemination vehicle and, counter intuitively, as a reproductive and protective niche environment. Resistance to phagocytosis and resistance to destruction from the phagolysosome are vital processes allowing *Cryptococcus* to be a viable pathogen. This thesis will explore the cryptococcal non-lytic exocytosis mechanism, termed vomocytosis. Vomocytosis is hypothesised to play a critical role in cryptococcal dissemination, immune evasion and promoting antifungal resistance. Understanding the molecular mechanisms of vomocytosis offers the potential of developing therapeutic approaches enabling the manipulation of vomocytosis to improve current antifungal treatments i.e. reducing pathogen dissemination around the host, enhancing immune recognition as cryptococci are less shielded by host macrophages and the release of cryptococci to the mercy of other antifungal agents/cells present in the blood.

The first results chapter discusses the results of a small molecule, leukocyte specific, kinase inhibitor screen. Macrophage ERK5 is shown to play a regulatory role in vomocytosis. Inhibition of ERK5, via small molecule ERK5 inhibitors (XMD17-109 or AX15836) or genetic knockdown of macrophage ERK5, results in an increase in the rates of vomocytosis, measured via time-lapse fluorescence microscopy. This effect could be achieved in both murine cell lines and primary human macrophages and with alternate strains of *C. neoformans* and *C. gattii*. The chapter further explores

intracellular proliferation rate (IPR), Colony Forming Units (CFU), cytokine profiling and phagosome maturation of cells treated with ERK5 inhibitors. A reproducible method of regulating vomocytosis was identified for use in the second results chapter. The data generated from this chapter enabled further hypotheses to be made concerning the molecular mechanisms of vomocytosis and consequences on pathogen dissemination.

The second results chapter uses the data gained from the first chapter to begin to explore the molecular mechanism of vomocytosis. Using stable isotope labelling of amino acids in cell culture (SILAC) and mass spectrometry, light is shed on the molecular mechanism of vomocytosis. The aim of this chapter was to begin to understand the molecular mechanics of vomocytosis and how it may affect *in vivo* dissemination and hence disease progression.

The final results chapter explores other biologically relevant ways to manipulate vomocytosis. These methods included investigating *Cryptococcus* mutants in order to associate pathogen genes with altered rates of vomocytosis. In addition, I discuss an investigation of co-infection of macrophages with *C. neoformans* and *M. marinum*, a close relative of *M. tuberculosis* –isolated in AIDS patients together. The aim of this chapter was to explore alternative methods of vomocytosis manipulation to gain a further understanding of the process.

CHAPTER 2: MATERIALS AND METHODS

All reagents and media were purchased from SIGMA™ unless specified otherwise.

Cryptococcus Strains

Strains used were: *C. neoformans var. grubii* serotype A WT strain H99, H99GFP (**Voelz *et al.,* 2010**), ATCC 90112 (**Ma 2009; Johnston and May 2010**), *C. gattii* serotype B R265, R265GFP (**Voelz *et al.,* 2010**) and Madhani Library *C. neoformans var. grubii* serotype A WT strain H99 and the mutant strains from this library (**Liu *et al.,* 2008**).

Candida Strains

Strains used were: *C. glabrata, C. glabrata GFP* (**Seider *et al.,* 2011**), *C. albicans* WT 529L (**Moyes *et al.,* 2010**) and *C. albicans* RH20 cyr1 + pSM2 (filamentation mutant) (**Hall *et al.,* 2011**).

Bacterial Strains

Strains used were: *E. coli* (mycobacterial shuttle plasmid (pMSP12-dsRed-Apr), containing dsRed and Apr^R) (**Chen *et al.,* 2010**) and *M. marinum* (pSMT-3 - mCherry) (**van Leeuwen *et al.,* 2014**). All bacterial strains used for this research were cultured and counted by the Bhatt group.

Culturing *C. neoformans*

Yeast Peptone Dextrose (YPD) broth (2% glucose, 1% peptone and 1% yeast extract) was used to culture *C. neoformans* strains. 3ml of YPD broth was inoculated with the cryptococcal strain of interest and incubated for 24 hours at 25^0C on an orbital rotator (20 rpm) – referred to as an overnight culture.

Yeast Peptone Dextrose (YPD) + 2% Agar was the solid culture media. Glycerol stocks, stored at -80^0C, of the strains were streaked onto YPD + Agar plates and incubated for 48 hours at 25^0C. These plates were stored at 4^0C and used for two weeks before fresh cultures were inoculated.

Culturing *Candida Species*

Yeast Peptone Dextrose (YPD) Broth (2% glucose, 1% peptone and 1% yeast extract) was used to culture *C. albicans* strains. For solid cultures 2% Agar was added to the media. Overnight cultures were made by inoculating 3ml of media and incubating at 37^0C, 200rpm overnight. *C. albicans* were then sub-cultured in fresh media and grown to log phase at 37^0C at 200rpm for ~4 hours.

C. neoformans Growth Curves

An overnight cryptococcal culture was diluted 1/10. 495µl of YPD was added to individual wells of a 48 well plate and inoculated with 5µl of the 1/10 dilution together with the recommended doses of kinase inhibitors and/or antibiotics. The 48 well plate was sealed with a breathable membrane and taken to a fully automated plate reader (BMG Omega Fluostar). Average Optical Density (OD 600) readings were taken per well every 30 minutes for 24 hours and graphs generated across the time course. The incubation chamber was set to 37^0C without CO_2. Constant shaking was used during the non-reading part of the cycle.

Tissue Culture

Dulbecco's Modified Eagle Media

J774A.1 and RAW264.7 murine macrophages were cultured in Complete Dulbecco's Modified Eagle Media (cDMEM). To DMEM, 2mM L-glutamine, 100 units/ml and 0.1mg/ml of streptomycin and penicillin respectively and 10% Foetal Bovine Serum (FBS) were added. The media was stored at 4^0C and warmed to 37^0C prior to use. Serum free media (sfDMEM) was made without the addition of the 10% FBS component.

Thawing Cell Lines

Cryovials of J774A.1 and RAW264.7 macrophages were defrosted quickly in a 37^0C water bath, added to 10ml of warmed cDMEM and centrifuged at 1000g at RT for 5-7 minutes, quickly removing the toxic DMSO present in the freezing media. The

supernatant was discarded and the pellet re-suspended in 15ml of warmed cDMEM and transferred to a T75 tissue culture flask for incubation at 37^0C, 5% CO_2 in a humidified incubator for 24 hours.

Passaging Cell Lines

Cultured macrophages were observed under a light microscope to check for confluency, contamination and macrophage health. Cells were passaged if confluent growth was observed. 10ml of warmed cDMEM was added to the culture flask and the cells re-suspended using a cell scraper. An appropriate dilution was made from the re-suspension and added to a fresh T75. These dilutions were returned to the humidified incubator at 37^0C in 5% CO_2.

Freezing Cell Lines

Freezing media contains; 50% FBS, 40% cDMEM and 10% DMSO. Flasks of confluent macrophages at passage two were frozen. The old media was removed and 8 flasks of cells were re-suspended in 10ml of warmed cDMEM using the cell scraper. The re-suspensions were centrifuged at 1000g for 5 -7 minutes. The pellets were re-suspended in the same 10ml of freezing media and aliquoted into 1ml cryovials. These were frozen at -80^0C for 24 hours, in a NALGENE™ Cryo 1^0C Freeze Container, before being transferred to liquid nitrogen.

Human Primary Macrophage Isolation and Culture

Donor blood was diluted 2x in cold (~4^0C) PBS and this dilution was carefully layered on top of 20ml Ficoll-Paque. The 50ml falcon tubes were centrifuged at 400g, 20^0C for

30 minutes, no Brake in a swing bucket rotor. A white disc of Peripheral Blood Mononuclear Cells (PBMCs) was produced which was pipetted into fresh falcon tubes. 50ml of cold PBS was added to the PBMCs and re-suspended. The suspension was centrifuged at 300g for 10 minutes. The pellet was re-suspended in a fresh 50ml of cold PBS and centrifuged at 200g for ten minutes. This step was repeated. The pellet was re-suspended in an appropriate volume of PBS and cell number calculated. If the preparation was clear of red blood cells (RBC) the suspension was centrifuged at 200g for 10 minutes and the pellet re-suspended in RPMI1640, 50ng/ml of GM-CSF and 10% FBS.

For samples contaminated with RBCs, purification was required. Samples were centrifuged for 10 minutes at 300g. Pellets were re-suspended in cold PBS + 2mM EDTA + 0.5% BSA (80µl per 10^7cells) and 20µl of $CD14^+$ MACS micro beads (per 10^7 beads) added. The solution was mixed and incubated at 4^0C for 15 minutes. Cells were washed by adding 2ml PBS + 2mM EDTA + 0.5% BSA buffer and centrifuged for 10 minutes at 300g. Cells were re-suspended in PBS + 2mM EDTA + 0.5% BSA buffers. A MACS column was placed in a magnetic field and rinsed in 3ml of PBS + 2mM EDTA + 0.5% BSA buffer. The cell suspension was applied to the column. The column was washed 3 times. The column was removed from the magnetic separator and placed over a collection tube. 5ml of PBS + 2mM EDTA + 0.5% BSA buffer was used to elute the samples. The elution was centrifuged at 300g for 10 minutes. The pellet was then re-suspended in RPMI1640, 10% FBS and 50ng/ml of GM-CSF. Cells were seeded into plates as required.

Murine Bone Marrow Derived Macrophage (BMDM) Isolation and Culture

All mouse work was conducted either at the [redacted] *Full ethical permission was obtained* [redacted] *prior to the work being undertaken.*

5.0 x 10^5 L929 cells were cultured in 50ml of cDMEM and incubated in a humidified incubator at 37^0C with 5% CO_2 for 7 days. The media was collected and filtered through a 0.45µm filter and stored at -20^0C. This was the L929 conditioned media.

Mice were sacrificed and the abdomen and hind legs sterilised with 70% ethanol. The femur was exposed and the bone flushed, using a 5ml syringe and 25-gauge needle, in lymphocyte media (RPMI-1640 GlutaMAX I, 10% FBS, 1% penicillin-streptomycin). The bone marrow cells were re-suspended and passed through a cell strainer. The strainer was washed with another 5ml of lymphocyte media. The cells were counted and adjusted to 2 x 10^6 cells/ml in BMM media (Lymphocyte media + 10% L929 conditioned media) and plated into 24 well plates. The cells were differentiated in a humidified incubator at 37^0C, 5% CO_2 for 7 days. Cells were washed twice in PBS every 2-3 days and fresh BMM media added until cells were fully differentiated.

Phagocytosis Assay

2.5 x 10^4 of murine macrophages were re-suspended in 200µl of cDMEM and seeded into individual wells of a 96 well plate and incubated at 37^0C, 5% CO_2 in a humidified incubator for 24 hours. An overnight culture of *C. neoformans* or *C. albicans* was made.

After 24 hours, macrophages were activated. For J774A.1 murine macrophages, 200µl of sfDMEM with 150ng/ml of phorbol myristate acetate (PMA) was added to the seeded macrophages inducing activation. For RAW264.7 murine macrophages, 1000IU (International Units) of IFNγ and 1µg/ml of LPS was added inducing the expression of the Fc receptor. Human primary macrophages and bone marrow derived murine macrophages were activated with 1000IU IFNγ and 1µg/ml of LPS. The macrophages were incubated for 1 hour at 37^0C, 5% CO_2 in a humidified incubator. 2.5 x 10^5 cryptococcal cells (MOI 10:1) were human serum opsonised, in 10% pooled human serum (4 human serum voluntary donors - Serum is frozen prior to use at -80^0C), for 1 hour at room temperature (RT) on an orbital rotator (20 rpm). *C. albicans*, *C. glabrata* and the bacterial species required no opsonisation

The activating media was replaced with sfDMEM or sfRPMI and 2.5 x 10^5 of serum opsonised cryptococcal cells, initiating infection. *Candida* species were added at an MOI of 2:1 and bacterial species were added at an MOI of 100:1. The recommended inhibitory concentrations of the respective kinase inhibitors, cytokines, dyes and/or antibiotics were added to the wells. After 2 hours the infection media was removed and washed 3-6 times in PBS. Fresh sfDMEM and the recommended inhibitory concentrations of the inhibitors, cytokines, dyes and/or antibiotics were added to the wells. This time point was noted as T_0. The samples were imaged using a Nikon Ti-E epifluorescence microscope.

Intracellular Proliferation Rate (IPR) and Colony Forming Units (CFU) Assays

1.0 x 10^5 murine macrophages were seeded into individual wells of a 24 well plate and left to incubate at 37^0C, 5% CO_2 in a humidified incubator for 24 hours. Two wells were required per treatment, one for time-point T_0 (0 hours) and one for T_{24} (24 hours). An overnight culture of the cryptococcal strain of interest was made.

A standard phagocytosis assay protocol was performed on these macrophages. At T_0 one set of wells were washed in PBS before being lysed in dd$H_2$0. The number of cryptococci in the lysate were counted using a haemocytometer and recorded. The T_{24} wells were PBS washed, provided with fresh sfDMEM and the appropriate treatments. These were incubated at 37^0C, 5% CO_2 in a humidified incubator for 24 hours. At T_{24} the second set of wells were washed in PBS before being lysed in ddH_2O. The numbers of cryptococci in the lysate were counted as before and a ratio between T_{24} and T_0 was calculated and recorded as the IPR.

Appropriate dilutions of the T_0 and T_{24} cell lysates were made and were plated onto YPD agar plates to assess the effects of individual drugs on pathogen viability. Colony forming units (CFU) were counted to assess drug efficiency on pathogen viability.

Fixed Sample Imaging

1.0 x 10^5 murine phagocytes were seeded onto coverslips in 24 well plates and incubated in a humidified incubator at 37^0C, 5% CO_2 for 24 hours. *C. neoformans* overnight cultures were made. A phagocytosis assay was performed on these cells.

After infection cells were washed in PBS to remove extracellular cryptococci. 250µl of 4% paraformaldehyde (PFA) was added to the washed cells for 10 minutes. Microscope coverslips were washed three times in PBS before being treated with 50mM NH_4Cl for 10 minutes before being washed three times in PBS and treated with 0.1% Triton X-100 in PBS for 5 minutes. Coverslips were washed three times in PBS before being treated in 0.5% (w/v) BSA for 40 minutes. Coverslips were washed three times in PBS before being treated with an appropriate dilution of the primary antibody (NFAT2) for 30 minutes. Coverslips were washed three times in PBS before being treated with the secondary antibody and DAPI for 60 minutes. Coverslips were washed three times in PBS and twice in water before being mounted, with Mowiol, onto a glass slide and imaged using a TE2000-U Nikon Epifluorescence Microscope.

Time-lapse Microscopy

Time-lapse movies were made using a Ti-E Nikon Epifluorescence Microscope. Samples were incubated at 37^0C, 5% CO_2 in the microscope imaging chamber. Images were taken every 5 minutes for 18 hours and compiled into single movie files for analysis.

Individual phagocytosed cryptococci were manually and blindly inspected over the 18-hour time course. Information concerning: the number of cryptococcal buds produced,

macrophage integrity, cryptococcal vomocytosis, percent of macrophages with successfully phagocytosed cryptococci and pathogen integrity were recorded in Microsoft Excel spreadsheets. These movies and analysis files were saved onto a secure server at the University of Birmingham, UK.

Western Blot

SDS PAGE Buffers

1x Sample Buffer = 50mM Tris-HCl pH6.8, 2% SDS, 10% glycerol, 1% β-mercaptoethanol, 12.5mM EDTA, Water and 0.02% bromophenol blue. 2x Separating Buffer (200ml) = 18.2g Tris-HCl pH 8.8 and 0.4 g SDS. 2x Stacking Buffer (200ml) = 6.1g Tris-HCl pH 6.8 and 0.4g SDS.

5x Running Buffer (500ml) = 7.5g Tris-Base, 36.0g glycine and 2.5g SDS. 1x Transfer Buffer (1000ml) = 5.8g Tris-Base, 2.9g glycine, 0.37g SDS, 200ml methanol, 800ml water. 1x Wash Buffer = 250mM Tris-Base, pH 7.4, 1.37M NaCl, 27mMKCl and 0.1% Tween 20.

SDS PAGE

SDS – PAGE plates were washed in 70% ethanol and assembled on Bio-Rad apparatus as described by the manufacturer. ERK5 is an 110Kda protein requiring an 8% separating gel for effective protein separation. 5ml of 2x Separating Buffer, 2.67ml of 30% Acrylamide (35.7:1), 1.6ml of Water (ELGA), 50µl of 10% AMPs and 10µl of

TEMED were mixed to produce the 8% gel and loaded into the apparatus. A water layer was added to the gel and left for 20 minutes at room temperature to set. 5ml of 2x Stacking Buffer, 1.7ml of 30% Acrylamide (37.5:1), 3.3ml Water (ELGA), 100µl of AMPS and 20µl TEMED were mixed to make the 5% stacking gel. The water layer was removed from the set separating gel and the stacking gel solution added before a comb was inserted. The stacking gel was left to set for 15 minutes at room temperature (RT).

Samples were lysed in 1x Sample Buffer and boiled for 5 minutes. A Bradford Assay was performed, according to the manufacturer instructions, to quantify the protein concentration. 20µg of protein was loaded onto the gel. Samples were run down the gel in 1x Running Buffer.

Wet Blotting and ECL Detection

After SDS-PAGE the proteins were transferred to a PVDF membrane. The PVDF was pre wetted in 100% methanol for 5 minutes. A transfer apparatus was set up. Samples were transferred to the PVDF membrane at 200mAmps for 2-3 hours.

The PVDF membrane was blocked with 5% milk powder in 1x Wash Buffer for 1 hour at RT. The ERK5 primary antibody was diluted appropriately (according to manufacturers recommendation) in 5-10ml of 5% milk powder and 1x Wash Buffer. This dilution was added to the PVDF membrane and incubated at 4^0C, overnight on an orbital rotator. The membrane was washed twice for one minute followed by three 5-minute washes in 1x Wash Buffer. The secondary antibody (GE Healthcare Ltd) was diluted appropriately in 1x Wash Buffer and incubated on an orbital rotator at RT. The

membrane was washed twice for one minute followed by three 5-minute washes in 1x Wash Buffer. 1ml of each of the Bio Rad ECL reagents (Clarity ™ Western ECL Substrate – Peroxide solution and Luminol/Enhancer solution) were added to the membrane and incubated at RT for 1 minute. Excess reagent was removed from the membrane and imaged in a Bio Rad gel imager.

ERK5 siRNA Gene/Protein silencing

5nmol of Accell™ Mouse MAPK7 (ERK5) – SMART pool siRNA was purchased from Dharmacon™ GE Healthcare.

The siRNA was re-suspended in 50µl of 1x siRNA buffer to produce a 100µM stock solution. The tube containing the siRNA was briefly centrifuged ensuring the siRNA was collected at the bottom of the tube. 5x siRNA buffer (Dharmacon™) was diluted in RNase free water (GIBCO) to produce a 1X siRNA buffer. The suspension was pipette mixed 2-3 times ensuring no air bubbles were added. The solution was placed on an orbital shaker for 30 minutes at room temperature. The tube was briefly centrifuged to collect the suspension to the bottom of the tube and then aliquoted into smaller volumes. Samples were stored in a -20^{0}C freezer as suggested by the manufacturer.

5.0 x 10^3 J774A.1 murine macrophages were seeded into a 96 well plate and incubated at 37^{0}C, 5% CO_2 in a humidified incubator for 24 hours. 1µl of 100µM siRNA solution was added to 100µl of Accell™ Delivery Media (Dharmacon™) producing a final concentration of siRNA at 1µM per well of a 96 well plate. The cDMEM was removed from the seeded macrophages and replaced with 100µl of siRNA containing Accell

Delivery Media. Macrophages were incubated at 37^0C, 5% CO_2 in a humidified incubator for 96 hours. Macrophage health was monitored over the 96 hours. Western Blot was used to assess protein knockdown. After siRNA treatment phagocytosis assays and time-lapse imaging were used for further studies.

ELISA

DuoSet ® ELISA Development kits for murine IFNγ, TNFα, IL-4, IL-10 and IL-1β and human IFNγ and IL-10, were purchased from R&Dsystems and used as the manufacturer instructed.

Multianalyte ELISA kits were purchased from Qiagen® capable of screening a single supernatant for 12 cytokines, including: IL-2, IL-4, IL-5, IL-6, IL-10, IL-12, IL-13, IL-17A, IFNγ, TNFα, G-CSF and TGFβ1. The multianalyte ELISA's were used as per the manufacturers instructions.

A standard phagocytosis protocol was performed on J774A.1 murine macrophages or human primary macrophages infected with cryptococci. These cells were incubated at 37^0C, 5% CO_2 in a humidified incubator for 18 - 24 hours. After 18 - 24 hours the tissue culture plates were centrifuged at 1000g for 5 minutes. The media supernatant was then used in the ELISA protocol.

SILAC – Stable Isotope Labelling of Amino Acids in Cell Culture

SILAC DMEM

500ml of DMEM lacking the amino acids Lysine and Arginine (Thermo™ Scientific) were supplemented with the appropriate volumes of Heavy, Medium and Light arginine and lysine isotopes as follows: Light Media – 146mg/l lysine + 84mg/l arginine, Medium Media – 178mg/l K4 lysine + 86.2mg/l R6 arginine, Heavy Media – 181.2mg/l K8 lysine + 87.8mg/l R10 arginine. The isotope-supplemented media was filtered through a 0.2µm vacuum filter. 2mM L-glutamine, 100 units/ml and 0.1mg/ml of streptomycin and penicillin respectively were added. 10% dialyzed foetal bovine serum was added. The medium was stored at 4^0C and warmed to 37^0C prior to use.

Adapting Cells in SILAC Media

J774A.1 murine macrophages growing in standard cDMEM were checked for confluency and macrophage health. Cells were split into three individual tissue culture flasks each containing the light, medium and heavy cDMEM. Cells were cultured in their individual SILAC media for 20 - 25 days, allowing multiple cell doubling times and were split into fresh media every two to three days. The number of flasks was increased, during the adaptation step, to expand the number of cells available for analysis.

Differential Treatment of SILAC Cell Populations

Confluent flasks of J774A.1 murine macrophages treated with various SILAC media were infected with *C. neoformans* H99 GFP at an MOI of 10:1. The macrophages were PMA activated and the H99 *C. neoformans* were 10% serum opsonised as described in the phagocytosis assay. For the first biological repeat, the SILAC heavy cells were treated with the ERK5 inhibitor and *C. neoformans* H99; whilst the light treated cells were treated with *C. neoformans* H99 only. The cells treated with medium SILAC media were PMA activated only. After a 24-hour infection the cells were lysed. These treatments were altered for the second biological repeat.

Ensuring Incorporation of the SILAC Amino Acids

Single flasks of J774A.1 murine macrophages, infected with H99 *C. neoformans* and cultured in the SILAC media were lysed in 1ml of the following lysis buffer: 10ml ddH_2O, 1 tablet Roche PhosSTOP and 1 tablet Roche Mini-complete protease (contains EDTA – final concentration 1mM in 10ml). The lysates were centrifuged at 13000 rpm for 10 minutes at 20^0C to pellet the cryptococcal component and the macrophage cell debris of the lysate. Supernatants were extracted and 100µl plated onto YPD + 2% Agar to ensure the removal of the cryptococcal cells. A second component of the lysis buffer, 2x stock – 5ml 1M Tris/HCl, pH7.4, 10ml TX-100 (10%), 3ml 5M NaCl, 32ml ddH_2O, was added to the supernatants in a 1:1 ratio. Supernatants were frozen at -80^0C.

A Bradford protein quantification assay, was performed on the cell lysates and 40µg of protein was loaded and run on a Pre-cast 12% gel (Bio-Rad). The gels were Coomassie

stained and systematically de-stained producing a characteristic-banding pattern. A small gel plug was excised from each band of the gel and taken to the University of Birmingham Genomics department for sample preparation and Mass Spectrometry. Mass spectrometry was performed on the samples and the data provided as an Excel file for analysis. The data files were analysed for the percentage of isotope incorporation.

Trypsin Digest of Lysates for SILAC

Cell lysates were removed from the -80^{0}C storage and thawed on ice. The Bradford protein quantification assays was performed on each of the protein lysates (one for each heavy, medium and light treatments) and the concentrations of the protein present per sample recorded. 5mg of protein per sample was required for the trypsin digest protocol. After protein quantification the required volumes of each treatment lysate were combined to produce a combined protein lysate with 15mg of protein. 0.5M of ammonium bicarbonate was added to give a final concentration of 50mM. The protein lysates were then treated with 8mM DTT and incubated at 56^{0}C for 45 minutes. After DTT treatment the samples were alkylated with 20mM iodacetamide in 50mM. The samples were kept in the dark for 45 minutes. After 45 minutes the samples were trypsin digested with 1µg/µl of Promega Gold Mass spec Grade Trypsin at 37^{0}C overnight.

SEP PAK – Desalting Trypsin Digested Lysates

SEP PAK columns (Plus Light x3, 130mg/0.3ml, 6.5mg) were washed with 4ml of 100% acetonitrile (ACN). The column was then conditioned with 1.5ml of 50% acetonitrile and 0.5% acetic acid (HaCO). After conditioning the columns were equilibrated with 4ml of 0.1% TFA after which 17ml of the trypsin-digested samples were loaded onto the column. These were passed through the column allowing the 5mg of protein to bind to the column – the flow through was collected. The column was washed with 4ml of 0.1%TFA to desalt the column. The column was washed with 1ml of 0.5% HaCO to remove the TFA. The peptides were eluted from the column using 2ml of 50% acetonitrile and 0.5% HaCO. The process was repeated for the rest of the protein lysate (50ml). The elution was aliquoted into six 1ml ependorf tubes and dried in a speed vac.

High Pressure Liquid Chromatography (HPLC) – Peptide Isolation:

HPLC Buffer Components

500ml of Buffer A contains – 400ml of dH_2O, 680.4mg (10mM) KH_2PO_4 made to pH3 and 100ml of 100% acetonitrile. 500ml of Buffer B contains – 400ml of dH_2O, 680.4mg (10mM) KH_2PO_4 made to pH3, 100ml of 100% acetonitrile and 18.638g (500mM) KCl. Both Buffers were filtered through a 0.2µm filter.

HPLC

The HPLC machine was set up with a constant flow through, overnight, of Buffer A to stabilise the pressure flowing down the Poly-Lysine A, 1ml column. Three of the dried samples were re-suspended in the same 1ml of Buffer A, making two concentrated peptide re-suspensions (one for each biological repeat). A single 1ml re-suspension was injected into the HPLC and the samples run through the HPLC machine. The peptides bound to the Poly-Lysine A column during the early stages of the run as the samples were passed through in Buffer A. During the course of the run Buffer B was introduced to the machine, increasing the conductivity of the buffer mix in the column inducing elution of the peptides. These peptides were detected via a UV detector at 214nm and a HPLC trace constructed by the Unicorn software. The samples were collected into individual collection tubes and dried down in a speed vac at 60^0C.

Macrotrap Desalting Protocol

The Macrotrap column (MiChrom) was cleaned and set up. The dried pellets from the HPLC flow through were re-suspended in 1ml of 2% acetonitrile (ACN) + 0.1%TFA. Column re-suspensions were combined according to the peptide concentrations noted in the HPLC trace i.e. multiple collections of small peptide concentrations were combined whereas high concentrations of peptides were re-suspended individually. This produced twenty individual re-suspensions. The Macrotrap column was cleaned with 0.5ml of 90% ACN + 0.1% TFA and then equilibrated with 0.5ml of 2% ACN + 0.1% TFA. A 1ml sample was loaded and passed through the column - the flow through was collected. The salts were removed by passing 0.5ml of 2% ACN + 0.1% TFA through the

column. Peptides were eluted and collected by passing 0.3ml of 90% ACN + 0.1% TFA through the column. The eluted peptides were dried in a speed vac at 45^0C.

Phosphopeptide Enrichment using Titanium Dioxide

The Titansphere Phos-TiO kit was purchased from HiChrom (Cat code: 5010-21310). The buffers required for the kit were made as follows: Buffer A - 2ml 2%TFA and 8ml 100% ACN, Buffer B – 0.5ml Lactic Acid (provided with the kit), and 1.5ml Buffer A, 5% Ammonia Solution and 5% pyrrolidine.

Centrifuge adaptors were added to the round bottom waste tubes. The titanium dioxide spin tips (provided with the kit) where added to the centrifuge adaptors. 20µl of Buffer A was loaded and spun at 5000rpm for 2 minutes to condition the tip. 20µl of Buffer B was loaded and spun at 5000rpm for 2 minutes to equilibrate the tip. The waste was discarded. The Macrotrap dried samples were re-suspended in 50µl of Buffer B. The samples were loaded onto the tip and spun at 3000rpm for 10 minutes. The flow through was re-loaded onto the tips and spun again at 3000rpm for 10minutes. The waste was collected and stored as the NON PHOSPHO FLOW THROUGH. 20µl of Buffer B was spun through the tip at 5000rpm for 2 minutes. 20µl of Buffer A was loaded and spun at 5000rpm for 2 minutes – this step was repeated. The waste was discarded. The spin tips and the centrifuge adapters were transferred to the recovery tubes. Samples were eluted by adding 50µl of 5% ammonia solution and spun at 3000rpm for 5 minutes. 50µl of pyrrolidine was added and spun at 3000rpm for 5 minutes. The samples were dried in a speed vac at 45^0C.

Desalting using Zip Tips – Preparing the Samples for Mass Spectrometry

Standard bed Zip Tip's C_{18}, Capacity 5µg, Volume 10µl were purchased from Millipore (Cat No. ZTC 18S 096). The phosphoenriched dried samples were re-suspended in 10µl of 0.1% TFA. The Tips were wetted with 10µl of 100% ACN, aspirated and dispensed twice. The tips were equilibrated with 10µl of 0.1% TFA, aspirated and dispensed twice. The samples were aspirated and dispensed 7 -10 times to allow for maximum binding on to the Zip Tip. The waste was stored. The tips were washed with 10µl of 0.1% TFA, aspirated and dispensed twice. 10µl of 0.1%TFA/70% ACN was used to elute the samples. The elution buffer was aspirated and dispensed through the column 7 – 10 times to remove all bound peptides. The samples were dried in a speed vac at 45^0C. Samples were re-suspended in 10µl of 0.1% formic acid and sent to the LTQ Orbitrap Elite mass spectrometer through the University of Birmingham, School of Biosciences, genomics facility.

Statistical Analysis

Statistical analysis was performed using a combination of Microsoft Excel, MaxQuant (Mass spec tools) and the statistical program, R (**Tyanova *et al.,* 2015**). Mass spec data analysis was performed using the software Cytoscape (***www.cytoscape.org***) and the online software DAVID (**Huang *et al.,* 2009**).

CHAPTER 3: MANIPULATION OF THE RATES OF CRYPTOCOCCAL VOMOCYTOSIS FROM MACROPHAGES

Summary

This results chapter will discuss the data obtained and developed from an initial kinase inhibitor library screen. A LRRK2 kinase inhibitor, LRRK2 IN1, was identified from our library of kinase inhibitors as having an affect on the rates of vomocytosis. LRRK2-IN1 was found to have multiple secondary targets, specifically, ERK5 and BRD4.

Specific inhibitors of LRRK2, ERK5 and Brd4 were used and the effects on vomocytosis analysed. Upon investigation, ERK5 was identified as a potent regulator of vomocytosis. Using a combination of pharmacological inhibition of ERK5 and non-pharmacological approaches, including ERK5 siRNA treatment and $ERK5^{-/-}$ conditional knockout murine bone marrow derived macrophages; similar effects on vomocytosis rates were observed. Such an approach potentially offers a powerful route to subtly modify the host-pathogen interaction during systemic cryptococcal infection.

Kinase Signalling

Kinase signalling cascades are important in both eukaryotic and prokaryotic cellular communication and are crucial in a variety of biological signalling processes, ranging from glucose metabolism, cell cycle checkpoint control, initiation of apoptosis, signal transduction, ligand detection and autophagy (**Munday *et al.,* 1980**; **Pines, 1994; Mogensen *et al.,* 2009**). The importance of kinases has also been reported in a vast array of immunological signalling process including: phagocytosis, Toll Like Receptor (TLR) signal transduction, MAP Kinase signalling in leukocytes, cytokine transcription, macrophage activation, cytokine secretion and activation (**Mogensen *et al.,* 2009**). The importance of kinases in cryptococcal vomocytosis are poorly understood, however, I hypothesised that a process as complex as vomocytosis must require intense cellular signalling both from the host macrophage and pathogen. Figure 6 shows the Toll Like Receptor (TLR) signalling pathways highlighting a range of kinases involved solely in pathogen recognition. The majority of the kinase inhibitors used in this research affect proteins in TLR signalling pathways including: IRAK4, IKKβ, and IKKε. Inhibitors of other MAPK signalling pathways including the JAK/STAT, MEK/ERK5 and JNK pathways were also used for this research.

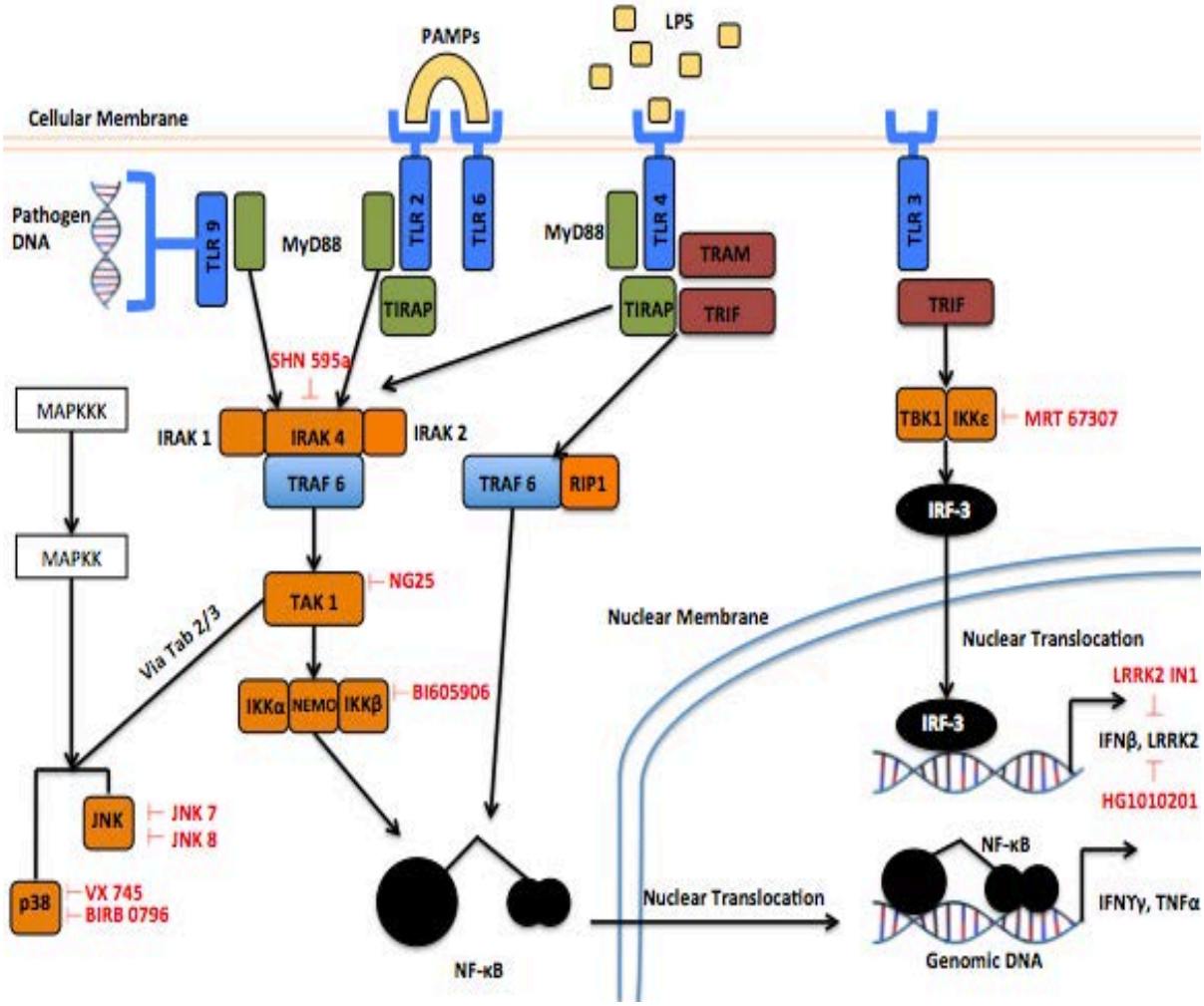

Figure 6: The Toll Like Receptor Signalling Pathways. Activation of Toll Like Receptors (TLRs 1, 2, 6, 7 and 9) leads to the recruitment of the Myeloid Differentiation primary response 88 (MyD88) proteins. For TLR 1, 2, 6 this is via Toll Interleukin 1 Receptor Adaptor Protein (TIRAP). MyD88 associates with Interleukin1 Receptor Associated Kinase 4 (IRAK-4) and TNF Receptor Associated Factor 6 (TRAF-6). IRAK-4 phosphorylates TRAF-6 triggering the enzymatic activity of TRAF-6. This results in the ubiquitylation of TRAF-6 and the recruitment of Nuclear Factor – κB (NF – κB) Modulator (NEMO) and TGFβ Activated Kinase 1 (TAK1) to the sites of ubiquitylation. NF – κB, Mitogen Activated Protein Kinases (MAPKs) and other transcription factors are activated and translocate to the nucleus to drive the transcription of pro-inflammatory

cytokine genes. Ligands of TLR 3 and 4 signals through the TIR-domain-containing adaptor – inducing interferonβ (TRIF) and the TRIF Related Adaptor Molecule (TRAM) pathway. TRIF binds directly to TLR4 and indirectly with TRAM binds to Receptor Interacting Protein 1 (RIP1) and TRAF-6 post receptor activation. This leads to NF – κB activation. Interferons (IFN) can also be activated through the TRIF pathway via the TANK (TRAF Family Member Associated NF – κB Activator) Binding Kinase and Interferon Regulatory Factor 3 pathway (**Ofengeim and Yuan 2013**). IKK – IκB Kinase. TLR9 detects bacterial DNA. The red labels indicate kinase inhibitors used in this study.

Macrophage and cryptococcal kinase signalling pathways, particularly those involved in immune signalling, may play a critical role in vomocytosis and therefore are worthy of investigation during cryptococcal-macrophage interactions. Investigation of cellular signalling during intracellular cryptococcal growth, cryptococcal quiescence, pathogen destruction and specifically cryptococcal vomocytosis may provide clues to tease apart the activity of kinases involved in these processes. In this research we screen a library of small molecule, leukocyte specific, kinase inhibitors and record their effects upon the vomocytosis rates of cryptococcal-infected macrophages using time-lapse microscopy (Figure 6 and Table 1).

An Initial Kinase Inhibitor Screen Indicated LRRK2 as a Regulator of Vomocytosis

To begin to dissect a potential role for kinase signalling in vomocytosis, cryptococcal (H99GFP) infected J774A.1 murine macrophages were treated with fifteen small molecule, leukocyte specific, kinase inhibitors (Table 1) kindly provided by the Alessi group (University of Dundee). The recommended inhibitory concentrations of each inhibitor used are shown in Table 1. Phagocytosis/Vomocytosis assays were performed on the infected macrophages and time-lapse imaging was used to manually and blindly quantify macrophage integrity, phagocytosis, intracellular cryptococcal proliferation rate (IPR), intracellular cryptococcal killing, colony forming units (CFU) and cryptococcal vomocytosis (Figure 7 and 8).

Table 1: The 15, small molecule, leukocyte specific, kinase inhibitors and the pathways/proteins affected.

Kinase Inhibitor (Recommended Inhibitor Concentration Used)	**Pathway/ Protein Inhibited**
SHN 595a (3μM)	**IRAK4** – a kinase, part of the MyD88 pathway of TLR4 signal transduction (**Wang *et al.,* 2009**).
NG25 (1μM)	**TAK1** – a kinase, part of the TLR4 signal transduction pathway activated both by theMyD88 and TRIF routes of activation (**Dzamko *et al.,* 2012**).
BI605906 (10μM)	**IKKβ** – a kinase involved in the activation of NFκB nuclear translocation (**Dzamko *et al.,* 2012**).
MRT67307 (2μM)	**IKKε** – a kinase involved in the phosphorylation of transcription factor IRF3 (**Dzamko *et al.,* 2012**).
JNK7 (10μM)	**JNK** – a mitogen activated protein kinase (MAPK)
JNK8 (10μM)	**JNK** – a mitogen activated protein kinase (MAPK)
VX745 (1μM)	**p38** – a MAPK similar to JNK and activated via phosphorylation to stress stimuli including cytokines (**Kuma *et al.,* 2005**).
BIRB0796 (100nM)	**p38** – a MAPK similar to JNK and activated via phosphorylation to stress stimuli including cytokines (**Kuma *et al.,* 2005**).
LRRK2-IN1 (1μM)	**LRRK2** – mutations in this kinase are associated with Parkinson's disease (**Zimprich *et al.,* 2004**). The protein is a multi domain protein, highly

	expressed in immune cells, particularly B-cells and macrophages (**Mata *et al.,* 2006**). LPS inhibits the kinase whilst IFNϒ up regulates its activity (**Gardet *et al.,* 2010**). LRRK2 is thought to affect the nuclear translocation of NFAT – a transcription factor involved in cytokine transcription (**Liu *et al.,* 2011**). LRRK2 is also phosphorylated via the TLR signal transduction pathway (**Dzamko *et al.,* 2012**).
HG1010201 (1µM)	**LRRK2** – see **LRRK2-IN1 (Dzamko *et al.,* 2012)**
Tofacitinib (5µM)	**JAK/STAT** – inhibits JAK/STAT signalling e.g. the signalling used by cell to detect IFNϒ.
Ruxolitinib (0.5µM)	**JAK/STAT** – see **Tofacitinib**
HG99101 (0.5µM)	**Tyrosine kinase -** a inhibitor of tyrosine kinases.
MRT199665 (1µM)	Inhibits AMPK related kinases (**Clark *et al.,* 2012**)
PD 1843452 (2µM)	Tyrosine Kinase Inhibitor

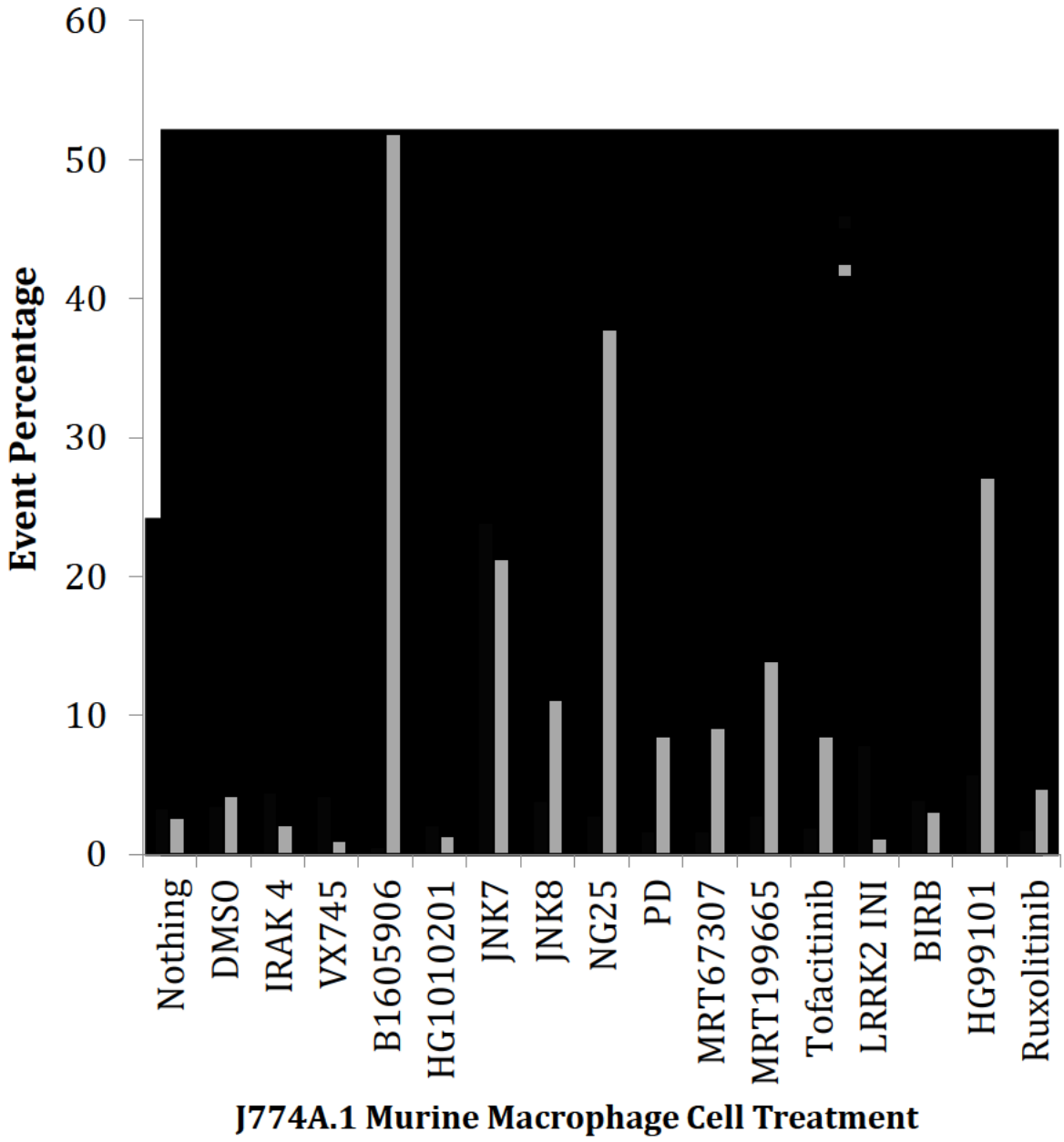

Figure 7: Vomocytosis assay of the original kinase inhibitor screen. The average percentage of cryptococci (H99GFP) that vomocytosed are shown in Black whilst the average percentage of lysed macrophages are shown in Grey (n=1). 10623 individual cryptococci were counted. (**, $p < 0.003$, *, $p < 0.005$ Chi squared test between the vomocytosis rates of the DMSO control and the inhibitor treatments).

Inhibitors that cause high rates of macrophage lysis are both clinically undesirable and complex from an assay quantification perspective, hence such compounds of this nature (e.g. B1605906) were discounted from further investigation. Vomocytosis rates of the "Nothing-Added" control and the DMSO control show no difference ($X^2 = 0.09$, p-value = 0.76, n=1) indicating that the DMSO solvent for the inhibitors has no effect on vomocytosis rates. The vomocytosis rates of the 15-kinase inhibitors were compared to the DMSO control. (Bonferroni correction. 0.05/15 = 0.003 = adjusted p-value for significance at the 5% level). A significant p-value was obtained for the JNK7 inhibitor ($X^2 = 45.70$, $p < 0.003$, n=1); however, the inhibitor also led to increased rates of macrophage lysis (21.23%) and was thus discounted. The p-value obtained for the LRRK2-IN1 inhibitor ($X^2 = 8.14$, p-value = 0.0043, n=1) was not significant using the stringent Bonferroni correction (designed to prevent the mis-interperation of false positives), however as LRRK2-IN1 increased vomocytosis (7.85%) without affecting macrophage lysis this inhibitor was the best candidate to investigate vomocytosis further.

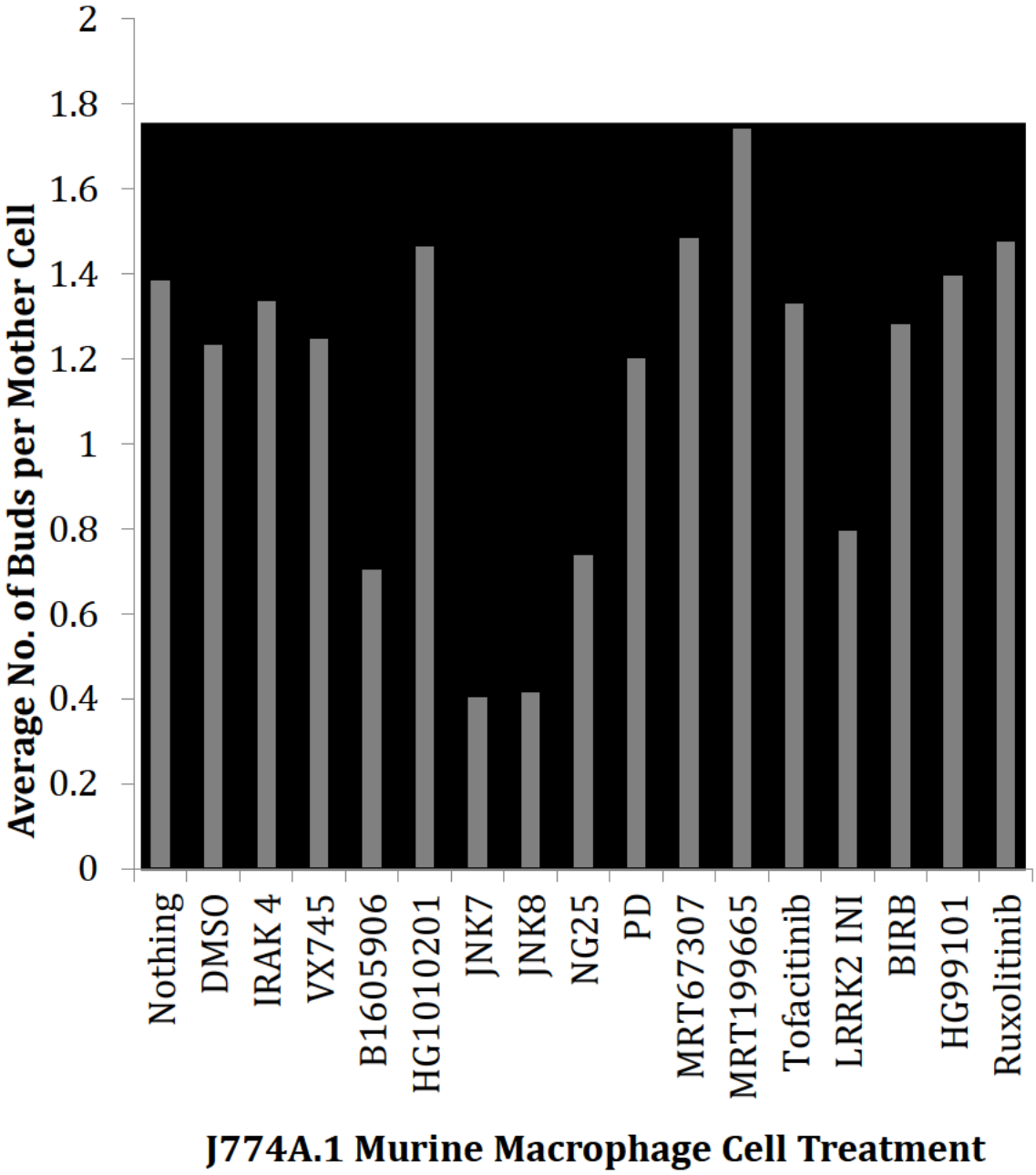

Figure 8: Time-lapse IPR of the original kinase inhibitor screen. The average number of buds individual mother cells produced during the 18-hour time-course in the presence of the kinase inhibitors (n=1). 10623 individual cryptococci were counted. These data were used a measure of overall cryptococcal health in response to the inhibitors, however the primary concern of this study was vomocytosis.

As a proxy measure for cryptococcal viability and overall health, the average number of buds produced per intracellular yeast cell during 18 hours of imaging was counted. Overall, as the levels of macrophage lysis and cryptococcal vomocytosis increase, the average number of buds decreases, presumably because the cryptococci are unable to remain within the macrophage for a substantial time period, reducing the rates of intracellular proliferation.

The effect of LRRK2 inhibition may result from activity within the macrophage, or through the interaction of the macrophage with the cryptococci. A cryptococcal genome search identified no annotated LRRK2 gene and given the inhibitors are mammalian specific, macrophage activity was considered as the primary target to investigate further. However, the effects of the inhibitors on extracellular cryptococcal growth could not be ignored and were analysed by performing growth curve experiments on cryptococci treated with the drug in the absence of the macrophages (n=5) (Figure 9). None of the 15 kinase inhibitors had detrimental or preferential effects on the growth rates of cryptococci, H99GFP(ANOVA – $F = 0.167$, $p < 0.936$, $n = 5$), indicating that the effects observed during time-lapse imaging have arisen due to inhibition of the host (macrophage) kinases and not a homologue or indirect target within the cryptococci.

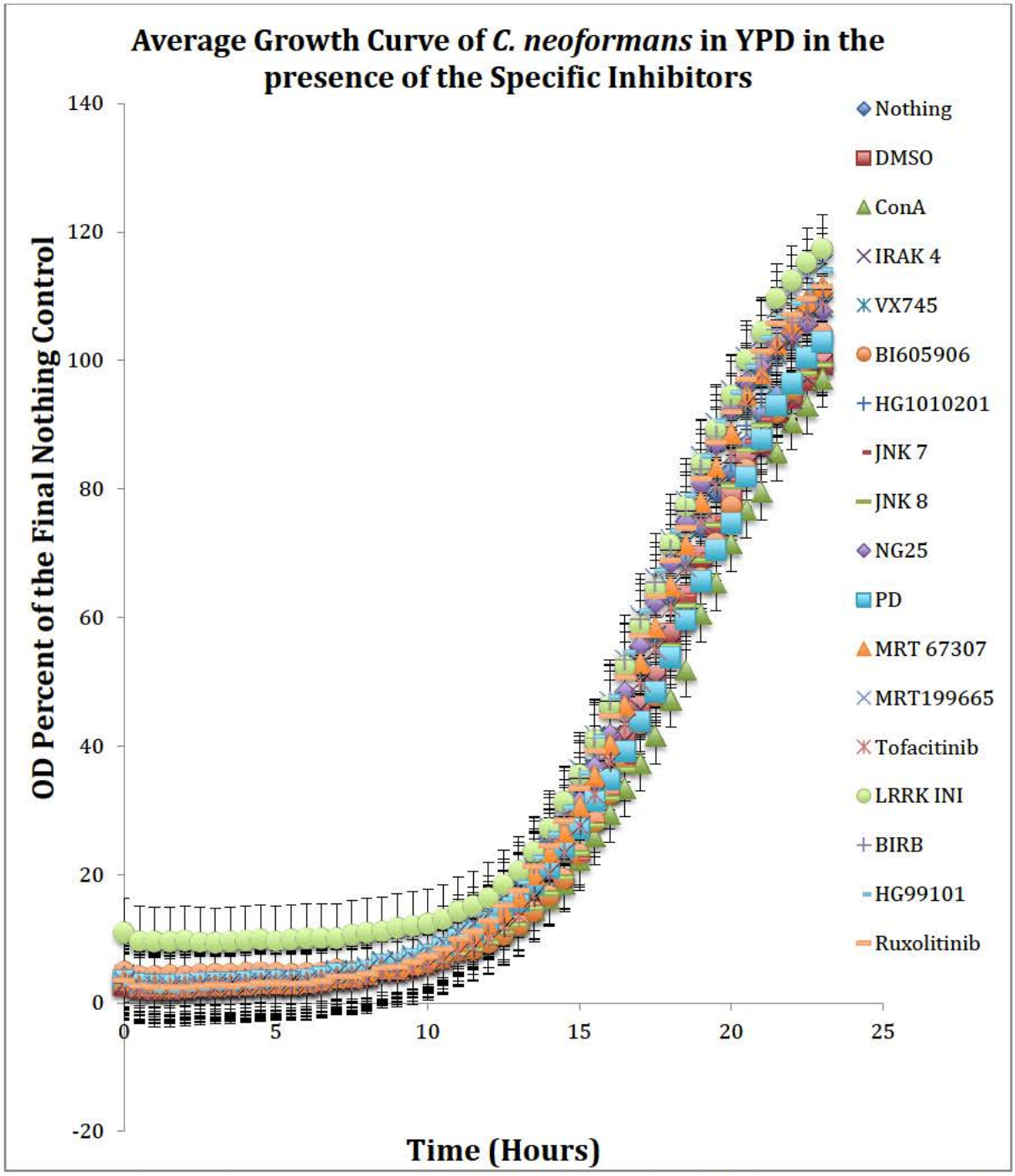

Figure 9: Extracellular growth curves for cryptococci. H99 GFP, in the presence of the 15-kinase inhibitors (ANOVA – $F = 0.167$, $p < 0.936$, $n = 5$) Error Bars = SD.

The LRRK2 inhibitor, LRRK2 – IN1, increased vomocytosis rates without increasing macrophage lysis and was therefore the most promising candidate to investigate vomocytosis further. Manually, scoring time-lapse movies for vomocytosis events was time consuming, therefore, further scoring focussed only on this inhibitor and the DMSO control (Figure 10). No difference was observed between the DMSO control and LRRK2–IN1 for macrophage lysis rates (n=3, $X^2 = 1.17$, $p = 0.28$). As previously seen, a significant difference was observed between the DMSO control and LRRK2-IN1 for vomocytosis rates (n=3, $X^2 = 9.32$, $p = 0.002$) indicating that vomocytosis is increased in the presence of LRRK2-IN1.

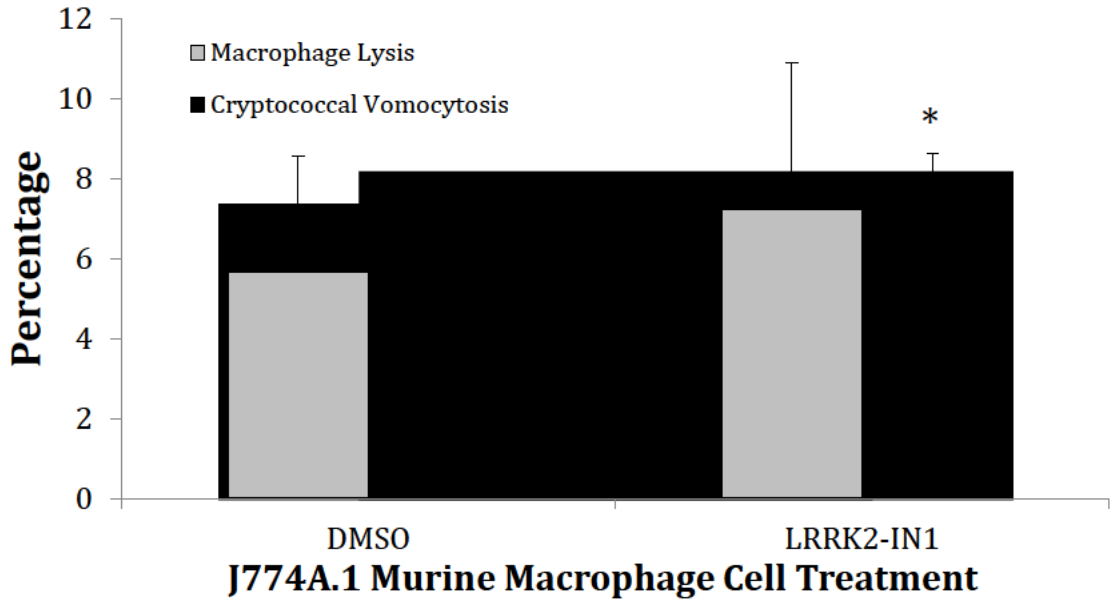

Figure 10: The effects of *LRRK2-IN1* treatment on macrophage lysis and cryptococcal (H99GFP) vomocytosis events. The percentage of macrophage (J774A.1) lysis events (**GREY**) and cryptococcal (H99 GFP) vomocytosis events (**BLACK**) when comparing cells treated with DMSO and LRRK2-IN1 (n = 3). Error bars = SEM. (*, p = 0.002, Chi Squared test for vomocytosis rates between the DMSO control and LRRK2-IN1).

To evaluate whether this effect was cryptococcal strain (H99GFP) specific; the experiment was repeated with a second cryptococcal strain, ATCC 90112, known to have a higher basal vomocytosis rate (**Ma 2009; Johnston and May 2010**)(Figure 11). No significant difference was observed between the macrophage lysis rates (n=3, X^2 = 0.009, p = 0.92). A significant difference was observed between the vomocytosis rates (n=3, X^2 = 9.55, p = 0.002), indicating that the effect on vomocytosis rates is not strain specific.

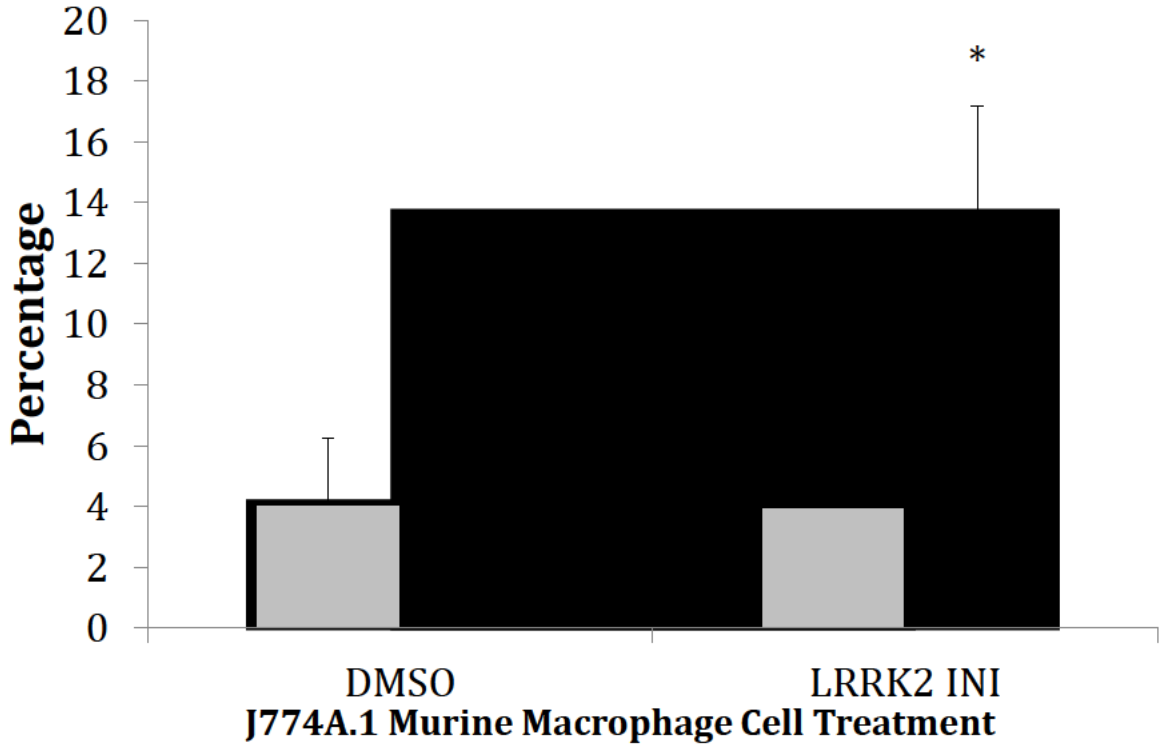

Figure 11: The effects of *LRRK2-IN1* treatment on macrophage lysis and cryptococcal (ATCC90112) vomocytosis events. The percentage of macrophage (J774A.1) lysis events (**GREY**) and cryptococcal vomocytosis events (**BLACK**) for the cryptococcal strain, ATCC 90112, when treated in DMSO and LRRK2-IN1 (n=3). Error bars = SEM. (*, p = 0.002, Chi Squared test for vomocytosis rates between the DMSO control and LRRK2-IN1).

Having established that LRRK2-IN1 is increasing the rates of vomocytosis in two independent cryptococcal strains (H99GFP and ATCC 90112), the effects of inhibitor dose was investigated. The Recommended inhibitor concentration of LRRK2-IN1 was 1μM (information supplied by Dario Alessi), therefore a range of concentrations (0.25 – 2μM) were examined for their effects on macrophage lysis and cryptococcal vomocytosis (see Figure 12).

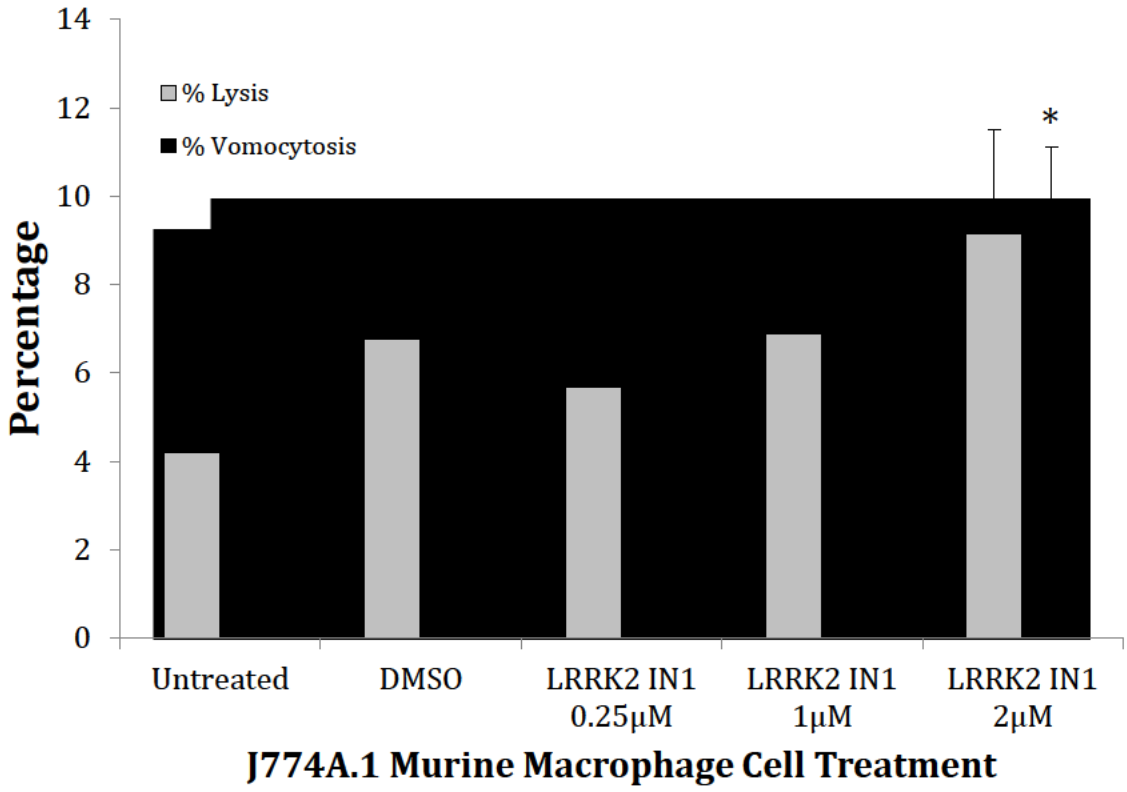

Figure 12: The effects of varying concentrations of *LRRK2-IN1* (0.25 - 2 μM) on macrophage lysis and cryptococcal (H99 GFP) vomocytosis. Error Bars = SEM. * = $p < 0.05$. Bonferroni correction $0.05/3 = 0.017$, $n = 3$.

As the concentration of the inhibitor is increased (0.25 - 2μM) the rates of vomocytosis increase to significantly different levels compared to the DMSO control (X^2 = 9.42 - 9.89, $p < 0.002$ (satisfies Bonferroni correction), n = 3). However, at higher concentrations of DMSO, macrophage lysis rates also increase and hence 1μM of the LRRK2-IN1 inhibitor was used as the rates of vomocytosis were increased but macrophage lysis rates were unaltered compared to the DMSO control.

LRRK2 is a large protein kinase (280KDa), recently discovered to play a critical role in the onset of genetic Parkinson's disease (**Zimprich *et al.,* 2004**). LRRK2 is highly expressed in inflammatory immune cells, such as macrophages and B-cells and this research shows evidence to suggest it may have a role in regulating cryptococcal vomocytosis. Inhibition of LRRK2 results in an increase in the rate of cryptococcal vomocytosis without altering macrophage physiology and these data made us question the molecular mechanisms of vomocytosis. As has been discussed in the introduction little is known about the molecular mechanisms of vomocytosis; it may involve the pathogen hijacking the natural exocytosis pathways adopted by the macrophage to eject indigestible material but equally could involve an active expulsion of prey from the host.

A recent paper by **Liu *et al.,* 2011** identified LRRK2 as a regulator, more specifically, an inhibitor of NFAT (Nuclear Factor of Activated T-Cells) nuclear translocation and hence immunomodulation in murine BMDMs. NFAT is a transcription factor prominently involved in the immune response (**Liu *et al.,* 2011**). We hypothesised that inhibition of LRRK2 may result in an increase of NFAT nuclear translocation in macrophages and

hence an increase in transcription of NFAT regulated genes, such as IFNγ, IL-2 and IL-10.

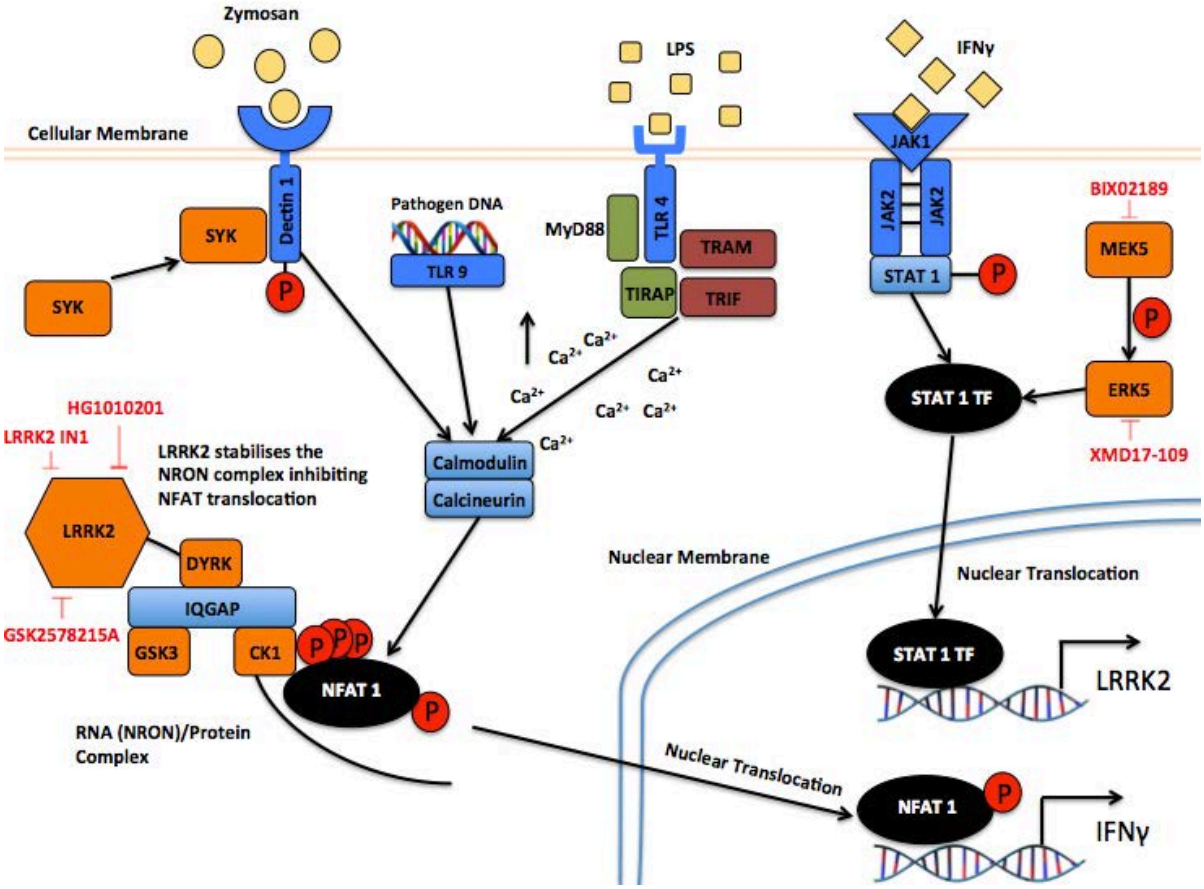

Figure 13: The role of LRRK2 in immunological signalling. LRRK2 (Leucine Rich Repeat Kinase 2) inhibits the nuclear translocation of the transcription factor NFAT (Nuclear Factor of Activated T-Cells), important in murine immune modulation, (**Liu *et al.,* 2011**). Inactivated NFAT remains cytoplasmic bound to a complex consisting of a single stranded RNA (NRON) and protein complex – IQGAP, GSK3, DYRK, CK1 and LRRK2 (Figure 4) (**Liu *et al.,* 2011**). Increased intracellular calcium levels induce NFAT activation via the Calmodulin/Calcineurin phosphatase activity; the resultant dephosphorylation of NFAT releases it from the NRON complex allowing nuclear translocation (**Liu *et al.,* 2011**). NFAT binds to several cytokine gene promotors including: IL-2, IL-6, IL-12p40 and IFNY. Increased IFNy detection increases

intracellular *lrrk2* transcription resulting in a negative feedback loop of NFAT activation (**Liu *et al.,* 2011**). ERK5 has been shown to mediate the cellular signalling initiated from IFNγ detection, via the JAK/STAT signalling pathway (**Kuss *et al.,* 2014**). IFNϒ signalling induces the transcription of *lrrk2* whilst LPS stimulation reduces it (**Gardet *et al.,* 2010**).

The effects of LRRK2 inhibition upon nuclear translocation of NFAT were investigated. Infected J774A.1 murine macrophages were treated with LRRK2-IN1 and fixed cell imaging was used to observe the nuclear translocation of NFAT. The macrophages were infected with GFP expressing cryptococci. After fixing, the NFAT protein were antibody bound and a TRITC bound secondary antibody was used for microscopy. The Hoechst stain was used to bind to macrophage DNA. We hypothesised that the LRRK2 inhibitor (LRRK2-IN1) would increase the percentage of macrophages with NFAT localised to the nucleus.

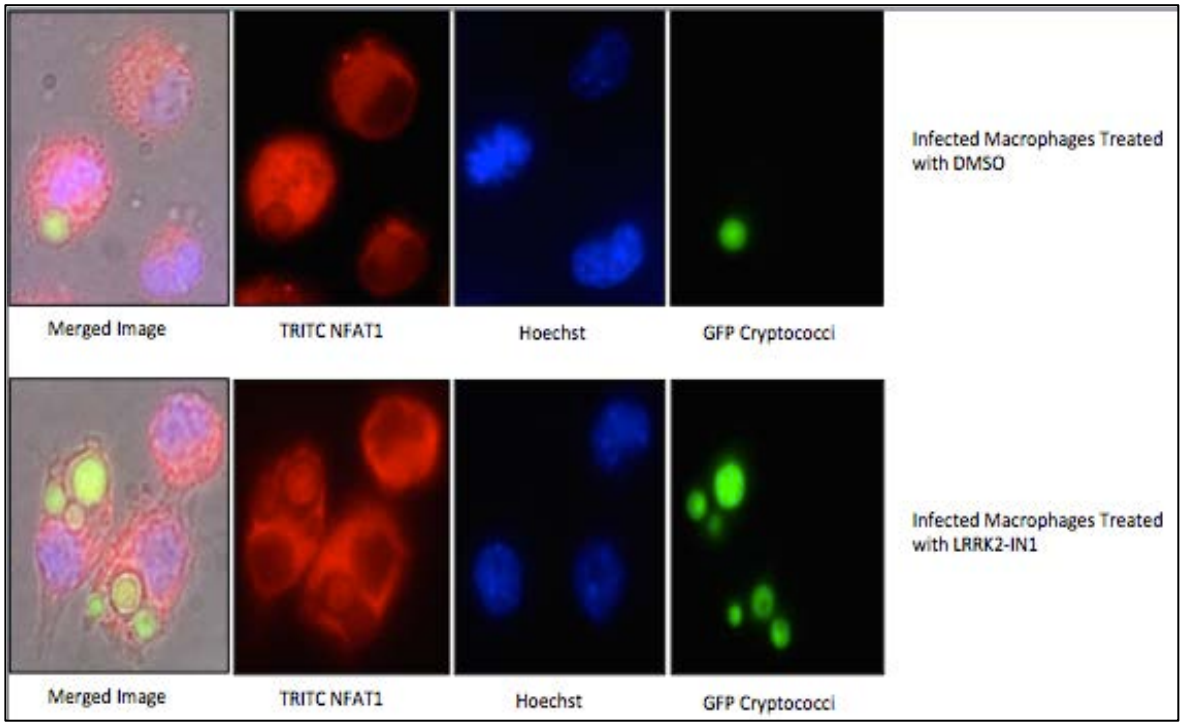

Figure 14: Fixed staining of NFAT of infected macrophages with and without LRRK2-IN1 treatment.

Upon cryptococcal infection of macrophages, no nuclear NFAT translocation was observed - see Figure 14. Addition of the LRRK2-IN1 inhibitor yielded no increase in the nuclear translocation of NFAT. Although discouraging, this result suggested a number of potential reasons for the observation. The first is that LRRK2 inhibition does not affect NFAT nuclear translocation. The second is that nuclear translocation may be fast and transient and therefore the protocol used is highly unlikely to detect the process. The third issue is that the LRRK2 inhibitor LRRK2-IN1 was not completely specific for LRRK2 (information supplied by the Alessi group) and therefore the effect on vomocytosis rates observed were actually due to the secondary inhibition of another protein.

Investigation of the Secondary Targets of LRRK2-IN1 Indicates ERK5 as a regulator of Vomocytosis

The initial inhibitor screen results posed a variety of questions concerning LRRK2-IN1 including its mode of action and how it caused an increase in vomocytosis rates. Curiously, addition of a second LRRK2 inhibitor, HG1010201, used during this screen, did not elicit a similar increase in vomocytosis as was observed with LRRK2-IN1. This, combined with information from our collaborators (Dario Alessi, University of Dundee) that LRRK2-IN1 has multiple secondary targets suggested that a secondary target might have been important. Secondary targets included ERK5 – a MAPK activated by MEK5 and implicated in a plethora of cellular processes, such as angiogenesis, apoptosis, cellular differentiation and recently macrophage efferocytosis (**Drew *et al.,* 2012; Heo *et al.,* 2014**), and Brd4 – an acetyl lysine reader protein involved in chromatin remodelling (**Spiltoir *et al.,* 2013**). Thus we considered the possibility that the phenotype first observed with LRRK2-IN1 was a result of secondary inhibition of one of these other targets. We therefore repeated the vomocytosis assay with two different LRRK2 inhibitors (HG1010201 and GSK2578215A) that do not inhibit these secondary targets. We also tested two inhibitors directed towards the "off targets": XMD17-109 a specific ERK5 inhibitor (**Elkins *et al.,* 2013**) and JQ1 a specific inhibitor for Brd4 (**Spiltoir *et al.,* 2013**).

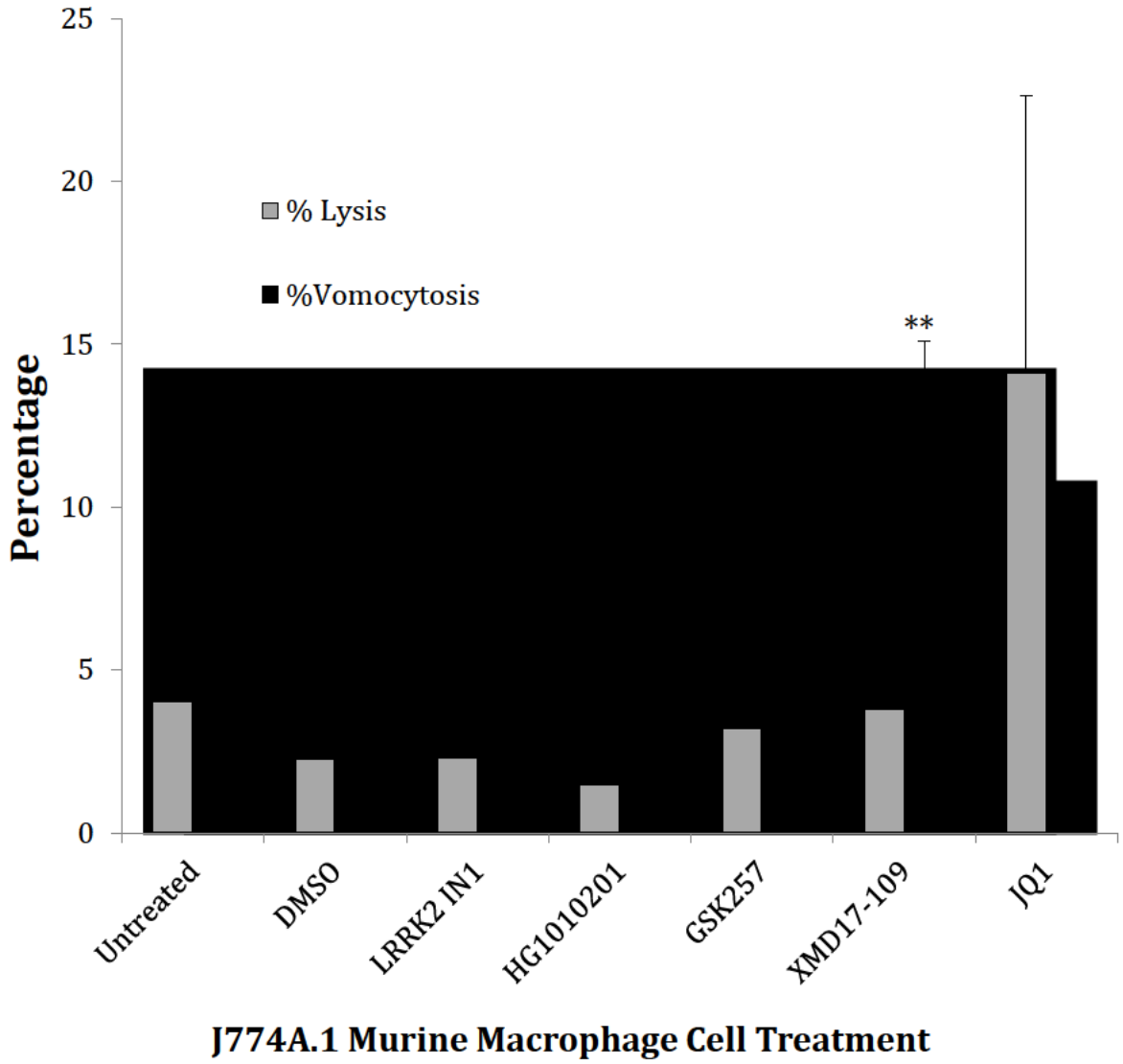

Figure 15: The effects of *LRRK2-IN1, HG1010201, GSK2578215A, XMD17-109* and *JQ1* on the rates of macrophage lysis and cryptococcal vomocytosis. The percentage of cryptococcal (H99 GFP) vomocytosis (**BLACK**) and macrophage (J774A.1) lysis (**GREY**) in the presence of 5 kinase inhibitors and the 2 controls (n=3). Error bars = SEM. (*, $p < 0.01$, **, $p<0.001$).

Differences in vomocytosis rates compared to the DMSO control were observed between three inhibitors (Bonferroni Correction 0.05/5 = 0.01): LRRK2-IN1 (X^2 = 6.90, p = 0.009, n=3), GSK2578215A (X^2 = 6.63, p = 0.01, n=3) and XMD17-109 (X^2 = 16.70, p > 0. 001, n=3). Two of these inhibitors were LRRK2 inhibitors (LRRK2-IN1 and GSK2578215A) whilst the third was an ERK5 inhibitor (XMD17-109). Interestingly the specific LRRK2 inhibitor, HG1010201, elicited no effect on the rates of vomocytosis whilst the GSK2578215A inhibitor crystallised and aggregated upon exposure to macrophages, potentially damaging the cells and thus resulting in vomocytosis like events (Figure 16).

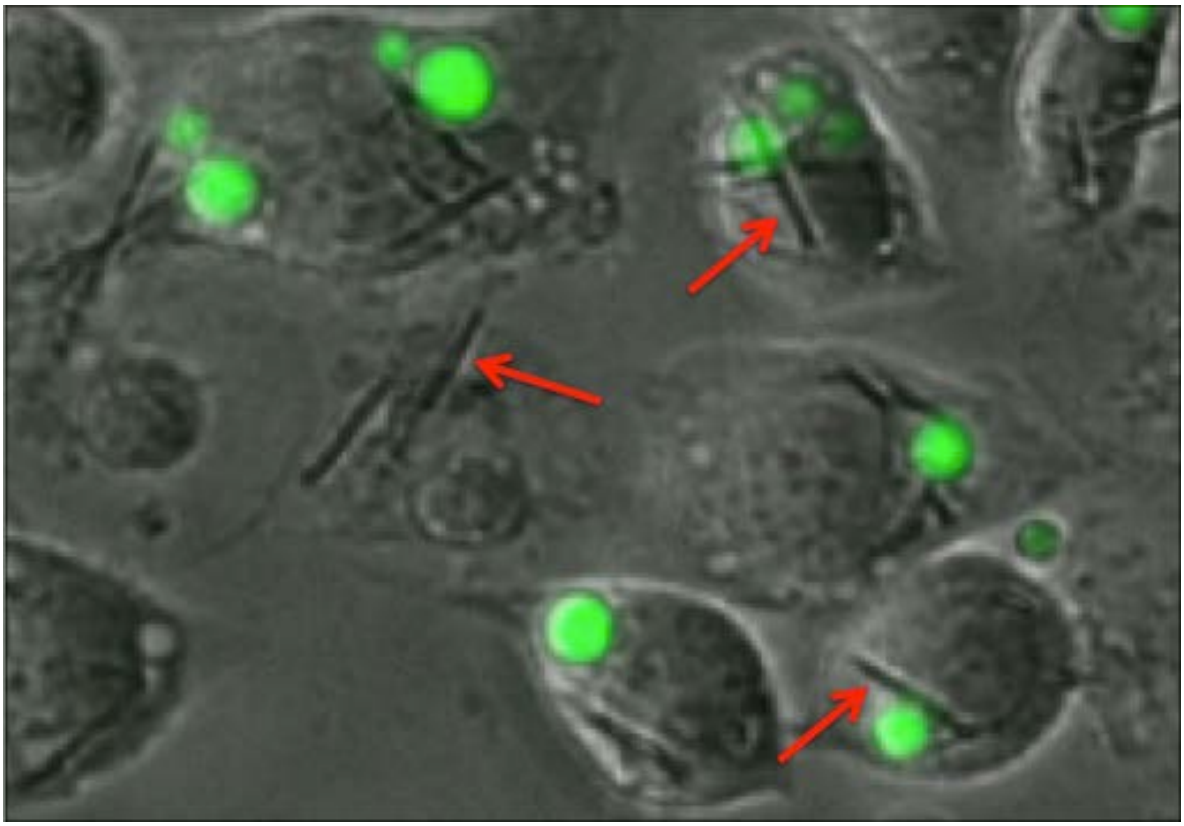

Figure 16: J774A.1 murine macrophages treated with *GSK2578251A* and the formation of crystal like structures. - (Highlighted with red arrows).

The Brd4 non-kinase inhibitor, JQ1, does not significantly increase the rate of cryptococcal vomocytosis when compared to the DMSO control ($X^2 = 0.36$, $p = 0.55$, n=3) but does increase the macrophage lysis rates considerably and variably suggesting that the inhibition of this protein is not the cause of the increase in vomocytosis first observed with LRRK2-IN1.

The specific ERK5 inhibitor, XMD17-109, increased the vomocytosis rates significantly when compared to the DMSO control ($X^2 = 16.70$, $p > 0.001$, n=3). The average vomocytosis rates were also elevated to higher rates then observed for the LRRK2 inhibitors – suggesting that the effects first observed with LRRK2-IN1 are potentially due to inhibition of the secondary target ERK5 that are enhanced when a more specific ERK5 inhibitor is used. Taken together, these data suggest that ERK5 plays a role in regulating vomocytosis and that the initial positive results with LRRK2-IN1 represent off-target effects on ERK5.

As a measure of cryptococcal well being whilst intracellular, we again measured intracellular budding capacity of *C. neoformans.* Only the ERK5 inhibitor, XMD17-109, significantly reduced budding relative to the DMSO control ($t = 4.19$, $p = 0.01$, n=3, Bonferroni correction $0.05/5 = 0.01$) (Figure 17). Interestingly we also noted that this inhibitor appeared to enhance the capacity of the macrophage to kill phagocytosed *C. neoformans* (assessed by loss of GFP signal and the fungi condensing in size). Thus it appears that XMD17-109 increases the antifungal activity of host macrophages and, either directly or indirectly, increases vomocytosis rates.

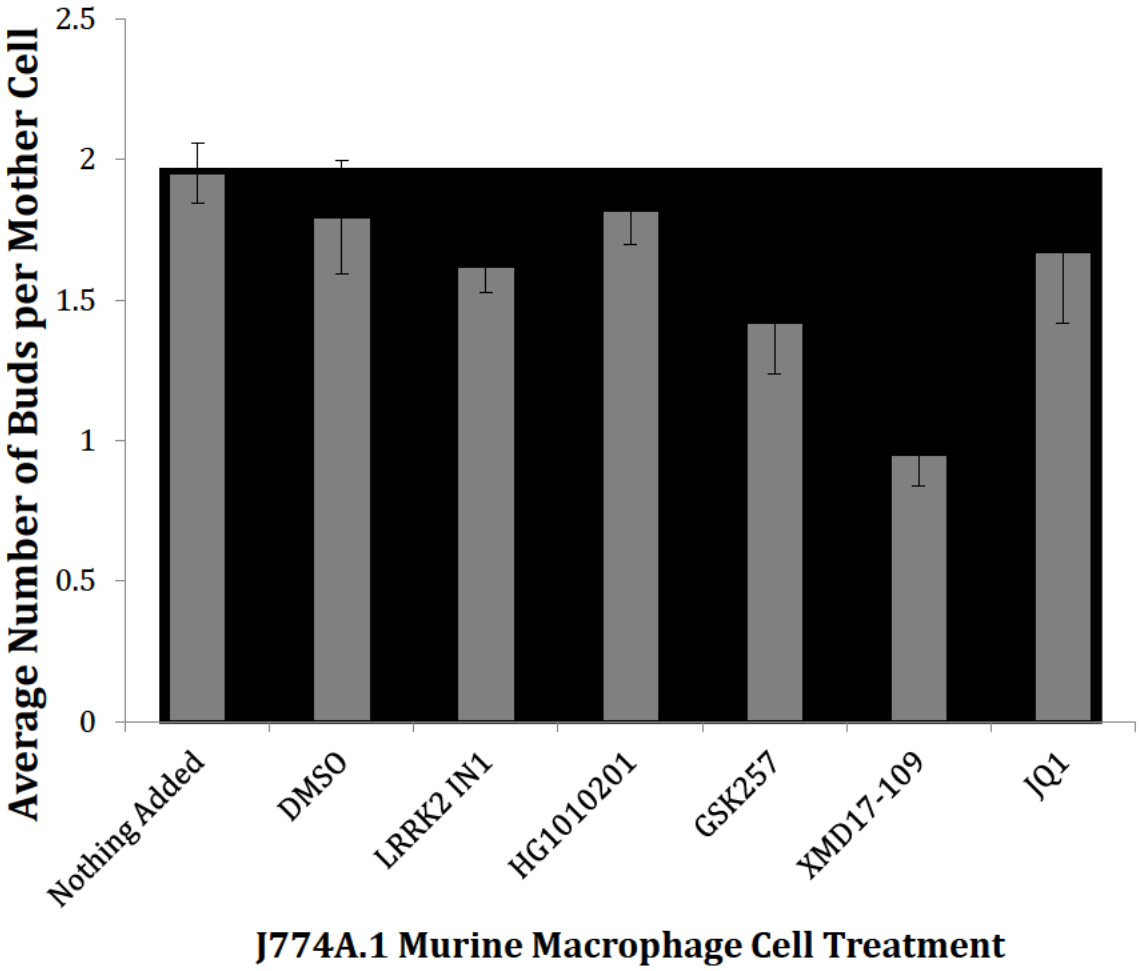

Figure 17: The intracellular budding capacity of H99 GFP cells during the 18-hour time-lapse movies whilst exposed to *LRRK2-IN1, HG1010201, GSK2578215A, XMD17-109* and *JQ1.* Error bars = SEM. (*, $p < 0.01$) n = 3.

As with the previous inhibitors, there was no impact upon cryptococcal growth in the absence of macrophages (Figure 18) indicating that the observed changes on the rates of vomocytosis are due to macrophage inhibition rather then cryptococcal inhibition, as previously discussed.

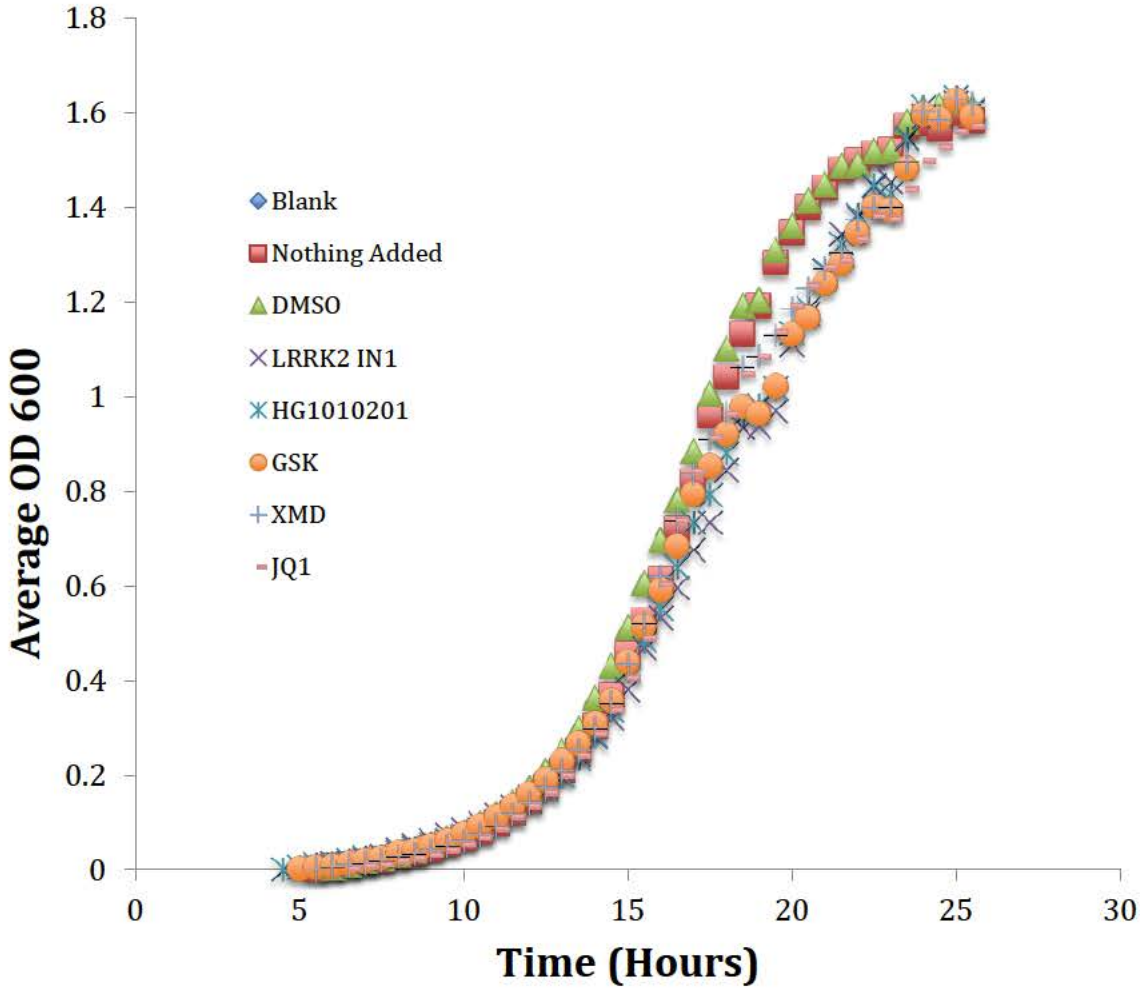

Figure 18: Extracellular growth curves for cryptococci exposed to *LRRK2-IN1, HG1010201, GSK2578215A, XMD17-109* and *JQ1* (n = 3).

ERK5

Extracellular Signal Regulated Kinase 5, ERK5, often referred to as MAPK7 or Big Map Kinase, is an atypical, poorly studied MAP Kinase (**Zhou *et al.,* 1995**). ERK5 is twice the size, 110KDa, of other better studied MAPKinases including: ERK1/2, JNK and p38 (**Lee *et al.,* 1995**) due to its large and unique C-terminal domain. ERK5, is phosphorylated and activated by the MAPKK, MEK5 (**Seyfried *et al.,* 2005**). The MEK5/ERK5 signalling pathway has been implicated in cell survival, cellular differentiation, anti-apoptotic signalling, motility, angiogenesis, cellular signalling, cellular proliferation, osteoclast differentiation (**Drew *et al.,* 2012; Amano *et al.,* 2015**) and, very recently, in efferocytosis – the canabalistic activity of macrophages to phagocytose dead/dying macrophages (**Heo *et al.,* 2014**). Due to its nature as a MAP kinase it has been implicated in many forms of cancer including prostrate and breast cancers (**Zhou *et al.,* 1995**).

Upon activation, the Mitogen Activated Protein Kinase Kinase Kinases (MAPKKK), MEKK2 and MEKK3, phosphorylate and activate the MAPKK, MEK5, a specific kinase and activator of ERK5 (**Seyfried *et al.,* 2005**) (Figure 19). ERK5 has been reported to respond to extracellular stress stimuli, such as oxidative stress and hyperosmolarity, commonly associated with the macrophage phagosome. These signals are common signalling cues to other MAPKs (**Drew *et al.,* 2012**). Both MEKK2 and MEKK3 have similar kinase activity but their regulatory N-terminal domains are different allowing varying responses to different environmental cues (**Drew *et al.,* 2012**). MEKK3 activates the MEK5/ERK5 pathway via predominantly growth factor- induced cellular stimulation and oxidative stress (**Chao *et al.,* 1999**). MEKK2 and MEKK3 bind to the

MEK5 PB1 domain located in the N-terminal, creating a MEKK2/3 and MEK5 complex (**Nakamura *et al.,* 2006**). MEKK/MEK5 complex formation exposes the Ser311 and Thr315 amino acid residues of MEK5 enabling its phosphorylation, hence resulting in the activation of MEK5 (**Nakamura *et al.,* 2006**).

The activated MEK5 is hypothesised to disassociate from the complex in order to bind to the functional domain of ERK5 (aa 78 – 139), however how it achieves this dissociation is little understood. The activated MEK5 can phosphorylate the two phosphorylation sites in the TEY motif of ERK5 (**Nakamura *et al.,* 2006**) (Figure 19). TEY motifs are common to ERK1/2, however the large C-terminal domain of ERK5 appears to regulate the activation status of ERK5 via autophosphorylation, affecting ERK5 cellular loaction and nuclear localisation (**Drew *et al.,* 2012**). Upon phosphorylation at the TEY motif the C-terminal domain becomes hyper-autophosphorylated and ERK5 enters its active state. The N-terminal and C-terminal of unactivated ERK5 are bound together in the cytosol (**Yan *et al.,* 2001**). Upon phosphorylation the bond between the C-terminal and the N-terminal degrades and the Nuclear Localisation Signal (NLS) of ERK5 becomes exposed, allowing nuclear translocation (**Kondoh *et al.,* 2006**) (Figure 19).

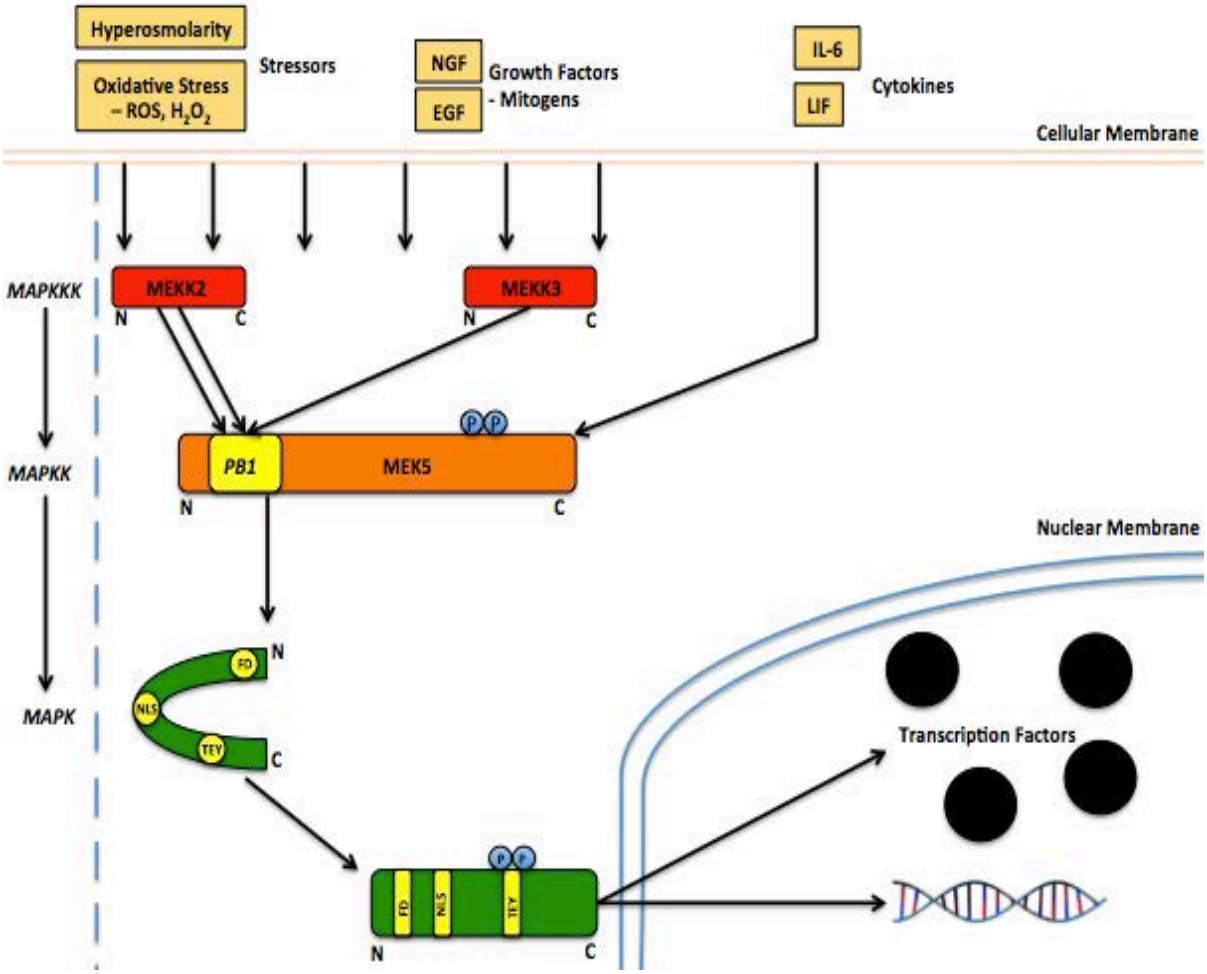

Figure 19: The ERK5 activation pathway. Activation of cytosolic ERK5 and nuclear transloaction is achieved through the detection of stressors, growth factors or cytokines. A kinase signalling cascade tranduces the signal through MEKK2 or MEKK3, capable of phosphorylating MEK5. MEK5 then phosphorylates the inactive, closed confirmation of ERK5 resulting in a change of protein confirmation and hyperphosphorylation of the C-terminal domain of ERK5. A nuclear localisation sequence is revealed and the phosphorylated ERK5 protein is capable of translocating the nucleus to phosphorylate a wide range of transcription factors and is hypothesised to act as a transcription (co)factor (**Drew *et al.*, 2012**).

Upon translocation to the nucleus, ERK5 is capable of phosphorylating a multitude of transcription factors and proteins involved in a wide range of cellular processes. These transcription factors include: cFOS, SAP1, MEF2C, Bad, CREB, FOXO3, SGK, C-Myc and Cyclin D1 (**Drew *et al.,* 2012**). The effects of ERK5 activation on cellular biology are profound and therefore regulation of its activity is essential. The MEK5/ERK5 signalling pathway has been implicated in a variety of tissue specific cancers such as prostate cancer and breast cancer (**Mehta *et al.,* 2003; Carlos Montero *et al.,* 2009**) and thus inhibition of the pathway may provide a therapeutic strategy for many aggressive cancers (**Carlos Montero *et al.,* 2009**). The role of ERK5 in innate cellular immunity against pathogenic infection and its roles in general cellular immunity are little known, however it has been shown to affect IL-10 synthesis and to be important for osteoclast differentiation (**Kozicky *et al.,* 2015; Amano *et al.,* 2015**). As macrophages are under a great deal of environmental stress upon ingestion of a pathogenic micro-organism, one can imagine that a plethora of downstream signalling is initiated to tolerate the stressor – ERK5 may be part of this global response. This study explores the role of murine macrophage ERK5 during cryptococcal infection of macrophages, specifically focussing on vomocytosis.

The ERK5 Inhibitor Increases Vomocytosis Rates of *C. neoformans* and *C. gattii* but not Dead Cryptococci or Latex beads in Murine Cell Lines

To begin to answer whether the increased vomocytosis phenotype observed with LRRK2-IN1 was due to indirect effects upon ERK5, the inhibitors were explored further. The initial assay used took both LRRK2-IN1 and XMD17-109 and repeated previous vomocytosis experiments. During this repeat experiment, both inhibitors were used either alone or together and vomocytosis rates measured (Figure 20).

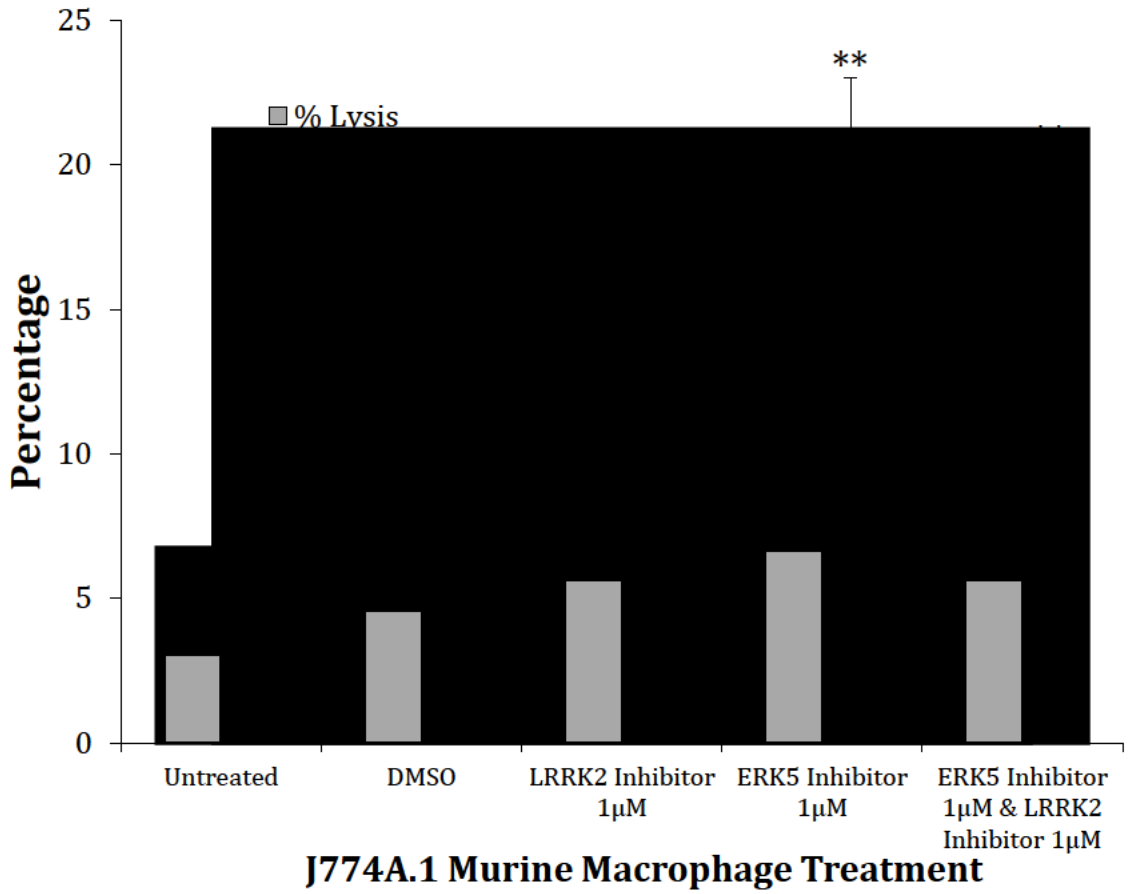

Figure 20: The effects of *LRRK2-IN1* and *XMD17-109* on the rates of macrophage lysis and cryptococcal vomocytosis. The percentage of cryptococcal (H99 GFP) vomocytosis events (**BLACK**) and macrophage (J774A.1) lysis events (**GREY**) (n=3). Error bars = SEM. * $p < 0.01$, ** $p < 0.001$, Chi squared test comparing the vomocytosis rates for the treatments with the DMSO control.

No difference was observed in macrophage lysis rates between the DMSO control and any of the treatments ($X^2 = 0.25 – 1.94$, $p = 0.16 – 0.62$, n=3, Bonferroni Correction $0.05/3 = 0.017$). As expected, significant differences were observed for the rates of vomocytosis for all treatments, particularly ERK5 inhibitor treatments, and the DMSO control ($X^2 = 6.77 – 65.77$, $p < 0.01$, n=3, Bonferroni Correction $0.05/3 = 0.017$).

However, the combination of 1μM of LRRK2-IN1 and 1μM of the ERK5 inhibitor, does not enhance vomocytosis rates further than the 1μM ERK5 inhibitor alone (T = 0.41, p = 0.71, n=3), suggesting that either the LRRK2 and ERK5 inhibitors affect the same cellular signalling pathway (ERK5), or that the macrophages are at the physiological limit of the how many cryptococci they can vomocytose without inducing macrophage lysis, therefore the rates cannot increase further.

To confirm that inhibition of ERK5 was the cause of the increase in the rates of vomocytosis a second specific ERK5 inhibitor, AX15836, was used to see if the results were reproducible (**Unpublished data**). Figure 21 shows that 1μM of AX15836 but not 2μM, is capable of significantly up regulating the rates of cryptococcal vomocytosis (X^2 = 6.399, p-value = 0.01, n = 4 – significant under the Bonferroni correction). 2μM of AX15836 generated a p-value of 0.04 after statistical analysis using X^2, however due to multiple comparisons being made these data are not significant under the Bonferroni correction. In this study, AX15836 is as effective at up regulating the rates of vomocytosis as XMD17-109 (X^2 = 6.521, p = 0.01, n=4), suggesting ERK5 is the protein of interest. Curiously recent unpublished data, from our collaborator, Alessi group (University of Dundee), suggests that the potency of this inhibitor *in vivo* is less effective then XMD17-109.

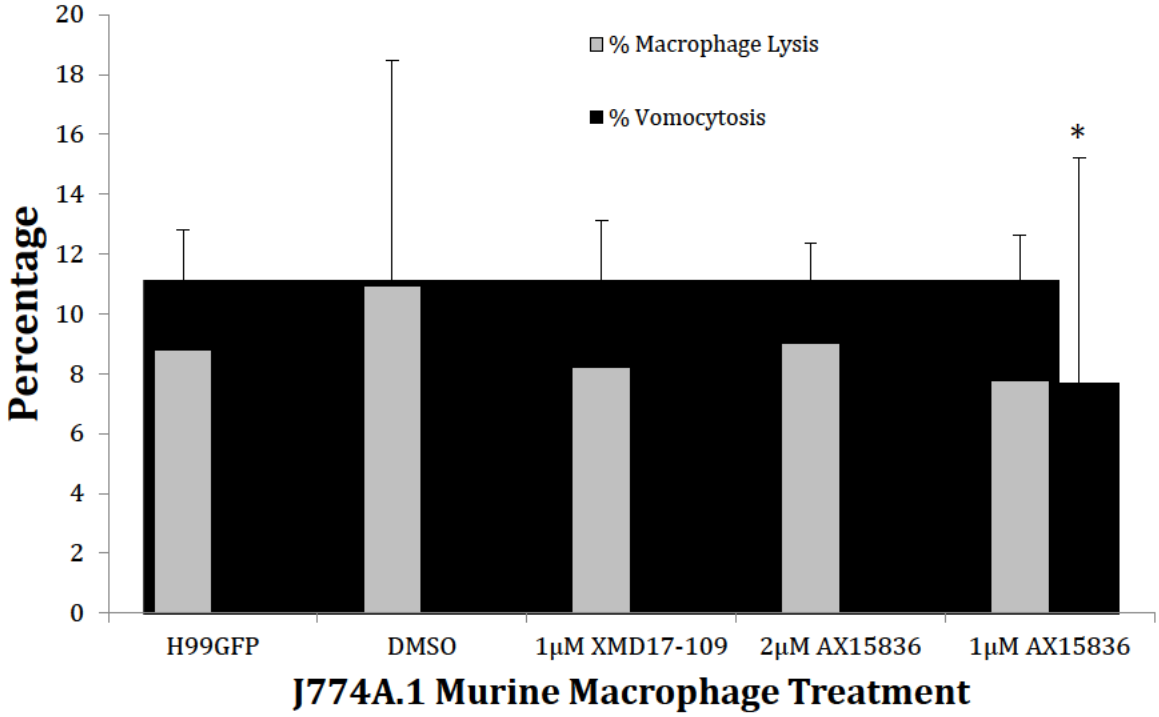

Figure 21: The effects of *XMD17-109* and *AX15836* on the rates of macrophage lysis and cryptococcal vomocytosis. The percentage of cryptococcal (H99 GFP) vomocytosis events (**BLACK**) and macrophage (J774A.1) lysis events (**GREY**) under the ERK5 inhibitor treatments (n=4). Error bars = SEM. * $p < 0.01$, Chi squared test comparing the vomocytosis rates for the treatments with the DMSO control. Bonferroni correction used.

Further to the observations that two separate ERK5 inhibitors enhanced the rate of cryptococcal vomocytosis, Western blotting and densitometry image quantification was used to confirm whether the inhibitors were capable of down regulating the murine ERK5 protein (Figure 22). Macrophages were infected with cryptococci and treated with the two ERK5 inhibitors, XMD17-109 and AX15836. Another infection was treated with a MEK5 inhibitor, BIX02189.

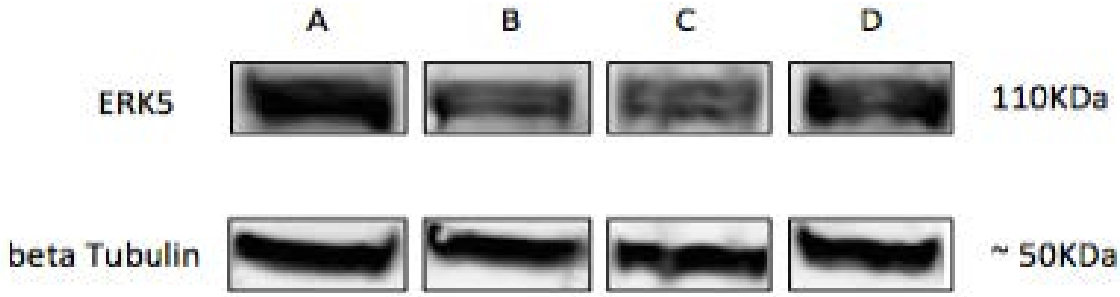

Figure 22: Western Blot of the murine ERK5 protein and the beta tubulin loading control. A – Cryptococcal infected macrophages treated with DMSO, B – Cryptococcal infected macrophages treated with XMD17-109, C – Cryptococcal infected macrophages treated with AX15836, D – Cryptococcal infected macrophages treated with BIX02189.

Visually, treatment with the inhibitors appears to have little effect on the overall regulation of the murine ERK5 protein. However, the band produced for the DMSO treatment could be perceived as more intense then the treated lanes. AX15836 and XMD17-109 treatments may induce a reduction in the ERK5 protein intensities (110KDa) with the characteristic double band of the antibody clearly visible for these treatments from the blot image. Ideally, densitometry was required to ratio the two separate bands, but as the separation between the bands is not sufficient this is difficult. Therefore, densitometry was used to quantify the whole gel band on the Western blot image to identify whether a difference was present, see Table 2.

Table 2: Densitometry quantification of the ERK5 inhibitor treatments Western Blot.

Infection Treatments	**Intensity Scores for beta Tubulin**	**Intensity Scores for ERK5**	**Normalised Scores for beta Tubulin**	**Quantified Protein Ratios**
DMSO	73.56	99.90	0.89	112.25
XMD17-109	78,17	87.30	0.95	91.89
AX15836	78.99	77.35	0.96	80.57
BIX02189	82.44	92.46	1.00	92.46

Densitometry quantification highlighted that treatment with all three inhibitors (XMD17-109, AX15836 and BIX02189) induced a reduction of the ERK5 protein intensity levels, as was suggested by the gel image. The protein levels were not dramatically reduced and this may have been due to the fact that the ERK5 antibody (SIGMA™) measures total ERK5 within the cell and not just the phosphorylated ERK5 protein. The second larger band located on the ERK5 protein represents the phosphorylated part of the protein, due to the hyper-phosphorylation of the C-terminal domain. The inhibitors are highly unlikely to cause the degradation of the protein and therefore a band will appear on the Western blot (110KDa). As the inhibitors prevent kinase activity, auto phosphorylation of the ERK5 C-terminal domain will not be achieved and therefore the second larger molecular weight band should have a reduction in intensity.

Having identified that the activity of two separate ERK5 inhibitors, AX15836 and XMD17-109, were reducing ERK5 kinase activity and inducing an enhanced vomocytosis phenotype, the next question was to ensure that the effect observed was

not cell line specific, therefore another cell line, RAW264.7, was investigated in the same way (Figure 23). Cryptococcal infected RAW264.7 cells had a significantly higher rate of vomocytosis when treated with XMD17-109 when compared to the DMSO treated control ($X^2 = 18.96$, ** $p < 0.001$, $n = 3$), suggesting that the phenotype observed is not cell line specific.

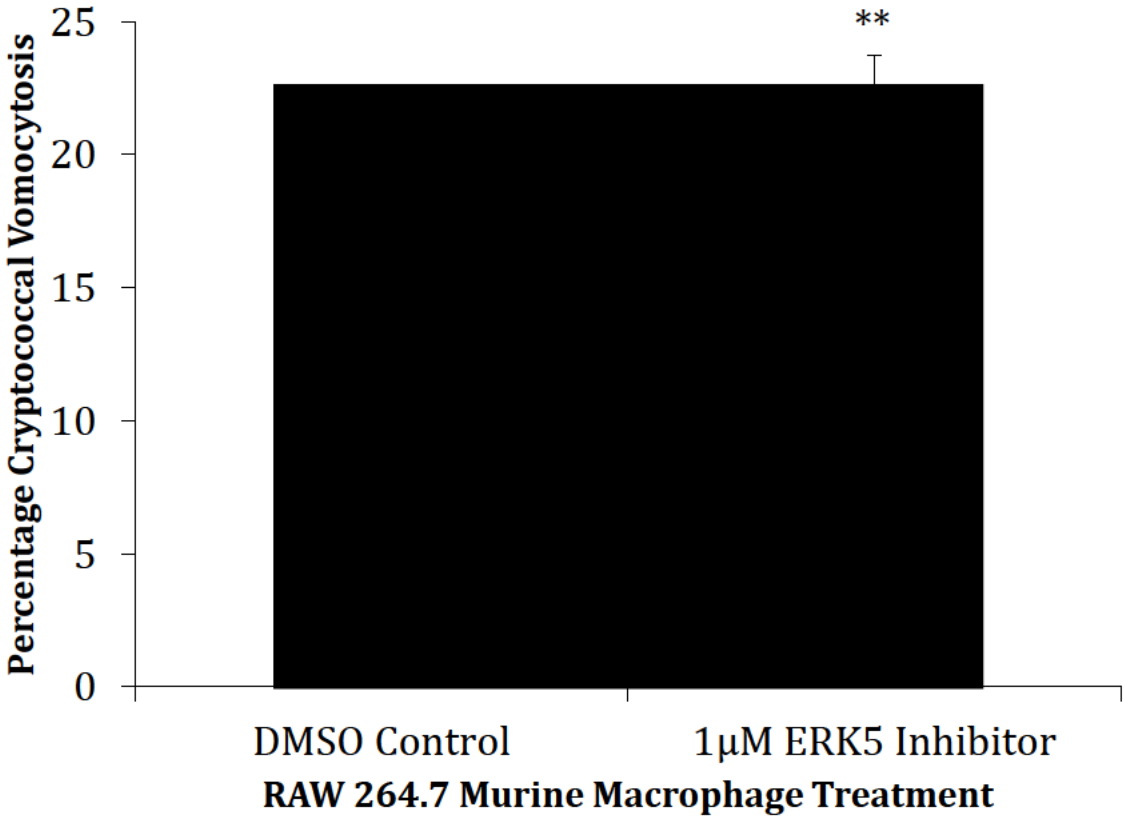

Figure 23: Vomocytosis rates for the treatment of cryptococcal (H99GFP) infected RAW264.7 macrophages with *XMD17-109*. Error bars = SEM. ** $p < 0.001$ comparing the vomocytosis rates for the ERK5 inhibitor treatment with the DMSO control ($n = 3$).

As vomocytosis has been reported in multiple species, including *C. gattii* and *C. albicans* (**Ma 2009; Bain *et al.,* 2012**), we were keen to investigate whether vomocytosis could be enhanced using the ERK5 inhibitor for a *C. gattii* and/or a *C. albicans* infection. Data would provide evidence as to whether *C. neoformans*, *C. gattii* and *C. albicans* share common cellular machinery to drive a vomocytosis event (Figure 24 and 25). Addition of the ERK5 inhibitor, XMD17-109, significantly increased the rate of *C. gattii* vomocytosis from J774A.1 murine macrophages when compared to the DMSO treated control ($n = 4$, $X^2 = 18.69$, $p < 0.001$). These data suggest that *C. gattii* and *C. neoformans* use possibly conserved evolutionarily similar cellular machinery, to elicit a vomocytosis event.

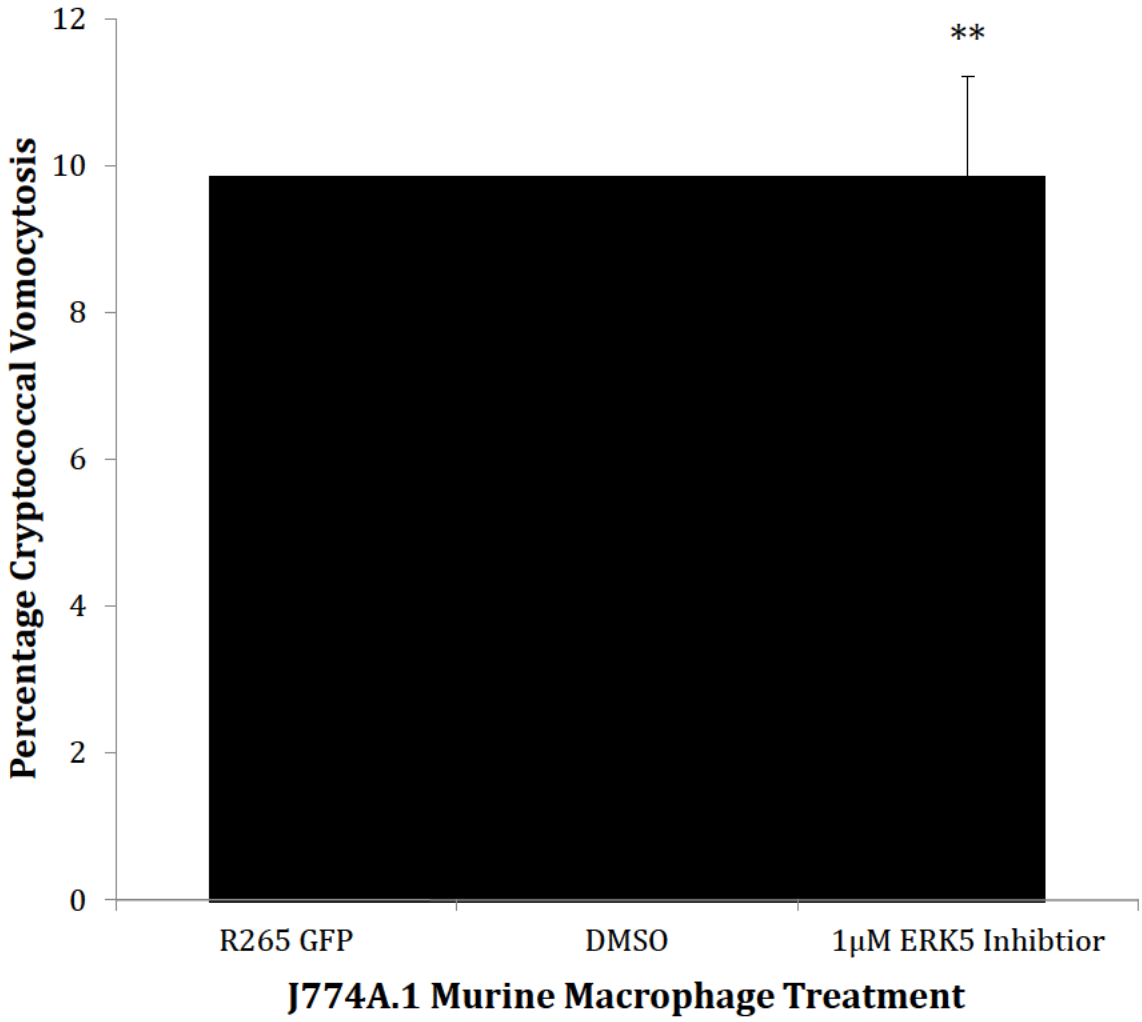

Figure 24: Vomocytosis rates for the treatment of *C. gattii* (R265 GFP) infected J774A.1 macrophages with *XMD17-109*. Error bars = SEM. ** $p < 0.001$ comparing the vomocytosis rates for the ERK5 inhibitor, XMD17-109, treatment with the DMSO control ($n = 4$).

The effects of the ERK5 inhibitor, XMD17-109, were investigated in relation to *C. albicans* vomocytosis. As the conditions used for the phagocytosis assay are strong inducers of filamentation (CO_2, 37ºC etc.), which results in macrophage lysis, complicating vomocytosis scoring, we used two strains with impaired filamentation

rates; a wild type strain, WT 529L (**Moyes *et al.,* 2010**), with a reduced filamentation rate and a RH20 cyr1 + pSM2 mutant incapable of filamenting (**Hall *et al.,* 2011**). Addition of the ERK5 inhibitor, XMD17-109, had no effect on the rates of vomocytosis from J774A.1 murine macrophages when compared to the DMSO control ($X^2 = 0.85$, $p = 0.356$, $n = 3$) (Figure 25). Although these data suggest that *C. albicans* may use alternative cellular machinery to elicit a vomocytosis event, this cannot be stated with certainty, as fewer phagocytosed *C. albicans* cells were counted inducing wide variation within the data set.

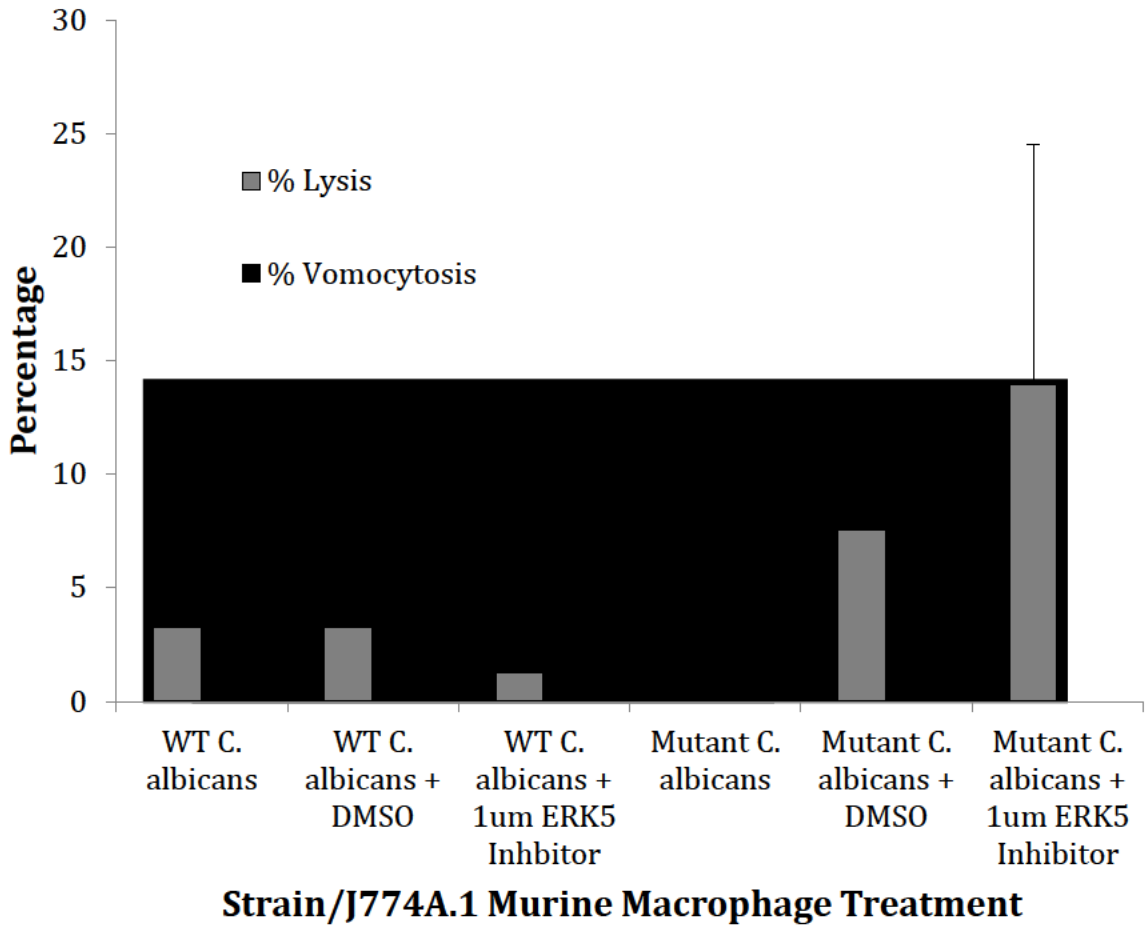

Figure 25: Vomocytosis rates for the treatment of *C. albicans* infected J774A.1 macrophages with *XMD17-109*. Error bars = SEM, n = 3. No significant differences were observed in the data set.

As has been previously reported (**Alvarez and Casadevall, 2006; Ma *et al.*, 2006**), heat killed cryptococci or latex beads are unable to undergo vomocytosis, suggesting that viable cryptococci are required. To investigate whether vomocytosis is predominantly macrophage driven or cryptococcal driven we treated latex bead infected J774A.1 macrophages with the ERK5 inhibitor, XMD17-109. As ERK5 inhibition has been shown to enhance vomocytosis in live *C. neoformans* and *C. gattii* we hypothesised that vomocytosis of latex beads may be observed when macrophages were treated with XMD17-109 (Figure 26).

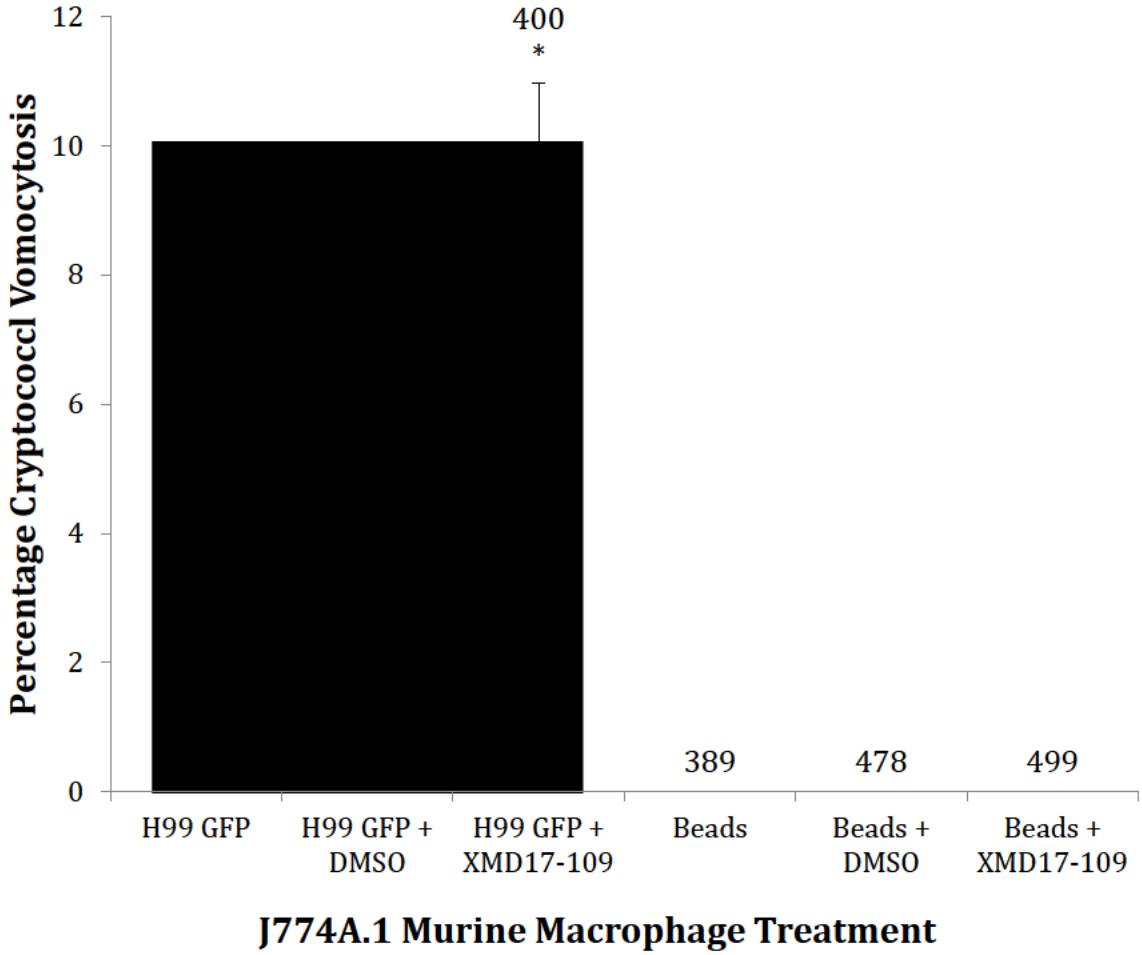

Figure 26: Vomocytosis rates for the treatment of *C. neoformans* (H99 GFP) and latex bead infected J774A.1 macrophages with *XMD17-109*. The percentage of *C. neoformans* (H99 GFP) vomocytosis events from J774A.1 murine macrophages when treated with 1μM XMD17-109 compared to the DMSO and untreated control (**BLACK**). The percentage of bead vomocytosis events from J774A.1 murine macrophages when treated with 1μM XMD17-109 compared to the DMSO and untreated control (**NO BARS**). Error bars = SEM, $X^2 = 4.81$, * $p < 0.05$, n = 3. The numbers above each treatment bar correspond to the number of phagocytosed particles (H99 GFP or Latex Bead) counted.

C. neoformans infected macrophages had an enhanced rate of vomocytosis when treated with the ERK5 inhibitor, XMD17-109 ($X^2 = 4.81$, * $p < 0.05$, $n = 3$). These data show that the ERK5 inhibitor was re-producing the phenotype previously reported for *C. neoformans*, however this effect is not seen for macrophages containing latex beads. Regardless of treatment no vomocytosis events were observed for latex bead containing macrophages, indicating that natural biological agents are essential to drive vomocytosis. Furthermore, the rates of vomocytosis were investigated with heat-killed cryptococci treated with the ERK5 inhibitor, XMD17-109 (Figure 27).

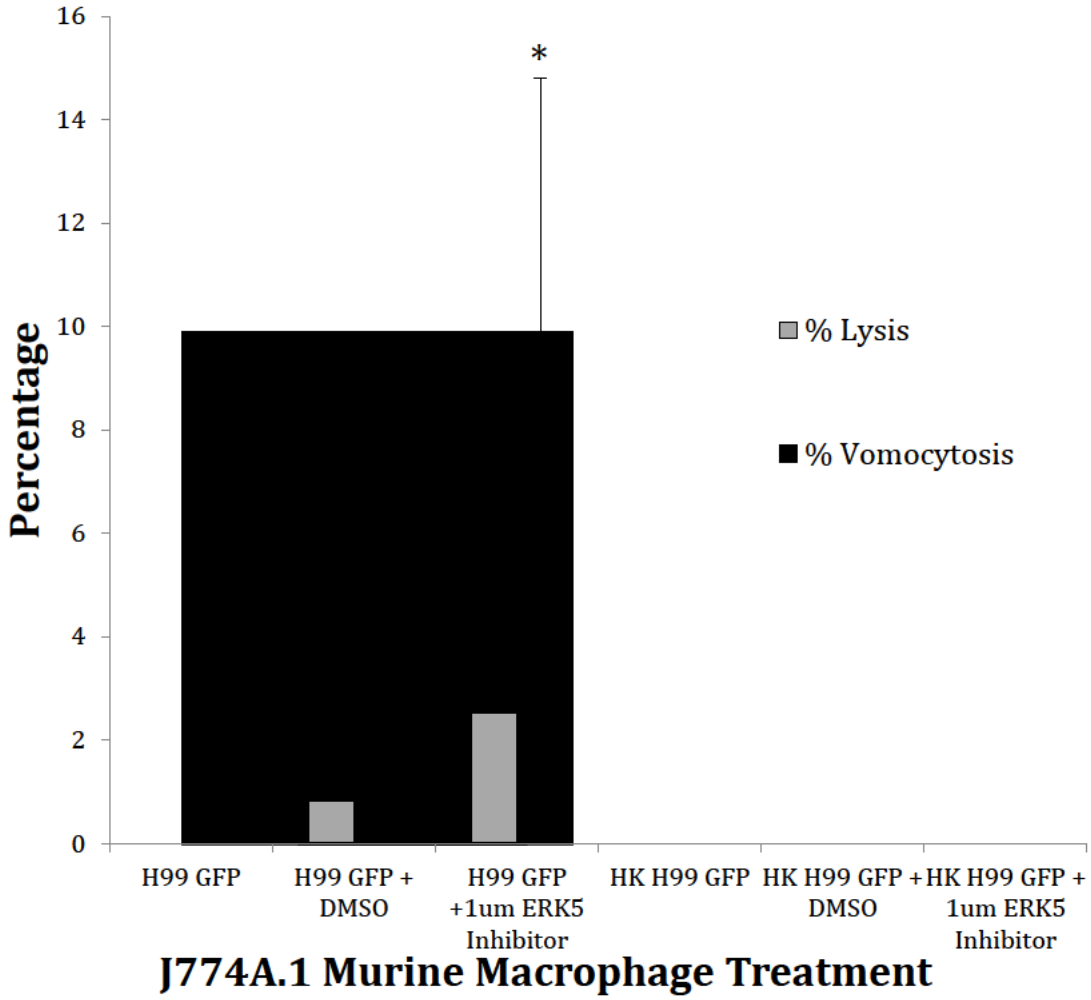

Figure 27: Vomocytosis rates for the treatment of live and dead *C. neoformans* infected J774A.1 macrophages with *XMD17-109*. The percentage of live *C. neoformans* (H99 GFP) vomocytosis events (**BLACK**) from J774A.1 murine macrophages when treated with 1μM XMD17-109 compared to the DMSO and untreated control. The **GREY** bars show macrophage lysis. No vomocytosis events were observed for the HK cryptococci as has been previously reported. Error bars = SEM, $X^2 = 4.81$, * $p < 0.05$, n = 2.

As previously reported no vomocytosis events were observed with Heat Killed (HK) cryptococci – confirmed via plating for Colony Forming Units (CFUs). The macrophage may detect that the pathogen is not metabolically active and resisting destruction; therefore, the prey is not expelled, as the macrophage should be capable of destroying the pathogen. This observation agrees with the literature and furthermore suggests that interplay between prey and host is required to induce a vomocytosis event.

The ERK5 Inhibitor Enhances Vomocytosis in Human Primary Macrophages

To test whether ERK5 inhibition also enhances vomocytosis in human primary macrophages, blood was taken from volunteer donors and monocyte-derived macrophages were isolated and differentiated, before being infected with cryptococci. Samples were treated with the ERK5 inhibitor and the rates of vomocytosis compared to the DMSO treated control were measured (Figure 28). A protein BLAST was run to compare the similarities of murine ERK5 and human ERK5. The two ERK5 proteins of humans and mice were shown to be 91.94% homologous and may therefore share a similar activation site, however this is not necessarily true as the activation site may be located in the non-homologous ~ 8% region.

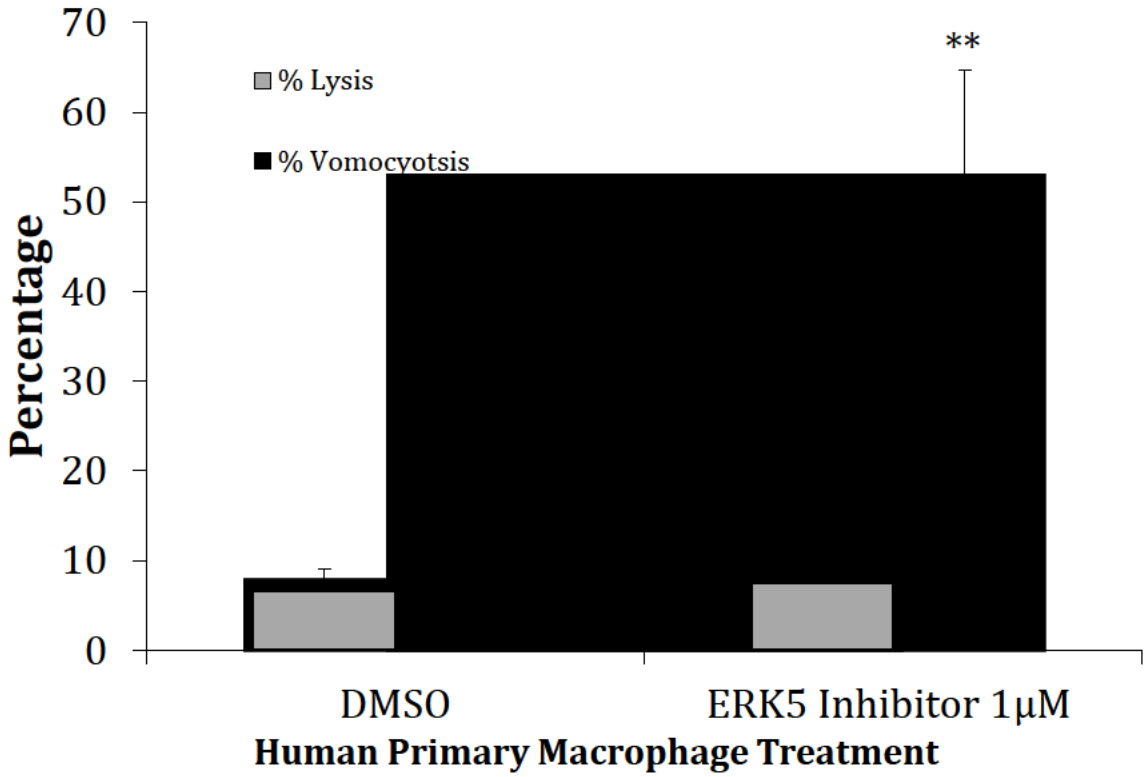

Figure 28: Vomocytosis rates for the treatment of *C. neoformans* (H99 GFP) infected human macrophages with *XMD17-109*. The percentage of cryptococcal (H99 GFP) vomocytosis events and human primary macrophage lysis events (n=6). Error bars = SEM, $X^2 = 21.93$, ** $p < 0.001$ comparing the vomocytosis rates for the ERK5 inhibitor treatment with the DMSO control.

As with J774A.1 and RAW264.7 cells, the presence of 1µM of the ERK5 inhibitor, XMD17-109, significantly enhances the rates of cryptococcal vomocytosis from human primary macrophages (Figure 28). Error bars = SEM, $X^2 = 21.93$, ** $p < 0.001$, n = 6. Human primary macrophages have been reported to vomocytose more frequently then cell lines and this effect has been observed in this study (**Alvarez and Casadevall, 2006; Ma *et al.*, 2006, Voelz *et al.*, 2009**).

The ERK5 Inhibitor has no Effect on Extracellular Cryptococcal Growth or Phagocytosis Rates of Human Primary Macrophages or Murine Cell Lines but does affect Intracellular Proliferation of Cryptococci

To test whether ERK5 inhibition impacted on phagocytic uptake of cryptococci, the first frames of the time-lapse movies were used to determine the differences in the phagocytosis rates between treatments. Percentage phagocytosis was calculated by counting the numbers of infected macrophages compared to the total macrophages. BIX02189, a MEK5 inhibitor was introduced into the studies. MEK5 is the only known upstream activator, via phosphorylation, of ERK5 and it was hypothesised that similar results to ERK5 inhibition would be observed with this inhibitor. Curiously, 3μM of BIX02189 induced rapid GFP loss and death of intracellular cryptococci over the course of the 18hr time-lapse – a similar effect had been previously noted with XMD17-109 treatment. The rate of vomocytosis, for the BIX02189 treatment, was significantly increased from the DMSO control ($X^2 = 3.69$, $p = 0.05$, $n = 3$) but intracellular *Cryptococcus* death rate was very high potentially masking any further vomocytosis rate differences (Figure 29).

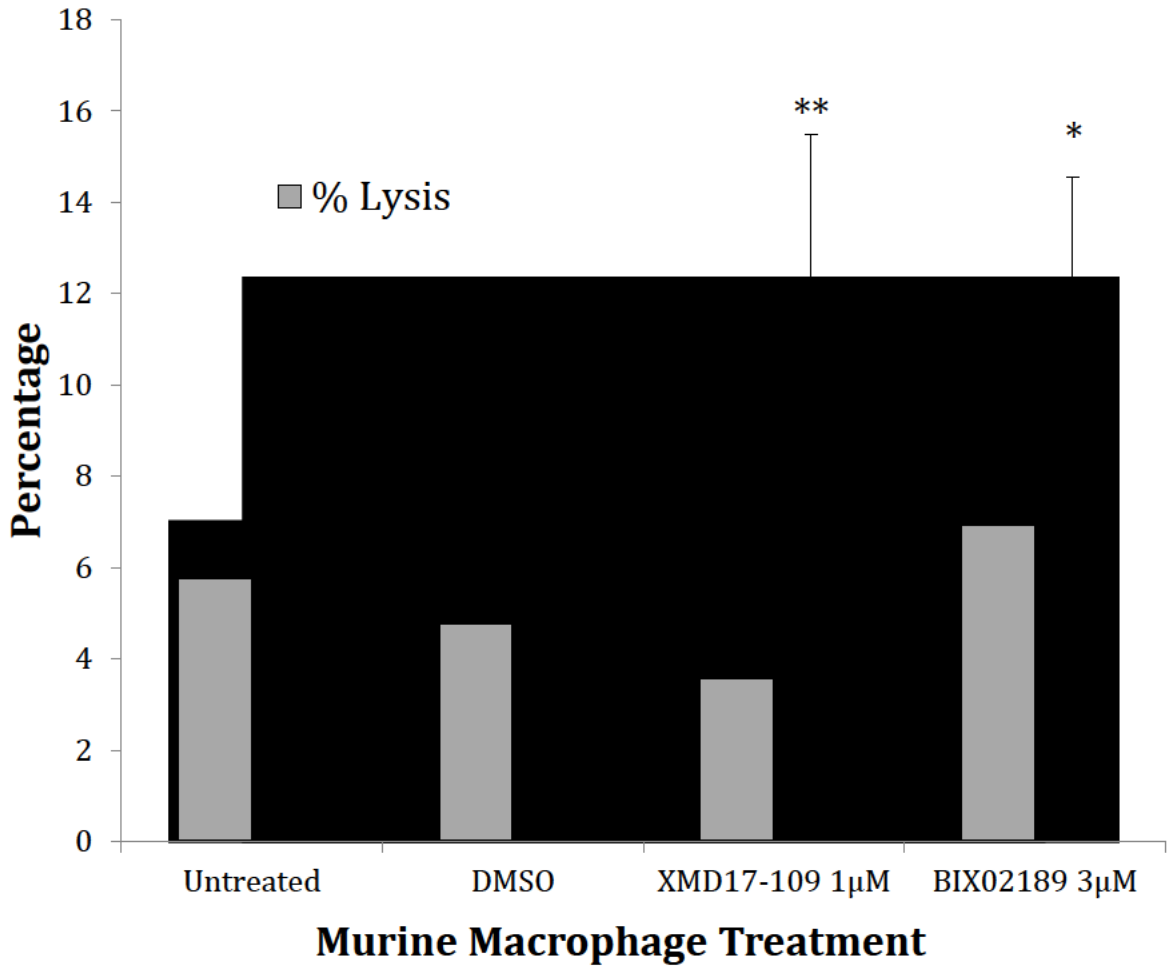

Figure 29: Vomocytosis rates for the treatment of *C. neoformans* (H99 GFP) infected J774A.1 murine macrophages with *XMD17-109* and *BIX02189*. The percentage of cryptococcal (H99 GFP) vomocytosis events (BLACK) and macrophage lysis events (GREY) (n=3). Error bars = SEM, * $p = 0.05$, ** $p < 0.01$ comparing the vomocytosis rates for the inhibitor treatments with the DMSO control.

No differences were observed between the original phagocytosis rates of the J774A.1 murine macrophage cell line when inhibitor treatments (XMD17-109 and LRRK2-IN1) were compared to the DMSO control (Figure 30) (ANOVA – $F = 0.526$, $p = 0.72$, $n = 3$). Similarly, no difference was observed between the phagocytosis rates of the human

primary macrophages when inhibitor treatments are compared to the DMSO control (Figure 31) (ANOVA – F = 0.037, p = 0.99, n = 6). No difference was observed between the extracellular growth curves of H99 GFP when treated with the ERK5 inhibitor (Figure 32). Interestingly the average number of buds that each phagocytosed "mother cell" produces over the course of the time-lapse movies, is significantly reduced, compared to the DMSO control, when cells are treated with the respective inhibitors (Figure 33).

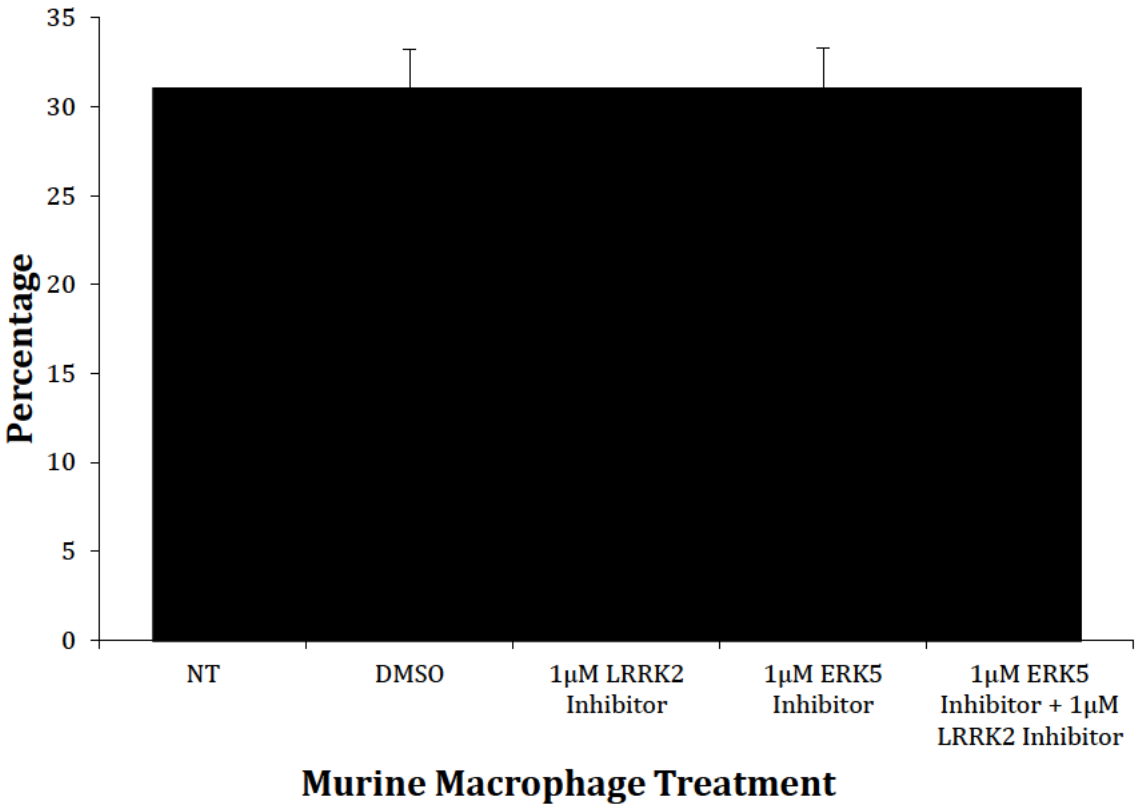

Figure 30: Phagocytosis rates for J774A.1 murine macrophages treated with *LRRK2-IN1* and *XMD17-109* combined. The percentage of J774A.1 murine macrophages that have successfully phagocytosed at least a single *Cryptococcus* when treated with both the LRRK2 inhibitor, LRRK2-IN1, and the ERK5 inhibitor, XMD17-109, (n = 3). Error Bars = SEM.

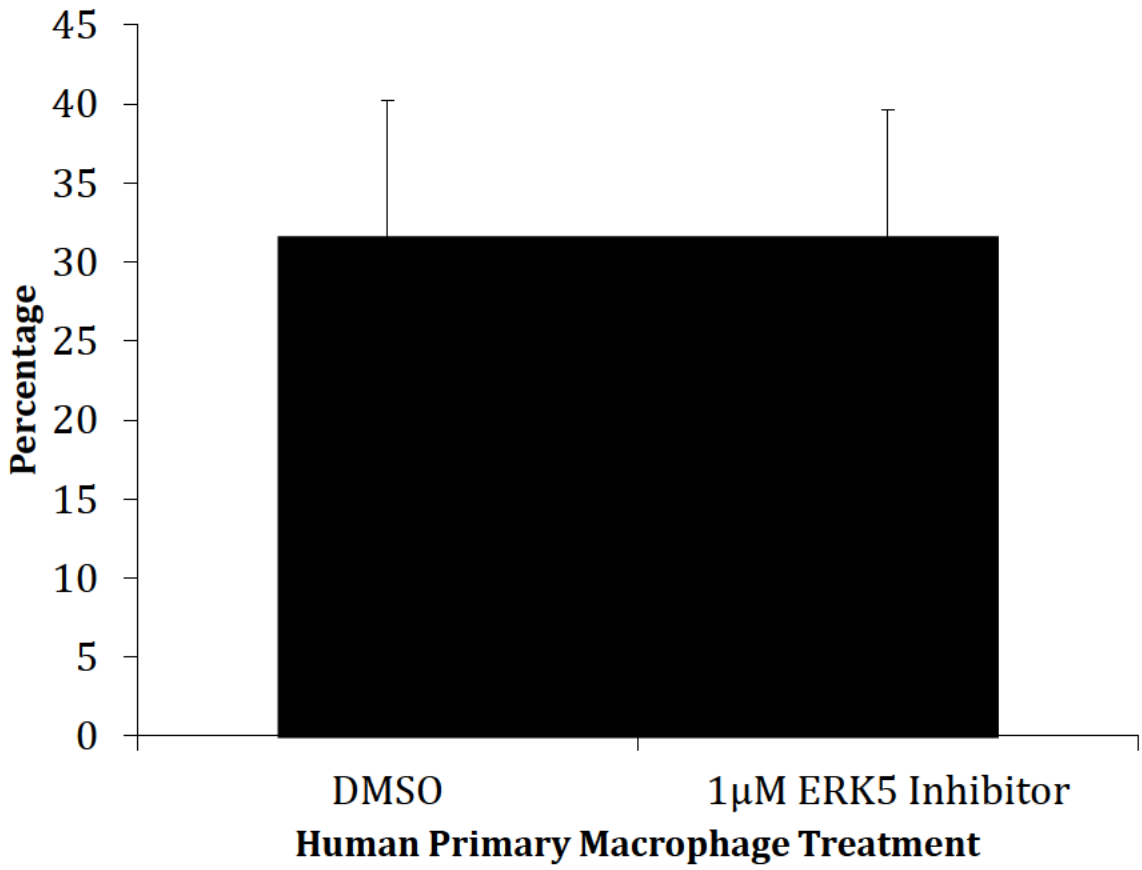

Figure 31: Phagocytosis rates for human primary macrophages treated with *XMD17-109*. The percentage of human primary macrophages that have successfully phagocytosed at least a single cryptococci when treated with the ERK5 inhibitor, XMD17-109 and the DMSO control (n = 6). Error Bars = SEM.

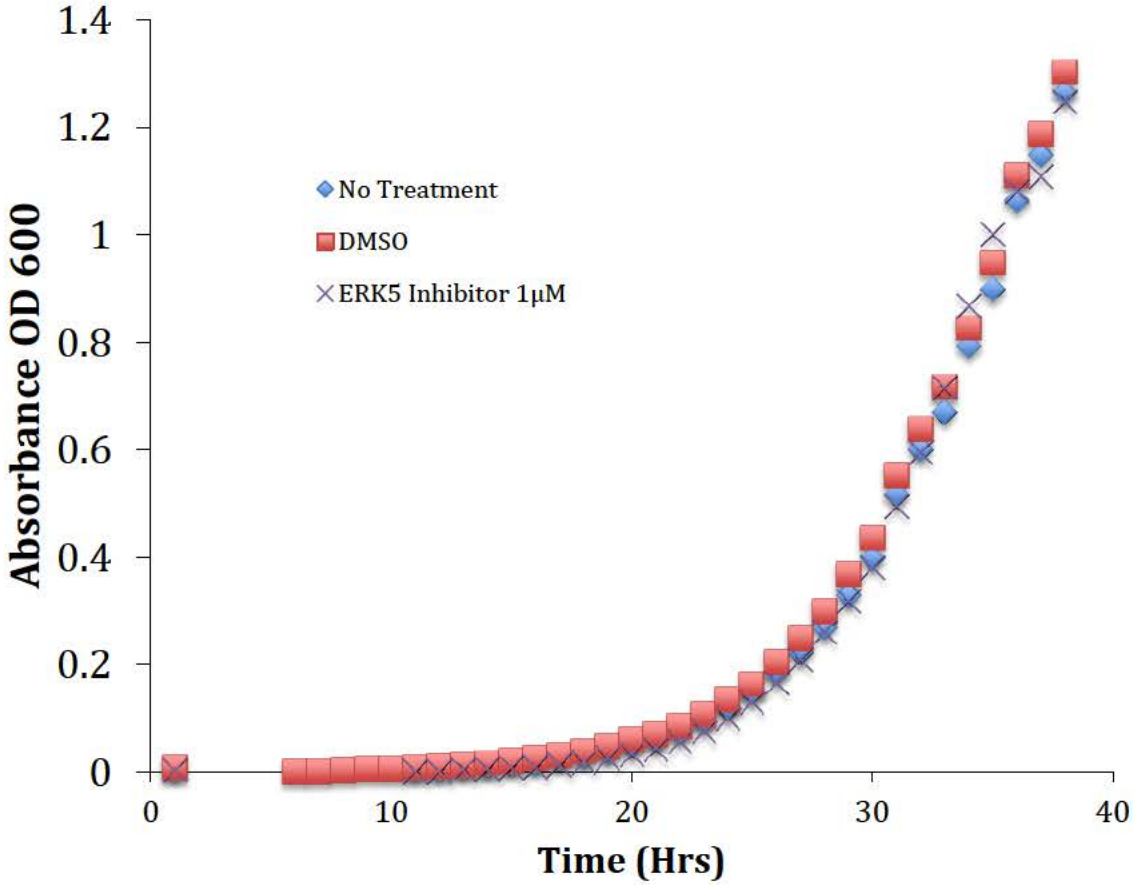

Figure 32: Extracellular growth curve of *C. neoformans*, H99 GFP when treated with controls and the ERK5 inhibitor, XMD17-109 (n = 3).

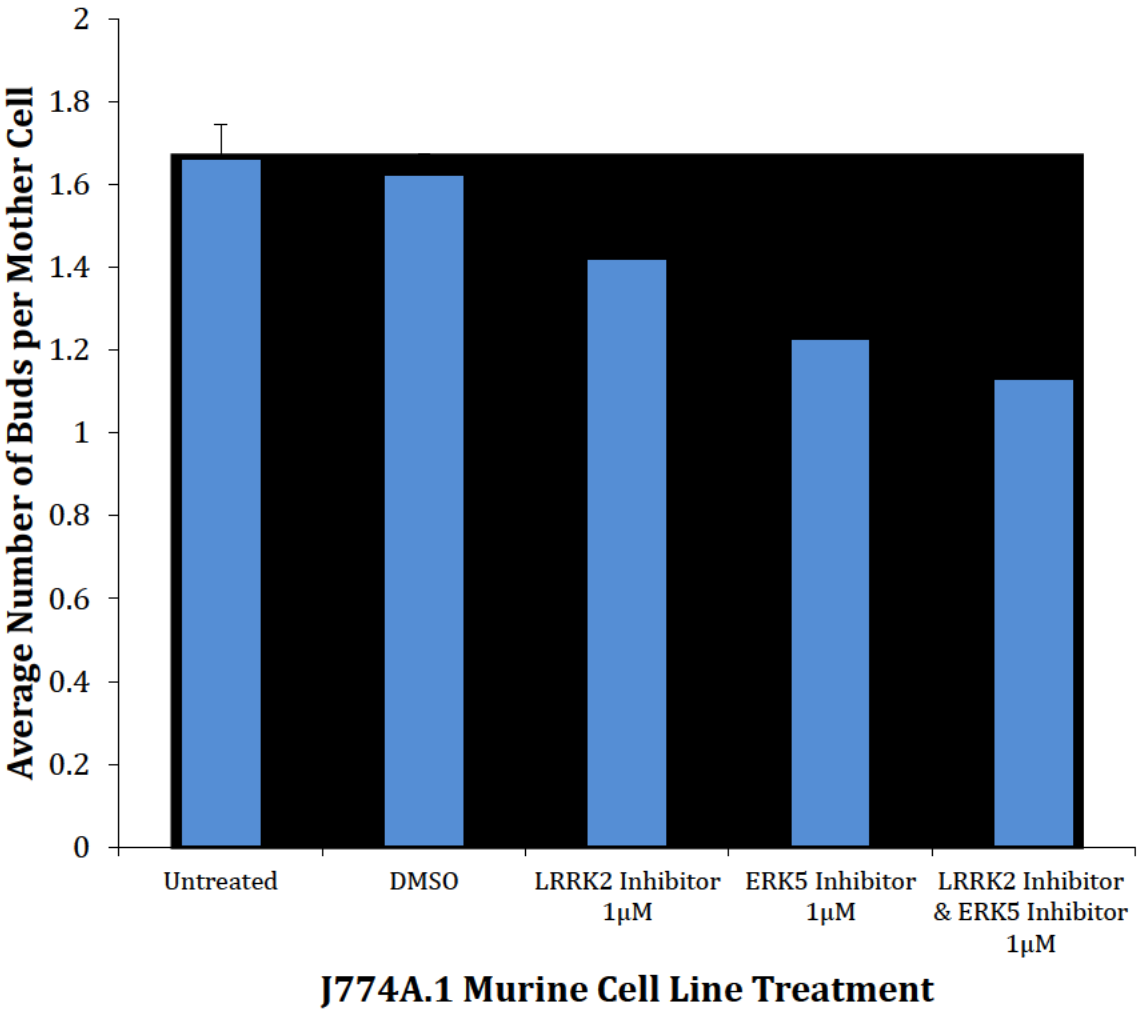

Figure 33: The average number of buds produced per "mother cell" in J774 A.1 murine macrophages when treated with *LRRK2-IN1* and *XMD17-109*. Error Bars = SEM, * $p < 0.01$, $n = 3$.

The reduction in intracellular cryptococcal replication was intriguing and worthy of further investigation. Intracellular proliferation rate (IPR) and Colony forming Unit (CFU) assays were performed on cryptococcal infected macrophages with and without treatment (Figure 34 and Figure 35). MEK5, the MAPKK and hence activator of ERK5 was inhibited in these studies using, BIX02189 and the effects on IPR and CFU observed.

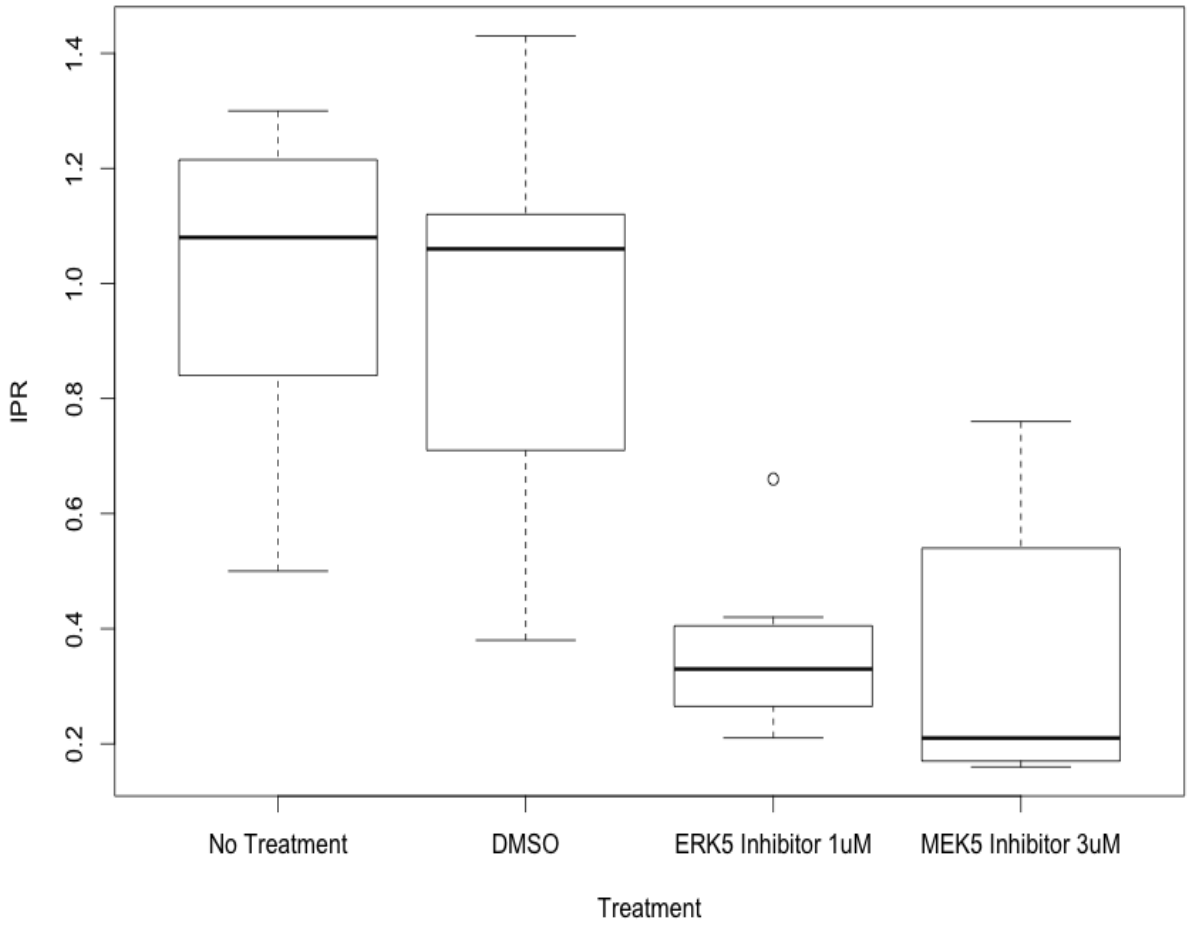

Figure 34: The Intracellular Proliferation Rate (IPR) of phagocytosed cryptococci and the respective inhibitor treatments in J774A.1 murine macrophages (n = 7).

An ANOVA statistical analysis highlighted a significant difference between the treatments (ANOVA – $F = 11.52$, $p < 0.001$, $n = 7$). Tukey's post-hoc analysis revealed significant differences as follows:

ERK5 Inhibitor – DMSO – $p = 0.003$, MEK5 Inhibitor – DMSO – $p = 0.003$, No Treatment – ERK5 Inhibitor – $p = 0.001$ and No Treatment – MEK5 Inhibitor – $p = 0.001$. No differences were seen between No Treatment and DMSO and between the ERK inhibitor and MEK5 inhibitor treated cells. These data show that the inhibitors reduce the intracellular proliferation rate of the cryptococci in macrophages. This reduction may be observed due to the increase in vomocytosis rates, hence reducing the IPR. To begin to answer this question we looked at the viability of the intracellular cryptococci present at the end of the 18-hour time course. The IPR lysates were diluted and plated out to measure the viability of the cryptococci.

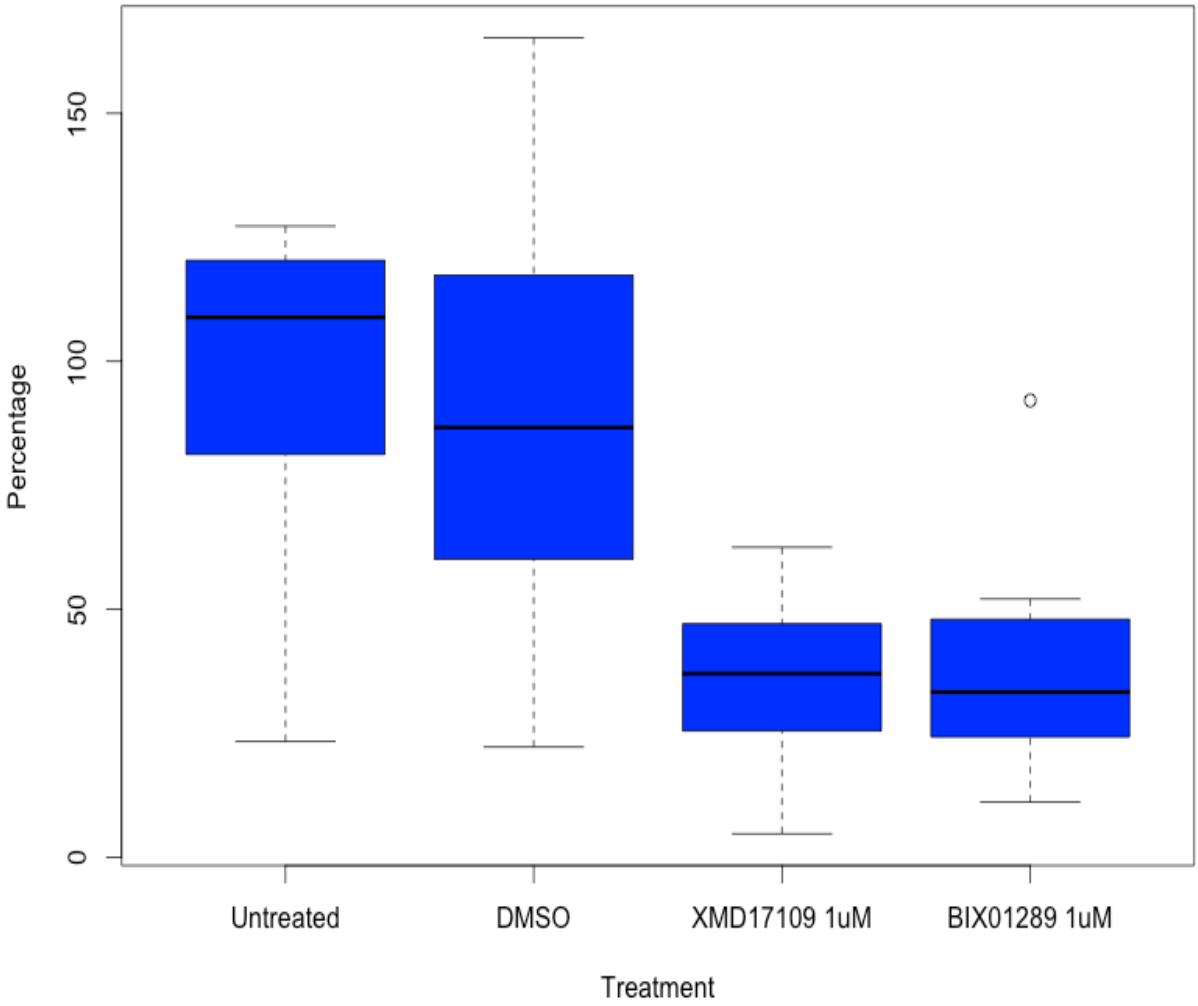

Figure 35. The Colony Forming Units (CFU) expressed as a percentage of the T_0 value, for phagocytosed cryptococci and the respective inhibitor treatments in J774A.1 murine macrophages (n = 7).

An ANOVA statistical analysis highlighted a significant difference between the treatments (ANOVA – $F = 6.673$, $p < 0.003$, $n = 7$). Tukey's post-hoc analysis revealed significant differences as follows:

ERK5 Inhibitor – DMSO – $p = 0.013$, MEK5 Inhibitor – DMSO – $p = 0.033$, No Treatment – ERK5 Inhibitor – $p = 0.017$ and No Treatment – MEK5 Inhibitor – $p = 0.043$. No

differences were seen between No Treatment and DMSO and between the ERK inhibitor and MEK5 inhibitor treated cells. These data show that the inhibitors reduce the colony forming units of the phagocytosed cryptococci; therefore the reduction in IPR can be attributed to both vomocytosis and intracellular cryptococcal killing.

These data suggest that the inhibitor is targeting and acting upon macrophage ERK5 and not cryptococcal ERK5. Cryptococcal extracellular growth is unaffected (Figure 32), however intracellular cryptococcal replication is reduced in the presence of the inhibitor. The reduction in IPR and CFU's may arise due to alterations in the maturation of the phagosome to a lysophagosome. The lysophagosome may become more antimicrobial (more acidic hence better proteolytic activities) in the presence of the ERK5 and MEK5 inhibitors, creating a more hostile environment for the intracellular cryptococci. In 2015, Smith *et al.,* used Lysotracker Red, a pH sensitive dye that illuminates red in acidic conditions, to investigate the phagosome maturation during *Cryptococcus* infection. A similar approach was used to investigate phagosome maturation of cryptococcal-infected macrophages in the presence of the two inhibitors.

Analysis of the movies identified that the presence of either of the inhibitors induces cryptococcal death-like events within macrophages. These events begin with a loss of the GFP signal, followed by the condensing of the cryptococcal particle and ultimately complete destruction of the pathogen. The results suggest that the cryptococci are either killed, vomocytose or induce macrophage lysis in the presence of the ERK5

inhibitor. To confirm that the lysophagosome is being manipulated by in the presence of ERK5 inhibitor, the cell dye Lysotracker Red was used, similar to the work undertaken by Smith *et al.,* in 2015 (Figure 36). J774A.1 murine macrophages were infected with H99GFP treated with the respective inhibitors and analysed for Lysotracker positivity. Figure 36 highlights that treatment of infected macrophages with the respective inhibitors increases the rate of Lysotracker positivity.

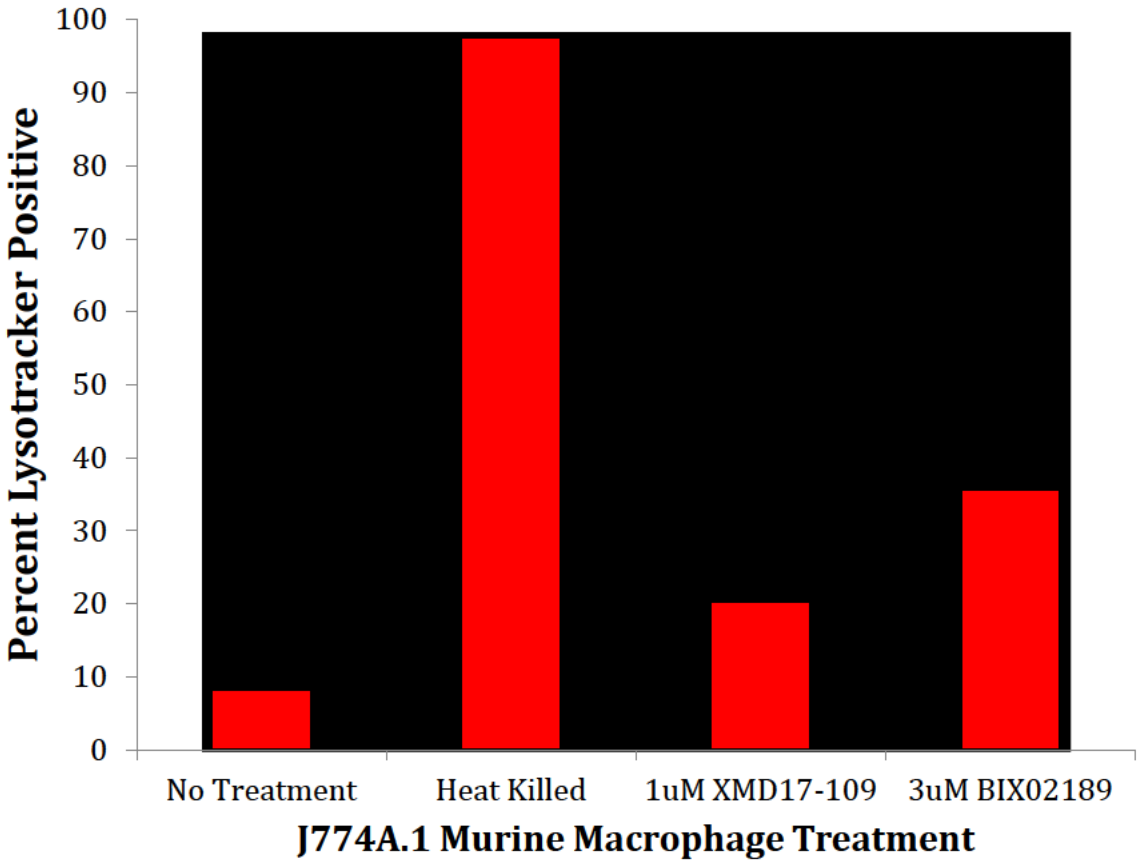

Figure 36: The percentage of Lysotracker positive phagocytosed cryptococci combined with inhibitor treatment. Error Bars = SEM, *** P<0.0001. Chi Squared (X^2) test comparing the inhibitor treatments to the no treatment control (Bonferroni Correction 0.05/2 = 0.025).

The ERK5 Inhibitor Modifies the Cytokine Profile Secreted by Infected Macrophages towards a Pro-inflammatory Response

Previous research suggested that human primary macrophages supplemented with IFNγ and TNFα have an enhanced rate of vomocytosis (**Voelz et al, 2009**). Augmenting amphotericin B treatment with IFNγ is known to improve the prognosis of many patients in the clinic and we hypothesise that this may be due to IFNγ enhancing vomocytosis in circulation, allowing better access of the amphotericin B and other immune cells, to destroy the pathogen (**Joly et al, 1994; Lutz et al 2000**). Thus it is possible that the effect of ERK5 inhibition acts via modulating the cytokine secretion levels in infected phagocytes. An initial screen of twelve human cytokines were analysed using the Qiagen Th_1, Th_2 and Th_{17} Multi-Analyte ELISA. The cytokines included were: IL-2, IL-4, IL-5, IL-6, IL-10, IL-12, IL-13, IL-17A, IFNγ, TNFα, G-CSF and TGF-β1. Primary human monocytes were differentiated into macrophages before being infected with *C. neoformans* (H99) and treated with the ERK5 inhibitor, XMD17-109. Multianalyte ELISAs were used to gauge the up and down regulation of individual cytokines (Figure 37 and 38).

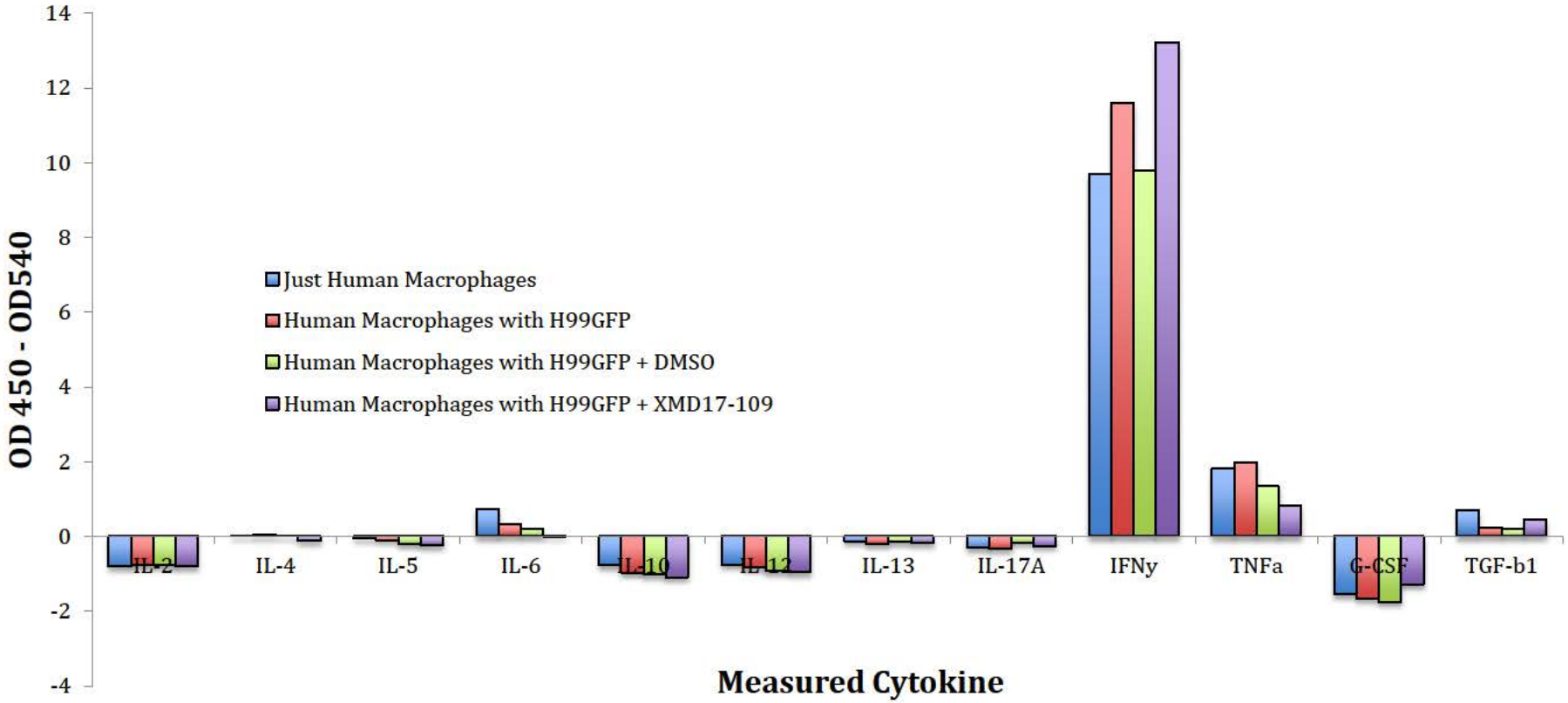

Figure 37: A multianalyte ELISA of 12 Th_1, Th_2 and Th_{17} cytokines comparing infected macrophages with infected macrophages treated plus *XMD17-109* – Repeat 1. Values above 0 represent the cytokines that are detectable above the background levels. The size of the bar represent how well detected an individual cytokine was and enables comparisons between treatments to be made. The multianalyte ELISA does not allow quantification of the cytokines present.

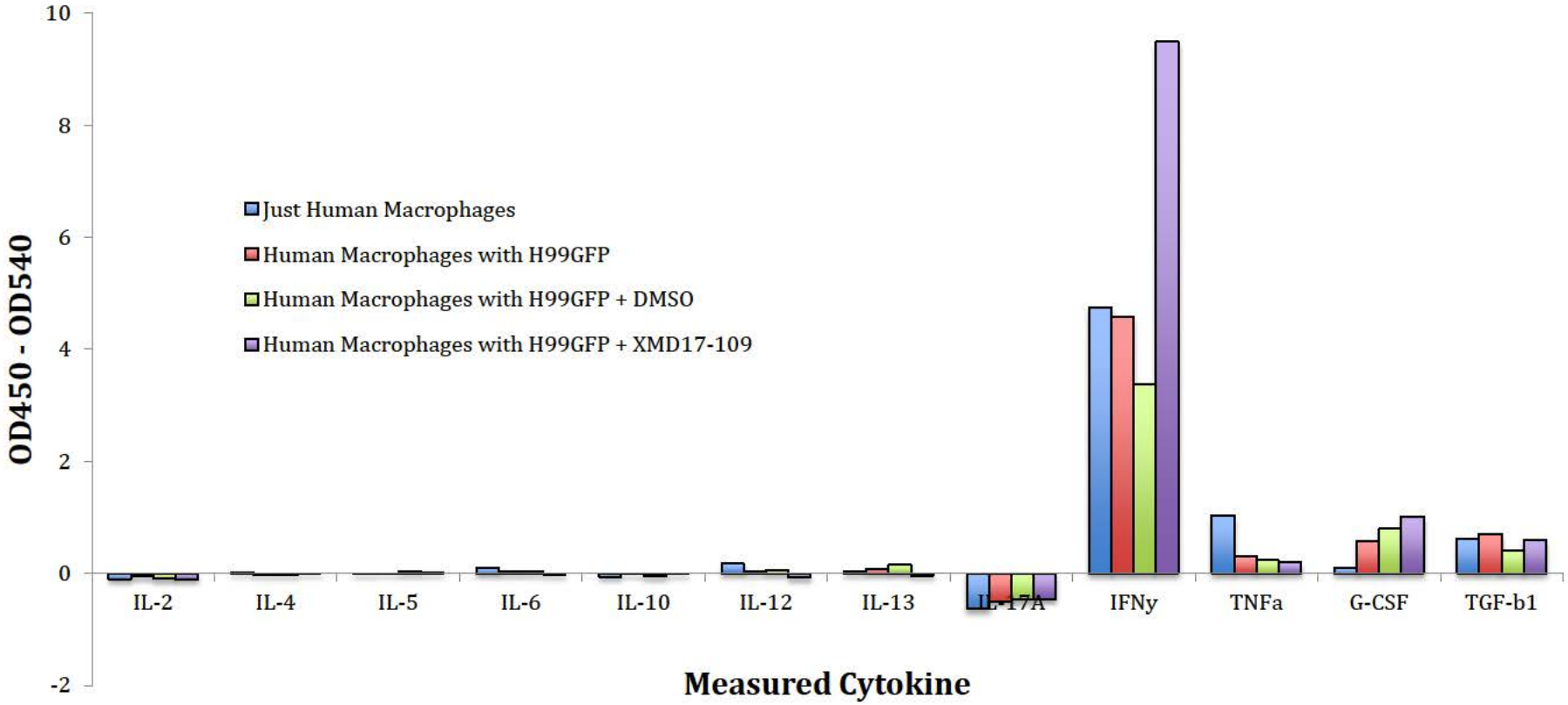

Figure 38: A multianalyte ELISA of 12 Th_1, Th_2 and Th_{17} cytokines comparing infected macrophages with infected macrophages treated plus *XMD17-109* – Repeat 2. Values above 0 represent the cytokines that are detectable above the background levels. The size of the bar represent how well detected an individual cytokine was and enables comparisons between treatments to be made. The multianalyte ELISA does not allow quantification of the cytokines present.

Figures 37 and 38 show the relative regulation of 12 individual cytokines. The assay is only able to demonstrate whether a cytokine is up or down regulated compared to controlled treatments. To quantify the cytokine present per treatment individual ELISAs for that given cytokine were required. From the multianalyte ELISA data IFNγ and TNFα were interesting. Upon treatment of human macrophages with the ERK5 inhibitor, XMD17-109, IFNγ was up regulated whilst TNFα was down regulated. The subtle changes noted in the cytokine profile may explain why we have observed the differences in vomocytosis rates and intracellular killing of cryptococci. Individual ELISAs (R&DSystems) were performed to quantify the amount of cytokines present in each treatment (Figure 39 and 40).

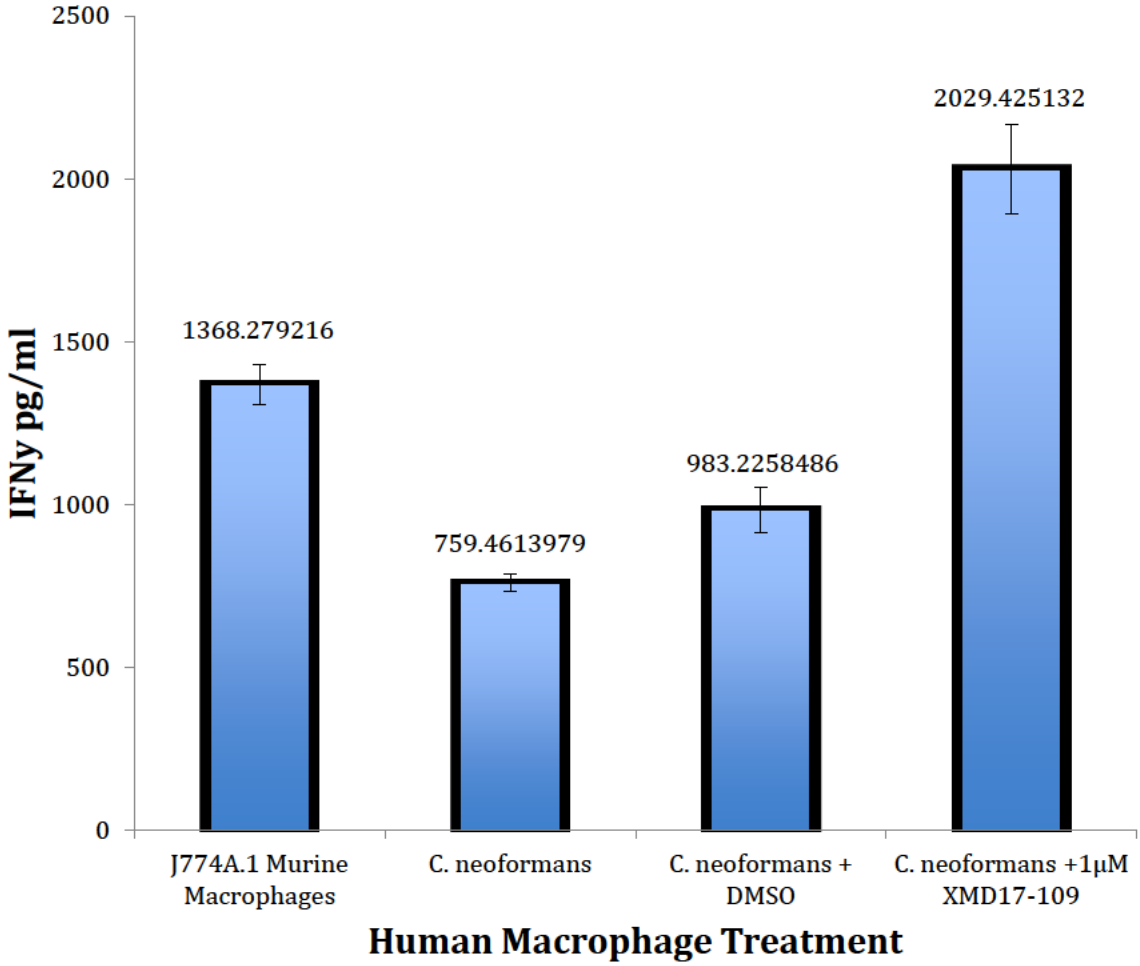

Figure 39: Quantification of IFNγ secreted by infected macrophages with and without ERK5 inhibitor treatment (ANOVA (F-value) = 43.79, p > 0.001, n=4).

Figure 39 shows the quantification of IFNγ secreted by human primary macrophages under a series of different treatment conditions. ANOVA identifies a significant difference between the treatment types (ANOVA (F-value) = 43.79, p > 0.001, n=4), however post hoc analysis is required to decipher where these differences lie. The Tukey's post hoc test revealed significant differences between: J774A.1 murine macrophages vs. *C. neoformans* infected macrophages (p = 0.001). This indicated that a significant reduction of IFNγ was induced upon infection of macrophages. This is in

agreement with the literature highlighting that *C. neoformans* induces an M2 (Th_2) like response from macrophages, aiding survival and overall pathogenesis. Upon treatment with the ERK5 inhibitor, XMD17-109, a significant increase in the secretion of IFNγ compared to all other treatment types ($p > 0.001$) is induced. The data suggests that the ERK5 inhibitor, XMD17-109 is inducing the production of IFNγ and driving macrophages to a more M1 aggressive antifungal phenotype. These data may explain why an increase in vomocytosis and intracellular killing is observed when macrophages are treated with this kinase inhibitor. The above analysis was repeated for TNFα. Human macrophages were treated in the same way and the concentration of TNFα levels were measured.

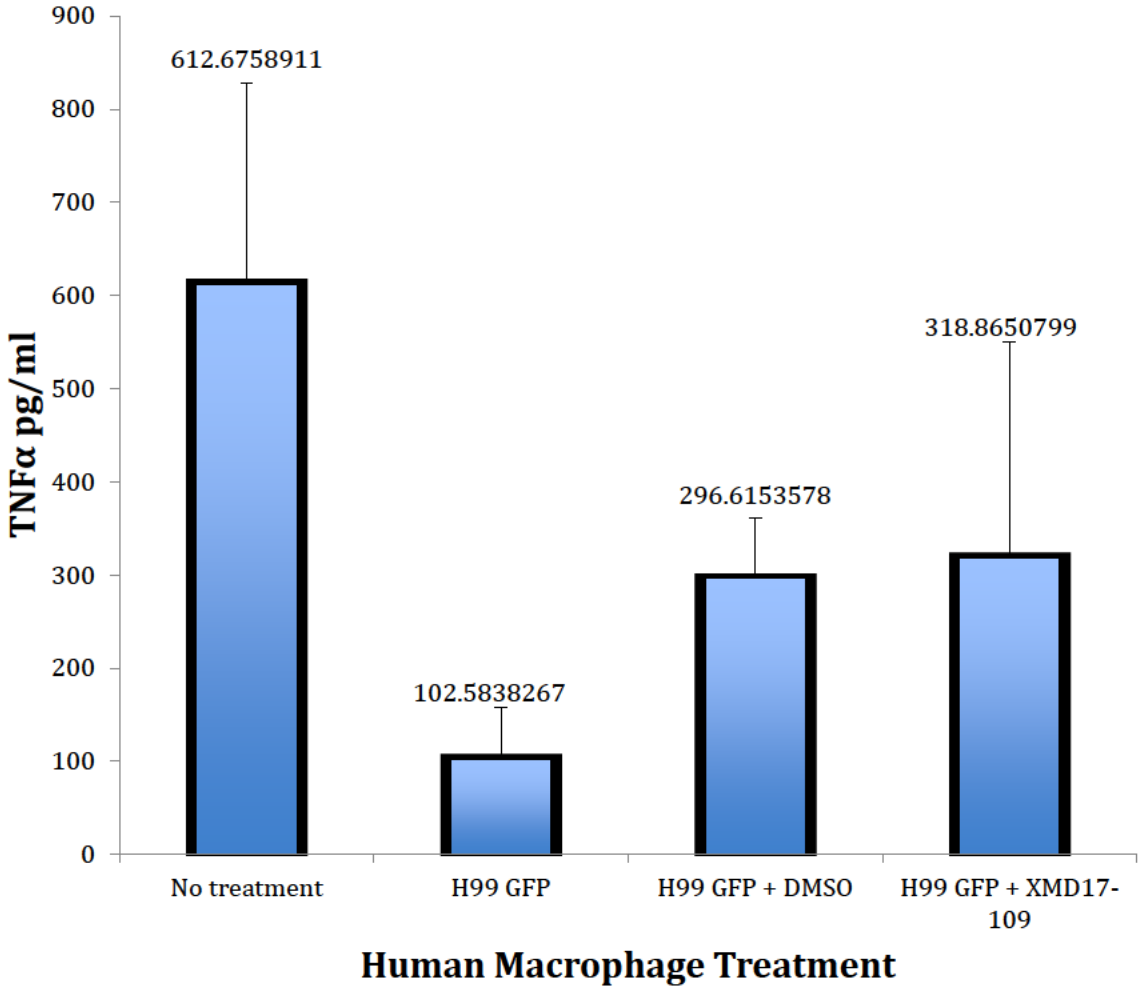

Figure 40: Quantification of TNFα secreted by infected macrophages with and without ERK5 inhibitor treatment (ANOVA (F-value) = 3.31, $p > 0.139$, n=2).

Figure 40 shows the quantification of TNFα secreted by human macrophages under a series of different treatment conditions. Although the graphical representation agrees with the multianalyte ELISA and the values of TNFα secreted appear to be reduced. ANOVA identified no significant differences between the treatment types (ANOVA (F-value) = 3.31, $p > 0.139$, n=2). Post hoc analysis using the Tukey's test revealed no

differences between any of the treatment options. TNFα is not significantly regulated in response to the ERK5 inhibitor treatment in human macrophages.

As the initial observation was observed in cell lines and a large aspect of the research is undertaken using cell lines, the cytokine secretion profiles were explored for J774A.1 murine macrophages. The two secreted cytokines; TNFα and IFNγ were measured, using the R&DSystems single quantification ELISA, for the J774A.1 murine macrophage cell line. J774A.1 murine macrophages were treated in the same way as the human macrophages. Figure 41 shows the ELISA for the murine TNFα ELISA.

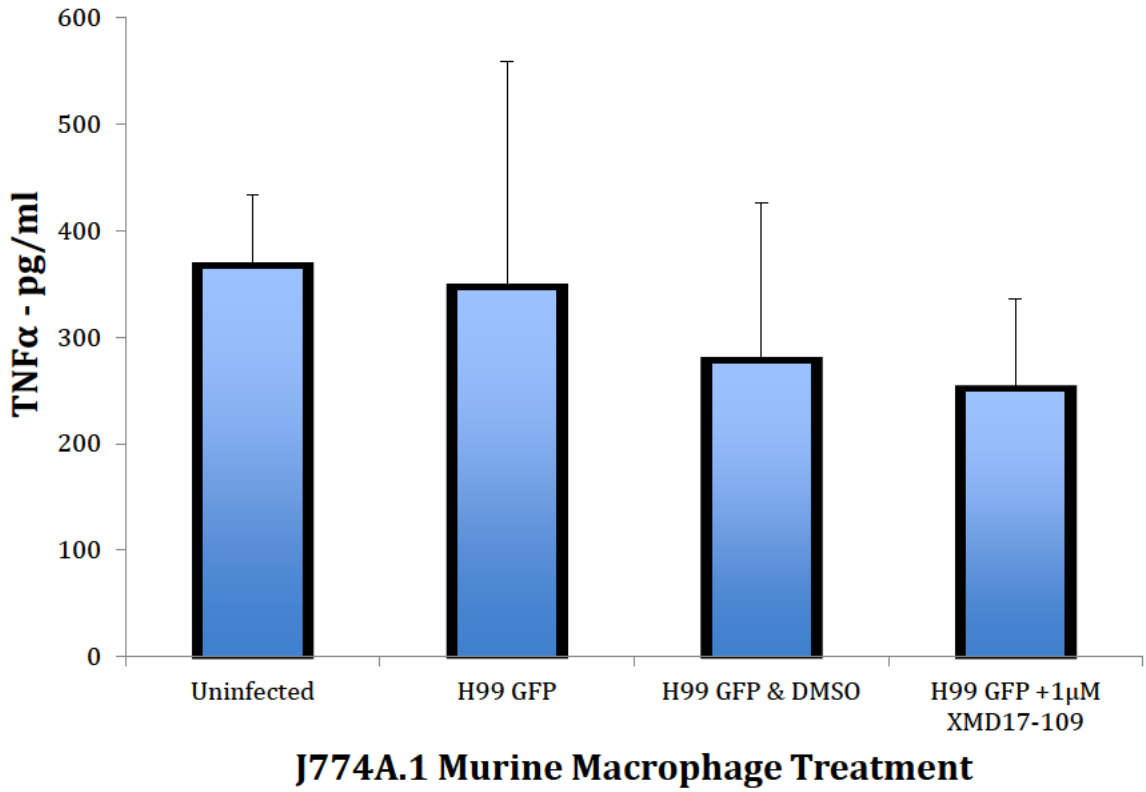

Figure 41: TNFα ELISA showing the concentration of TNFα detected after infecting J774A.1 murine macrophages with *C. neoformans* (H99GFP) and applying different treatments (ANOVA (F-Value) = 0.152, p = 0.925, n = 3). Error Bars = SEM.

The murine TNFα ELISA shows that the levels of the cytokine secreted between treatments are not significantly different (ANOVA (F-Value) = 0.152, p = 0.925, n = 3). The Tukey's post hoc test reveals no significant difference between any of the treatment groups. Similar to the treatment of human macrophages with XMD17-109, the reduction of TNFα is not significant in murine macrophages. These data suggest that TNFα is not regulated by a significantly measurable degree, therefore the ERK5 inhibitor; XMD17-109 has no effect on the secretion of TNFα for both murine and human macrophages. Human cytokine profiling and cytokine quantification, identified IFNγ as a cytokine with a significant increase in secretion from cryptococcal infected macrophages treated with the ERK5 inhibitor, XMD17-109. The concentration of secreted IFNγ was measured from murine macrophages, however the ELISA was incapable of detecting IFNγ in any of the treatments tested. The cause of this was possibly due to the J774A.1 murine macrophages not secreting measureable levels of IFNγ into the media, possibly due to too few macrophages seeded for the assay.

As the data for IFNγ secretion from human macrophages was compelling, the cytokine was deemed worthy of further investigation. We hypothesised that addition of the ERK5 inhibitor was increasing the secretion of IFNγ. This acts as a paracrine signal to other macrophages skewing the macrophage population towards the M1 phenotype, enhancing antifungal activity of the lysophagosome, hence leading to pathogen escape or destruction of the cryptococci from the host. Previous reports suggest that addition of exogenous IFNγ result in an increase in the vomocytosis rates (**Voelz *et al.,* 2009**).

Therefore the addition of increasing concentrations of exogenous IFNγ was performed and the rates of vomocytosis from each condition measured (Figure 42).

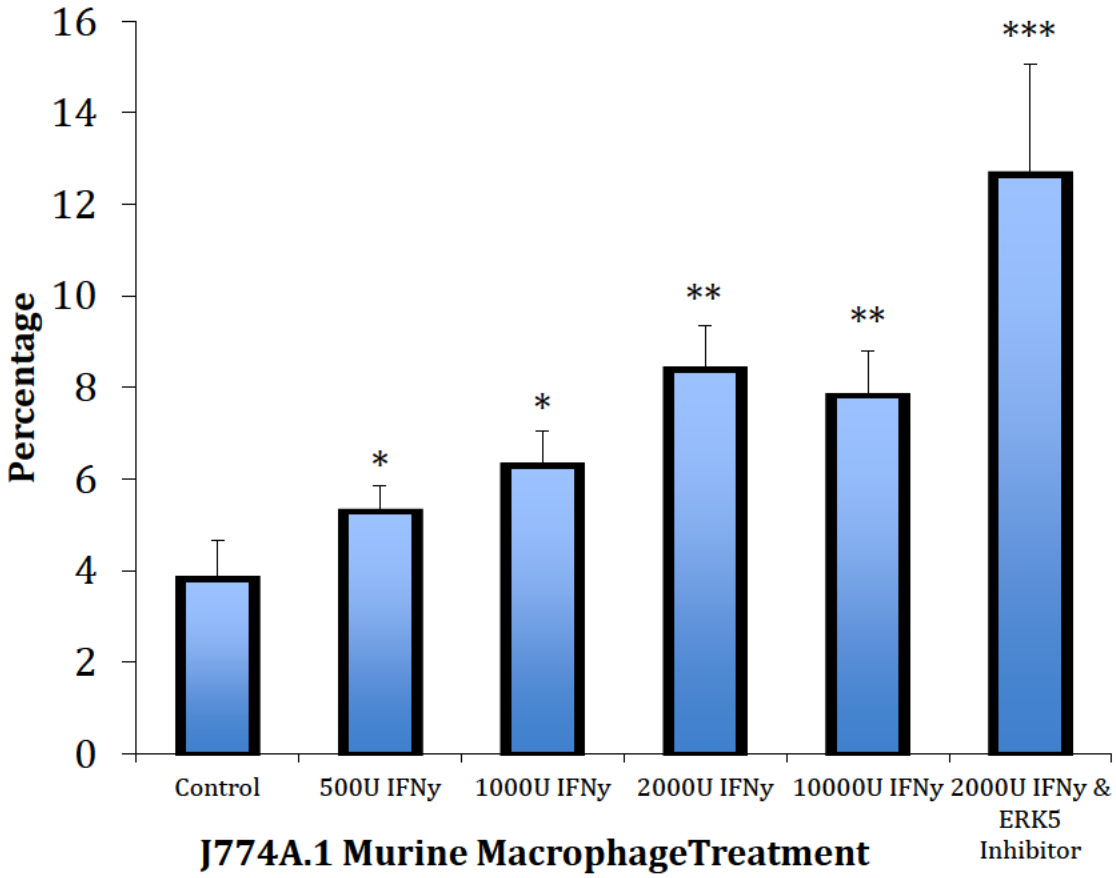

Figure 42: Vomocytosis rates for *C. neoformans* (H99GFP) infected murine macrophages (J774A.1) when treated with increasing concentrations of IFNγ. Error Bars = SEM, * $p < 0.05$, ** $p < 0.01$, $p < 0.001$, $n = 9$.

Figure 42 shows that increasing the exogenous IFNγ added to infected macrophages increases the rates of vomocytosis. Initially gradual increasing concentrations of IFNγ induce higher vomocytosis rates at higher concentrations of IFNγ, up to 2000U of IFNγ. However upon saturation of macrophages with IFNγ, 10000U, the rates of vomocytosis are unable to climb higher then ~8%. The maximum vomocytosis rate of macrophages treated with IFNγ was reached. The cytokine profiling and ELISA data suggest that addition of the ERK5 inhibitor; XMD17-109 increases the secretion of IFNγ in human macrophages. These data suggest that we have reached the limit of IFNγ driven vomocytosis, therefore, XMD17-109 was combined with 2000U of IFNγ to see if the rates of vomocytosis could be further increased. This was the case suggesting that the alteration of the IFNγ secretion profile from macrophages treated with XMD17-109 only partially contributed to the phenotype observed. This indicates that alterations in other biological process must be occurring upon inhibitor treatment to increase vomocytosis rates further. The next results chapter will look at the molecular mechanisms of vomocytosis further.

Genetic Reduction of Macrophage ERK5 Enhances Vomocytosis

To independently test a role for ERK5 in regulating vomocytosis, cryptococcal escape from murine macrophages in which ERK5 expression was reduced either by siRNA or genetic knockout approaches, were analysed. J774A.1 murine macrophages were treated for 96 hours with siRNA against ERK5 (Accell SMARTpool MAPK7 siRNA, 1μM) and then infected with H99 GFP and the rates of vomocytosis recorded (Figure 43).

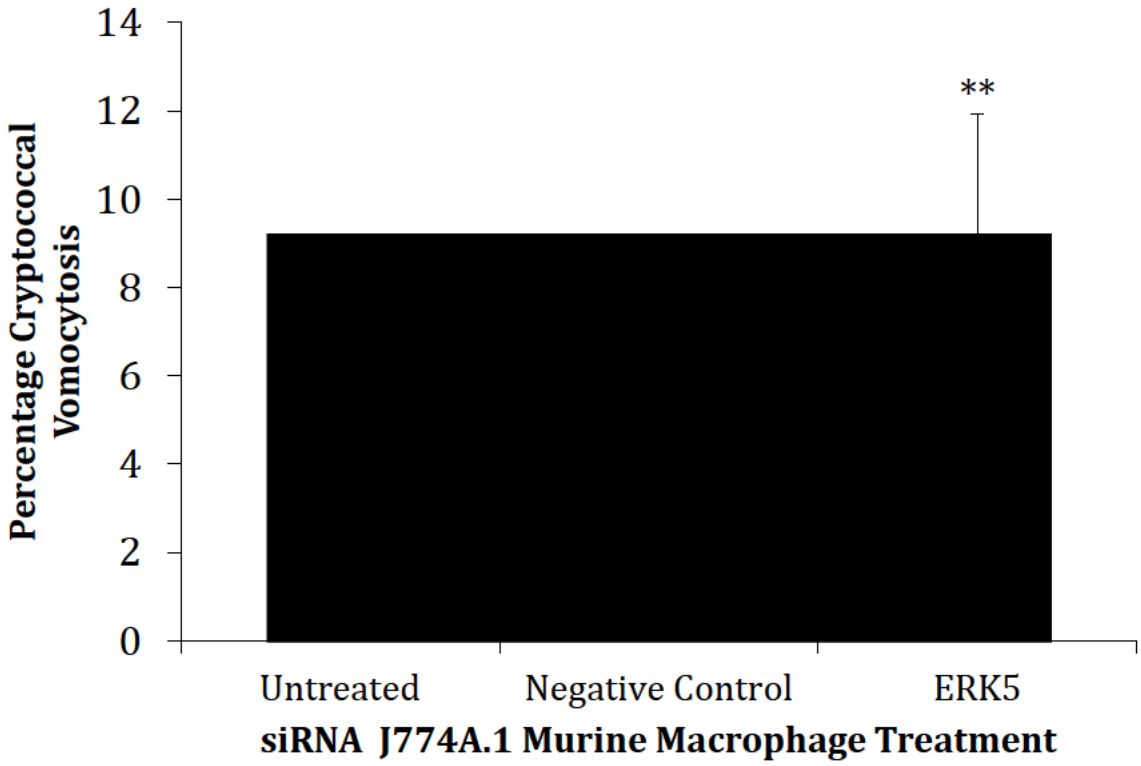

Figure 43: The rates of H99 GFP vomocytosis from J774A.1 murine macrophages treated with ERK5 siRNA. Error Bars = SEM. ** $p < 0.001$, $n = 3$. The siRNA negative control was scrambled siRNA, ensuring that nonsense siRNA did not elicit the same phenotype.

As with pharmacological inhibition, treatment of cells with ERK5 siRNA causes a higher rate of vomocytosis when compared to the untreated control ($X^2 = 10.92$, $p < 0.001$, $n = 3$). These results support the data presented for the inhibitor screen. To confirm that the protein had been down-regulated, Western Blotting was performed using an ERK5 primary antibody (SIGMA ™) (Figure 44).

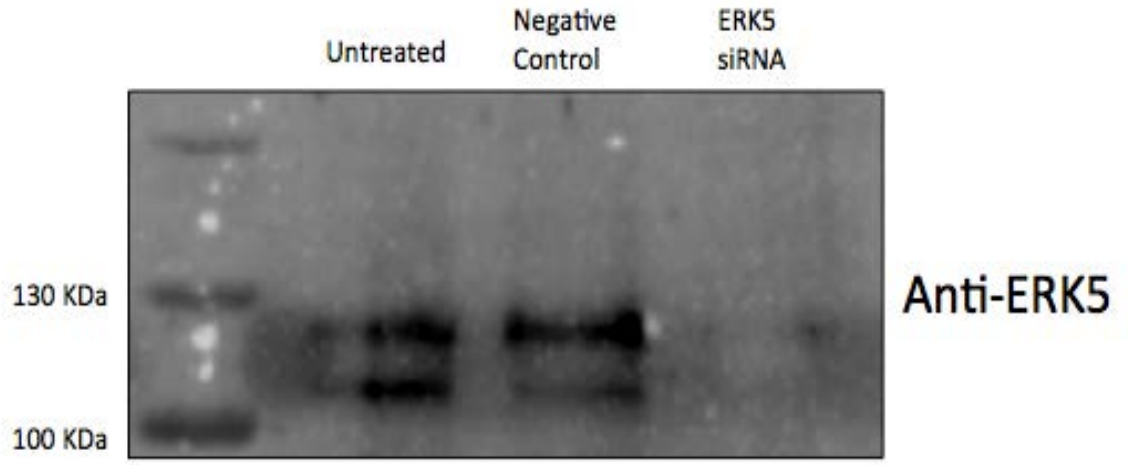

Figure 44: ERK5 Western Blot showing the characteristic double band pattern produced by ERK5 presence when run on a protein gel. Inactivated ERK5 is 110Kda however upon activation the protein becomes hyper-phosphorylated on the C-terminal domain resulting in a band shift when run on a protein gel. All treatments are shown on the gel as well as the band sizes.

Treatment of cells with ERK5 siRNA has no effect on the phagocytosis rates of the macrophages (Figure 45) similar to the results observed with the kinase inhibitor studies. Thus siRNA knockdown of ERK5 produces the same effect as pharmacological ERK5 inhibition.

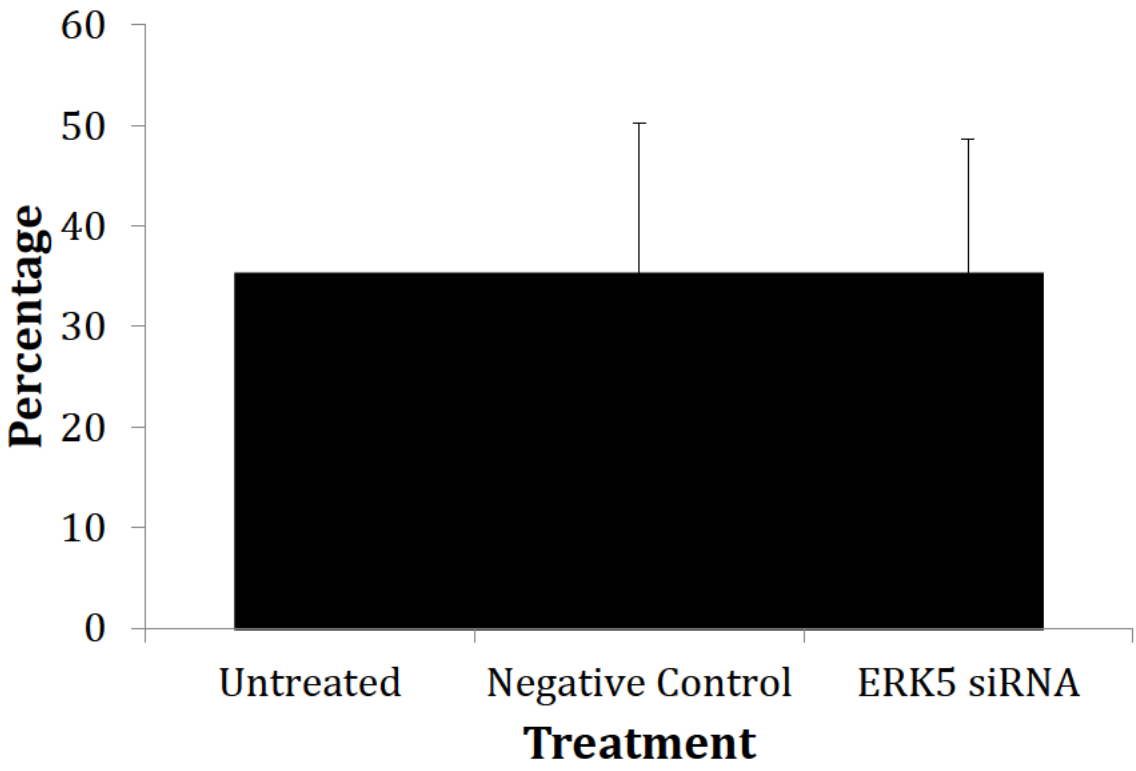

Figure 45: The percentage of siRNA treated J774A.1 murine macrophages that have successfully phagocytosed at least a single cryptococci. Error Bars = SEM, n = 3.

Lastly, vomocytosis rates in ERK5 -/- murine Bone Marrow Derived Macrophages (BMDM) (a kind gift from [redacted] were tested. Mice expressing ERK5 $^{fl/fl}$ are bred with mice expressing a tamoxifen inducible Cre endonuclease. BMDM are harvested from the progeny and treated with tamoxifen to suppress ERK5. Western Blotting is used to confirm the knockdown (Figure 47). Note that this inducible knockout is not 100% effective, so residual ERK5 remains in a subset of the cell population.

No differences in the rates of macrophage lysis rates were observed ($X^2 = 3.716$, $p = 0.053$, $n = 3$) (Figure 46). Significant differences were observed in the rates of vomocytosis between the WT and ERK5 -/- cells ($X^2 = 31.028$, ** $p < 0.001$, $n = 3$)

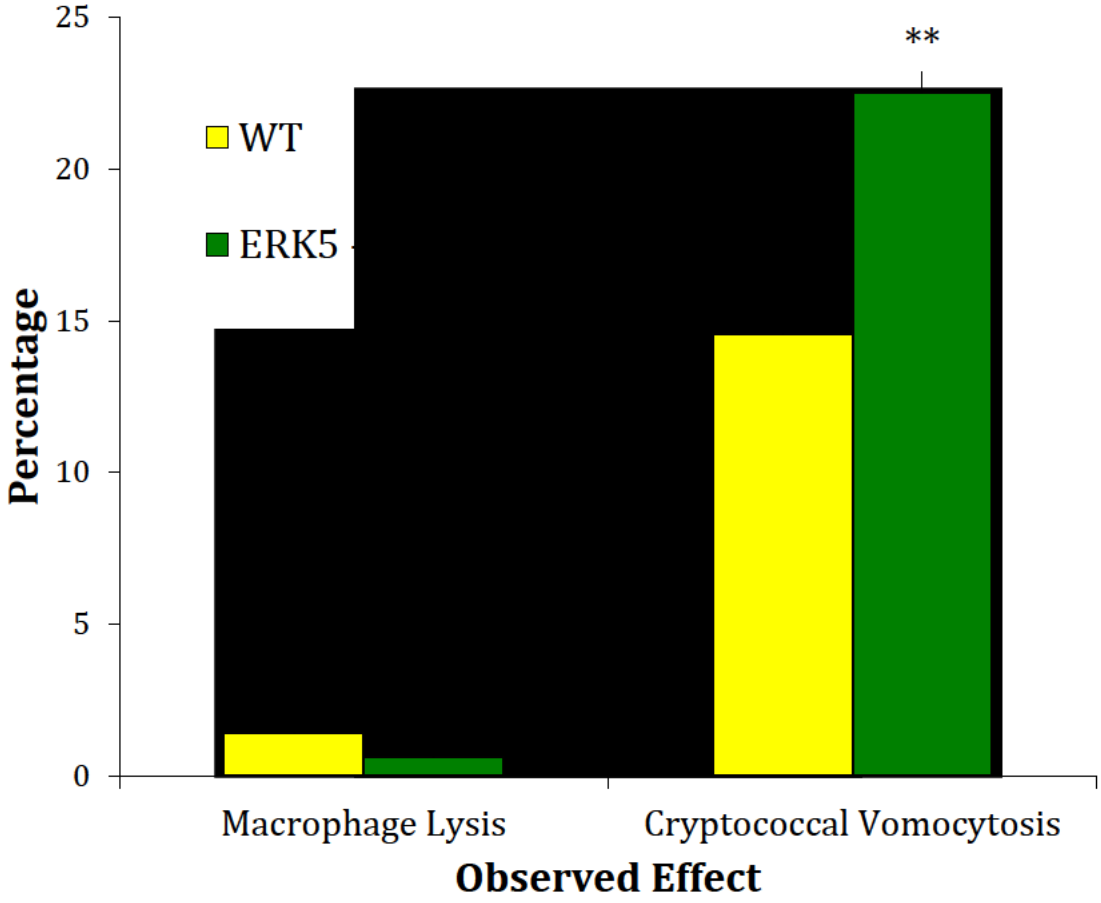

Figure 46: The percentage of cryptococcal vomocytosis events and macrophage lysis events in WT (YELLOW) and ERK5 -/- (GREEN) murine BMDM. Error Bars = SEM, ** $p < 0.001$, $n = 3$.

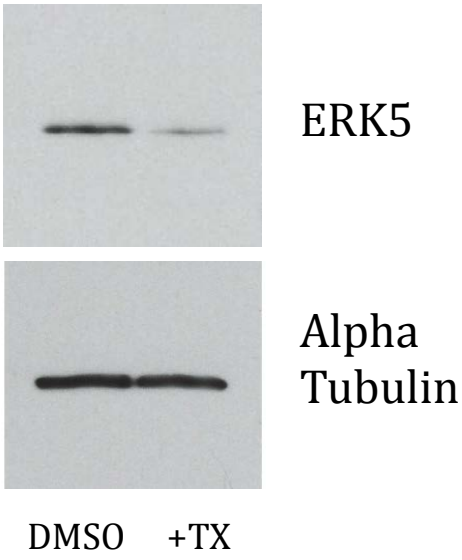

Figure 47: Western Blot showing ERK5 presence in WT BMDM and absence in ERK5 -/- BMDM. One parent contains a floxed ERK5 gene whilst the second contains the Cre endo-nuclease controlled by a tamoxifen-induced promotor. These mutations are organism wide. The offspring of these mice contain white blood cells with floxed ERK5 and the Cre-endonuclease awaiting tamoxifen to cleave ERK5 from the DNA of the cell. The mice can be bled and the monocytes harvested and differentiated into macrophages. Addition of tamoxifen to the media induces the cleavage of ERK5 from the white blood cells, producing the Western blot shown above. *This Western blot was performed* [redacted] *due to availability of a large quantity of the macrophages. Time-lapse imaging was performed at the University of Birmingham.*

Activation of ERK5 in Macrophages by IGF2 Reduces Vomocytosis Rates

In differentiating muscle myoblasts, ERK5 activity is enhanced by insulin like growth factor 2 (IGF2) (**Carter *et al.*, 2009**). To test whether we could use this approach to activate ERK5 in macrophages and potentially suppress vomocytosis, J774A.1 murine macrophage cells were treated with IGF2 and the rates of cryptococcal (H99 GFP) vomocytosis recorded (Figure 48). A significant difference was observed in vomocytosis rates between the PBS control and the IGF2 treated infected macrophages ($X^2 = 11.139$, ** $p < 0.001$, $n = 3$). Thus, together, these data demonstrate that we can subtly modify the rates of cryptococcal vomocytosis by the loss or activation of ERK5.

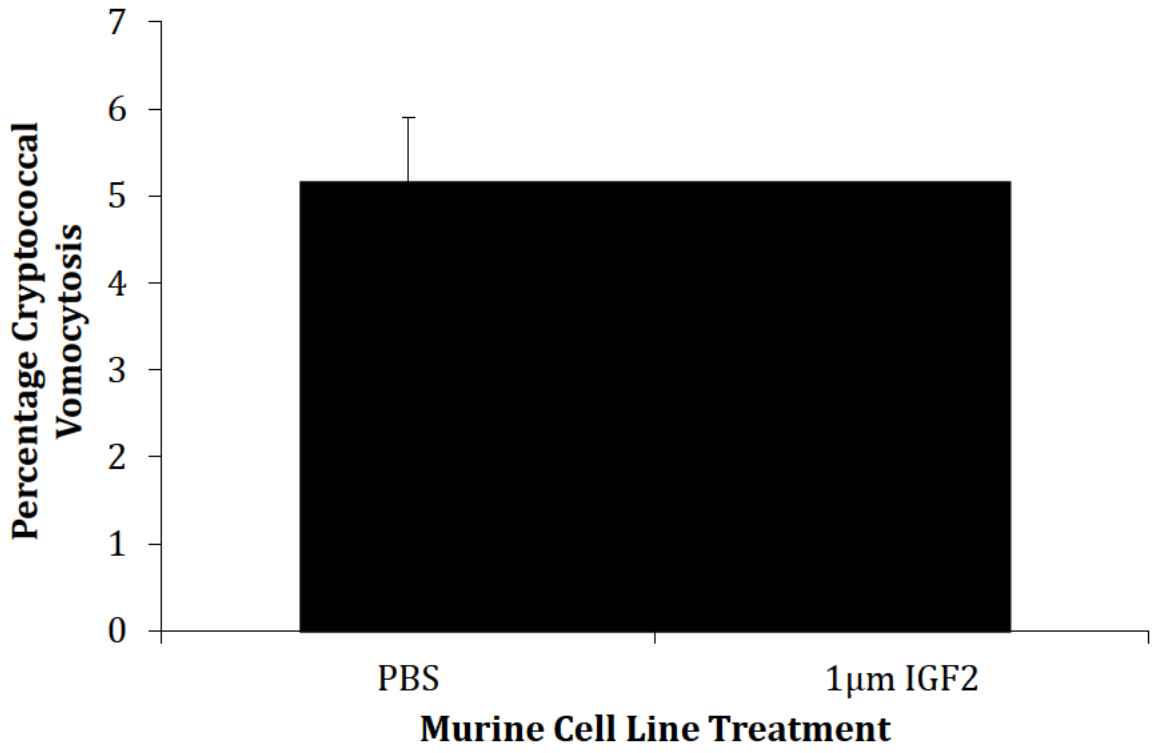

Figure 48: The percentage of cryptococcal vomocytosis events for cells treated with a PBS control and 1µM IGF2 (n = 3). Error Bars = SEM, ** $p < 0.001$.

Discussion of Results

Vomocytosis was discovered a decade ago with many predicting its biological importance in pathogen dissemination, pathogenicity and patient prognosis (**Alvarez and Casadevall 2006; Ma *et al.,* 2006**). The ability of cryptococci to escape phagocyte cells is not a unique process; with multiple microorganisms capable of some form of phagocyte escape (**Lee *et al.,* 2011; Andersen *et al.,* 2012; Bain *et al.,* 2012**), suggesting that escape from a phagocyte is a useful strategy for survival. Furthermore, the demonstration that cryptococci are capable of escape from amoebae suggests that vomocytosis may be a cryptococcal evolutionarily developed escape strategy or a universally adopted "discard" pathway by the host (**Steenbergen *et al.,* 2001; Chrisman *et al.,* 2010**). Amoebal vomocytosis may use a different cellular mechanism as opposed to macrophages; therefore an excellent experiment would be to investigate the effects of XMD17-109 on amoebal vomocytosis. Enhanced vomocytosis rates, using XMD17-109, have been observed from murine cell lines, primary human macrophages and from macrophages of the *in vivo* zebrafish embryo model (**Johnston Unpublished Data**). The aim of this research was to begin to understand the molecular mechanism of vomocytosis and begin to explore the consequences on pathogen dissemination within a host.

The molecular mechanism of vomocytosis is poorly understood. Current evidence suggests that secretion of cryptococcal PLB affects the rate of vomocytosis as mutants in the *Plb1* gene have a reduced rate of vomocytosis compared to their WT counterparts (**Chayakulkeeree *et al.,* 2011**). This is the only known cryptococcal gene identified as having an affect on the rates of vomocytosis. Many of the factors attributed to

manipulating vomocytosis rates are due to chemical modification of the macrophage and specifically the lysophagosome. Treatment of macrophages with chloroquine, a basic compound capable of neutralising lysophagosome pH, enhances the rates of vomocytosis (**Ma *et al.,* 2006**) however, treatment of macrophages with concanamycin, a v-ATPase inhibitor that inhibits the acidification of the phagosome, reduces the rate of vomocytosis (**Ma *et al.,* 2006**). Interestingly the addition of exogenous TNFα and IFNγ induces and increase in the rates of vomocytosis in human macrophages (**Voelz *et al.,* 2009**). These cytokines are Th_1 derived and skew macrophages towards an aggressive antifungal M1 phenotype (**Voelz *et al.,* 2009**), furthermore *C. neoformans* is capable of reducing the M1 response of macrophages by secreting prostaglandins capable of driving macrophage towards the more tolerable M2 phenotype (**Noverr *et al.,* 2001**). The increase in vomocytosis rates may arise due to the cryptococci sensing the harsh, antifungal environment created, therefore the pathogen vomocytoses to avoid destruction. Equally the macrophage may sense that even at its most antimicrobial it is still incapable of destroying the pathogen and ejects the cryptococci via a non-lytic exocytosis event. The addition of exogenous IFNγ and the resulting increase in vomocytosis rates may explain why clinics see an improvement in patient prognosis. The additional IFNγ may increase vomocytosis rates within the host, revealing the cryptococci to antifungal agents and immune cells better equipped at destroying them (e.g. neutrophils).

The formation of macrophage derived actin cages surrounding the cryptococcal containing phagosome restricts the occurrence of vomocytosis events (**Johnston and May 2010**). This was identified using macrophage actin polymerising and de-

polymerising compounds and measuring vomocytosis rates. The addition of actin polymerising compounds (jaspokinolide) increases the incidence of actin cage like structures forming around the cryptococcal containing phagosome (**Johnston and May, 2010**). The research in this thesis identifies ERK5, an atypical MAPK, which when inhibited or genetically reduced induces the largest enhancement in vomocytosis rates ever reported. Activation of ERK5 also induces a reduction in the rates of vomocytosis suggesting that ERK5 is playing a critical role in regulating vomocytosis rates.

Over-expression of ERK5 is associated with many forms of cancer, including prostate and breast cancer, however its contribution to innate immunity is poorly understood. Curiously, activation of ERK5 in macrophages has been recently reported to enhance the cannibalistic, efferocytosis activity of macrophages (**Heo *et al.*, 2014**). Efferocytosis is the process of macrophages sensing and phagocytosing apoptotic macrophages within the host environment and is likely to use similar machinery, such as actin cytoskeleton re-arrangement and SNAP/SNARE formation to achieve this. These data combined with this research suggest that ERK5 plays a critical regulatory role in what enters and leaves a macrophage.

The research in this chapter has clearly identified that inhibition of ERK5 activity enhances the rate of cryptococcal vomocytosis. This was observed in two murine cell lines (J774A.1 and RAW246.7) and in human primary macrophages and was observed with two different ERK5 inhibitors (XMD17-109 and AX15836). Vomocytosis rates could be enhanced through ERK5 siRNA treatment and by genetic knockdown of the ERK5 gene. Furthermore, activation of ERK5 reduces the rates in vomocytosis providing us

with the pharmacological tools to regulate vomocytosis rates *in vitro* now begging to be tested *in vivo*.

The variability in vomocytosis rates when J774A.1 murine macrophages were treated with the ERK5 inhibitor, XMD17-109 was noted. The highest rates of vomocytosis achieved were ~25% and the lowest ~8%. The variability could be due to a plethora of explanations including: batch variation between XMD17-109 inhibitor stocks, stock macrophage variation, variability in *C. neoformans*, timing of experiment – evidence suggests macrophage activity can be regulated via circadian rhythms (**Keller *et al.*, 2009**) and temperature, CO_2 and humidity fluctuations within the incubating chamber of the fluorescence microscope used.

The research also demonstrates that the addition of the ERK5 inhibitor, XMD17-109 and particularly the MEK5 inhibitor, BIX02189, has significant consequences upon intracellular proliferation rate and the colony forming units. It was demonstrated that the lysophagosome of macrophages treated with the respective inhibitors matured more efficiently then untreated cells, giving rise to the notion that inhibition of ERK5 allows better maturation of the of the lysophagosome, resulting in increased rates of vomocytosis and reduced intracellular proliferation rates. Why inhibition of ERK5 induces this response is an enigma. Clearly it is beneficial for the macrophage to induce phagosome maturation, so are the cryptococci activating ERK5 by some unknown mechanism, in order to prevent phagosome maturation? Additional to this is the evidence of the increase in IFNγ secretion from macrophages treated with XMD17-109. These data add further evidence to skewing the macrophage to an M1 like phenotype,

suggesting that the more antimicrobial the macrophage the greater the rate of vomocytosis.

Interestingly evidence from the latex bead study and the heat killed (HK) cryptococci study suggest that viable pathogens are required for vomocytosis, indicating some form of cellular communication between host and prey to initiate a vomocytosis event. Evidence of this has been reported before and the fact that XMD17-109 cannot trigger vomocytosis events of these particles further suggests vomocytosis is dependant upon the presence of live yeast cells.

The results from this chapter feed into the next chapter of the thesis, whereby the molecular mechanism of vomocytosis and its potential consequences in pathogen dissemination and host prognosis are explored.

CHAPTER 4: INVESTIGATION OF THE MOLECULAR MECHANISM OF VOMOCYTOSIS USING SILAC

This results chapter will discuss the data generated from phosphoproteome experiments and begin to further question the effects on pathogen dissemination and host prognosis. Stable isotope labelling of amino acids in cell culture (SILAC) was used to investigate the phosphopeptides involved in vomocytosis. As ERK5 phosphorylates downstream transcription factors and other proteins it has been hypothesised that inhibition of this kinase may result in dramatic changes in the phospho-proteome of the treated macrophages. The aim of this approach was to begin to determine the phosphoproteins involved in vomocytosis to tease apart the molecular mechanism of the process. Three individual batches of macrophages were differentially labelled with three isotopes (Heavy, Medium and Light) of both lysine and arginine. These different batches were then treated differently such as: uninfected cells, cryptococcal infected cells and cryptococcal-infected cells with the ERK5 inhibitor, XMD17-109. The macrophages undergoing these treatments were lysed post infection and the protein concentration of the lysate quantified. The lysates were combined, the proteins were trypsin digested, phosphopeptide enriched and sent for mass spectrometry analysis through the University of Birmingham Proteomics and Genomics Facility. The Mass Spectrometer is capable of detecting the variations in amino acid isotopes allowing comparisons between the proteins and phosphoproteins present in separate treatments to be assessed. Two biological repeats and four technical repeats were performed on the samples. Mass spec analysis identified a group of cytoskeletal proteins upregulated in

infected macrophages treated with the ERK5 inhibitor, XMD17-109 when compared to infected macrophages in the absence of the inhibitor.

To further investigate the effects of vomocytosis *in vivo* and its potential consequences on pathogen dissemination, murine and zebrafish *in vivo* models are currently being used. Our collaborators at [redacted] generated mice deficient in ERK5 in the myeloid cell lineage, controlled by the LysM (lysozyme M) promotor. These mice were infected with H99 *C. neoformans* and the dissemination of pathogen, mortality and morbidity of the mouse and the infection burden of multiple organs investigated. The data from these studies are currently being analysed. Zebrafish embryos have been infected with H99 *C. neoformans* and treated with the ERK5 inhibitor, XMD17-109. Vomocytosis rates within the zebrafish macrophages were investigated with the added advantage of the *in vivo* cell-to-cell interactions capable of being visualised. Our collaborators have discovered that the addition of XMD17-109 drives an increase in the rate of vomocytosis in zebrafish similar to our previous *in vitro* work.

SILAC – Investigating the Molecular Mechanism of Vomocytosis

SILAC Experiment Organisation

As inhibition of macrophage ERK5 has been shown to increase the rate of cryptococcal vomocytosis, exploration of the macrophage biology and hence the molecular mechanisms that may be driving an increase in vomocytosis rates was investigated. Stable Isotope Labelling of Amino Acids in Cell Culture or SILAC was used to explore

these questions. This method isotopically labels lysine and arginine within the media of the cells of interest. The isotope labels can be light (Lys0, Arg0), medium (Lys+4, Arg+6) or heavy (Lys+8, Arg+10). These batches of cells are then distinguishable by a mass spectrometer, enabling three different treatments to be studied and compared at a given time. In this research the three treatments to compare were uninfected macrophages, cryptococcal infected macrophages and cryptococcal infected macrophage plus 1μM XMD17-109 (ERK5 inhibitor). The experimental set up is shown in Figure 49. Upon completion of infection the samples were lysed and stored for further processing.

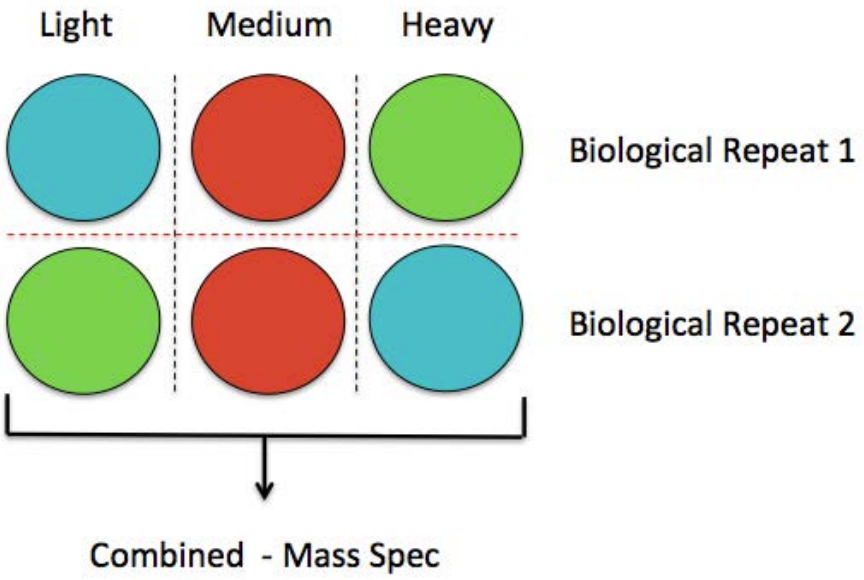

Figure 49: SILAC experimental setup. RED – Uninfected macrophages, GREEN – Infected Macrophages and BLUE – Infected macrophages plus 1μM XMD17-109. Macrophages were infected for two hours with the infection dose of *C. neoformans* (H99), before being washed and incubated in the required conditions for 24 hours.

Confirming Incorporation of the Heavy and Medium Amino Acid Isotopes

Prior to running the samples through the mass spectrometer, it was essential to confirm that the J774A.1 murine macrophages were capable of incorporating the varying amino acid isotopes into their synthesised proteins. Macrophages were cultured in the differentially labelled media for seven complete division cycles. The health of the macrophages was monitored, via microscopy and, once confluent, cells were infected and then lysed. The concentration of peptides in individual lysates was quantified using the Bradford protein quantification assay, examples shown in Figure 50 and the values obtained for each lysate are shown in Table 3.

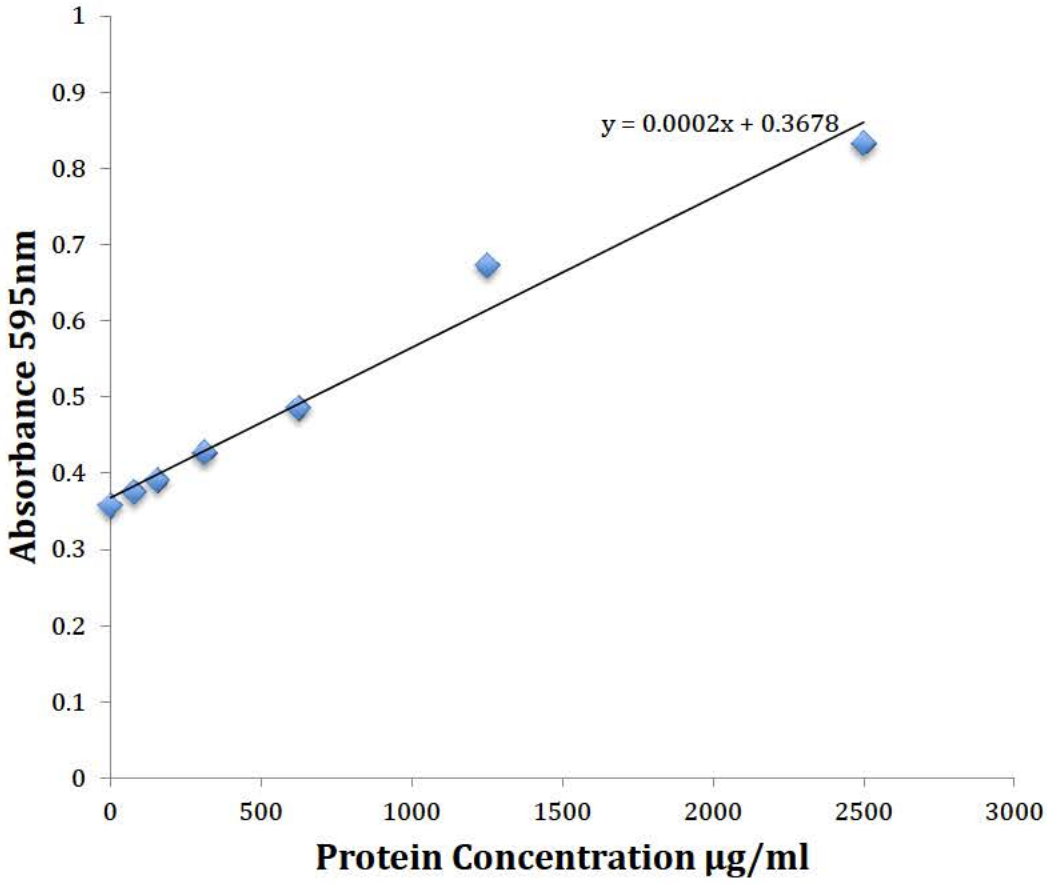

Figure 50: Example of a Bradford assay standard curve.

Table 3: The protein concentrations (mg/ml) for each biological repeat.

Isotope Labelling	**Macrophage Treatment**	**Protein Concentration (mg/ml)**
Heavy (Biological Repeat 1)	H99 GFP Infection	0.83
Medium (Biological Repeat 1)	Uninfected	0.74
Light (Biological Repeat 1)	H99 GFP Infection + ERK5 Inhibitor (XMD17-109)	0.55
Heavy (Biological Repeat 2)	H99 GFP Infection + ERK5 Inhibitor (XMD17-109)	1.59
Medium (Biological Repeat 2)	Uninfected	0.88
Light (Biological Repeat 2)	H99 GFP Infection	1.48

20 - 40μg of protein for each treatment was loaded onto a protein gel. The samples were run down the gel and Coomassie stained to highlight the in gel protein. In a Class 2 safety cabinet a fragment of these lanes were cut from the gel, to avoid keratin contamination. The gel plugs were in-gel digested at the University of Birmingham's Genomics department and sent for mass spec analysis. The isotope incorporation was then determined from the mass spec data using the software MaxQuant and Microsoft Excel (Figures 51 and 52).

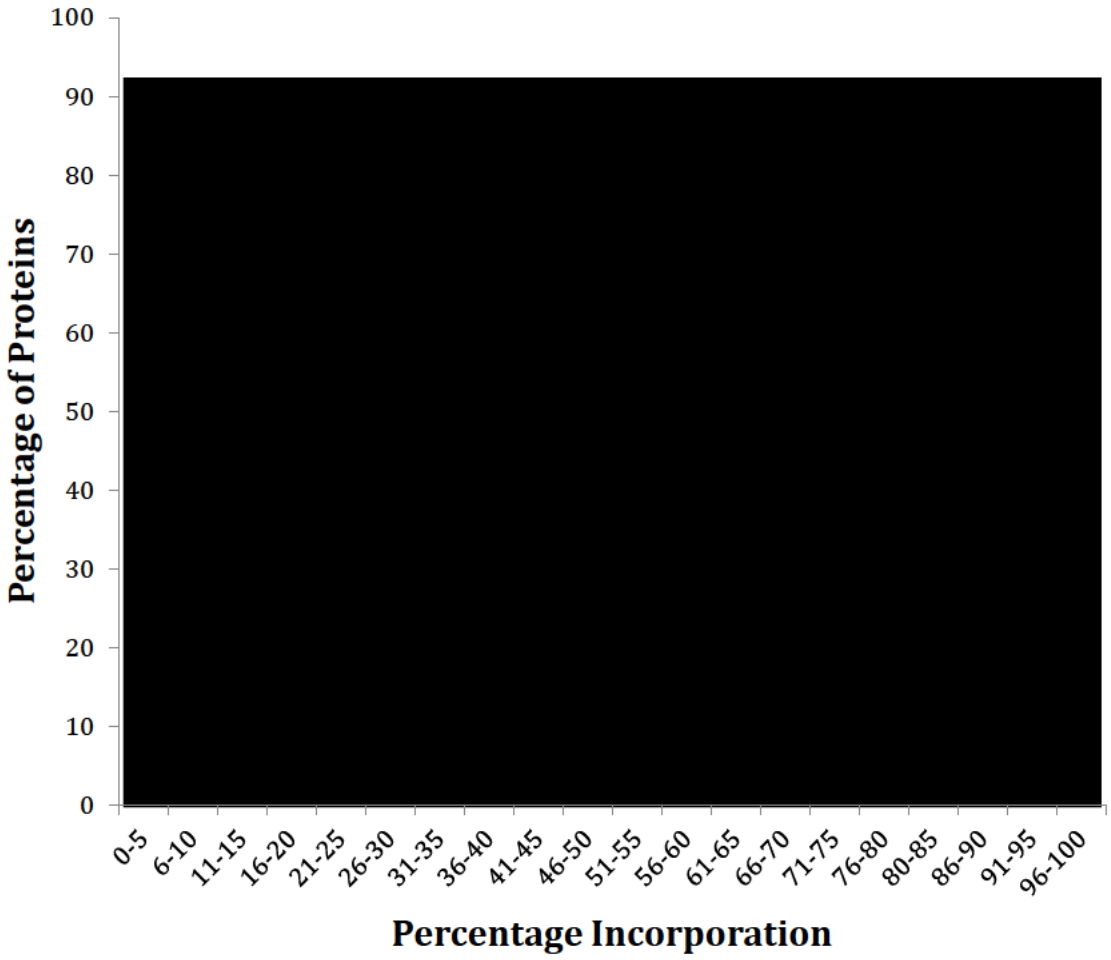

Figure 51: The percentage of Heavy isotope (Heavy, Lys8, Arg10) incorporation into proteins of the infected J774A.1 murine macrophages.

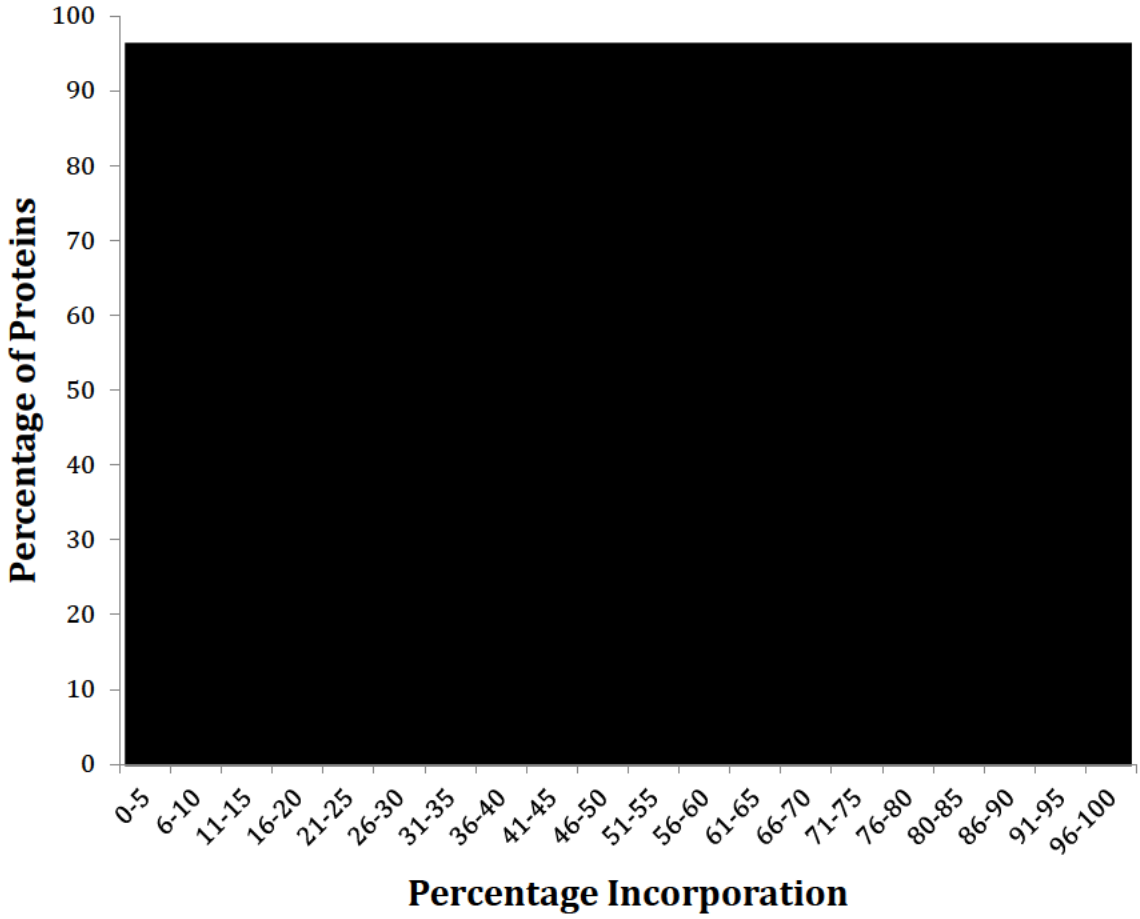

Figure 52: The percentage of Medium isotope (Medium, Lys4, Arg6) incorporation into proteins of the infected J774A.1 murine macrophages.

Figures 51 and 52 show that the incorporation of the isotopes for both Heavy (Figure 51) and Medium (Figure 52) lysine and arginine has been incorporated extensively into the proteins of the J774A.1 murine macrophages. Over 95% of all proteins for both isotope treatments have between 95 - 100% isotope incorporation after 7 macrophage lifecycles. These incorporation values and the reasonably high concentration of proteins in the lysates ensured that SILAC was a method we could use to investigate the phospho-

proteome further and hence shed more light on the molecular mechanisms of vomocytosis.

Separating the peptides from the Complex Macrophage Lysate

The macrophage lysate is a complex mixture of proteins, lipids, glycoproteins and polysaccharides, however for this study we were specifically interested in the protein component of this mixture and more specifically the phospho-peptides. High Pressure Liquid Chromatography (HPLC) was used separate the mixture isolating the peptide component. 5mg of protein from the individual lysates were combined, totalling 15mg (all three treatments), trypsin digested, to cleave proteins into peptides, before being loaded into the HPLC machine with a poly-lysine A butoryl column. The peptides bind to the adsorbent column from which they can be eluted using a gradually increasing salt buffer over the course of the HPLC run. The peptides are then detected and a HPLC trace drawn. The trace for the first biological repeat is shown in Figure 53 and the second biological repeat is shown in Figure 54. The elutions were collected into individual tubes for drying and phosphopeptide enrichment using titanium dioxide tips, before being sent to the mass spectrometer. The mass spectrometer used was the LTQ Orbitrap Elite mass spectrometer (Thermo Fisher Scientific) as used by **Sarhan *et al.,* 2016**. This mass spectrometer was used due to its good resolving power (**Sarhan *et al.,* 2016**).

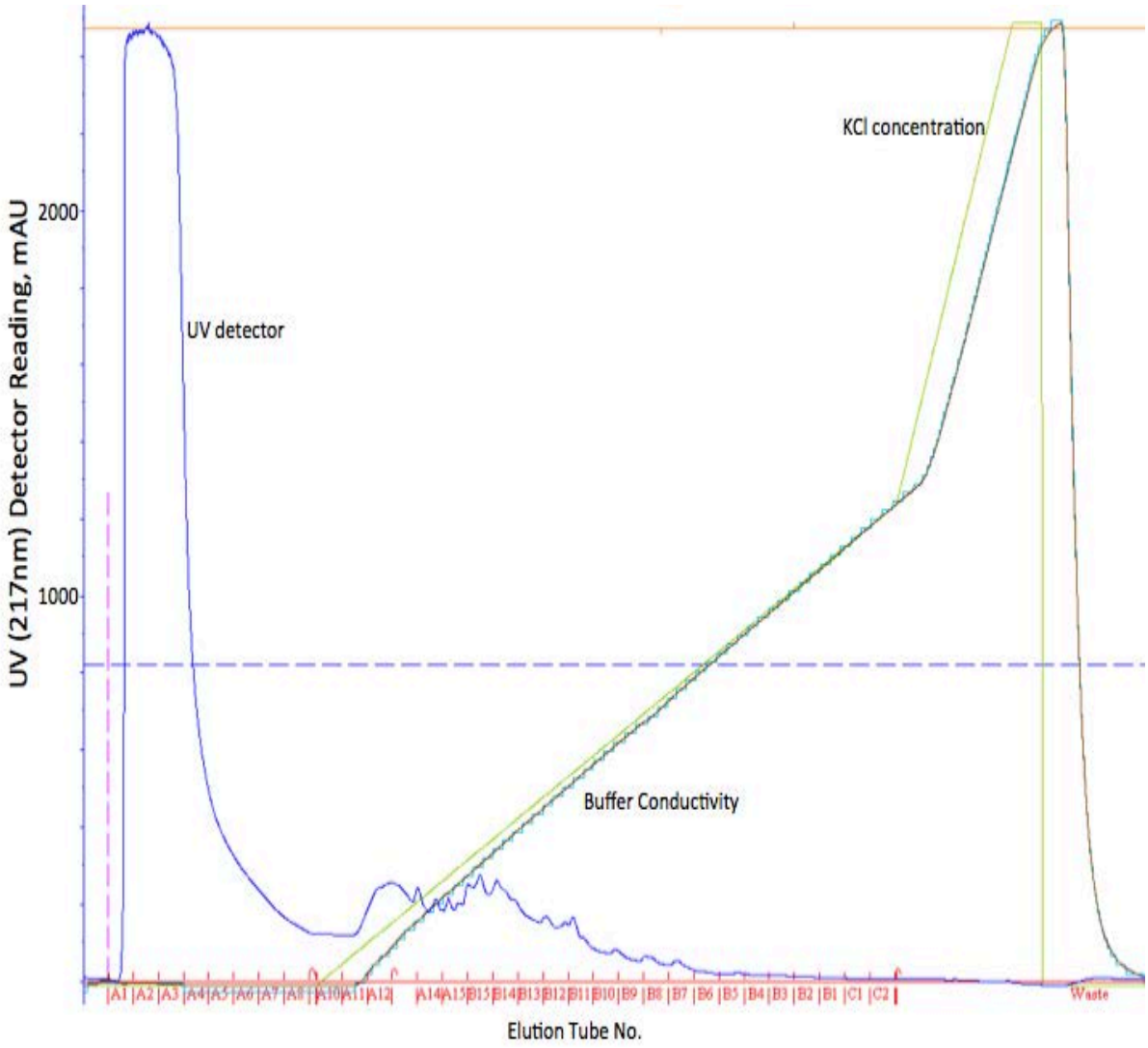

Figure 53: The HPLC trace for the first biological repeat showing the elution of the peptides from the complex macrophage lysate. The **Blue** trace corresponds to the UV 214nm detector, capable of detecting changes in the samples running through the HPLC machine. The peak at the start of this trace highlights the complex lysate passing through the HPLC machine. The peptides bind to the adsorbent column. The fluctuations in the line approximately midway through the graph show the peptides being eluted from the column as the salt (KCl) concentration (**Green**) of the elution buffer increases. The increase in KCl concentration increases the buffer conductivity (**Light Blue** and **Brown** (%)) eluting the peptides into individual collection tubes (**Red**).

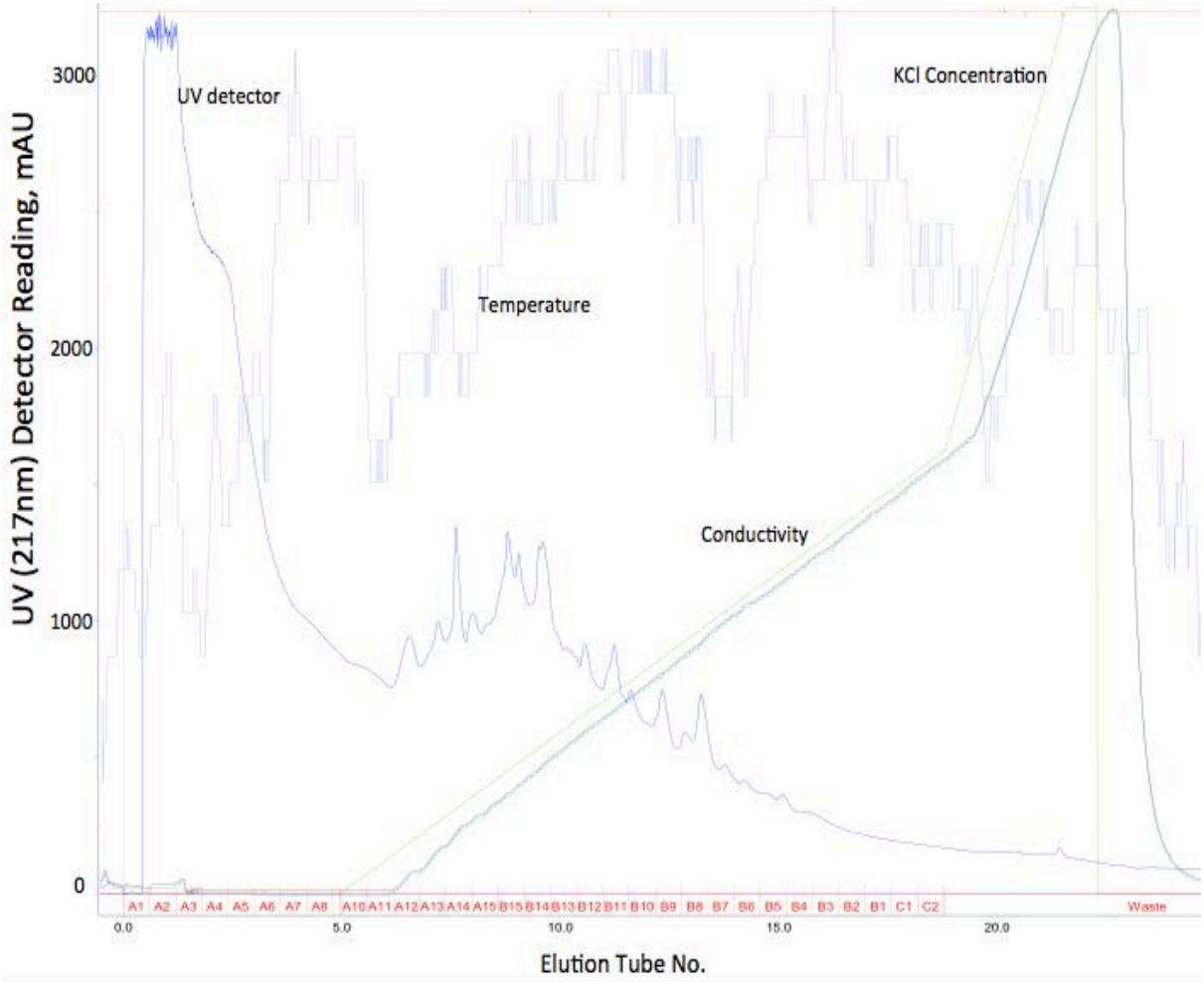

Figure 54: The HPLC trace for the second biological repeat showing the elution of the peptides from the complex macrophage lysate. The **Blue** trace corresponds to the UV 217nm detector, capable of detecting minute changes in the samples running through the HPLC machine. The peak at the start of this trace highlights the complex lysate passing through the HPLC machine UV detector. The peptides bind to the adsorbent column. The fluctuations in the line approximately midway through the graph show the peptides being eluted from the column as the salt (KCl) concentration (**Green**) of the elution buffer increases. The increase in KCl concentration increases the buffer conductivity (**Light Blue** and **Brown** (%)) eluting the peptides into individual collection tubes (**Red**). The variable **Grey** line represents the temperature fluctuations over the course of the run.

The peptides detected for the first biological repeat are much less concentrated then the second biological repeat; the explanation for this is unclear. Table 3 shows the concentrations of protein in the first biological and second biological repeats. The first repeat is approximately half as concentrated and the second repeat. These values have consequences on the trypsin digest reaction mix. The lower concentration of protein in repeat 1 results in a higher volume of lysate required to ensure 15mg of protein is present in the digest. The lysis buffer contains a high percentage of the Triton X-100 detergent. In turn more lysate was required and hence an increase in the detergent was present in the trypsin digest buffer. The detergent may have interfered with the biological activity of the trypsin, resulting in reduced proteolytic activity. These conditions were optimised for the second biological repeat resulting in greater proteolytic degradation and hence more binding to the column during the HPLC run. This produced greater peaks on the HPLC trace.

Mass Spectrometry – Results

Identifying the Peptides of Interest

Elutions from the HPLC were dried in a speed vac and phosphoenriched using chromatography with titanium dioxide tips. Titanium dioxide has a high affinity for phosphate groups and therefore strongly binds the phospho-peptides. After phosphoenrichment samples were dried, desalted and re-suspended in 0.1% formic acid. Samples were run down a LC-MS facility at the University of Birmingham. Two technical repeats for each biological repeat were gathered.

Data from the mass spec was generated and our collaborator, Debbie Cunningham, used MaxQuant to create a Microsoft Excel File, summarising these data. The Microsoft Excel files were analysed to identify peptides and peptide groups of interest. A total of 2318 phospho-peptides were identified over the course of the four repeats (biological and technical). For the Complete Raw Data File – See Appendix.

As SILAC was used the ratio of peptides between treatments could be calculated. These ratios were used to identify which, if any, peptides were up or down-regulated depending upon treatment type, allowing comparisons to be made and potentially highlighting biological differences between treatments. Individual ratios per peptide identified were calculated per comparison: Infected (Heavy, H) vs. Uninfected (Medium, M), HM, Infected (Heavy, H) vs. Infected + ERK5 inhibitor (XMD17-109) (Light, L), HL and Uninfected (Medium, M) vs. Infected + ERK5 inhibitor (XMD17-109) (Light, L), ML.

1383 similar peptides were identified between uninfected and infected + ERK5 inhibitor (ML) treatments, 1381 similar peptides were identified between infected and infected + ERK5 inhibitor (HL) treatments and 1383 similar peptides were identified between infected and uninfected (HM) treatments.

Thresholding was performed on the ratio values (Figure 55). Ratio values below 0.5 were retained for analysis. 0.5 was chosen as peptides with ratio values lower then this were equal to or below half as well expressed for a given treatment. Ratio values above 1.5 were retained for further analysis. 1.5 was chosen as peptides with ratio values above this were increasingly expressed for a given treatment. Figure 55 shows the thresholding for the Infected vs. Infected + ERK5 inhibitor (HL) comparison. Both Infected vs. Uninfected (HM) and Uninfected vs. Infected + ERK5 inhibitor (ML) were analysed in the same way. Peptides that were located above the positive dotted red line were retained as well as those located below the negative dotted red line (Figure 55). Peptides located between the two dotted red lines did not match the threshold criteria and were removed from analysis. 139 peptides remained for the ML comparison, 114 peptides remained for the HL comparison and 142 peptides remained for the HM comparison.

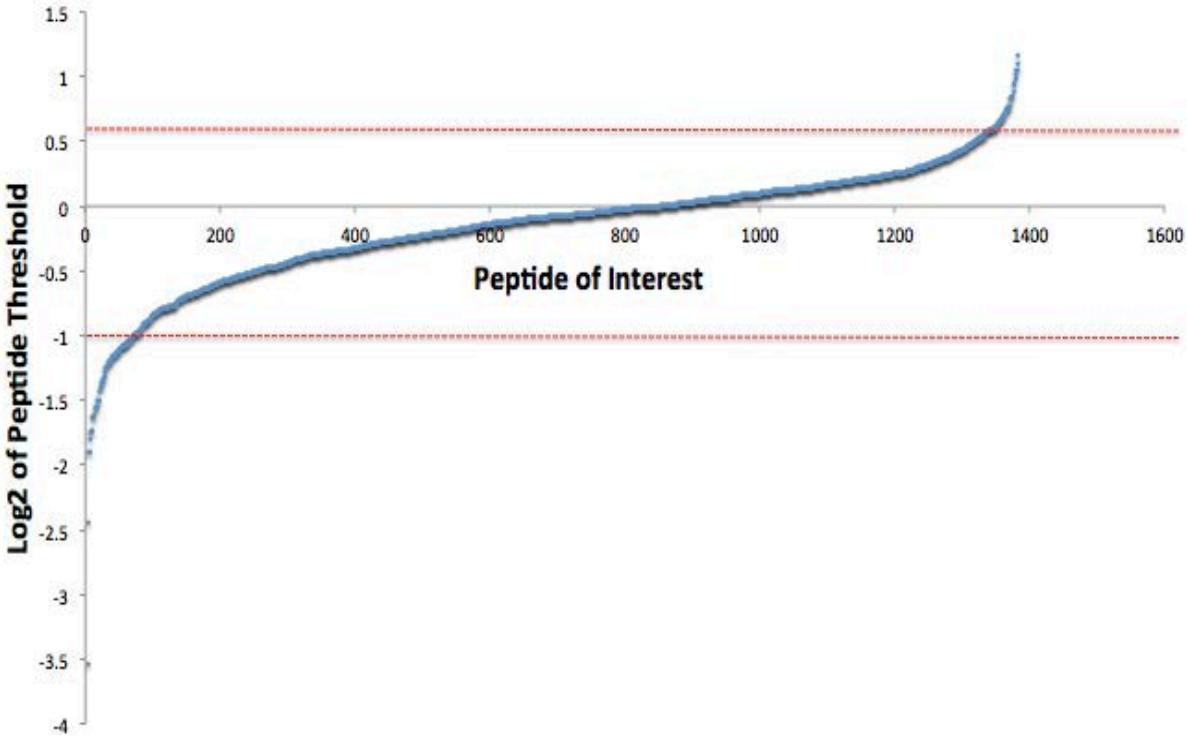

Figure 55: The ratio values for each of the peptides identified per comparison were transformed using the logarithmic function (Log_2). The peptides were assigned a number and plotted against the Log_2 values. All peptides with a Log_2 value of 0.58 (positive red dashed line) or above and all peptides with a Log_2 value of -1 (negative red dashed line) or below were selected for further analysis.

Individual peptides, that satisfied the threshold criteria, were analysed to confirm whether they were also present in either a second technical repeat or in another biological repeat. Peptides identified in two separate biological repeats were considered more reliable then peptides only identified in a single biological repeat, as they were identified on two separate occasions. However, as the experiment has only two biological repeats we are unable to rule out peptides that were only present in a single biological repeat, as these may have been critical to the biological process, but did not

show in the second repeat. The mass spectrometer is reported to detect approximately 60-80% of peptides per run and hence many proteins will be missed per repeat (**Sarhan *et al.,* 2016**). Due to this we ensured two technical repeats were done for each biological repeat to maximise phospho-proteome coverage. Mass spec data analysis commonly identified peptides found in a single biological repeat but in both technical repeats. Further biological and technical repeats would improve the peptide representation under the conditions tested. Figure 56 shows the representation of the identified peptides and whether they were detected in separate biological repeats.

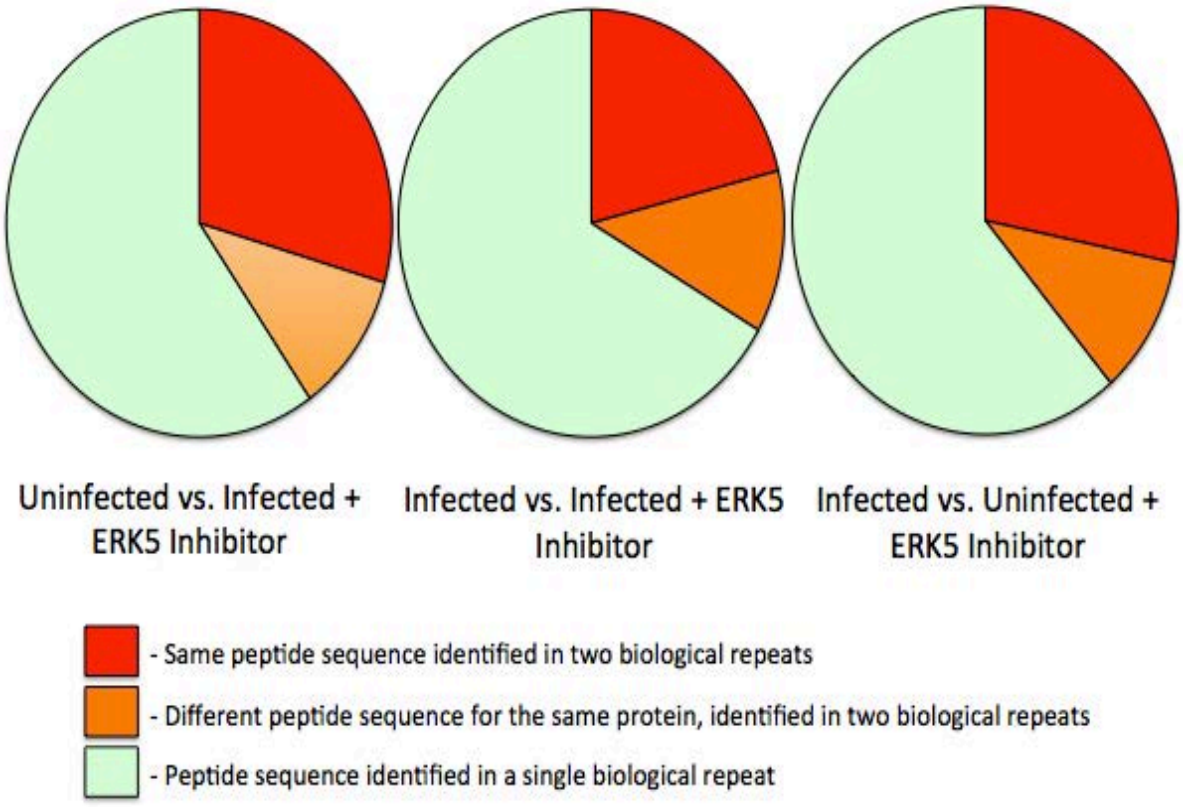

Figure 56: The peptide representation for the two biological repeats and the four technical repeats.

Figure 56 clearly shows that ~33% of proteins were detected in at least two separate biological repeats regardless of the treatment strategies being compared. The identified proteins have been identified through the detection of the same peptide sequence (**RED**) or an alternative peptide sequence (**ORANGE**). Approximately 66% of proteins were only identified in one biological repeat (**GREEN**), however many were detected in both technical repeats of this biological repeat. For each treatment comparison an average of 132 peptides were identified, that matched the threshold criteria, therefore 87 of these peptides were only found in a single biological repeat – to exclude these from further analysis would remove a vast amount of data that may be relevant to the biological problem posed. These singly represented peptides may reveal significant clues about the process of vomocytosis but have not been detected in the second biological repeat.

Functional Analysis

Having identified the peptides of interest, further analysis was required to begin to answer the biological questions of what proteins are involved in regulating the rate of vomocytosis. Functional analysis of the peptides was used to investigate the functions of the selected peptides, to reveal up or down regulated functions within the cell in relation to the treatment strategies. The online tool DAVID was used to achieve this (**Huang *et al.*, 2009**). DAVID, clusters peptides based on the GO term annotation, identifying significant over-representation within the treatment population as opposed to a normal population. The Microsoft Excel spreadsheets assigned a protein ID to each of the individual peptides. Both up and down regulated peptides were combined as the effects on key cellular functions were of interest. These combined protein IDs were then fed

into DAVID and the functions of the individual peptides were assigned, fold enrichment analysis performed and the peptides were clustered into functional groups.

A protein “Fold Enrichment” analysis of the peptides for each comparison was performed and the significantly enriched functional groups identified. The enrichment analysis identifies groups of genes that are over-represented within the gene set and hence points towards significantly modified cellular functions via our treatments. Table 4 highlights the enriched groups of genes for the ML comparison. See the appendices for the HM and HL comparisons (Appendix Table 1 and Table 2).

Table 4: The enrichment analysis for the comparison between infected macrophages vs. infected macrophages + XMD17-109 (ML).

Enrichment Term	Gene Count	Fold Enrichment
compositionally biased region:Arg/Ser-rich (RS domain)	5	58.38556851
RRM2	6	11.14633581
RRM 1	6	11.14633581
spliceosome	7	11.02923387
compositionally biased region:Arg-rich	6	10.89863946
nuclear speck	5	10.85416667
mrna splicing	11	10.38627109
RNA splicing	11	9.914958541
Spliceosome	6	9.748293748
compositionally biased region:Lys-rich	6	9.52308302
Spliceosome	5	9.25483871
mrna processing	12	9.017171717
mRNA metabolic process	14	8.398763797
mRNA processing	12	8.298015267
nuclear body	6	8.25528169
RNA recognition motif, RNP-1	9	8.196626333
Nucleotide-binding, alpha-beta plait	9	8.158144519
RRM	9	6.683392973
rna-binding	17	6.321316255
regulation of organelle organization	5	5.882251082
RNA processing	13	5.389595728
RNA binding	18	4.80984556
ribonucleoprotein complex	11	4.651785714

short sequence motif:Nuclear localization signal	8	4.525386625
methylation	5	4.080168198
actin-binding	5	3.98989899
endosome	5	3.876488095
actin binding	6	3.740990991
chromosomal part	6	3.686320755
chromosome	7	3.618055556
acetylation	43	3.335383947
cytoskeletal protein binding	7	3.036166601
compositionally biased region:Pro-rich	13	3.005989666
GTPase regulator activity	6	2.984502508
nuclear lumen	13	2.876415629
phosphoprotein	97	2.771876586
nucleoplasm part	7	2.665935673
intracellular organelle lumen	14	2.414165931
organelle lumen	14	2.407790493
cell cycle	8	2.372154937
membrane-enclosed lumen	14	2.329855196
non-membrane-bounded organelle	21	2.138027619
intracellular non-membrane-bounded organelle	21	2.138027619
nucleus	45	2.131159282
nucleotide binding	25	2.056431145
zinc-finger	13	1.947229773
coiled coil	18	1.874238925
atp-binding	13	1.821650852
alternative splicing	44	1.770834883
ATP binding	14	1.742166283

purine nucleoside binding	15	1.73999581
nucleoside binding	15	1.728827672
cytoplasm	28	1.667090182
splice variant	44	1.617154236

Table 4 shows the enrichment analysis for the ML (uninfected macrophages vs. infected macrophages + XMD17-109) comparison. The groups are selected based on the EASE Score threshold. This value highlights how significantly enriched the genes within this functional group are. The value of 0.05 was selected. Proteins within these groups were therefore identified more frequently than expected based on their representation within the proteome as a whole. Functional groups were selected on whether 5 or more genes were present in the group. This gave a clear indication of whether this functional group had multiple genes present. The fold enrichment score gives and indication of how well enriched individual groups are. 97 genes were identified as phosphoproteins; this was encouraging as we purposely selected for phosphopeptides via titanium dioxide enrichment. Furthermore, the phosphopeptide genes are significantly enriched which was as expected, as we treated infected macrophages with a kinase inhibitor. Other protein groups of interest were actin binding and cytoskeletal proteins, as previous reports suggest that actin cage formation may play an important role in vomocytosis regulation (**Johnston and May 2010**). Enrichment analysis also identified multiple proteins involved in mRNA binding and regulation, nuclear proteins and chromatin remodelling proteins, suggesting that transcription and translation are being regulated upon inhibitor treatment. This result seems plausible, as genetic regulation in response to both cryptococcal phagocytosis and inhibitor treatment would be expected and

therefore the genes involved would be expressed more then for a non infected population.

Having identified significantly enriched groups of genes, the next stage of analysis was to cluster the genes of interest into functional groups within the cell to begin to identify which groups of proteins may have a role in vomocytosis. Using the Uniprot gene-mapping tool, the protein ID numbers were converted to their gene names for each comparison. The gene names were assigned a regulation status depending upon whether the genes were up-regulated or down-regulated within a given treatment, i.e. upregulated genes in the HL comparison had a greater then 1.5 ratio value, indicating that the gene is up-regulated in infected macrophages compared to those that were treated with XMD17-109. Using the DAVID clustering analysis (**Huang *et al.,* 2009**) the gene function of each individual genes were assigned and whether or not the gene was assigned to a significant cluster, a significant cluster being whether multiple genes are clustered together due to having related roles within the macrophage cell. Furthermore the gene functions were also manually assigned via their GeneCard information. The DAVID analysis and manual analysis provided similar functions for each gene. Table 5: shows the clusters used for this analysis.

Table 5: The titles of the clusters identified in this cluster analysis and a list of cellular functions encompassed within the cluster.

Cluster Title	**Cellular Functions**
Transcription and Translation Regulation	Nuclear protein, chromatin remodelling, nuclear speck, nuclear body, mRNA binding, mRNA regulation, DNA binding, nucleotide binding, splicing factors.
Transmembrane and Endoplasmic Reticulum	Golgi apparatus, membrane proteins, transmembrane, endoplasmic reticulum, vacuolar proteins.
Cytoskeleton	Actin binding, microtubule proteins, cytoskeletal proteins, myosin.
Autophagy and Apoptosis	Caspases.
Leukocyte Activation	Complement receptors, antibody receptors.
Signalling	Kinases, GTPases, signal transduction, ubiquitylation.
Metabolism	Superoxide dismutase

Having assigned a general cellular function/location to each individual gene product, Cytoscape (*www.cytoscape.org*) was used to cluster the genes into groups and highlight whether genes were up or down regulated per treatment condition. Cytoscape also enabled the identification of genes that were significantly or non-significantly clustered. DAVID annotation clusters proteins/peptides based on their GO terms, however many proteins would be associated with our groups but assigned multiple Go terms and hence

are not significantly clustered. The cytoscape images were then used to infer biological meaning from the mass spec data, see figures (57, 59 and 61).

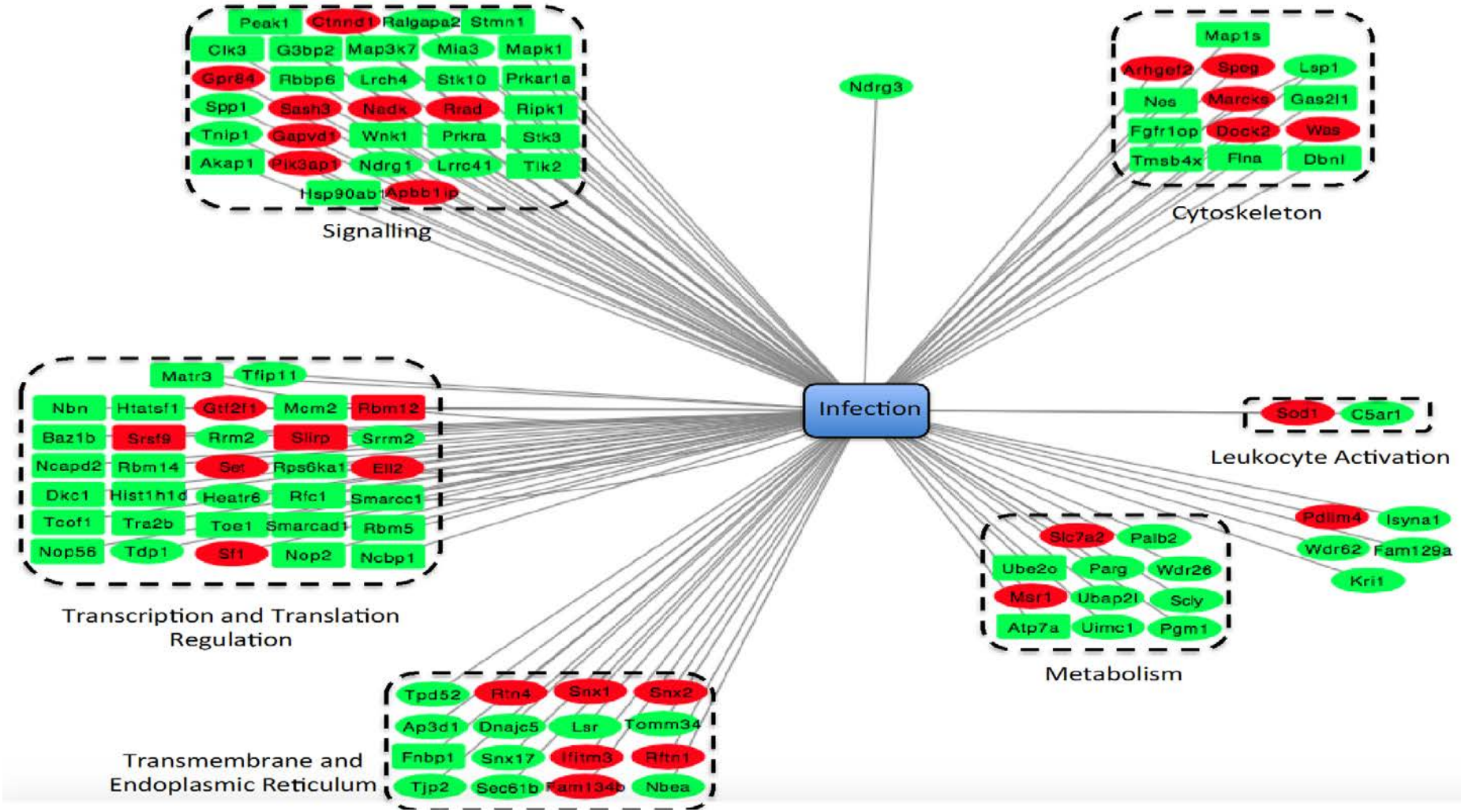

Figure 57: A Cytoscape plot showing the up and down regulated proteins, sorted into functional clusters, for the comparison between infected macrophages and uninfected macrophages (HM). Red = down regulated proteins, Green = up regulated proteins, rectangle = significantly clustered and ellipse = non-significantly clustered.

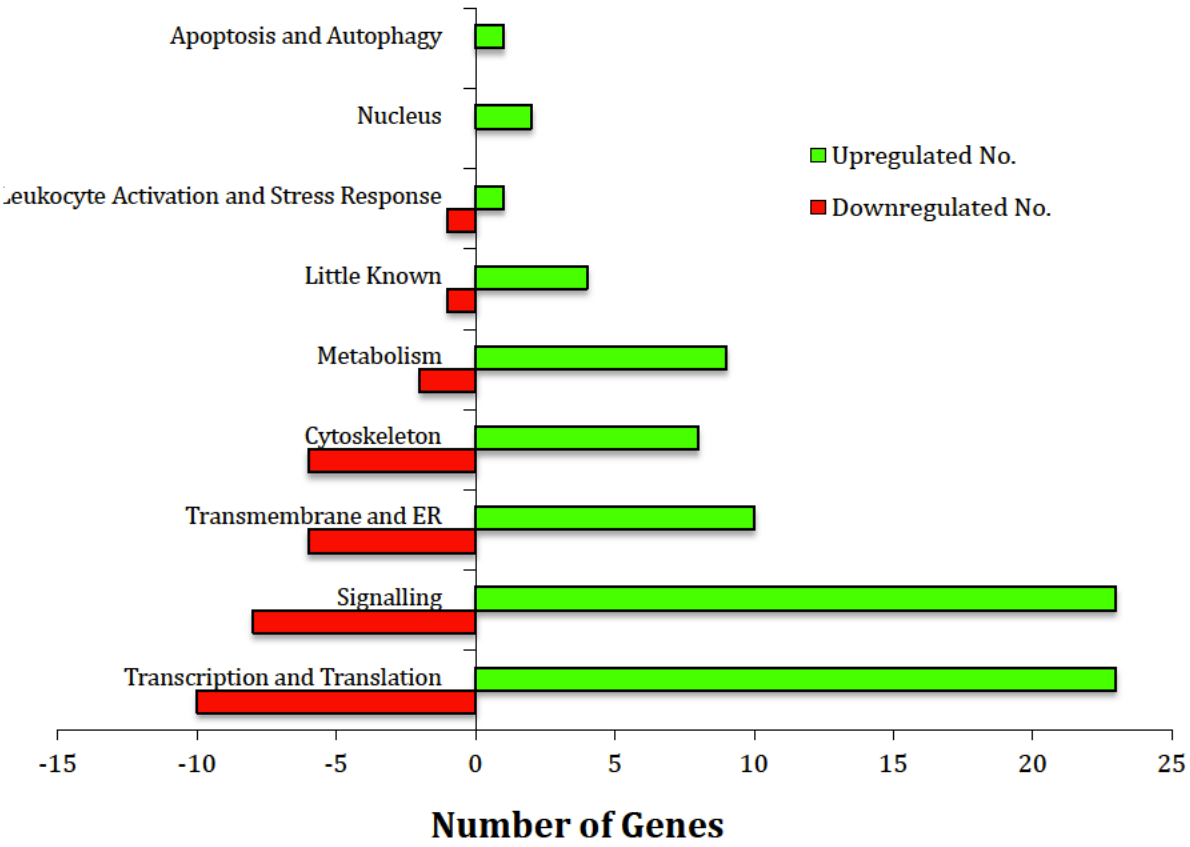

Figure 58: The number of genes up and down regulated in cryptococcal infected macrophages compared to uninfected macrophages (HM), sorted by functional group.

Upon cryptococcal infection macrophages regulate a wide range of genes. As expected, many of these genes encode signalling proteins and transcription/translation regulation proteins (Figure 57 and 58), many of which are significantly clustered into their respective functional groups (Figure 57). Macrophage cellular signalling and transcription/translation regulation will be critical upon response to a phagocytosed pathogen. Modulating the correct genes and organisation of appropriate cellular signalling will ensure the macrophage is capable of dealing with the cryptococci. Cytoskeletal genes are also regulated in response to cryptococcal phagocytosis, enabling

the macrophage to organise its cellular structure to cope with physiological changes. Other regulated genes include metabolic, apoptotic and leukocyte activation genes, however many of these identified genes have not been significantly clustered into these groups based on their gene ontology. The next comparison was between infected macrophages and infected macrophages treated with the ERK5 inhibitor, XMD17-109.

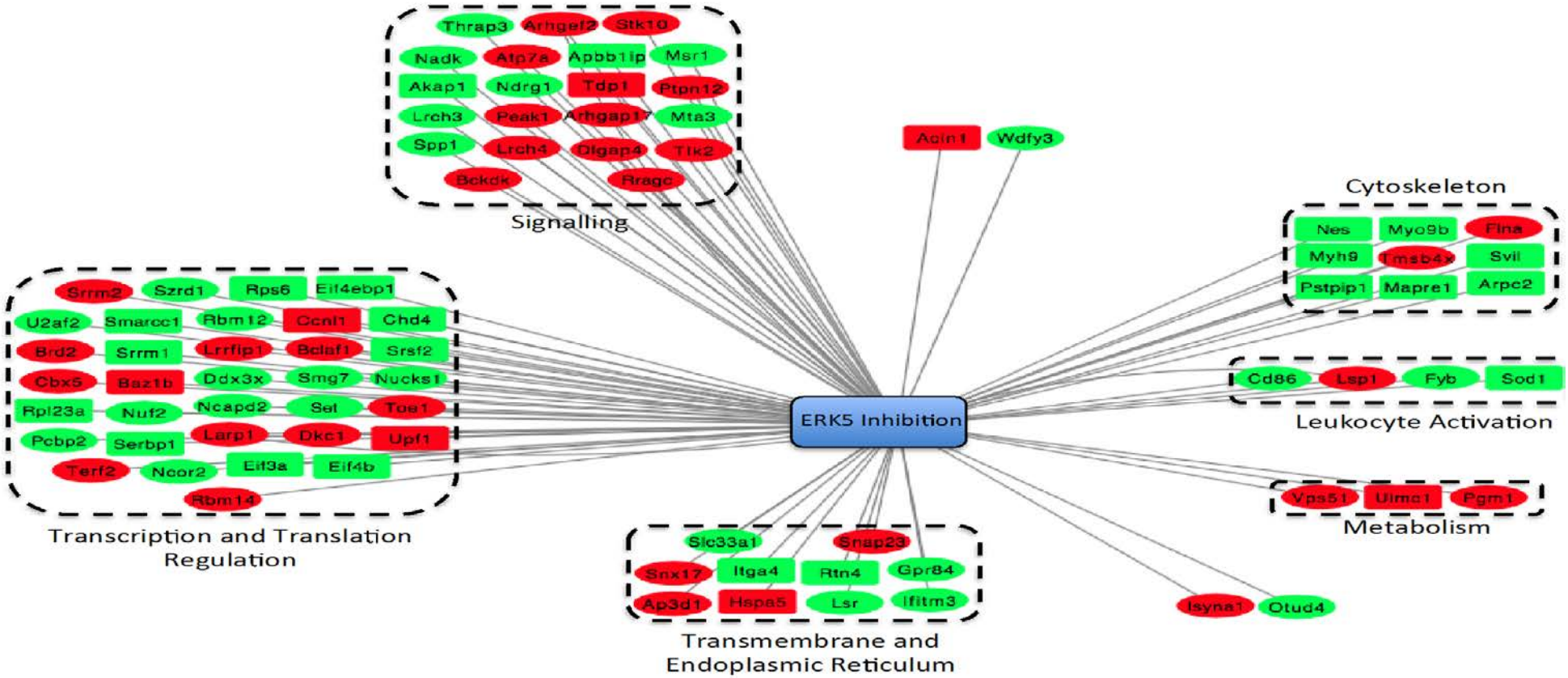

Figure 59: A Cytoscape plot showing the up and down regulated proteins, sorted into functional clusters, for the comparison between infected macrophages and infected macrophages + *XMD17-109* (HL). Red = down regulated proteins in infected macrophages treated with XMD17-109, Green = up regulated proteins in infected macrophages treated with *XMD17-109*, rectangle = significantly clustered and ellipse = not significantly clustered.

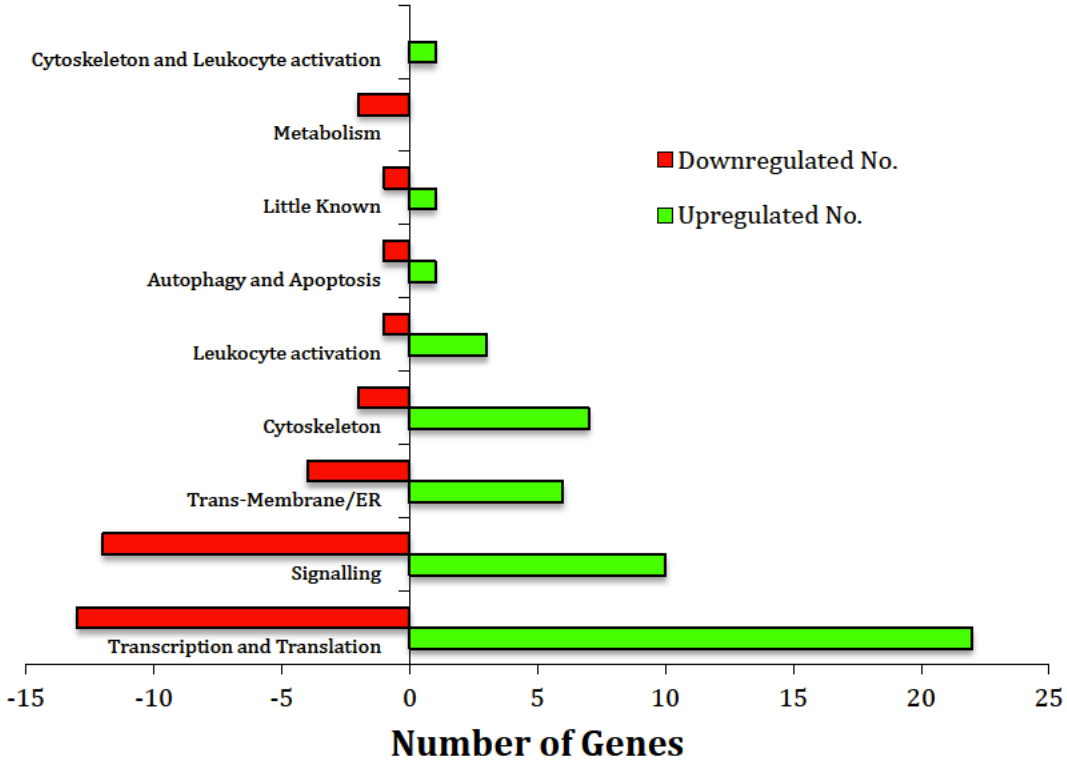

Figure 60: The number of genes up and down regulated in cryptococcal infected macrophages treated with *XMD17-109* compared to just infected macrophages, sorted by functional group.

Treatment of infected macrophages with XMD17-109 induced up and down-regulation of multiple genes when compared to infected only macrophages (Figure 60). The major groups of regulated proteins are associated with transcription/translation regulation and signalling proteins. As XMD17-109 is an ERK5 inhibitor, the downstream effects of blocking the molecular activity of this kinase will result in significant changes in gene regulation and signalling, hence the differences between treatments. An exciting result is the upregulation of multiple cytoskeletal genes in inhibitor treated cells compared to non-inhibitor treated macrophages. Upon treatment with the ERK5 inhibitor, 7/9 of the

identified cytoskeletal proteins are shown to be upregulated and significantly clustered. Two cytoskeletal proteins of particular interest include: Arpc2 and Myo9b. The ARP2/3 complex has been shown to play a significant role in the regulation of vomocytosis and therefore its presence in the mass spec data is encouraging. Significant cytoskeletal activity upon inhibitor treatment is interesting and the potential explanations for this will be discussed later on in the chapter. Smaller functional groups include regulation of transmembrane, metabolic and leukocyte activation proteins.

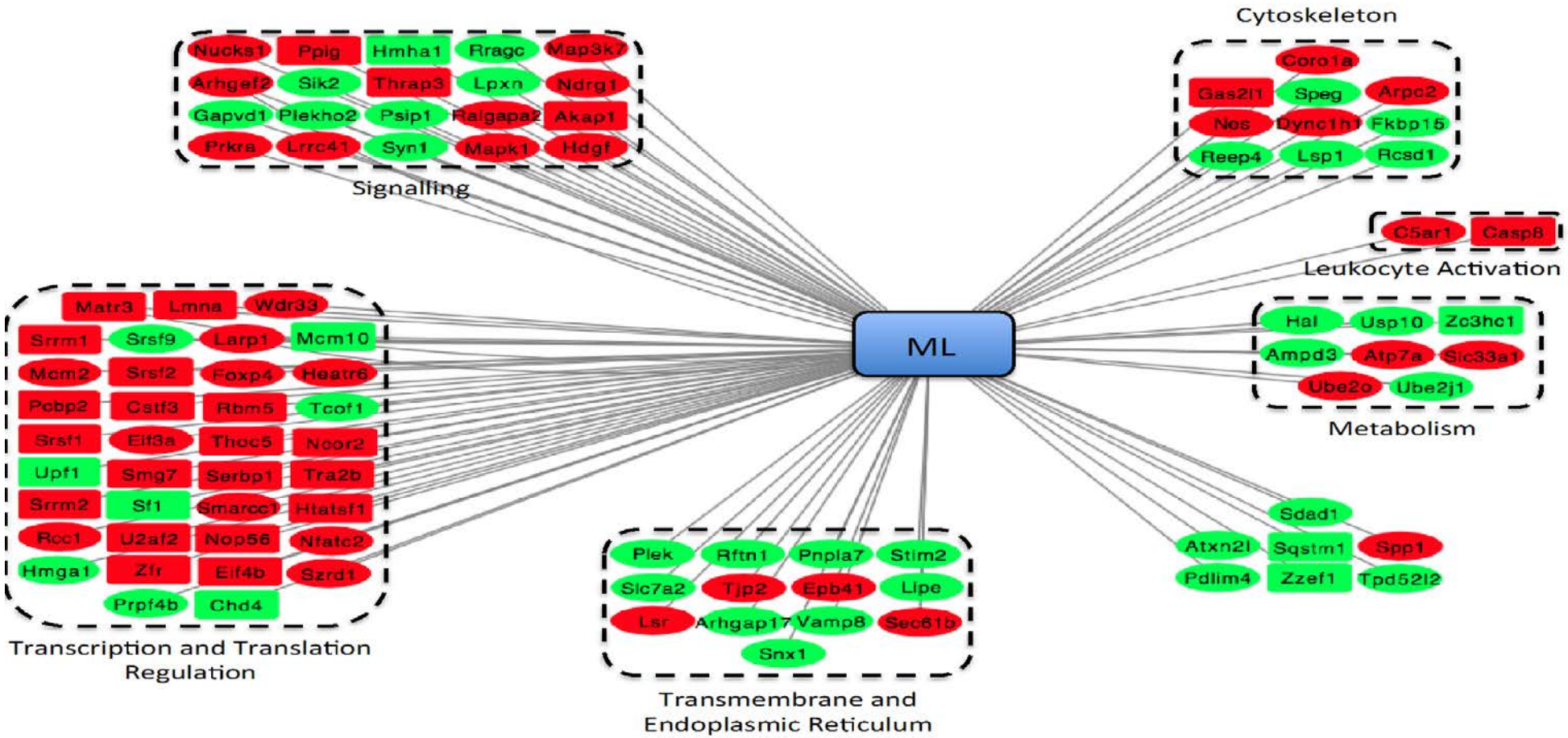

Figure 61: A Cytoscape plot showing the up and down regulated proteins, sorted into functional clusters, for the comparison between uninfected macrophages and infected macrophages + *XMD17-109* (ML). Red = down regulated proteins in uninfected macrophages, Green = up regulated proteins in uninfected macrophages, rectangle = significantly clustered and ellipse = not significantly clustered.

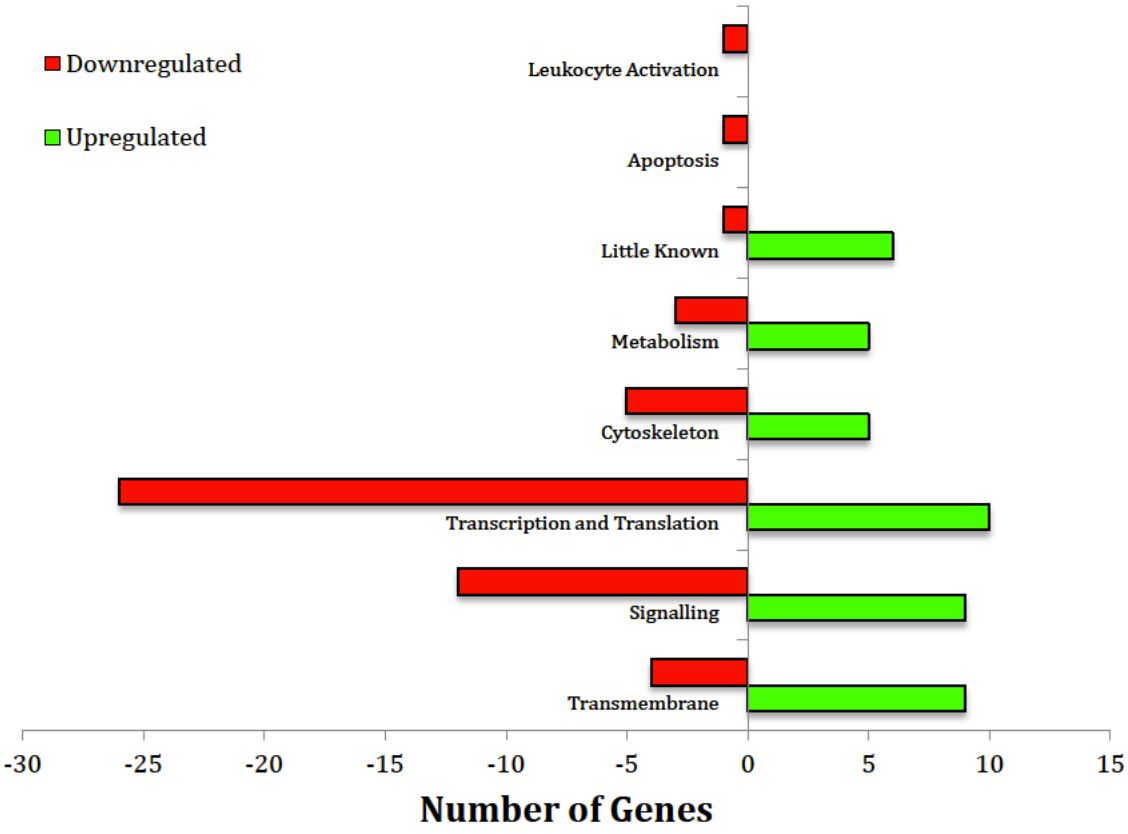

Figure 62: The number of genes up and down regulated in uninfected macrophages compared to infected macrophages treated with *XMD17-109.*

The final comparison made is between uninfected macrophages and infected macrophages treated with XMD17-109. As two variables have changed (infection and inhibitor treatment) this comparison has the most biological variability and interpreting the results from this study is far more difficult then previous comparisons. A point of note is that the three treatments are auto-correlated; i.e. if a protein/peptide is upregulated in the inhibitor vs. infected and upregulated in the infected versus uninfected, then by definition, it is also upregulated in the inhibitor vs. uninfected. Upon infection and treatment of macrophages, multiple signalling and

transcription/translational regulation proteins are upregulated when compared to the uninfected control. This is understandable as the biological changes between treatments are drastic and therefore the macrophage must respond accordingly. Cytoskeletal proteins are also regulated in response to the macrophage treatment. Similarly to the HL comparison Arpc2 is upregulated in response to the infection and inhibitor treatment. Arpc2 is not upregulated for the comparison between uninfected macrophages and infected macrophages (HM) indicating that Arpc2 may be under the control of ERK5. Conversely the protein Nes, is present in the HM comparison, the HL comparison and the ML comparison, therefore it is likely that infection triggers the expression of this protein. Other smaller groups including those for transmembrane, metabolic and leukocyte activation proteins are also present in this comparison.

To begin to understand the differences in cytoskeletal protein regulation between treatments Table 6 was constructed to visualise the comparison. Arpc2 is upregulated in macrophages treated with the ERK5 inhibitor, XMD17-109, against both other treatment types. Arpc2 is also not identified in infected macrophages when compared to the uninfected control. This suggests that Arpc2 is regulated by the addition of the ERK5 inhibitor, however this is likely to be very indirect. On the other hand the Nes gene is present in all comparisons and is likely to be triggered by cryptococcal infection.

Table 6: The identified cytoskeletal proteins and their relative regulation status for each comparison.

Gene	***Regulation during infection (relative to uninfected cells)***	***Regulation during infection + XMD17-109 (relative to infected only cells)***	***Regulation during no infection (relative to infected cells treated with XMD17-109)***
Coro1a			
Gas2l1			
Speg			
Arpc2			
Nes			
Dync1h1			
FKbp15			
Reep4			
Lsp1			
Rcsd1			
Myo9b			
Fina			
Myh9			
Tmsb4x			
Svil			
Pstpip1			
Mapre1			
Map1s			
Arhgef2			
Marcks			

Fgfr1op			
Dock 2			
Was			
Dbn1			

Discussion of Results

These data indicate that significant gene/protein regulation occur upon either cryptococcal infection of macrophages and/or cryptococcal infection of macrophages plus a treatment of the ERK5 inhibitor XMD17-109. The macrophage is likely to require significant changes in gene regulation to deal with both infection and/or macrophage treatment, therefore these data are unsurprising. A similar result was obtained for the regulation of signalling proteins and for proteins involved in plasma membrane and endoplasmic reticulum regulation. A multitude of signalling and membrane regulation would enable the macrophages to manage pathogenic attack and allow adaptation to the ERK5 inhibitor, XMD17-109.

A fascinating result is the evidence suggesting significant cytoskeletal modification upon ERK5 inhibition. **Johnston *et al.,* 2010**, identified actin cage formation around the cryptococcal containing phagosomes involving the WASH/WASP and the ARP2/3 complex and hypothesised that the formation of these "cage" like structures resulting in vomocytosis inhibition. Identification of upregulated cytoskeletal genes through the mass spec data, combined with the work from **Johnston *et al.,* 2010**, suggests that cytoskeletal activity is fundamental in the molecular process of vomocytosis. The data in the previous results chapter indicated that ERK5 inhibition results in an increase in the vomocytosis rates, therefore inhibition of ERK5 may result in the modification of cytoskeletal proteins, hence inducing the phenotype observed. Conversely, ERK5 inhibition may increase vomocytosis rates via an alternative mechanism and the

resulting upregulation of cytoskeletal proteins, observed in the mass spec data, is a result of an increase in actin cage formation to try and supress more vomocytosis events. A great experiment would be to treat infected macrophages with XMD17-109 and measure actin cage formation as performed by **Johnston *et al.,* 2010**. An increase in actin cage formation would indicate that the increase in vomocytosis rates drive more actin cage formation however, a reduction in actin cage formation would indicate that ERK5 inhibition is modulating the cytoskeletal proteins to modify vomocytosis rates.

Proteins of particular interest were the ARP2/3 proteins (Arpc2), identified as important for actin cage formation (**Johnston *et al.,* 2010**), and Myo9b – a myosin protein. Literature searches have revealed that phosphorylation of ARP2/3 proteins induce a nucleation of actin filaments driving the production of more actin filaments (**LeClaire *et al.,* 2008**), therefore potentially driving the production of more actin cages. The mass spec data shows that ERK5 inhibition of infected macrophages induces an upregulation or enhanced phosphorylation of these proteins. The specific subunit identified in the mass spec data was the Arpc2 subunit. Arpc2 is a 34KDa subunit and is one of seven peptides making up the ARP2/3 complex, involved in actin polymerisation and branching, however, its precise mode of action is poorly understood (**Welch *et al.,* 1997**). Phosphorylation of the particular phosphorylation site on the Arpc2 subunit may have a various affects on protein activity and hence actin cage formation.

Due to project time constraints the activity of majority of the identified cytoskeletal genes has not been explored extensively within the literature. How these genes may then have an affect on the cryptococcal macrophage interaction is yet to be explored. Further research into the roles of these proteins in cryptococcal infection is necessary, to begin to understand the enhanced vomocytosis phenotype recorded. This research is currently on-going within the lab.

CHAPTER 5: INVESTIGATING VOMOCYTOSIS RATES IN ALTERNATIVE BIOLOGICALLY RELEVANT SYSTEMS AND INVESTIGATION OF *C. NEOFORMANS* MUTANTS

The previous results chapters have explored the host driven aspect of the cryptococcal – macrophage interaction and how these affect the rates of vomocytosis. In this chapter the role of pathogen derived factors and other biologically relevant phenomena will be considered. Research to date has identified only a single virulence factor, PLB, as capable of altering the rate of vomocytosis (**Chayakulkeeree *et al.,* 2011**). As PLB is a cryptococcal secreted phospholipid-modifying enzyme, the plasma and lysophagosomal membranes may be modulated by PLB, inducing the changes in the rates of vomocytosis reported (**Chayakulkeeree *et al.,* 2011**). To begin to understand pathogen derived factors attributable to altered vomocytosis rates, mutants were targeted from the **Santiago-Tirado *et al.,* 2015** research data. These data show a range of cryptococcal mutants with reportedly poor phagocytosis rates, however it could be argued that these mutants have a high vomocytosis rate, which was detected in early screens. This approach was adopted as a prelude to a whole genome screen; hence targeting specific mutants for potential vomocytosis rate altered candidates.

This chapter also explores the effects of cryptococcal and *Mycobacteria* co-infection of macrophages. Cryptococcosis and tuberculosis are diseases commonly found in sub-Saharan Africa where, as a result of the HIV/AIDS epidemic, significant numbers of patients are co-infected with both pathogens. This chapter thus begins to explore the co-

infection of macrophages with both species to observe potential differences in the interaction between the pathogens and the macrophages.

A small-scale selective screen for C. *neoformans* mutants exhibiting altered vomocytosis rates

A multitude of genes from the *C. neoformans* H99 genome have been successfully mutated, using biolistics, by the Madhani group and stored as a library (**Liu *et al.,* 2008**). The *C. neoformans* library created by **Liu *et al.,* 2008**, was initially screened for melanisation, capsule formation, growth a physiological relevant temperature and intracellular proliferation rate (**Liu *et al.,* 2008**). Further to this in 2015 the library was further used to screen mutants investigating the differences in phagocytosis rates (**Santiago-Tirado *et al.,* 2015**). The methods used in this paper explore phagocytosis rates but do not consider the effects of cryptococcal vomocytosis or pathogen derived macrophage lysis. These two processes have significant consequences on the reported phagocytosis rate. The question asked was, do the reportedly poor phagocytosis mutants (**Santiago-Tirado *et al.,* 2015**) induce an increase in macrophage lysis or increase in vomocytosis rates which in-turn indicates a poor phagocytosis rate using the method **Santiago-Tirado *et al.,*** used in 2015. We were particularly interested in mutants with an increased vomocytosis rate, as these mutants are easier to analysis in comparison to the WT (H99) control. Ten of these reportedly poorly phagocytic strains were selected at random and the rates of cryptococcal vomocytosis and macrophage lysis investigated using time-lapse microscopy, as has been shown in previous chapters. The mutants selected are shown in Table 7.

Table 7: The selected mutant strains and the gene mutation described.

Mutant Strain/ Protein	Library Location	Protein Activity
Wild Type H99	-	-
Wild Type Kn99	-	-
OPT1	4 – H8	Proton-coupled oligopeptide transporter
GPB1	9 EE4	G-protein beta sub-unit involved in pheromone sensing and mating
LP15	10 – H1	Transporter of the major facilitator superfamily
LP19	9 – G10	Endoglucanase
HRK1	10 EE9	Serine and threonine – protein kinase
CAS33	7 – H6	Capsular associated protein; involved in modification of GXM polysaccharides.
LPI15	9 – D2	Membrane protein; domains typical of WSC proteins, polycystin and fungal exoglucanase
LPI16	7 – D9	3-oxo-5-alpha-steroid 4-dehydrogenase (steroid reductase.
DHA1	1 – D5	Glycoprotein that elicits a delayed type hypersensitivity in mice
SNF3/HXT2	1 EE6	Low affinity glucose (hexose) transporter

J774A.1 murine macrophages were infected with the individual mutants of *C. neoformans*, highlighted in table 7, with an MOI of 10:1. The rates of macrophage lysis and cryptococcal vomocytosis were recorded from the time-lapse movies and recorded in Figure 63.

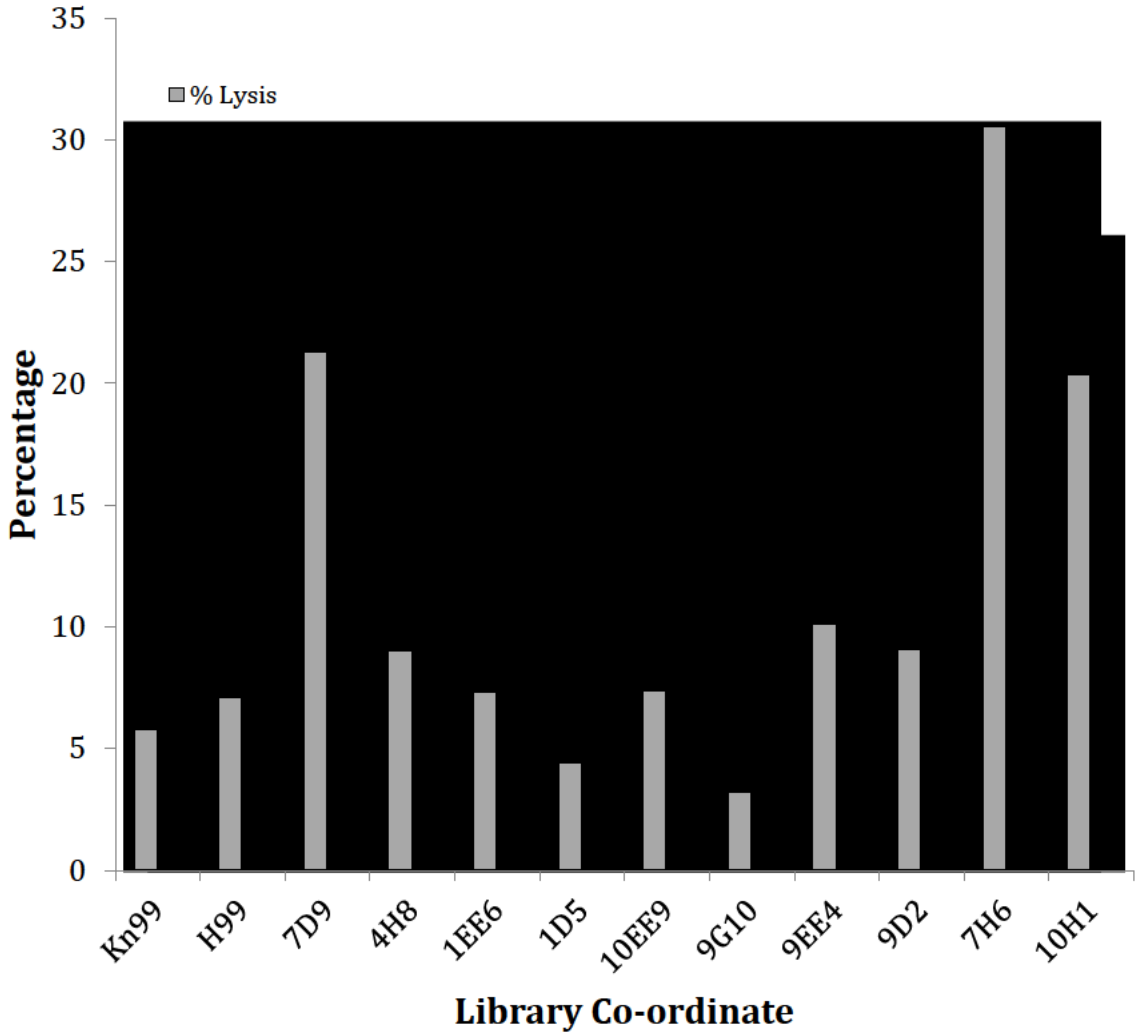

Figure 63: The lysis rates (GREY) and vomocytosis rates (BLACK) of the individual selected mutants from the Madhani library. (n = 1)

The range (10) of selected cryptococcal mutants was screened for vomocytosis and pathogen driven macrophage lysis by analysing three technical repeats of a single biological repeat. Analysis of these movies is a time consuming and visually demanding process, therefore mutants drastically different from the WT control were selected for further experiments. Figure 63 shows the initial vomocytosis and macrophage lysis screen. The data is variable with some mutant strains generating an increased rate of macrophage lysis, such as *CAS33* (7-H6), *LPI16* (7-D9) and *LP15* (9-D2) compared to the H99 WT control. Other mutant strains had higher vomocytosis rates, such as *DHA1* (1-D5), *HRK1* (10EE9), *SNF3/HXT2* (1EE6) and *LPI15* (9-D2). Our primary interest in this study was naturally the modulation of vomocytosis. The mutant strains to be carried forward were *DHA1* (1-D5) and *HRK1* (10EE9) due to the changes in vomocytosis and relatively small effects on macrophage lysis. The two strains, *LP15* (10-H1) and *CAS33* (7-H6), induced extremely high levels of macrophage lysis and were therefore included in the second experiment to investigate whether this effect was reproducible or whether the macrophages in the area of the well used for imaging had become sensitive, possibly due to the wash procedure. This selection enabled four separate mutants to be explored more closely. During the initial screen the intracellular proliferation rate was also measured by counting the number of buds individual mother cryptococci produced over the course of an 18-hour time-lapse (Figure 64).

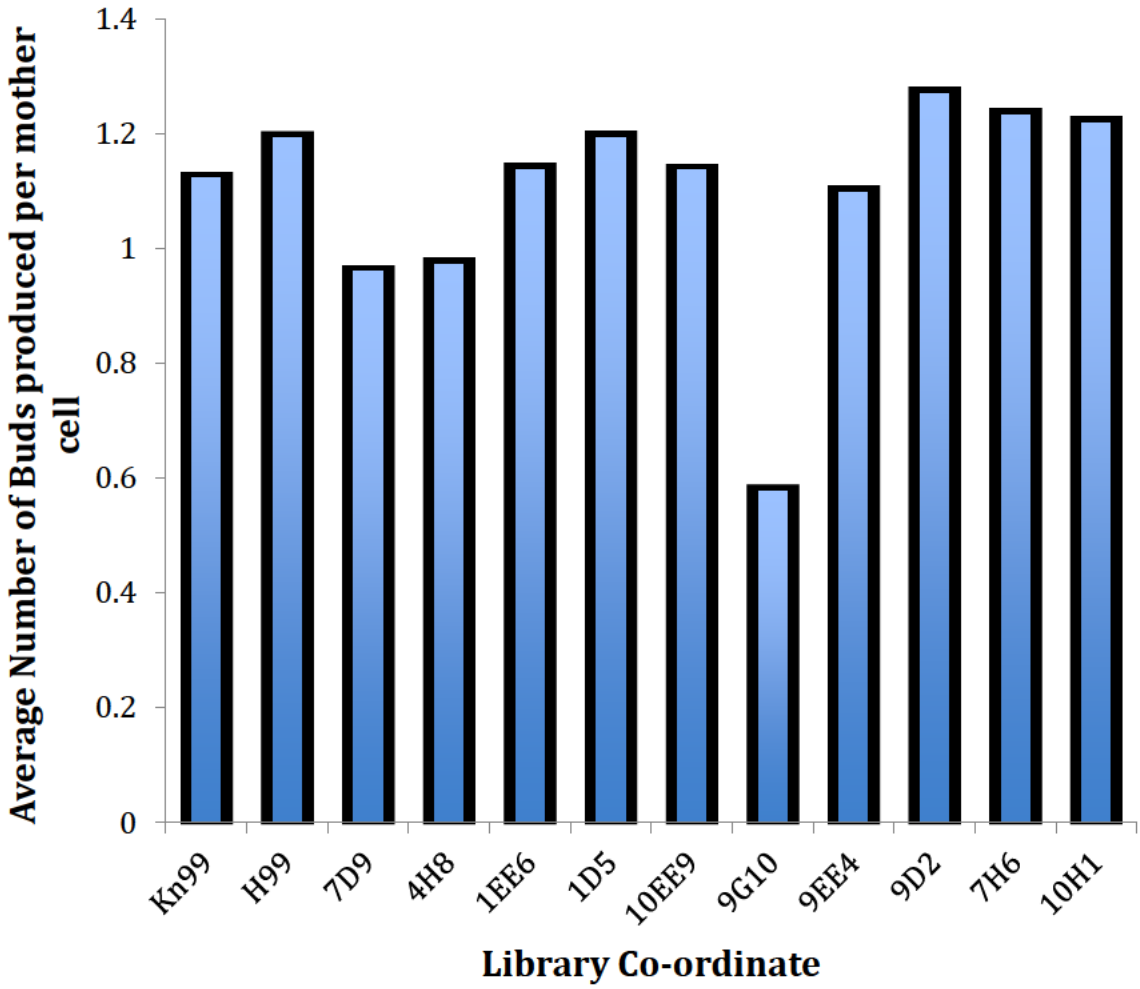

Figure 64: The time-lapse calculated IPR's of the individual selected mutants from the Madhani library. (N = 1)

The IPRs show little difference between the mutant strains and WT control (H99), with the exception of *LP19* (9-G10), which appears to be significantly impaired in intracellular survival.

The *DHA1* (1-D5), *HRK1* (10EE9), *LP15* (10-H1) and *CAS33* (7-H6) mutants were used for further analysis. The results of the second experiment are shown in Table 8.

Table 8: Analysis of the second experiment involving the "poorly phagocytic" mutant strains (n = 2).

Library Location	**Gene Mutated**	**Number Counted**	**Vomocytosis (%)**	**Macrophage Lysis (%)**	**IPR**
H99	N/A	104	2.88	0.00	1.50
10-H1	LP15	125	6.40	0.00	1.34
10EE9	HRK1	86	5.81	0.00	2.02
7-H6	CAS33	129	17.05	0.78	1.16
1–D5	DHA1	132	15.91	3.03	1.62

From the data shown in Table 8, it can clearly be seen that two of the mutants, *CAS33* and *DHA1*, have much higher rates of vomocytosis that the H99 WT control. For the *DHA1* mutant this agrees with the initial study and therefore this mutant was carried forward for further analysis. For the *CAS33* mutant the rates of macrophage lysis have decreased dramatically and the rates of vomocytosis have increased. This indicated that in the initial study the area of the well imaged was sensitive – commonly occurring at the point where the macrophages are washed prior to imaging. The rates of vomocytosis for this strain were as high as the *DHA1* mutant and therefore the mutant was carried forward for further studies. The IPR for the *DHA1* mutant are not dramatically different from the H99 WT control, however the IPR for the *CAS33* mutant are lower then the H99 WT control. As *CAS33* is involved in capsule modification, this agrees with the literature that capsule is the most prominent virulence factor, commonly required for persistence within a macrophage. Alterations in the capsule may reduce the resistant properties of the cryptococci.

These two strains, *DHA1* (1-D5) and *CAS33* (7-H6), were analysed for their effects on vomocytosis rates a further four times ensuring that six separate biological repeats were obtained for each mutant strain and the H99 WT control. Figure 65 shows the data for the complete study of these mutant strains.

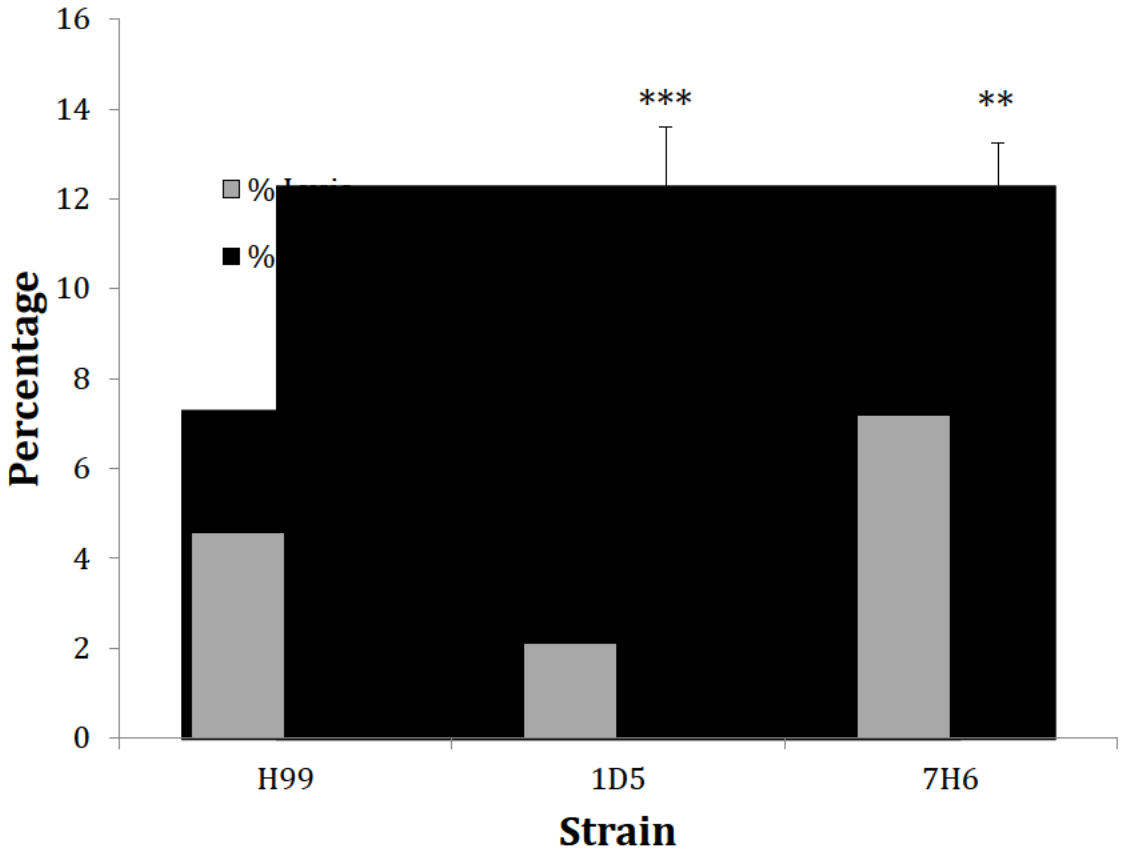

Figure 65: The macrophage lysis rates (GREY) and vomocytosis rates (BLACK) shown for the WT H99 strain and the two mutant strains, *DHA1* (1-D5) and *CAS33* (7-H6). Error Bar = SEM. *** $p > 0.0001$, ** $p > 0.001$. Bonferroni correction = 0.05/2 = 0.025 for significance at the 5% level (n = 6).

The rates of cryptococcal vomocytosis for both mutant strains are significantly higher then the WT H99 control, *DHA1* (1-D5) $X^2 = 34.68$, $p > 0.0001$ and *CAS33* (7-H6) $X^2 = 14.16$, $p > 0.001$, $n = 6$. This suggests that both the cryptococcal genes investigated may play significant roles in the regulation of cryptococcal driven vomocytosis and therefore are worthy of further investigation. The next stage is to mutate these genes in a separate *C. neoformans* strain and observe whether these effects are reproducible; this is currently being performed in the lab.

Mycobacteria Co-infection

Although rare, cryptococcal and mycobacterial co-infections occur clinically in endemic regions (**Huang *et al.,* 2010; Chandrashekar *et al.,* 2012**). The immunological effects of harbouring two such infections may be severe and have drastic consequences on disease progression for both infectious parties. The research in this thesis is particularly interested in vomocytosis and as mycobacterial species are capable of parasitizing macrophages, the effects on vomocytosis rate were investigated in relation to co-infection. Dr. Apoorva Bhatt provided all the bacterial strains used in this study and these can be found in the methods chapter. Initial experiments were conducted using the mCherry tagged *M. marinum* and dsRed tagged *E. coli* strains. These bacterial strains were co-infected in macrophages with *C. neoformans*. *M. marinum* was used as it is safer and shares many commonalities with *M. tuberculosis* such as cell wall structure and the ability to parasitise macrophages*. M. marinum* is commonly found in aquatic environments but rarely causes infections, however when infections do occur they are

commonly associated with aquarium fish keepers (**Lewis *et al.,* 2003**; **Rallis *et al.,* 2007**).

Macrophages were infected with serum opsonised *C. neoformans* H99 GFP and unopsonised bacteria simultaneously. The optimum number of bacterial cells used was determined in preliminary studies. The cellular concentrations used, provided the greatest number of double phagocytic (fungi and bacteria) events without inducing adverse macrophage effects. The rates of vomocytosis, macrophage lysis and cryptococcal budding of macrophages infected with both bacteria and fungi were counted similarly to the kinase inhibitor study (Figure 66 and 67).

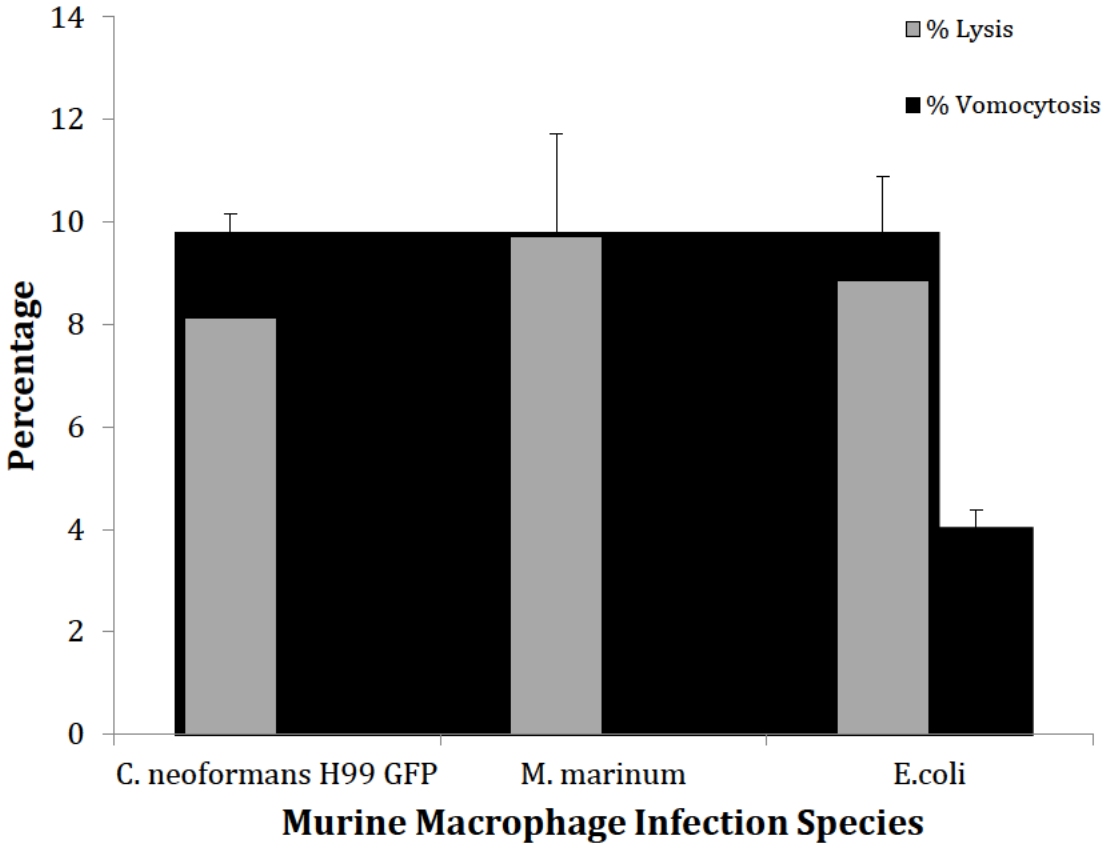

Figure 66: The effects of bacterial and cryptococcal co-infection on the percentage macrophage lysis and vomocytosis events (n = 6). Error bars = SD. Bonferroni correction 0.05/2 = 0.025 for significance at the 5% level. * = p >0.05.

The H99 GFP data shows macrophages singly infected with cryptococci alone, counted - 1264. The *M. marinum* data shows macrophages that were co-infected with cryptococci and *M. marinum,* counted - 350. The *E. coli* data shows macrophages that were co-infected with cryptococci and *E. coli,* counted - 811. *E.coli* was used as a control to help identify whether the effects observed were bacteria specific.

No significant difference was observed in the rates of macrophage lysis between H99 GFP and *M. marinum* co-infection ($X^2 = 0.86$, $p = 0.35$, $n = 6$) or *E. coli* co-infection ($X^2 = 0.34$, $p = 0.56$, $n = 6$). Whilst no significant difference was observed in the rates of cryptococcal vomocytosis between H99 GFP and *E.coli* co-infection ($X^2 = 0.38$, $p = 0.54$, $n = 6$), a significant reduction was observed in the rates of cryptococcal vomocytosis between H99 GFP single infection and *M. marinum* co-infection ($X^2 = 8.54$, $p = 0.003$, $n = 6$). Furthermore, the number of co-infected macrophages with *E.coli* compared to *M. marinum* are far higher (811 - *E. coli* vs. 350- *M. marinum*), suggesting that *M. marinum* may have an effect on the phagocytosis rates of *C. neoformans*.

The movies were also used to gain an indication of the effects of cryptococcal-infected macrophages upon the intracellular proliferation rate of the cryptococci. The intracellular budding capacity of cryptococci, in macrophages co-infected with both strains of bacteria, showed no significant differences between the infection status (Figure 67).

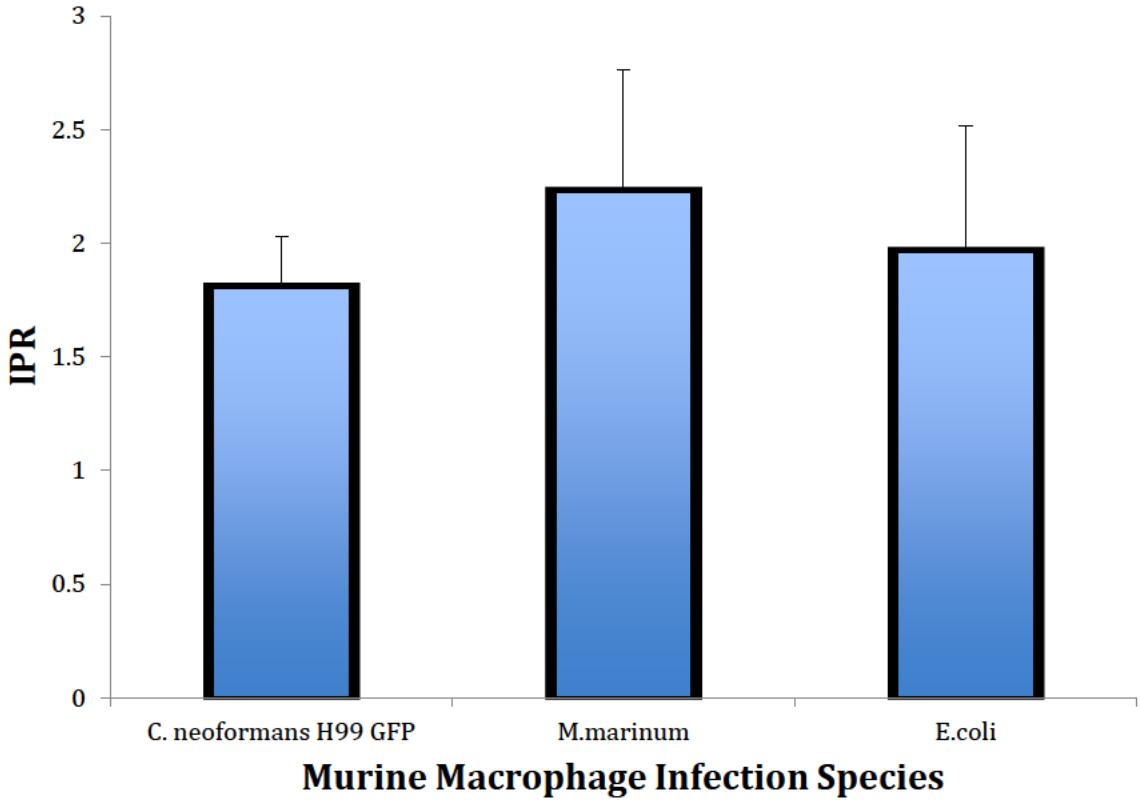

Figure 67: The intracellular budding capacity of *C. neoformans* H99 GFP cells produced during the 18-hour time-lapse movies whilst singularly or co-infected with the two bacterial strains (n = 6). Error bars = SD.

To ensure that the effects seen were not *C. neoformans* H99 GFP strain specific, a second strain ATCC 90112, with a naturally higher basal vomocytosis rate, was used in repeat experiments (Figure 68). No difference was observed in the intracellular budding capacity of ATCC 90112 whilst co-infected with *E. coli* or *M. marinum,* when compared to the nothing-added control, similar to the results for *C. neoformans* H99 GFP. A significant difference was observed for the vomocytosis rates between the macrophages singularly infected with *C. neoformans* H99 GFP and those co-infected with *M. marinum* ($X^2 = 3.83$, $p = 0.05$, $n = 3$). No significant difference was observed between the

macrophages singularly infected with *C. neoformans* H99 GFP and those co-infected with *E. coli* ($X^2 = 1.28$, $p = 0.26$, $n = 3$). These results are similar to the *C. neoformans* H99GFP experiments suggesting that the effects observed are not cryptococcal strain specific. Similarly, addition of *M. marinum* reduces the phagocytic uptake of *C. neoformans*, suggestive of an effect on phagocytosis.

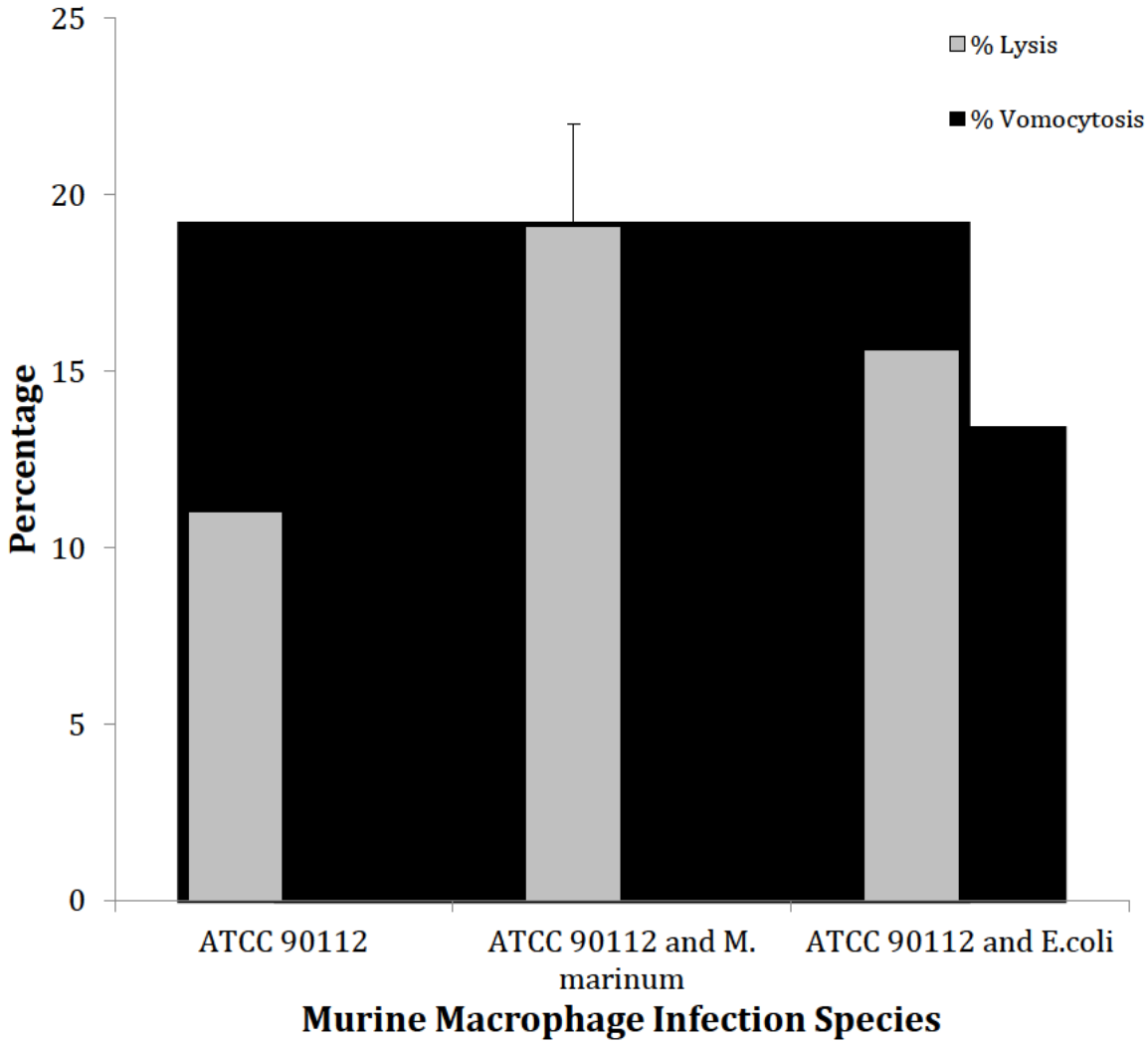

Figure 68: The effects of bacterial and cryptococcal co-infection on the percent (%) of macrophage lysis and the percent (%) of vomocytosis events (n = 3). Error bars = SD.

The ATCC90112 data shows macrophages singly infected with cryptococci alone, counted -353. The *M. marinum* data shows macrophages that were co-infected with cryptococci and *M. marinum,* counted - 184. The *E. coli* data shows macrophages that were co-infected with cryptococci and *E. coli,* counted - 448*. E.coli* was used as a control to help identify whether the effects observed were bacteria specific.

These data indicate that the addition of *M. marinum* during co-infection of macrophages reduces phagocytosis rates and the vomocytosis rate but has little effect on intracellular proliferation rates and macrophage physiology. How the presence of mycobacteria induces a reduction in the rate of cryptococcal vomocytosis is unknown, however co-infection is likely to induce a plethora of genetic, biochemical and physiological changes to the host macrophage.

Discussion

The data presented in this chapter begin to explore the cryptococcal-derived factors associated within changes in the rates of cryptococcal vomocytosis. Until recently the only known cryptococcal virulence factor to affect vomocytosis rates was phospholipase B (**Chayakulkeeree *et al.,* 2011**). Mutants of *plb1* have been shown to have a reduced vomocytosis rate compared to the WT counterparts, possibly due to the reduction in plasma membrane modification of these mutants (**Chayakulkeeree *et al.,* 2011**). In this study, mutants with reportedly poor phagocytosis rates (**Liu *et al.,* 2008; Santiago-Tirado *et al.,* 2015**) were investigated and the rates of vomocytosis of these mutants were compared to the WT control.

These data highlight two mutants, which have enhanced rates of vomocytosis compared to the WT (H99) control. These mutants have no effect on macrophage lysis or intracellular proliferation rate. The first is a *DHA1* mutant. *DHA1* encodes a glycoprotein, highly expressed on the cell surface, which elicits a delayed type hypersensitive response in mice (**Mandel *et al.,* 2000; Santiago-Tirado *et al.,* 2015**). The presence of this glycoprotein partly drives the immunological response towards the protective M2 phenotype, hence deletion of this gene would reduce the ability of the *C. neoformans* to induce this response; macrophages would be less protective and potentially more skewed towards the aggressive M1 phenotype (**Mandel *et al.,* 2000**). The ability of *C. neoformans* to skew the immunological response toward an M2 phenotype is well-documented (**Monari *et al.,* 2006; Shen and Liyun 2015).** Immunological modification enables the survival and replication of cryptococci within macrophages. These data

agree with our earlier conclusions that the generation of an aggressive M1 phenotype drives cryptococci to vomocytose more frequently. Cytokine profiling and Lysotracker Red phagosome testing are essential experiments to confirm this.

The second mutant was a *CAS33* mutant. CAS33 is a capsule associated protein involved in polysaccharide modification of the cryptococcal capsule (**Moyrand e*t al.,* 2004**). CAS33 is associated with the O-acetylation of xylose residues, potential antigens on the surface of the cryptococcal capsule. Interestingly, deletion of *CAS33* does not reduce the overall size of the polysaccharide capsule (**Moyrand *et al.,* 2004**). Subtle polysaccharide changes to the biochemistry of the capsule via CAS33 induce the vomocytosis phenotype observed. How this phenotype arises is unknown and further experiments, such as cytokine profiling and phagosome dynamics needs to be considered to begin to understand the process. The alterations in cellular capsule modification may induce changes to the immunological responses to the pathogen similar to hypotheses previously described, however it is equally likely that the changes to the cryptococcal capsule my drive an alternative mechanisms resulting in the increase vomocytosis phenotype observed. The genes of interest are now being deleted in a separate strain of *C. neoformans* to observe whether the effect is reproducible within multiple different strains.

Another important aspect of cryptococcal biology is the fact that *C. neoformans* infections rarely operate in isolation. *C. neoformans* predominantly affects the immunocompromised such as those with HIV/AIDS (**Park *et al.,* 2009**). However, multiple other species also endemic to similar regions, such as *M. tuberculosis*, operate in

a similar way, therefore it is feasible that a person infected with HIV would not only acquire a cryptococcal infection but also a TB infection. The literature has case reports of this occurring (**Huang *et al.,* 2010; Chandrashekar *et al.,* 2012).** The affect of co-infection of macrophages was investigated and the rates of vomocytosis specifically looked at. The data from this chapter suggests that the presence of mycobacteria within the macrophage, simultaneously infected with *C. neoformans,* induces a reduction in the rate of cryptococcal vomocytosis and phagocytosis. The data presented in this chapter indicate that the reduction in vomocytosis is slight but reproducible, with two separate cryptococcal strains tested. Repeating the experiments with separate strains of *M. marinum* and *M. tuberculosis* would indicate whether the effect is reproducible with separate bacterial strains/species. Other bacterial species such as *M. smegmatis* – a non-pathogenic mycobacterial species with a similar cell wall to *M. marinum* and *Corneybacterium species* - a bacterium with a similar cell wall structure but is not a mycobacteria may shed further light onto the vomocytosis phenotype observed. Bacterial cell wall, a major pathogen associated molecular pattern, may induce an altered immunological response, hence reducing vomocytosis, however much more work is required to ascertain this.

Co-infection and polymicrobial interactions are interesting areas of research. The methods used in these studies enabled the visualisation of a complex multicellular interaction between macrophages, *C. neoformans* and *M. marinum*. The *in vivo* effects of co-infection upon cryptococcal dissemination, lung and brain fungal burden, immunological responses during co-infection and extracellular cryptococcal growth are experiments that would reveal more about the co-infection relationship between *C. neoformans* and *M. marinum*.

THESIS SUMMARY

This thesis has concentrated on characterising the enigmatic process of cryptococcal vomocytosis from both the host and pathogen perspective. The non-lytic exocytosis mechanism of vomocytosis has been hypothesised to have severe consequences on pathogen dissemination and hence patient prognosis, however until recently little was known about the molecular mechanism governing the process. The data in this thesis highlights macrophage ERK5 as a potent regulator of vomocytosis by demonstrating that down-regulation or inhibition of ERK5 results in enhanced vomocytosis. Using mass spectrometry, I implicate a variety of actin cytoskeletal genes in playing a role in the process of vomocytosis. Finally pathogen derived virulence factors have been explored implicating cryptococcal *CAS33* and *DHA1* as factors potentially associated with the process. This research sheds light on the process of vomocytosis, potentially enabling alternative therapeutic strategies to be developed concerning reducing cryptococcal dissemination within the host.

Reference:

Aimanianda, V., Bayry, J., Bozza, S., Kniemeyer, O., Perruccio, K., Elluru, S. R., Clavaud, C., Paris, S., Brakhage, A. A., Kaveri, S. V., Romani, L. and Latge, J.-P. (2009) 'Surface hydrophobin prevents immune recognition of airborne fungal spores', Nature, 460(7259), 1117-U79.

Albert-Weissenberger, C., Cazalet, C. and Buchrieser, C. (2007) 'Legionella pneumophila - a human pathogen that co-evolved with fresh water protozoa', Cellular and Molecular Life Sciences, 64(4), 432-448.

Alspaugh, J. A. and Granger, D. L. (1991) 'INHIBITION OF CRYPTOCOCCUS-NEOFORMANS REPLICATION BY NITROGEN-OXIDES SUPPORTS THE ROLE OF THESE MOLECULES AS EFFECTORS OF MACROPHAGE-MEDIATED CYTOSTASIS', Infection and Immunity, 59(7), 2291-2296.

Alvarez, M. and Casadevall, A. (2006) 'Phagosome extrusion and host-cell survival after Cryptococcus neoformans phagocytosis by macrophages', Curr Biol, 16(21), 2161-5.

Amano, S., Chang, Y.T. and Fukui, Y. (2015) ‘ERK5 activation is essential for osteoclast differentiation’, PLoS One, 10(4).

Andersen, T. E., Khandige, S., Madelung, M., Brewer, J., Kolmos, H. J. and Moller-Jensen, J. (2012) 'Escherichia coli Uropathogenesis In Vitro: Invasion, Cellular Escape, and Secondary Infection Analyzed in a Human Bladder Cell Infection Model', Infection and Immunity, 80(5), 1858-1867.

Anthony, R. M., Urban, J. F., Jr., Alem, F., Hamed, H. A., Rozo, C. T., Boucher, J.-L., Van Rooijen, N. and Gause, W. C. (2006) 'Memory T(H)2 cells induce alternatively activated macrophages to mediate protection against nematode parasites', Nature Medicine, 12(8), 955-960.

Bain, J., Lewis, L., Okai, B., Quinn, J., Gow, N. and Erwig, L. (2012) 'Non-lytic expulsion/exocytosis of Candida albicans from macrophages', Fungal Genetics and Biology, 49(9), 677-678.

Ballabh, P., Braun, A. and Nedergaard, M. (2004) 'The blood-brain barrier: an overview - Structure, regulation, and clinical implications', Neurobiology of Disease, 16(1), 1-13.

Beaman, L. (1987) 'FUNGICIDAL ACTIVATION OF MURINE MACROPHAGES BY RECOMBINANT GAMMA-INTERFERON', Infection and Immunity, 55(12), 2951-2955.

Beaman, L. and Holmberg, C. (1980) 'In vitro Response of Alveolar Macrophages to Infection with Coccidioides immitis', Infection and Immunity, 28(2), 594-600.

Biswas, S. and Mantovani, A. (2010) 'Macrophage plasticity and interaction with lymphocyte subsets: cancer as a paradigm', Nature Immunology, 11(10), 889-896.

Blanco, J., Hontecillas, R., Bouza, E., Blanco, I., Pelaez, T., Munoz, P., Molina, J. and Garcia, M. (2002) 'Correlation between the elastase activity index and invasiveness of clinical isolates of Aspergillus fumigatus', Journal of Clinical Microbiology, 40(5), 1811-1813.

Bolanos, B. and Mitchell, T. G. (1989) 'PHAGOCYTOSIS OF CRYPTOCOCCUS-NEOFORMANS BY RAT ALVEOLAR MACROPHAGES', Journal of Medical and Veterinary Mycology, 27(4), 203-217.

Borchers, A. and Gershwin, M. (2010) 'The immune response in Coccidioidomycosis', Autoimmunity Reviews, 10(2), 94-102.

Bose, I., Reese, A., Ory, J., Janbon, G. and Doering, T. (2003) 'A yeast under cover: the capsule of Cryptococcus neoformans', Eukaryotic Cell, 2(4), 655-663.

Brothers, K. M., Gratacap, R. L., Barker, S. E., Newman, Z. R., Norum, A. and Wheeler, R. T. (2013) 'NADPH oxidase-driven phagocyte recruitment controls Candida albicans filamentous growth and prevents mortality', PLoS Pathog, 9(10), e1003634.

Brothers, K. M., Newman, Z. R. and Wheeler, R. T. (2011) 'Live imaging of disseminated candidiasis in zebrafish reveals role of phagocyte oxidase in limiting filamentous growth', Eukaryot Cell, 10(7), 932-44.

Brown, G. D., Denning, D. W., Gow, N. A., Levitz, S. M., Netea, M. G. and White, T. C. (2012) 'Hidden killers: human fungal infections', Sci Transl Med, 4(165), 165rv13.

Brown, S., Campbell, L. and Lodge, J. (2007) 'Cryptococcus neoformans, a fungus under stress', Current Opinion in Microbiology, 10(4), 320-325.

Byrnes, E. J., III, Li, W., Ren, P., Lewit, Y., Voelz, K., Fraser, J. A., Dietrich, F. S., May, R. C., Chatuverdi, S., Chatuverdi, V. and Heitman, J. (2011) 'A Diverse Population of Cryptococcus gattii Molecular Type VGIII in Southern Californian HIV/AIDS Patients', Plos Pathogens, 7(9).

Calderone, R. and Sturtevant, J. (1994) 'Macrophage interactions with Candida', Immunol Ser, 60, 505-15.

Cambier, C. J., Falkow, S. and Ramakrishnan, L. (2014) 'Host Evasion and Exploitation Schemes of Mycobacterium tuberculosis', Cell, 159(7), 1497-1509.

Carlos Montero, J., Ocana, A., Abad, M., Jesus Ortiz-Ruiz, M., Pandiella, A. and Esparis-Ogando, A. (2009) 'Expression of Erk5 in Early Stage Breast Cancer and Association with Disease Free Survival Identifies this Kinase as a Potential Therapeutic Target', Plos One, 4(5).

Carter, E. J., Cosgrove, R. A., Gonzalez, I., Eisemann, J. H., Lovett, F. A., Cobb, L. J. and Pell, J. M. (2009) 'MEK5 and ERK5 are mediators of the pro-myogenic actions of IGF-2', Journal of Cell Science, 122(17), 3104-3112.

Casadevall, A. (2010) 'Cryptococci at the brain gate: break and enter or use a Trojan horse?', Journal of Clinical Investigation, 120(5), 1389-1392.

Casadevall, A., Rosas, A. L. and Nosanchuk, J. D. (2000) 'Melanin and virulence in Cryptococcus neoformans', Current Opinion in Microbiology, 3(4), 354-358.

Chakrabarti, A., Jatana, M., Kumar, P., Chatha, L., Kaushal, A. and Padhye, A. A. (1997) 'Isolation of Cryptococcus neoformans var. gattii from Eucalyptus camaldulensis in India', Journal of Clinical Microbiology, 35(12), 3340-3342.

Chandrashekar, U. K., Acharya, V., Varghese, G. K. and Rao, L. (2012) 'An unusual presentation of pulmonary cryptococcosis with co-existing disseminated tuberculosis in an AIDS patient', Tropical Doctor, 42(1), 60-62.

Chang, Y. C., Stins, M. F., McCaffery, M. J., Miller, G. F., Pare, D. R., Dam, T., Paul-Satyasee, M., Kim, K. S. and Kwon-Chung, K. J. (2004) 'Cryptococcal yeast cells invade the central nervous system via transcellular penetration of the blood-brain barrier', Infection and Immunity, 72(9), 4985-4995.

Chao, T. H., Hayashi, M., Tapping, R. I., Kato, Y. and Lee, J. D. (1999) 'MEKK3 directly regulates MEK5 activity as part of the big mitogen-activated protein kinase 1 (BMK1) signaling pathway', Journal of Biological Chemistry, 274(51), 36035-36038.

Chaturvedi, V. and Chaturvedi, S. (2011) 'Cryptococcus gattii: a resurgent fungal pathogen', Trends in Microbiology, 19(11), 564-571.

Chayakulkeeree, M., Johnston, S., Oei, J., Lev, S., Williamson, P., Wilson, C., Zuo, X., Leal, A., Vainstein, M., Meyer, W., Sorrell, T., May, R. and Djordjevic, J. (2011) 'SEC14 is a specific requirement for secretion of phospholipase B1 and pathogenicity of Cryptococcus neoformans', Molecular Microbiology, 80(4), 1088-1101.

Chen, H., Langer, R. and Edwards, D. (1997) 'A film tension theory of phagocytosis', Journal of Colloid and Interface Science, 190(1), 118-133.

Chen, J., Varma, A., Diaz, M. R., Litvintseva, A. P., Wollenberg, K. K. and Kwon-Chung, K. J. (2008) 'Cryptococcus neoformans strains and infection in apparently immunocompetent patients, China', Emerging Infectious Diseases, 14(5), 755-762.

Chrisman, C. J., Alvarez, M. and Casadevall, A. (2010) 'Phagocytosis of Cryptococcus neoformans by, and Nonlytic Exocytosis from, Acanthamoeba castellanii', Applied and Environmental Microbiology, 76(18), 6056-6062.

Chu, J., Feudtner, C., Heydon, K., Walsh, T. and Zaoutis, T. (2006) 'Hospitalizations for endemic mycoses: A population-based national study', Clinical Infectious Diseases, 42(6), 822-825.

Clark, K., MacKenzie, K. F., Petkevicius, K., Kristariyanto, Y., Zhang, J., Choi, H. G., Peggie, M., Plater, L., Pedrioli, P. G. A., McIver, E., Gray, N. S., Arthur, J. S. C. and Cohen, P. (2012) 'Phosphorylation of CRTC3 by the salt-inducible kinases controls the interconversion of classically activated and regulatory macrophages', Proceedings of the National Academy of Sciences of the United States of America, 109(42), 16986-16991.

Cox, G. M., Mukherjee, J., Cole, G. T., Casadevall, A. and Perfect, J. R. (2000) 'Urease as a virulence factor in experimental cryptococcosis', Infection and Immunity, 68(2), 443-448.

Day, J. N., Hoang, T. N., Duong, A. V., Hong, C. T. T., Diep, P. T., Campbell, J. I., Sieu, T. P. M., Hien, T. T., Bui, T., Boni, M. F., Lalloo, D. G., Carter, D., Baker, S. and Farrar, J. J. (2011) 'Most Cases of Cryptococcal Meningitis in HIV-Uninfected Patients in Vietnam Are Due to

a Distinct Amplified Fragment Length Polymorphism-Defined Cluster of Cryptococcus neoformans var. grubii VN1', Journal of Clinical Microbiology, 49(2), 658-664.

Derengowski, L., Paes, H., Albuquerque, P., Tavares, A., Fernandes, L., Silva-Pereira, I. and Casadevall, A. (2013) 'The Transcriptional Response of Cryptococcus neoformans to Ingestion by Acanthamoeba castellanii and Macrophages Provides Insights into the Evolutionary Adaptation to the Mammalian Host', Eukaryotic Cell, 12(5), 761-774.

Dewar, G. J. and Kelly, J. K. (2008) 'Cryptococcus gattii: An emerging cause of pulmonary nodules', Canadian Respiratory Journal, 15(3), 153-157.

Diamond, R. and Bennett, J. (1973) 'Growth of Cryptococcus neoformans within Human Macrophages In vitro', Infection and Immunity, 7(2), 231-236.

Doering, T. (2009) 'How Sweet it is! Cell Wall Biogenesis and Polysaccharide Capsule Formation in Cryptococcus neoformans', Annual Review of Microbiology, 63, 223-247.

Drew, B. A., Burow, M. E. and Beckman, B. S. (2012) 'MEK5/ERK5 pathway: The first fifteen years', Biochimica Et Biophysica Acta-Reviews on Cancer, 1825(1), 37-48.

Dromer, F., Casadevall, A., Perfect, J. R. and Sorrel, T. (2011) Cryptococcus neoformans: Latency and Disease., In Cryptococcus: From Human Pathogen to Model Yeast., Washington, DC: ASM Press.

Dutcher, J. D. (1968) 'The discovery and development of amphotericin B', Diseases of the chest, 54, Suppl 1:296-8.

Dzamko, N., Inesta-Vaquera, F., Zhang, J., Xie, C., Cai, H., Arthur, S., Tan, L., Choi, H., Gray, N., Cohen, P., Pedrioli, P., Clark, K. and Alessi, D. R. (2012) 'The IkappaB Kinase Family Phosphorylates the Parkinson's Disease Kinase LRRK2 at Ser935 and Ser910 during Toll-Like Receptor Signaling', Plos One, 7(6).

Edwards, L., Acquaviv.FA, Levesay, V., Cross, F. and Palmer, C. (1969) 'An Atlas of Sensitivity to tuberculin PPD-B and Histoplasmin in United States', American Review of Respiratory Disease, 99(4P2), 1-&.

Eichner, R. D., Alsalami, M., Wood, P. R. and Mullbacher, A. (1986) 'THE EFFECT OF GLIOTOXIN UPON MACROPHAGE FUNCTION', International Journal of Immunopharmacology, 8(7), 789-797.

Elkins, J. M., Wang, J., Deng, X., Pattison, M. J., Arthur, J. S. C., Erazo, T., Gomez, N., Lizcano, J. M., Gray, N. S. and Knapp, S. (2013) 'X-ray Crystal Structure of ERK5 (MAPK7) in Complex with a Specific Inhibitor', Journal of Medicinal Chemistry, 56(11), 4413-4421.

Ellerbroek, P. M., Ulfman, L. H., Hoepelman, A. I. and Coenjaerts, F. E. J. (2004a) 'Cryptococcal glucuronoxylomannan interferes with neutrophil rolling on the endothelium', Cellular Microbiology, 6(6), 581-592.

Ellerbroek, P. M., Walenkamp, A. M. E., Hoepelman, A. I. M. and Coenjaerts, F. E. J. (2004b) 'Effects of the capsular polysaccharides of Cryptococcus neoformans on phagocyte migration and inflammatory mediators', Current Medicinal Chemistry, 11(2), 253-266.

Ellis, D. H. and Pfeiffer, T. J. (1990) 'NATURAL HABITAT OF CRYPTOCOCCUS-NEOFORMANS VAR GATTII', Journal of Clinical Microbiology, 28(7), 1642-1644.

Emmons, C. W. (1955) 'SAPROPHYTIC SOURCES OF CRYPTOCOCCUS-NEOFORMANS ASSOCIATED WITH THE PIGEON (COLUMBA-LIVIA)', American Journal of Hygiene, 62(3), 227-232.

Enjalbert, B., Nantel, A. and Whiteway, M. (2003) 'Stress-induced gene expression in Candida albicans: absence of a general stress response', Mol Biol Cell, 14(4), 1460-7.

Evans, E. E. (1950) 'THE ANTIGENIC COMPOSITION OF CRYPTOCOCCUS NEOFORMANS .1. A SEROLOGIC CLASSIFICATION BY MEANS OF THE CAPSULAR AND AGGLUTINATION REACTIONS', Journal of Immunology, 64(5), 423-430.

Evans, R. J., Li, Z., Hughes, W. S., Djordjevic, J. T., Nielsen, K. and May, R. C. (2015) 'Cryptococcal Phospholipase B1 Is Required for Intracellular Proliferation and Control of Titan Cell Morphology during Macrophage Infection', Infection and Immunity, 83(4), 1296-1304.

Fadok, V. A., Bratton, D. L., Konowal, A., Freed, P. W., Westcott, J. Y. and Henson, P. M. (1998) 'Macrophages that have ingested apoptotic cells in vitro inhibit proinflammatory cytokine production through autocrine/paracrine mechanisms involving TGF-beta, PGE2, and PAF', Journal of Clinical Investigation, 101(4), 890-898.

Fairhurst, T. M. and Pegues, D. A. (2002) 'Pulmonary cryptococcal granulomas', New England Journal of Medicine, 347(7), 497-497.

Fairn, G. and Grinstein, S. (2012) 'How nascent phagosomes mature to become phagolysosomes', Trends in Immunology, 33(8), 397-405.

Feldmesser, M., Kress, Y. and Casadevall, A. (2001) 'Dynamic changes in the morphology of Cryptococcus neoformans during murine pulmonary infection', Microbiology-Sgm, 147, 2355-2365.

Fernandez-Arenas, E., Bleck, C., Nombela, C., Gil, C., Griffiths, G. and Diez-Orejas, R. (2009) 'Candida albicans actively modulates intracellular membrane trafficking in mouse macrophage phagosomes', Cellular Microbiology, 11(4), 560-589.

Fields, B. S. (1996) 'The molecular ecology of legionellae', Trends in Microbiology, 4(7), 286-290.

Flannagan, R. S., Jaumouillé, V. and Grinstein, S. (2012) 'The cell biology of phagocytosis', Annu Rev Pathol, 7, 61-98.

Fradin, C., De Groot, P., MacCallum, D., Schaller, M., Klis, F., Odds, F. and Hube, B. (2005) 'Granulocytes govern the transcriptional response, morphology and proliferation of Candida albicans in human blood', Molecular Microbiology, 56(2), 397-415.

Franzot, S. P., Salkin, I. F. and Casadevall, A. (1999) 'Cryptococcus neoformans var. grubii: Separate varietal status for Cryptococcus neoformans serotype A isolates', Journal of Clinical Microbiology, 37(3), 838-840.

Frey, C. L. and Drutz, D. J. (1986) 'Influence of fungal surface components on the interaction of Coccidioides immitis with polymorphonuclear neutrophils', J Infect Dis, 153(5), 933-43.

Ganendren, R., Carter, E., Sorrell, T., Widmer, F. and Wright, L. (2006) 'Phospholipase B activity enhances adhesion of Cryptococcus neoformans to a human lung epithelial cell line', Microbes and Infection, 8(4), 1006-1015.

Garcia-Hermoso, D., Janbon, G. and Dromer, F. (1999) 'Epidemiological evidence for dormant Cryptococcus neoformans infection', Journal of Clinical Microbiology, 37(10), 3204-3209.

García-Rodas, R., González-Camacho, F., Rodríguez-Tudela, J. L., Cuenca-Estrella, M. and Zaragoza, O. (2011) 'The interaction between Candida krusei and murine macrophages results in multiple outcomes, including intracellular survival and escape from killing', Infect Immun, 79(6), 2136-44.

Gardet, A., Benita, Y., Li, C., Sands, B. E., Ballester, I., Stevens, C., Korzenik, J. R., Rioux, J. D., Daly, M. J., Xavier, R. J. and Podolsky, D. K. (2010) 'LRRK2 Is Involved in the IFN-gamma Response and Host Response to Pathogens', Journal of Immunology, 185(9), 5577-5585.

Goldman, D. L., Khine, H., Abadi, J., Lindenberg, D. J., Pirofski, L., Niang, R. and Casadevall, A. (2001) 'Serologic evidence for Cryptococcus neoformans infection in early childhood', Pediatrics, 107(5).

Gonzalez, A., Hung, C. and Cole, G. (2011) 'Coccidioides releases a soluble factor that suppresses nitric oxide production by murine primary macrophages', Microbial Pathogenesis, 50(2), 100-108.

Gonzalez, G. M., Casillas-Vega, N., Garza-Gonzalez, E., Hernandez-Bello, R., Rivera, G., Rodriguez, J. A. and Bocanegra-Garcia, V. (2016) 'Molecular typing of clinical isolates of Cryptococcus neoformans/Cryptococcus gattii species complex from Northeast Mexico', Folia Microbiologica, 61(1), 51-56.

Gordon, S. and Martinez, F. (2010) 'Alternative Activation of Macrophages: Mechanism and Functions', Immunity, 32(5), 593-604.

Grunberg, E., Titsworth, E. and Bennett, M. (1963) 'CHEMOTHERAPEUTIC ACTIVITY OF 5-FLUOROCYTOSINE', Antimicrobial agents and chemotherapy, 161, 566-8.

Gyawali, R. and Lin, X. (2011) 'Mechanisms of Uniparental Mitochondrial DNA Inheritance in Cryptococcus neoformans', Mycobiology, 39(4), 235-42.

Hall, R. A., Turner, K. J., Chaloupka, J., Cottier, F., De Sordi, L., Sanglard, D., Levin, L. R., Buck, J. and Muhlschlegel, F. A. (2011) 'The Quorum-Sensing Molecules Farnesol/Homoserine Lactone and Dodecanol Operate via Distinct Modes of Action in Candida albicans', Eukaryotic Cell, 10(8), 1034-1042.

Hardison, S. E., Ravi, S., Wozniak, K. L., Young, M. L., Olszewski, M. A. and Wormley, F. L., Jr. (2010) 'Pulmonary Infection with an Interferon-gamma-Producing Cryptococcus neoformans Strain Results in Classical Macrophage Activation and Protection', American Journal of Pathology, 176(2), 774-785.

Harriff, M. J., Purdy, G. E. and Lewinsohn, D. M. (2012) 'Escape from the Phagosome: The Explanation for MHC-I Processing of Mycobacterial Antigens?', Frontiers in immunology, 3, 40-40.

Haslett, C., Savill, J. S., Whyte, M. K. B., Stern, M., Dransfield, I. and Meagher, L. C. (1994) 'GRANULOCYTE APOPTOSIS AND THE CONTROL OF INFLAMMATION', Philosophical Transactions of the Royal Society of London Series B-Biological Sciences, 345(1313), 327-333.

He, K., Zhou, H.-R. and Pestka, J. J. (2012) 'Mechanisms for ribotoxin-induced ribosomal RNA cleavage', Toxicology and Applied Pharmacology, 265(1), 10-18.

Heinekamp, T., Thywissen, A., Macheleidt, J., Keller, S., Valiante, V. and Brakhage, A. A. (2013) 'Aspergillus fumigatus melanins: interference with the host endocytosis pathway and impact on virulence. ', Front Micro, 3, 440.

Helmbright, A. and Larsh, H. (1952) 'Size of the Spores of Histoplasma capsulatum', Proceedings of the Society For Experimental Biology and Medicine, 81(2), 550-551.

Heo, K.-S., Cushman, H. J., Akaike, M., Woo, C.-H., Wang, X., Qiu, X., Fujiwara, K. and Abe, J.-i. (2014) 'ERK5 Activation in Macrophages Promotes Efferocytosis and Inhibits Atherosclerosis', Circulation, 130(2), 180-U184.

Hoang, L., Maguire, J., Doye, P., Fyfe, M. and Roscoe, D. (2004) 'Cryptococcus neoformans infections at Vancouver Hospital and Health Sciences Centre (1997-2002): epidemiology, microbiology and histopathology', Journal of Medical Microbiology, 53(9), 935-940.

Holbrook, E., Smolnycki, K., Youseff, B. and Rappleye, C. (2013) 'Redundant Catalases Detoxify Phagocyte Reactive Oxygen and Facilitate Histoplasma capsulatum Pathogenesis', Infection and Immunity, 81(7), 2334-2346.

Huang, C. T., Tsai, Y. J., Fan, J. Y., Ku, S. C. and Yu, C. J. (2010) 'Cryptococcosis and tuberculosis co-infection at a university hospital in Taiwan, 1993-2006', Infection, 38(5), 373-379.

Huang, D. W., Sherman, B. T. and Lempicki, R. A. (2009) 'Systematic and integrative analysis of large gene lists using DAVID bioinformatics resources', Nature Protocols, 4(1), 44-57.

Hubber, A. and Roy, C. R. (2010) 'Modulation of Host Cell Function by Legionella pneumophila Type IV Effectors', Annual Review of Cell and Developmental Biology, Vol 26, 26, 261-283.

Hung, C., Ampel, N., Christian, L., Seshan, K. and Cole, G. (2000) 'A major cell surface antigen of Coccidioides immitis which elicits both humoral and cellular immune responses', Infection and Immunity, 68(2), 584-593.

Hung, C., Seshan, K., Yu, J., Schaller, R., Xue, J., Basrur, V., Gardner, M. and Cole, G. (2005) 'A metalloproteinase of Coccidioides posadasii contributes to evasion of host detection', Infection and Immunity, 73(10), 6689-6703.

Hung, C., Xue, J., Cole, G., Clemons, K., LaniadoLaborin, R. and Stevens, D. (2007) 'Virulence mechanisms of Coccidioides', Coccidioidomycosis: Sixth International Symposium, 1111, 225-235.

Hwang, C., Rhie, G., Oh, J., Huh, W., Yim, H. and Kang, S. (2002) 'Copper- and zinc-containing superoxide dismutase (Cu/ZnSOD) is required for the protection of Candida albicans against oxidative stresses and the expression of its full virulence', Microbiology-Sgm, 148, 3705-3713.

Inglis, D. O., Voorhies, M., Hocking Murray, D. R. and Sil, A. (2013) 'Comparative transcriptomics of infectious spores from the fungal pathogen Histoplasma capsulatum

reveals a core set of transcripts that specify infectious and pathogenic states', Eukaryot Cell, 12(6), 828-52.

Jain, C., Pastor, K., Gonzalez, A. Y., Lorenz, M. C. and Rao, R. P. (2013) 'The role of Candida albicans AP-1 protein against host derived ROS in in vivo models of infection', Virulence, 4(1), 67-76.

Janbon, G., Himmelreich, U., Moyrand, F., Improvisi, L. and Dromer, F. (2001) 'Cas1p is a membrane protein necessary for the O-acetylation of the Cryptococcus neoformans capsular polysaccharide', Molecular Microbiology, 42(2), 453-467.

Jarvis, J. N., Wainwright, H., Harrison, T. S., Rebe, K. and Meintjes, G. (2010) 'Pulmonary cryptococcosis misdiagnosed as smear-negative pulmonary tuberculosis with fatal consequences', International Journal of Infectious Diseases, 14, E310-E312.

Jimenez-Lopez, C., Collette, J. R., Brothers, K. M., Shepardson, K. M., Cramer, R. A., Wheeler, R. T. and Lorenz, M. C. (2013) 'Candida albicans Induces Arginine Biosynthetic Genes in Response to Host-Derived Reactive Oxygen Species', Eukaryotic Cell, 12(1), 91-100.

Johnston, S. and May, R. (2010) 'The Human Fungal Pathogen Cryptococcus neoformans Escapes Macrophages by a Phagosome Emptying Mechanism That Is Inhibited by Arp2/3 Complex-Mediated Actin Polymerisation', Plos Pathogens, 6(8).

Johnston, S. and May, R. (2013) 'Cryptococcus interactions with macrophages: evasion and manipulation of the phagosome by a fungal pathogen', Cellular Microbiology, 15(3), 403-411.

Johnston, S.A., Voelz, K., and May, R. (2016) ‘Cryptococcus neoformans Thermotolerance to Avian Body Temperature is Sufficient for Extracellular Growth But Not Intracellular Suvival in Macrophages’, Scientific Reports, Nature, **6**

Joly, V., Saintjulien, L., Carbon, C. and Yeni, P. (1994) 'IN-VIVO ACTIVITY OF INTERFERON-GAMMA IN COMBINATION WITH AMPHOTERICIN-B IN THE TREATMENT OF EXPERIMENTAL CRYPTOCOCCOSIS', Journal of Infectious Diseases, 170(5), 1331-1334.

Jong, A., Wu, C. H., Shackleford, G. M., Kwon-Chung, K. J., Chang, Y. C., Chen, H. M., Ouyang, Y. and Huang, S. H. (2008) 'Involvement of human CD44 during Cryptococcus neoformans infection of brain microvascular endothelial cells', Cellular Microbiology, 10(6), 1313-1326.

Jong, A., Wu, C.H., Gonzales-Gomez, I., Kwon-Chung, K.J., Chang, Y.C., Tseng, H., Cho, W and Huang S.H. (2012) 'Hyaluronic Acid Receptor CD44 Deficiency Is Associated with Decreased Cryptococcus neoformans Brain Infection', J. Biol Chem, 287(19), 15298 – 15306.

Kangogo, M., Bader, O., Boga, H., Wanyoike, W., Folba, C., Worasilchai, N., Weig, M., Gross, U. and Bii, C. C. (2015) 'Molecular types of Cryptococcus gattii/Cryptococcus neoformans species complex from clinical and environmental sources in Nairobi, Kenya', Mycoses, 58(11), 665-670.

Kaocharoen, S., Ngamskulrungroj, P., Firacative, C., Trilles, L., Piyabongkarn, D., Banlunara, W., Poonwan, N., Chaiprasert, A., Meyer, W. and Chindamporn, A. (2013) 'Molecular Epidemiology Reveals Genetic Diversity amongst Isolates of the Cryptococcus neoformans/C. gattii Species Complex in Thailand', Plos Neglected Tropical Diseases, 7(7).

Kaur, R., Ma, B. and Cormack, B. (2007) 'A family of glycosylphosphatidylinositol-linked aspartyl proteases is required for virulence of Candida glabrata', Proceedings of the National Academy of Sciences of the United States of America, 104(18), 7628-7633.

Keller, M., Mazuch, J., Abraham, U., Eom, G. D., Herzog, E. D., Volk, H. D., Kramer, A. and Maier, B. (2009) 'A circadian clock in macrophages controls inflammatory immune responses', Proceedings of the National Academy of Sciences of the United States of America, 106(50), 21407-21412.

Kidd, S. E., Chow, Y., Mak, S., Bach, P. J., Chen, H., Hingston, A. O., Kronstad, J. W. and Bartlett, K. H. (2007) 'Characterization of environmental sources of the human and animal pathogen Cryptococcus gattii in British Columbia, Canada, and the Pacific northwest of the United States', Applied and Environmental Microbiology, 73(5), 1433-1443.

Kinchen, J. and Ravichandran, K. (2008) 'Phagosome maturation: going through the acid test', Nature Reviews Molecular Cell Biology, 9(10), 781-795.

Kitahara, N., Morisaka, H., Aoki, W., Takeda, Y., Shibasaki, S., Kuroda, K. and Ueda, M. (2015) 'Description of the interaction between Candida albicans and macrophages by mixed and quantitative proteome analysis without isolation', Amb Express, 5.

Klengel, T., Liang, W., Chaloupka, J., Ruoff, C., Schroppel, K., Naglik, J., Eckert, S., Mogensen, E., Haynes, K., Tuite, M., Levin, L., Buck, J. and Muhlschlegel, F. (2005) 'Fungal adenylyl cyclase integrates CO2 sensing with cAMP signaling and virulence (vol 15, pg 2021, 2005)', Current Biology, 15(23), 2177-2177.

Kobayashi, M., Murata, K., Hiroshi, H. O. and Tokura, Y. (2004) 'Cryptococcosis: Long-lasting presence of fungi after successful treatment', Acta Dermato-Venereologica, 84(4), 320-321.

Kondoh, K., Terasawa, K., Morimoto, H. and Nishida, E. (2006) 'Regulation of nuclear translocation of extracellular signal-regulated kinase 5 by active nuclear import and export mechanisms', Molecular and Cellular Biology, 26(5), 1679-1690.

Kozicky, L.K., Zhao, Z.Y., Menzies, S.C., Fidanza, M., Reid, G.S., Wilhelmsen, K., Hellman, J., Hotte, N., Madsen, K.L and Sly, L.M. (2015) ‘Intravenous immunoglobulin skews macrophages to an anti-inflammatory, IL-10-producing activation state’ J Leukoc Biol, 98(6), 983-984.

Kroetz, D. and Deepe, G. (2012) 'The role of cytokines and chemokines in Histoplasma capsulatum infection', Cytokine, 58(1), 112-117.

Krombach, F., Münzing, S., Allmeling, A. M., Gerlach, J. T., Behr, J. and Dörger, M. (1997) 'Cell size of alveolar macrophages: an interspecies comparison', Environ Health Perspect, 105 Suppl 5, 1261-3.

Kuma, Y., Sabio, G., Bain, J., Shpiro, N., Marquez, R. and Cuenda, A. (2005) 'BIRB796 inhibits all p38 MAPK isoforms in vitro and in vivo', Journal of Biological Chemistry, 280(20), 19472-19479.

Kuss, M., Adamopoulou, E. and Kahle, P. J. (2014) 'Interferon- induces leucine-rich repeat kinase LRRK2 via extracellular signal-regulated kinase ERK5 in macrophages', Journal of Neurochemistry, 129(6), 980-987.

Kwon-Chung, K. J., Boekhout, T., Fell, J. W. and Diaz, M. (2002) '(1557) Proposal to conserve the name Cryptococcus gattii against C. hondurianus and C. bacillisporus (Basidiomycota, Hymenomycetes, Tremellomycetidae)', Taxon, 51(4), 804-806.

Kwon-Chung, K. J., Fraser, J. A., Doering, T. L., Wang, Z. A., Janbon, G., Idnurm, A. and Bahn, Y.-S. (2014) 'Cryptococcus neoformans and Cryptococcus gattii, the Etiologic Agents of Cryptococcosis', Cold Spring Harbor Perspectives in Medicine, 4(7).

Kwonchung, K. J. and Bennett, J. E. (1978) 'DISTRIBUTION OF ALPHA AND A MATING TYPES OF CRYPTOCOCCUS-NEOFORMANS AMONG NATURAL AND CLINICAL ISOLATES', American Journal of Epidemiology, 108(4), 337-340.

Kwonchung, K. J. and Bennett, J. E. (1984a) 'EPIDEMIOLOGIC DIFFERENCES BETWEEN THE 2 VARIETIES OF CRYPTOCOCCUS-NEOFORMANS', American Journal of Epidemiology, 120(1), 123-130.

Kwonchung, K. J. and Bennett, J. E. (1984b) 'HIGH PREVALENCE OF CRYPTOCOCCUS-NEOFORMANS VAR GATTII IN TROPICAL AND SUB-TROPICAL REGIONS', Zentralblatt Fur Bakteriologie Mikrobiologie Und Hygiene Series a-Medical Microbiology Infectious Diseases Virology Parasitology, 257(2), 213-218.

Kwonchung, K. J., Polacheck, I. and Bennett, J. E. (1982) 'IMPROVED DIAGNOSTIC MEDIUM FOR SEPARATION OF CRYPTOCOCCUS-NEOFORMANS VAR NEOFORMANS (SEROTYPE-A AND SEROTYPE-D) AND CRYPTOCOCCUS-NEOFORMANS VAR GATTII (SEROTYPE-B AND SEROTYPE-C)', Journal of Clinical Microbiology, 15(3), 535-537.

Latge, J. (1999) 'Aspergillus fumigatus and aspergillosis', Clinical Microbiology Reviews, 12(2), 310-+.

LeClaire, L. L., Baumgartner, M., Iwasa, J. H., Mullins, R. D. and Barber, D. L. (2008) 'Phosphorylation of the Arp2/3 complex is necessary to nucleate actin filaments', Journal of Cell Biology, 182(4), 647-654.

Lee, J., Repasy, T., Papavinasasundaram, K., Sassetti, C. and Kornfeld, H. (2011) 'Mycobacterium tuberculosis Induces an Atypical Cell Death Mode to Escape from Infected Macrophages', Plos One, 6(3).

Lee, J. D., Ulevitch, R. J. and Han, J. H. (1995) 'PRIMARY STRUCTURE OF BMK1 - A NEW MAMMALIAN MAP KINASE', Biochemical and Biophysical Research Communications, 213(2), 715-724.

Levitz, S., Nong, S., Seetoo, K., Harrison, T., Speizer, R. and Simons, E. (1999) 'Cryptococcus neoformans resides in an acidic phagolysosome of human macrophages', Infection and Immunity, 67(2), 885-890.

Lewis, F. M. T., Marsh, B. J. and von Reyn, C. F. (2003) 'Fish tank exposure and cutaneous infections due to Mycobacterium marinum: Tuberculin skin testing, treatment, and prevention', Clinical Infectious Diseases, 37(3), 390-397.

Lionakis, M. S. (2014) 'New insights into innate immune control of systemic candidiasis', Medical Mycology, 52(6), 555-564.

Liu, L., Tewari, R. P. and Williamson, P. R. (1999a) 'Laccase protects Cryptococcus neoformans from antifungal activity of alveolar macrophages', Infection and Immunity, 67(11), 6034-6039.

Liu, L., Wakamatsu, K., Ito, S. and Williamson, P. R. (1999b) 'Catecholamine oxidative products, but not melanin, are produced by Cryptococcus neoformans during neuropathogenesis in mice', Infection and Immunity, 67(1), 108-112.

Liu, O., Chun, C., Chow, E., Chen, C., Madhani, H. and Noble, S. (2008) 'Systematic genetic analysis of virulence in the human fungal pathogen Cryptococcus neoformans', Cell, 135(1), 174-188.

Liu, Z., Lee, J., Krummey, S., Lu, W., Cai, H. and Lenardo, M. J. (2011) 'The kinase LRRK2 is a regulator of the transcription factor NFAT that modulates the severity of inflammatory bowel disease', Nature Immunology, 12(11), 1063-U65.

Lo, H. J., Köhler, J. R., DiDomenico, B., Loebenberg, D., Cacciapuoti, A. and Fink, G. R. (1997) 'Nonfilamentous C. albicans mutants are avirulent', Cell, 90(5), 939-49.

Lorenz, M., Bender, J. and Fink, G. (2004) 'Transcriptional response of Candida albicans upon internalization by macrophages', Eukaryotic Cell, 3(5), 1076-1087.

Lutz, J. E., Clemons, K. V. and Stevens, D. A. (2000) 'Enhancement of antifungal chemotherapy by interferon-gamma in experimental systemic cryptococcosis', Journal of Antimicrobial Chemotherapy, 46(3), 437-442.

Ma, H. (2009) Intracellular Parasitism of Macrophages by Cryptococcus unpublished thesis University of Birmingham.

Ma, H., Croudace, J., Lammas, D. and May, R. (2006) 'Expulsion of live pathogenic yeast by macrophages', Current Biology, 16(21), 2156-2160.

Ma, H., Croudace, J. E., Lammas, D. A. and May, R. C. (2007) 'Direct cell-to-cell spread of a pathogenic yeast', Bmc Immunology, 8.

Mambula, S. S., Simons, E. R., Hastey, R., Selsted, M. E. and Levitz, S. M. (2000) 'Human neutrophil-mediated nonoxidative antifungal activity against Cryptococcus neoformans', Infection and Immunity, 68(11), 6257-6264.

Mandel, M. A., Grace, G. G., Orsborn, K. I., Schafer, F., Murphy, J. W., Orbach, M. J. and Galgiani, J. N. (2000) 'The Cryptococcus neoformans gene DHA1 encodes an antigen that elicits a delayed-type hypersensitivity reaction in immune mice', Infection and Immunity, 68(11), 6196-6201.

Mansour, M., Tam, J., Vyas, J., Clemons, K., Perlin, D. and Richardson, M. (2012) 'The cell biology of the innate immune response to Aspergillus fumigatus', Advances Against Aspergillosis Ii, 1273, 78-84.

Marcil, A., Harcus, D., Thomas, D. Y. and Whiteway, M. (2002) 'Candida albicans killing by RAW 264.7 mouse macrophage cells: Effects of Candida genotype, infection ratios, and gamma interferon treatment', Infection and Immunity, 70(11), 6319-6329.

Mata, I. F., Wedemeyer, W. J., Farrer, M. J., Taylor, J. P. and Gallo, K. A. (2006) 'LRRK2 in Parkinson's disease: protein domains and functional insights', Trends in Neurosciences, 29(5), 286-293.

Mayer, F., Wilson, D. and Hube, B. (2013) 'Candida albicans pathogenicity mechanisms', Virulence, 4(2), 119-128.

McClelland, C. M., Chang, Y. C., Varma, A. and Kwon-Chung, K. J. (2004) 'Uniqueness of the mating system in Cryptococcus neoformans', Trends in Microbiology, 12(5), 208-212.

McNeil, M., Nash, S., Hajjeh, R., Phelan, M., Conn, L., Plikaytis, B. and Warnock, D. (2001) 'Trends in mortality due to invasive mycotic diseases in the United States, 1980-1997', Clinical Infectious Diseases, 33(5), 641-647.

Meagher, L. C., Savill, J. S., Baker, A., Fuller, R. W. and Haslett, C. (1992) 'PHAGOCYTOSIS OF APOPTOTIC NEUTROPHILS DOES NOT INDUCE MACROPHAGE RELEASE OF THROMBOXANE-B2', Journal of Leukocyte Biology, 52(3), 269-273.

Mehta, P. B., Jenkins, B. L., McCarthy, L., Thilak, L., Robson, C. N., Neal, D. E. and Leung, H. Y. (2003) 'MEK5 overexpression is associated with metastatic prostate cancer, and stimulates proliferation, MMP-9 expression and invasion', Oncogene, 22(9), 1381-1389.

Meredith, P. and Riesz, J. (2004) 'Radiative relaxation quantum yields for synthetic eumelanin', Photochemistry and Photobiology, 79(2), 211-216.

Meyer, W., Castaneda, A., Jackson, S., Huynh, M., Castaneda, E. and IberoAmerican Cryptococcal, S. (2003) 'Molecular typing of IberoAmerican Cryptococcus neoformans isolates', Emerging Infectious Diseases, 9(2), 189-195.

Miao, Y., Li, G., Zhang, X., Xu, H. and Abraham, S. N. (2015) 'A TRP Channel Senses Lysosome Neutralization by Pathogens to Trigger Their Expulsion', Cell, 161(6), 1306-19.

Miramon, P., Kasper, L. and Hube, B. (2013) 'Thriving within the host: Candida spp. interactions with phagocytic cells', Medical Microbiology and Immunology, 202(3), 183-195.

Miramón, P., Dunker, C., Windecker, H., Bohovych, I. M., Brown, A. J., Kurzai, O. and Hube, B. (2012) 'Cellular responses of Candida albicans to phagocytosis and the extracellular activities of neutrophils are critical to counteract carbohydrate starvation, oxidative and nitrosative stress', PLoS One, 7(12), e52850.

Mirbod-Donovan, F., Schaller, R., Hung, C., Xue, J., Reichard, U. and Cole, G. (2006) 'Urease produced by Coccidioides posadasii contributes to the virulence of this respiratory pathogen', Infection and Immunity, 74(1), 504-515.

Missall, T. A., Moran, J. M., Corbett, J. A. and Lodge, J. K. (2005) 'Distinct stress responses of two functional laccases in Cryptococcus neoformans are revealed in the absence of the thiol-specific antioxidant Tsa1', Eukaryotic Cell, 4(1), 202-208.

Mogensen, T. H. (2009) 'Pathogen Recognition and Inflammatory Signaling in Innate Immune Defenses', Clinical Microbiology Reviews, 22(2), 240-+.

Monari, C., Bistoni, F. and Vecchiarelli, A. (2006) 'Glucuronoxylomannan exhibits potent immunosuppressive properties', Fems Yeast Research, 6(4), 537-542.

Moore, T. D. E. and Edman, J. C. (1993) 'THE ALPHA-MATING TYPE LOCUS OF CRYPTOCOCCUS-NEOFORMANS CONTAINS A PEPTIDE PHEROMONE GENE', Molecular and Cellular Biology, 13(3), 1962-1970.

Morton, C. O., Bouzani, M., Loeffler, J. and Rogers, T. R. (2012) 'Direct interaction studies between Aspergillus fumigatus and human immune cells; what have we learned about pathogenicity and host immunity?', Front Microbiol, 3, 413.

Moyes, D. L., Runglall, M., Murciano, C., Shen, C. G., Nayar, D., Thavaraj, S., Kohli, A., Islam, A., Mora-Montes, H., Challacombe, S. J. and Naglik, J. R. (2010) 'A Biphasic Innate Immune MAPK Response Discriminates between the Yeast and Hyphal Forms of Candida albicans in Epithelial Cells', Cell Host & Microbe, 8(3), 225-235.

Moyrand, F., Chang, Y. C., Himmelreich, U., Kwon-Chung, K. J. and Janbon, G. (2004) 'Cas3p belongs to a seven-member family of capsule structure designer proteins', Eukaryotic Cell, 3(6), 1513-1524.

Munday, K. A., Giles, I. G. and Poat, P. C. (1980) 'REVIEW OF THE COMPARATIVE BIOCHEMISTRY OF PYRUVATE-KINASE', Comparative Biochemistry and Physiology B-Biochemistry & Molecular Biology, 67(3), 403-411.

Nailis, H., Kucharikova, S., Ricicova, M., Van Dijck, P., Deforce, D., Nelis, H. and Coenye, T. (2010a) 'Real-time PCR expression profiling of genes encoding potential virulence factors in Candida albicans biofilms: identification of model-dependent and -independent gene expression', Bmc Microbiology, 10.

Nailis, H., Vandenbosch, D., Deforce, D., Nelis, H. J. and Coenye, T. (2010b) 'Transcriptional response to fluconazole and amphotericin B in Candida albicans biofilms', Research in Microbiology, 161(4), 284-292.

Nakamura, K., Uhlik, M. T., Johnson, N. L., Hahn, K. M. and Johnson, G. L. (2006) 'PB1 domain-dependent signaling complex is required for extracellular signal-regulated kinase 5 activation', Molecular and Cellular Biology, 26(6), 2065-2079.

Nierman, W., Pain, A., Anderson, M., Wortman, J., Kim, H., Arroyo, J., Berriman, M., Abe, K., Archer, D., Bermejo, C., Bennett, J., Bowyer, P., Chen, D., Collins, M., Coulsen, R., Davies, R., Dyer, P., Farman, M., Fedorova, N., Feldblyum, T., Fischer, R., Fosker, N., Fraser, A., Garcia, J., Garcia, M., Goble, A., Goldman, G., Gomi, K., Griffith-Jones, S., Gwilliam, R., Haas, B., Haas, H., Harris, D., Horiuchi, H., Huang, J., Humphray, S., Jimenez, J., Keller, N., Khouri, H., Kitamoto, K., Kobayashi, T., Konzack, S., Kulkarni, R., Kumagai, T., Lafton, A., Latge, J., Li, W., Lord, A., Majoros, W., May, G., Miller, B., Mohamoud, Y., Molina, M., Monod, M., Mouyna, I., Mulligan, S., Murphy, L., O'Neil, S., Paulsen, I., Penalva, M., Pertea, M., Price, C.,

Pritchard, B., Quail, M., Rabbinowitsch, E., Rawlins, N., Rajandream, M., Reichard, U., Renauld, H., Robson, G., de Cordoba, S., Rodriguez-Pena, J., Ronning, C., Rutter, S., Salzberg, S., Sanchez, M., Sanchez-Ferrero, J., Saunders, D., Seeger, K., Squares, R., Squares, S., Takeuchi, M., Tekaia, F., Turner, G., de Aldana, C., Weidman, J., White, O., Woodward, J., Yu, J., Fraser, C., Galagan, J., Asai, K., Machida, M., Hall, N., Barrell, B. and Denning, D. (2005) 'Genomic sequence of the pathogenic and allergenic filamentous fungus Aspergillus fumigatus', Nature, 438(7071), 1151-1156.

Nosanchuk, J. D., Rosas, A. L., Lee, S. C. and Casadevall, A. (2000) 'Melanisation of Cryptococcus neoformans in human brain tissue', Lancet, 355(9220), 2049-2050.

Noverr, M. C., Phare, S. M., Toews, G. B., Coffey, M. J. and Huffnagle, G. B. (2001) 'Pathogenic yeasts Cryptococcus neoformans and Candida albicans produce immunomodulatory prostaglandins', Infection and Immunity, 69(5), 2957-2963.

O'Meara, T. R. and Alspaugh, J. A. (2012) 'The Cryptococcus neoformans Capsule: a Sword and a Shield', Clinical Microbiology Reviews, 25(3), 387-408.

Ofengeim, D. and Yuan, J. (2013) 'Regulation of RIP1 kinase signalling at the crossroads of inflammation and cell death', Nature Reviews Molecular Cell Biology, 14(11), 727-736.

Okagaki, L. and Nielsen, K. (2012) 'Titan Cells Confer Protection from Phagocytosis in Cryptococcus neoformans Infections', Eukaryotic Cell, 11(6), 820-826.

Okagaki, L., Strain, A., Nielsen, J., Charlier, C., Baltes, N., Chretien, F., Heitman, J., Dromer, F. and Nielsen, K. (2010) 'Cryptococcal Cell Morphology Affects Host Cell Interactions and Pathogenicity', Plos Pathogens, 6(6).

Osterholzer, J. J., Chen, G.-H., Olszewski, M. A., Zhang, Y.-M., Curtis, J. L., Huffnagle, G. B. and Toews, G. B. (2011) 'Chemokine Receptor 2-Mediated Accumulation of Fungicidal Exudate Macrophages in Mice That Clear Cryptococcal Lung Infection', American Journal of Pathology, 178(1), 198-211.

Panepinto, J., Komperda, K., Frases, S., Park, Y. D., Djordjevic, J. T., Casadevall, A. and Williamson, P. R. (2009) 'Sec6-dependent sorting of fungal extracellular exosomes and laccase of Cryptococcus neoformans', Molecular Microbiology, 71(5), 1165-1176.

Pappas, P., Alexander, B., Andes, D., Hadley, S., Kauffman, C., Freifeld, A., Anaissie, E., Brumble, L., Herwaldt, L., Ito, J., Kontoyiannis, D., Lyon, G., Marr, K., Morrison, V., Park, B., Patterson, T., Perl, T., Oster, R., Schuster, M., Walker, R., Walsh, T., Wannemuehler, K. and Chiller, T. (2010) 'Invasive Fungal Infections among Organ Transplant Recipients: Results of the Transplant-Associated Infection Surveillance Network (TRANSNET)', Clinical Infectious Diseases, 50(8), 1101-1111.

Park, B., Wannemuehler, K., Marston, B., Govender, N., Pappas, P. and Chiller, T. (2009) 'Estimation of the current global burden of cryptococcal meningitis among persons living with HIV/AIDS', Aids, 23(4), 525-530.

Patterson, M. J., McKenzie, C. G., Smith, D. A., da Silva Dantas, A., Sherston, S., Veal, E. A., Morgan, B. A., Maccallum, D. M., Erwig, L. P. and Quinn, J. (2013) 'Ybp1 and Gpx3 Signaling in Candida albicans Govern Hydrogen Peroxide-Induced Oxidation of the Cap1 Transcription Factor and Macrophage Escape', Antioxid Redox Signal.

Perfect, J. R., Dismukes, W. E., Dromer, F., Goldman, D. L., Graybill, J. R., Hamill, R. J., Harrison, T. S., Larsen, R. A., Lortholary, O., Nguyen, M.-H., Pappas, P. G., Powderly, W. G., Singh, N., Sobel, J. D. and Sorrell, T. C. (2010) 'Clinical Practice Guidelines for the Management of Cryptococcal Disease: 2010 Update by the Infectious Diseases Society of America', Clinical Infectious Diseases, 50(3), 291-322.

Pericolini, E., Cenci, E., Monari, C., De Jesus, M., Bistoni, F., Casadevall, A. and Vecchiarelli, A. (2006) 'Cryptococcus neoformans capsular polysaccharide component galactoxylomannan induces apoptosis of human T-cells through activation of caspase-8', Cellular Microbiology, 8(2), 267-275.

Pfeiffer, T. and Ellis, D. (1991) 'ENVIRONMENTAL ISOLATION OF CRYPTOCOCCUS NEOFORMANS-GATTII FROM CALIFORNIA', Journal of Infectious Diseases, 163(4), 929-930.

Pines, J. (1994) 'Protein kinases and cell cycle control', Seminars in Cell Biology, 5(6), 399-408.

Polak, A. (1977) '5-Fluorocytosine--current status with special references to mode of action and drug resistance', Contributions to microbiology and immunology, 4, 158-67.

Polak, A. and Scholer, H. J. (1975) 'MODE OF ACTION OF 5-FLUOROCYTOSINE AND MECHANISMS OF RESISTANCE', Chemotherapy, 21(3-4), 113-130.

Powderly, W. G., Cloud, G. A., Dismukes, W. E. and Saag, M. S. (1994) 'MEASUREMENT OF CRYPTOCOCCAL ANTIGEN IN SERUM AND CEREBROSPINAL-FLUID - VALUE IN THE MANAGEMENT OF AIDS-ASSOCIATED CRYPTOCOCCAL MENINGITIS', Clinical Infectious Diseases, 18(5), 789-792.

Price, J. V. and Vance, R. E. (2014) 'The Macrophage Paradox', Immunity, 41(5), 685-693.

Rallis, E. and Koumantaki-Mathioudaki, E. (2007) 'Treatment of Mycobacterium marinum cutaneous infections', Expert Opinion on Pharmacotherapy, 8(17), 2965-2978.

Ramage, G., Mowat, E., Jones, B., Williams, C. and Lopez-Ribot, J. (2009) 'Our Current Understanding of Fungal Biofilms', Critical Reviews in Microbiology, 35(4), 340-355.

Ramirez, M. A. and Lorenz, M. C. (2009) 'The Transcription Factor Homolog CTF1 Regulates beta-Oxidation in Candida albicans', Eukaryotic Cell, 8(10), 1604-1614.

Rappleye, C., Eissenberg, L. and Goldman, W. (2007) 'Histoplasma capsulatum alpha-(1,3)-glucan blocks innate immune recognition by the beta-glucan receptor', Proceedings of the National Academy of Sciences of the United States of America, 104(4), 1366-1370.

Richardson, K., Cooper, K., Marriott, M. S., Tarbit, M. H., Troke, P. F. and Whittle, P. J. (1990) 'DISCOVERY OF FLUCONAZOLE, A NOVEL ANTIFUNGAL AGENT', Reviews of Infectious Diseases, 12, S267-S271.

Rosas, A. L. and Casadevall, A. (1997) 'Melanization affects susceptibility of Cryptococcus neoformans to heat and cold (vol 153, pg 265, 1997)', Fems Microbiology Letters, 156(1), 171-171.

Sabiiti, W. and May, R. C. (2012) 'Capsule Independent Uptake of the Fungal Pathogen Cryptococcus neoformans into Brain Microvascular Endothelial Cells', Plos One, 7(4).

Sabiiti, W., Robertson, E., Beale, M. A., Johnston, S. A., Brouwer, A. E., Loyse, A., Jarvis, J. N., Gilbert, A. S., Fisher, M. C., Harrison, T. S., May, R. C. and Bicanic, T. (2014) 'Efficient phagocytosis and laccase activity affect the outcome of HIV-associated cryptococcosis', Journal of Clinical Investigation, 124(5), 2000-2008.

Santangelo, R. T., Nouri-Sorkhabi, M. H., Sorrell, T. C., Cagney, M., Chen, S. C. A., Kuchel, P. W. and Wright, L. C. (1999) 'Biochemical and functional characterisation of secreted phospholipase activities from Cryptococcus neoformans in their naturally occurring state', Journal of Medical Microbiology, 48(8), 731-740.

Santiago-Tirado, F. H., Peng, T., Yang, M., Hang, H. C. and Doering, T. L. (2015) 'A Single Protein S-acyl Transferase Acts through Diverse Substrates to Determine Cryptococcal Morphology, Stress Tolerance, and Pathogenic Outcome', Plos Pathogens, 11(5).

Sarhan, A. R., Patel, T. R., Creese, A. J., Tomlinson, M. G., Hellberg, C., Heath, J. K., Hotchin, N. A. and Cunningham, D. L. (2016) 'Regulation of Platelet Derived Growth Factor Signaling by Leukocyte Common Antigen-related (LAR) Protein Tyrosine Phosphatase: A

Quantitative Phosphoproteomics Study', Molecular & Cellular Proteomics, 15(6), 1823-1836.

Schrettl, M. and Haas, H. (2011) 'Iron homeostasis-Achilles' heel of Aspergillus fumigatus?', Current Opinion in Microbiology, 14(4), 400-405.

SCULLY, C., ELKABIR, M. and SAMARANAYAKE, L. (1994) 'CANDIDA AND ORAL CANDIDOSIS - A REVIEW', Critical Reviews in Oral Biology & Medicine, 5(2), 125-157.

Seider, K., Brunke, S., Schild, L., Jablonowski, N., Wilson, D., Majer, O., Barz, D., Haas, A., Kuchler, K., Schaller, M. and Hube, B. (2011) 'The Facultative Intracellular Pathogen Candida glabrata Subverts Macrophage Cytokine Production and Phagolysosome Maturation', Journal of Immunology, 187(6), 3072-3086.

Seyfried, J., Wang, X., Kharebava, G. and Tournier, C. (2005) 'A novel mitogen-activated protein kinase docking site in the N terminus of MEK5 alpha organizes the components of the extracellular signal-regulated kinase 5 signaling pathway', Molecular and Cellular Biology, 25(22), 9820-9828.

Shah, A., Kannambath, S., Herbst, S., Rogers, A., Soresi, S., Carby, M., Reed, A., Mostowy, S., Fisher, M.C., Shaunak, S., and Armstrong-James, D.P. (2016) ' Calcineurin Orchestrates Lateral Transfer of Aspergillus fumigatus During Macrophage Cell Death', AM J Respir Crit Care Med, 194(4),

Shen, L. and Liu, Y. (2015) 'Prostaglandin E2 blockade enhances the pulmonary anti-Cryptococcus neoformans immune reaction via the induction of TLR-4', International Immunopharmacology, 28(1), 376-381.

Sionov, E., Chang, Y. C., Garraffo, H. M., Dolan, M. A., Ghannoum, M. A. and Kwon-Chung, K. J. (2012) 'Identification of a Cryptococcus neoformans Cytochrome P450 Lanosterol 14 alpha-Demethylase (Erg11) Residue Critical for Differential Susceptibility between Fluconazole/Voriconazole and Itraconazole/Posaconazole', Antimicrobial Agents and Chemotherapy, 56(3), 1162-1169.

Sionov, E., Chang, Y. C., Garraffo, H. M. and Kwon-Chung, K. J. (2009) 'Heteroresistance to Fluconazole in Cryptococcus neoformans Is Intrinsic and Associated with Virulence', Antimicrobial Agents and Chemotherapy, 53(7), 2804-2815.

Sionov, E., Lee, H., Chang, Y. C. and Kwon-Chung, K. J. (2010) 'Cryptococcus neoformans Overcomes Stress of Azole Drugs by Formation of Disomy in Specific Multiple Chromosomes', Plos Pathogens, 6(4).

Smith, D., Nicholls, S., Morgan, B., Brown, A. and Quinn, J. (2004) 'A conserved stress-activated protein kinase regulates a core stress response in the human pathogen Candida albicans', Molecular Biology of the Cell, 15(9), 4179-4190.

Smith, L. M., Dixon, E. F. and May, R. C. (2015) 'The fungal pathogen Cryptococcus neoformans manipulates macrophage phagosome maturation', Cellular Microbiology, 17(5), 702-713.

Smith, L. M. and May, R. C. (2013) 'Mechanisms of microbial escape from phagocyte killing', Biochem Soc Trans, 41(2), 475-90.

Spiltoir, J. I., Stratton, M. S., Cavasin, M. A., Demos-Davies, K., Reid, B. G., Qi, J., Bradner, J. E. and McKinsey, T. A. (2013) 'BET acetyl-lysine binding proteins control pathological cardiac hypertrophy', Journal of Molecular and Cellular Cardiology, 63, 175-179.

Spitzer, E. D., Spitzer, S. G., Freundlich, L. F. and Casadevall, A. (1993) 'PERSISTENCE OF INITIAL INFECTION IN RECURRENT CRYPTOCOCCUS-NEOFORMANS MENINGITIS', Lancet, 341(8845), 595-596.

Staib, F. (1962) 'CRYPTOCOCCUS NEOFORMANS UND GUIZOTIA ABYSSINICA (SYN-G-OLEIFERA-DC) - (FARBREAKTION FUR CR-NEOFORMANS)', Zeitschrift Fur Hygiene Und Infektionskrankheiten, 148(5), 466-475.

Stano, P., Williams, V., Villani, M., Cymbalyuk, E., Qureshi, A., Huang, Y., Morace, G., Luberto, C., Tomlinson, S. and Del Poeta, M. (2009) 'App1: An Antiphagocytic Protein That Binds to Complement Receptors 3 and 2', Journal of Immunology, 182(1), 84-91.

Steenbergen, J. N., Shuman, H. A. and Casadevall, A. (2001) 'Cryptococcus neoformans interactions with amoebae suggest an explanation for its virulence and intracellular pathogenic strategy in macrophages', Proceedings of the National Academy of Sciences of the United States of America, 98(26), 15245-15250.

Stockli, J., Fazakerley, D. J. and James, D. E. (2011) 'GLUT4 exocytosis', Journal of Cell Science, 124(24), 4147-4158.

Strasser, J., Newman, S., Ciraolo, G., Morris, R., Howell, M. and Dean, G. (1999) 'Regulation of the macrophage vacuolar ATPase and phagosome-lysosome fusion by Histoplasma capsulatum', Journal of Immunology, 162(10), 6148-6154.

Stukes, S. A., Cohen, H. W. and Casadevall, A. (2014) 'Temporal Kinetics and Quantitative Analysis of Cryptococcus neoformans Nonlytic Exocytosis', Infection and immunity, 82(5), 2059-67.

Swamydas, M., Gao, J. L., Break, T. J., Johnson, M. D., Jaeger, M., Rodriguez, C. A., Lim, J. K., Green, N. M., Collar, A. L., Fischer, B. G., Lee, C. C. R., Perfect, J. R., Alexander, B. D., Kullberg, B. J., Netea, M. G., Murphy, P. M. and Lionakis, M. S. (2016) 'CXCR1-mediated neutrophil degranulation and fungal killing promote Candida clearance and host survival', Science Translational Medicine, 8(322), 12.

Tassel, D. and Madoff, M. A. (1968) 'TREATMENT OF CANDIDA SEPSIS AND CRYPTOCOCCUS MENINGITIS WITH 5-FLUOROCYTOSINE - A NEW ANTIFUNGAL AGENT', Journal of the American Medical Association, 206(4), 830-&.

Thywißen, A., Heinekamp, T., Dahse, H. M., Schmaler-Ripcke, J., Nietzsche, S., Zipfel, P. F. and Brakhage, A. A. (2011) 'Conidial Dihydroxynaphthalene Melanin of the Human Pathogenic Fungus Aspergillus fumigatus Interferes with the Host Endocytosis Pathway', Front Microbiol, 2, 96.

Tyanova, S., Temu, T., Carlson, A., Sinitcyn, P., Mann, M. and Cox, J. (2015) 'Visualization of LC-MS/MS proteomics data in MaxQuant', Proteomics, 15(8), 1453-1456.

Ullmann, B., Myers, H., Chiranand, W., Lazzell, A., Zhao, Q., Vega, L., Lopez-Ribot, J., Gardner, P. and Gustin, M. (2004) 'Inducible defense mechanism against nitric oxide in Candida albicans', Eukaryotic Cell, 3(3), 715-723.

Uppuluri, P., Chaturvedi, A., Srinivasan, A., Banerjee, M., Ramasubramaniam, A., Kohler, J., Kadosh, D. and Lopez-Ribot, J. (2010) 'Dispersion as an Important Step in the Candida albicans Biofilm Developmental Cycle', Plos Pathogens, 6(3).

van Leeuwen, L. M., van der Kuip, M., Youssef, S. A., de Bruin, A., Bitter, W., van Furth, A. M. and van der Sar, A. M. (2014) 'Modeling tuberculous meningitis in zebrafish using Mycobacterium marinum', Disease Models & Mechanisms, 7(9), 1111-1122.

Velagapudi, R., Hsueh, Y., Geunes-Boyer, S., Wright, J. and Heitman, J. (2009) 'Spores as Infectious Propagules of Cryptococcus neoformans', Infection and Immunity, 77(10), 4345-4355.

Voelz, K., Johnston, S. A., Rutherford, J. C. and May, R. C. (2010) 'Automated Analysis of Cryptococcal Macrophage Parasitism Using GFP-Tagged Cryptococci', Plos One, 5(12).

Voelz, K., Lammas, D. and May, R. (2009) 'Cytokine Signaling Regulates the Outcome of Intracellular Macrophage Parasitism by Cryptococcus neoformans', Infection and Immunity, 77(8), 3450-3457.

Vylkova, S., Carman, A., Danhof, H., Collette, J., Zhou, H. and Lorenz, M. (2011) 'The Fungal Pathogen Candida albicans Autoinduces Hyphal Morphogenesis by Raising Extracellular pH', Mbio, 2(3).

Vázquez-Torres, A. and Balish, E. (1997) 'Macrophages in resistance to candidiasis', Microbiol Mol Biol Rev, 61(2), 170-92.

Wager, C. M. L. and Wormley, F. L. (2014) 'Classical versus alternative macrophage activation: the Ying and the Yang in host defense against pulmonary fungal infections', Mucosal Immunology, 7(5), 1023-1035.

Wang, Y., Cao, Y., Jia, X., Cao, Y., Gao, P., Fu, X., Ying, K., Chen, W. and Jiang, Y. (2006) 'Cap1p is involved in multiple pathways of oxidative stress response in Candida albicans', Free Radical Biology and Medicine, 40(7), 1201-1209.

Wang, Z., Wesche, H., Stevens, T., Walker, N. and Yeh, W.-C. (2009) 'IRAK-4 Inhibitors for Inflammation', Current Topics in Medicinal Chemistry, 9(8), 724-737.

Watabe, T., Miyaji, M. and Nishimura, K. (1984) 'STUDIES ON RELATIONSHIP BETWEEN CYSTS AND GRANULOMAS IN MURINE CRYPTOCOCCOSIS', Mycopathologia, 86(2), 113-120.

Welch, M. D., DePace, A. H., Verma, S., Iwamatsu, A. and Mitchison, T. J. (1997) 'The human Arp2/3 complex is composed of evolutionarily conserved subunits and is localized to cellular regions of dynamic actin filament assembly', Journal of Cell Biology, 138(2), 375-384.

Wellington, M., Koselny, K. and Krysan, D. J. (2012) 'Candida albicans morphogenesis is not required for macrophage interleukin 1β production', MBio, 4(1), e00433-12.

Welsh, O., Vera-Cabrera, L., Rendon, A., Gonzalez, G. and Bonifaz, A. (2012) 'Coccidioidomycosis', Clinics in Dermatology, 30(6), 573-591.

Wheeler, R., Kombe, D., Agarwala, S. and Fink, G. (2008) 'Dynamic, Morphotype-Specific Candida albicans beta-Glucan Exposure during Infection and Drug Treatment', Plos Pathogens, 4(12).

Whiston, E., Wise, H., Sharpton, T., Jui, G., Cole, G. and Taylor, J. (2012) 'Comparative Transcriptomics of the Saprobic and Parasitic Growth Phases in Coccidioides pp', Plos One, 7(7).

Wiesner, D. L., Smith, K. D., Kotov, D. I., Nielsen, J. N., Bohjanen, P. R. and Nielsen, K. (2016) 'Regulatory T Cell Induction and Retention in the Lungs Drives Suppression of Detrimental Type 2 Th Cells During Pulmonary Cryptococcal Infection', Journal of immunology (Baltimore, Md. : 1950), 196(1), 365-74.

Williamson, P. R., Wakamatsu, K. and Ito, S. (1998) 'Melanin biosynthesis in Cryptococcus neoformans', Journal of Bacteriology, 180(6), 1570-1572.

Wilson, D. E., Bennett, J. E. and Bailey, J. W. (1968) 'SEROLOGIC GROUPING OF CRYPTOCOCCUS NEOFORMANS', Proceedings of the Society for Experimental Biology and Medicine, 127(3), 820-&.

Wormley, F. L., Jr., Perfect, J. R., Steele, C. and Cox, G. M. (2007) 'Protection against cryptococcosis by using a murine gamma interferon-producing Cryptococcus neoformans strain', Infection and Immunity, 75(3), 1453-1462.

Wu, L. G., Hamid, E., Shin, W. and Chiang, H. C. (2014) 'Exocytosis and Endocytosis: Modes, Functions, and Coupling Mechanisms', Annual Review of Physiology, Vol 76, 76, 301-331.

Yan, C., Luo, H. L., Lee, J. D., Abe, J. I. and Berk, B. C. (2001) 'Molecular cloning of mouse ERK5/BMK1 splice variants and characterization of ERK5 functional domains', Journal of Biological Chemistry, 276(14), 10870-10878.

Yan, Z., Hull, C. M., Heitman, J., Sun, S. and Xu, J. P. (2004) 'SXI1 alpha controls uniparental mitochondrial inheritance in Cryptococcus neoformans', Current Biology, 14(18), R743-R744.

Yan, Z., Hull, C. M., Sun, S., Heitman, J. and Xu, J. (2007) 'The mating type-specific homeodomain genes SXI1 alpha and SXI2a coordinately control uniparental mitochondrial inheritance in Cryptococcus neoformans', Current Genetics, 51(3), 187-195.

Youseff, B., Holbrook, E., Smolnycki, K. and Rappleye, C. (2012) 'Extracellular Superoxide Dismutase Protects Histoplasma Yeast Cells from Host-Derived Oxidative Stress', Plos Pathogens, 8(5).

Zaragoza, O., Chrisman, C., Castelli, M., Frases, S., Cuenca-Estrella, M., Rodriguez-Tudela, J. and Casadevall, A. (2008) 'Capsule enlargement in Cryptococcus neoformans confers resistance to oxidative stress suggesting a mechanism for intracellular survival', Cellular Microbiology, 10(10), 2043-2057.

Zaragoza, O. and Nielsen, K. (2013) 'Titan cells in Cryptococcus neoformans: cells with a giant impact', Curr Opin Microbiol, 16(4), 409-13.

Zhou, G. C., Bao, Z. Q. and Dixon, J. E. (1995) 'COMPONENTS OF A NEW HUMAN PROTEIN-KINASE SIGNAL-TRANSDUCTION PATHWAY', Journal of Biological Chemistry, 270(21), 12665-12669.

Zhu, X., Gibbons, J., Garcia-Rivera, J., Casadevall, A. and Williamson, P. (2001) 'Laccase of Cryptococcus neoformans is a cell wall-associated virulence factor', Infection and Immunity, 69(9), 5589-5596.

Zimprich, A., Biskup, S., Leitner, P., Lichtner, P., Farrer, M., Lincoln, S., Kachergus, J., Hulihan, M., Uitti, R. J., Calne, D. B., Stoessl, A. J., Pfeiffer, R. F., Patenge, N., Carbajal, I. C., Vieregge, P., Asmus, F., Muller-Myhsok, B., Dickson, D. W., Meitinger, T., Strom, T. M., Wszolek, Z. K. and Gasser, T. (2004) 'Mutations in LRRK2 cause autosomal-dominant Parkinsonism with pleomorphic pathology', Neuron, 44(4), 601-607.

APPENDIX

Movie 1: A Cryptococcal Vomocytosis Event from a Murine Macrophage. (See Attached CD).

Excel File 1: Complete Mass Spec Raw Data File. (See Attached CD)

Table 1: *The enrichment analysis for the comparison between infected macrophages vs. uninfected macrophages + XMD17-109 (HM).*

Term	Gene Count	Fold Enrichment
RRM 2	7	11.17892743
RRM 1	7	11.17892743
negative regulation of cellular component organization	5	8.208288027
RNA recognition motif, RNP-1	10	7.830629519
Nucleotide-binding, alpha-beta plait	10	7.793866
DNA packaging	5	7.558126599
chromatin assembly or disassembly	5	7.003401711
cell soma	5	6.93972694
RRM	10	6.242138365
protein tyrosine kinase activity	6	5.857184837
mrna splicing	7	5.689870248
RNA splicing	7	5.317010453
SH3	6	5.173070714
cytoskeleton organization	11	5.151581995
regulation of organelle organization	5	4.956953159
leukocyte activation	7	4.879995896
short sequence motif:Nuclear localization signal	10	4.862805803
Src homology-3 domain	6	4.720644904
actin cytoskeleton organization	5	4.626489615
Serine/threonine protein kinase, active site	10	4.611370717
sh3 domain	6	4.566240409
mrna processing	7	4.528188406
rna-binding	14	4.481506051
Serine/threonine protein kinase-related	10	4.438752561
Serine/threonine protein kinase	7	4.38515253

cellular macromolecular complex subunit organization	7	4.36211878
cell activation	7	4.34438659
actin filament-based process	5	4.337334014
response to DNA damage stimulus	8	4.255725639
cellular macromolecular complex assembly	6	4.221405271
enzyme binding	6	4.194665123
mRNA processing	7	4.079080539
membrane invagination	5	4.060482907
endocytosis	5	4.060482907
serine/threonine-protein kinase	10	4.043025362
DNA damage	5	4.001344688
lymphocyte activation	5	3.996705689
compositionally biased region:Glu-rich	7	3.982775765
membrane organization	7	3.929114342
chromatin organization	8	3.877438916
mmu04010:MAPK signaling pathway	6	3.82108768
RNA binding	16	3.811818703
protein serine/threonine kinase activity	10	3.802764502
cellular response to stress	10	3.7790633
chromosome organization	10	3.7790633
SM00326:SH3	6	3.763033175
macromolecular complex subunit organization	9	3.744052904
Protein kinase, core	11	3.719150313
macromolecular complex assembly	8	3.613589522
protein amino acid phosphorylation	15	3.578300562
Protein kinase, ATP binding site	10	3.554803978
mRNA metabolic process	7	3.538804971
kinase	16	3.513486255
SM00220:S_TKc	7	3.495597484
RNA processing	10	3.49368781
cytoskeleton	13	3.461883809
internal side of plasma membrane	6	3.394904747
actin binding	6	3.335341365
protein kinase activity	12	3.295294385
vesicle-mediated transport	10	3.27626947
phosphorylation	15	3.189571531
nucleolus	6	3.143024717
cytoskeletal protein binding	8	3.093649962
membrane-bounded vesicle	8	3.093135436
chromosomal part	6	3.063954913
chromosome	7	3.007215007
GO:0005829~cytosol	10	2.957916401
acetylation	44	2.938105657
binding site:ATP	11	2.836488009

vesicle	9	2.816004804
compositionally biased region:Pro-rich	14	2.782873024
cytoplasmic membrane-bounded vesicle	7	2.74571805
phosphoprotein	110	2.706027433
domain:Protein kinase	9	2.657176028
phosphorus metabolic process	15	2.644471547
phosphate metabolic process	15	2.644471547
cytoplasmic vesicle	8	2.557316699
protein localization	12	2.4330543
non-membrane-bounded organelle	28	2.369415889
intracellular non-membrane-bounded organelle	28	2.369415889
intracellular signaling cascade	14	2.335998035
active site:Proton acceptor	11	2.335175174
establishment of protein localization	10	2.327349959
atp-binding	19	2.291990135
nucleotide binding	31	2.273471348
cell cycle	9	2.248882841
nuclear lumen	12	2.206880322
adenyl ribonucleotide binding	20	2.193101172
cytoskeleton	15	2.170984096
nucleotide phosphate-binding region:ATP	14	2.169229579
ATP binding	19	2.107991216
adenyl nucleotide binding	20	2.085946391
purine nucleoside binding	20	2.068428754
nucleoside binding	20	2.055152574
cytoplasm	40	2.050210286
nucleotide-binding	21	1.998955029
ribonucleotide binding	21	1.871951056
purine ribonucleotide binding	21	1.871951056
organelle lumen	13	1.858331809
purine nucleotide binding	21	1.796912932
nucleus	43	1.753110157
alternative splicing	50	1.732338473
coiled coil	19	1.703112762
splice variant	49	1.548160813

Table 2: *The enrichment analysis for the comparison between infected macrophages vs. infected macrophages + XMD17-109 (HL).*

Term	Gene Count	Fold Enrichment
nuclear speck	6	13.025
nuclear body	9	12.38292254
compositionally biased region:Lys-rich	6	10.97955454
chromatin assembly or disassembly	5	9.166216945
Nucleotide-binding, alpha-beta plait	8	8.0380112
chromatin binding	6	7.913449132
regulation of organelle organization	6	7.785332315
cell cortex	5	7.75297619
RNA recognition motif, RNP-1	7	7.066435554
actin filament-based process	6	6.812165775
actin cytoskeleton organization	5	6.055258467
RRM	7	6.02990566
chromatin	5	5.920454545
actin binding	8	5.678632479
rna-binding	13	5.564660753
cytoskeleton organization	9	5.516600505
actin-binding	6	5.511627907
ATPase activity, coupled	6	5.500379441
leukocyte activation	6	5.474617244
chromosome organization	11	5.440739662
compositionally biased region:Glu-rich	7	5.341605144
mitosis	5	5.258513932
nuclear division	5	5.258513932
M phase of mitotic cell cycle	5	5.150090964
chromatin modification	6	5.080259222
chromatin organization	8	5.074883287
organelle fission	5	5.071663183
cytoskeletal protein binding	10	4.937941286
response to DNA damage stimulus	7	4.87374462
cell activation	6	4.87374462
actin cytoskeleton	5	4.765243902
nucleoplasm part	12	4.570175439
enzyme binding	5	4.463553913
cellular response to stress	9	4.451514269
ATPase activity	6	4.365069806
chromosomal part	7	4.300707547
cell division	6	4.266694578
transcription factor binding	6	4.258974359

nucleoplasm	13	4.240191987
M phase	6	4.23654126
chromosome	8	4.134920635
mitotic cell cycle	5	4.094744455
mRNA metabolic process	6	3.970003896
RNA binding	13	3.954761905
cytoskeleton	11	3.91706889
ribonucleoprotein	5	3.902343067
ribonucleoprotein complex	9	3.806006494
acetylation	42	3.750277569
compositionally biased region:Pro-rich	14	3.732323821
cell cycle phase	6	3.655308465
cell projection	10	3.397826087
negative regulation of biosynthetic process	7	3.222960152
nuclear lumen	14	3.097678369
cell cycle process	6	3.050740907
compositionally biased region:Ser-rich	6	2.976037152
cell cycle	9	2.943390777
organelle lumen	17	2.923745599
membrane-enclosed lumen	17	2.829109881
negative regulation of macromolecule metabolic process	7	2.764357126
intracellular organelle lumen	16	2.759046778
phosphoprotein	82	2.697445951
protein localization	10	2.65369893
non-membrane-bounded organelle	25	2.545270974
intracellular non-membrane-bounded organelle	25	2.545270974
establishment of protein localization	8	2.43687231
cytoskeletal part	9	2.271802326
cytoplasm	33	2.26178722
atp-binding	14	2.258325654
coiled coil	18	2.157554111
nucleotide binding	23	2.153874344
cytoskeleton	12	2.089572193
nucleus	37	2.017167041
alternative splicing	43	1.992189243
ATP binding	14	1.983389306
purine nucleoside binding	15	1.980918306
nucleoside binding	15	1.968203812
adenyl ribonucleotide binding	14	1.960295047
nucleotide-binding	15	1.9093009
adenyl nucleotide binding	14	1.864515159
splice variant	42	1.779734448
purine ribonucleotide binding	15	1.70738393